L.B. Klyashtorin, A.A. Lyubushin

CYCLIC CLIMATE CHANGES AND FISH PRODUCTIVITY

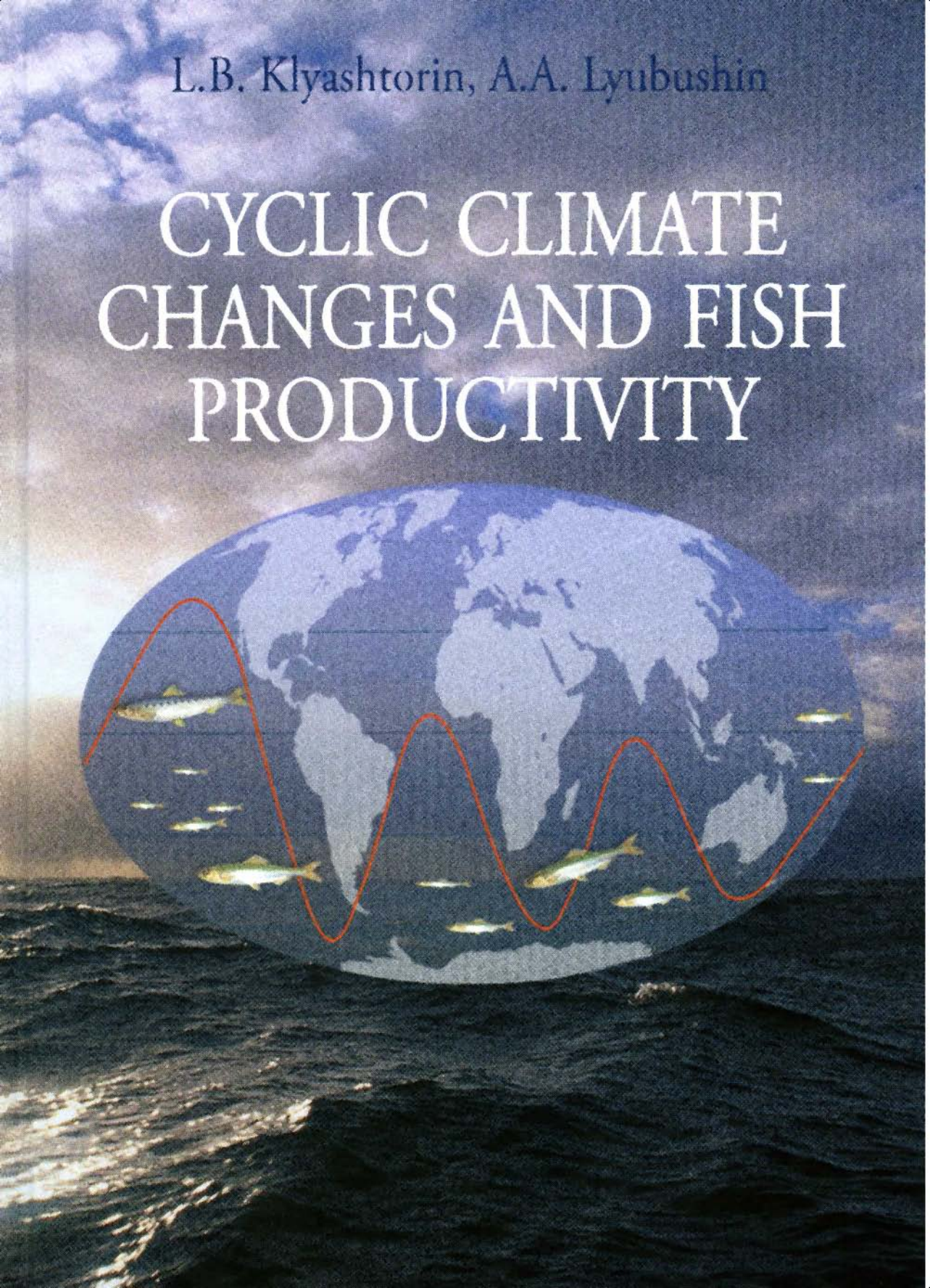

GOVERNMENT OF THE RUSSIAN FEDERATION
STATE COMMITTEE FOR FISHERIES OF THE RUSSIAN FEDERATION

FEDERAL STATE UNITARY ENTERPRISE
«RUSSIAN FEDERAL RESEARCH INSTITUTE OF FISHERIES
AND OCEANOGRAPHY» (FSUE «VNIRO»)

L.B. KLYASHTORIN, A.A. LYUBUSHIN

CYCLIC CLIMATE CHANGES AND FISH PRODUCTIVITY

EDITOR OF ENGLISH VERSION OF THE BOOK
DR. GARY D. SHARP
CENTER FOR CLIMATE / OCEAN RESOURCES STUDY
SALINAS, CALIFORNIA, USA

MOSCOW VNIRO PUBLISHING 2007

УДК 639.2.053.8:551.465.7:639.2.053.1

Klyashtorin L.B., Lyubushin A.A.

K47 Cyclic climate changes and fish productivity.— M.: VNIRO Publishing, 2007.— 224 p.

The book considers relationships between climate changes and fish productivity of oceanic ecosystems. Long-term time series of various climatic indices, dynamics of phyto- and zooplankton and variation of commercial fish populations in the most productive oceanic areas are analyzed. Comparison of climate index fluctuations and populations of major commercial species for the last 1500 years indicates on a coherent character of climate fluctuations and fish production dynamics. A simple stochastic model is suggested that makes it possible to predict trends of basic climatic indices and populations of some commercial fish species for several decades ahead. The approach based on the cyclic character of both climate and marine biota changes makes it possible to improve harvesting of commercial fish stocks depending on a phase (ascending or descending) of the long-term cycle of the fish population. In addition, this approach is helpful for making decisions on long-term investments in fishing fleet, enterprises, installations, etc. The results obtained also elucidate the old discussion: which factor is more influential on the long-term fluctuations of major commercial stocks, climate or commercial fisheries?

ISBN 978-5-85382-339-6

INTRODUCTION

Many century-long fishery practices indicated that the populations and catches of massive commercial fishes, herrings, codfish, sardines, anchovies, salmons and some other species are subject to significant long-term fluctuations [Rothschild, 1986; Sharp, 2003].

The periods of «good» or «poor» fisheries have caused and still cause significant economic and social consequences. As indicated in Japanese annals, outbursts in population and catches of Japanese sardine attracted people to the sea and caused expansion of seaboard industrial fishing settlements, whereas diminution of the fished populations and catches caused withdrawal of the people, and some settlements disappeared. Within the recent 400 years this process repeated every 50 to 70 years [Kawasaki, 1994].

The written history of rises and falls of Bohuslan herring catches at the southern extremity of Sweden in the Skagerrak Strait embraces over a thousand years. The first documented attempts to detect the periodicity of this process were initiated in the 19th century [Ljuingman, 1880]. The average duration of «good» or «poor» periods has been shown to be about 55 years, and the full fluctuation cycle for the Bohuslan herring bloom / bust pattern is 110 to 120 years. This repeating pattern has tended to associate with secular alteration of the solar activity (sun spot dynamics) and polar lights (galactic rays). Modern researchers suggest that the periodicity of Bohuslan fishery relates to long-period meteorological processes proceeding in North Atlantic and specificity of herring migration in the North Sea as a response to the changes in oceanographic contexts [Alheit, Hagen, 1997; Corten, 1999].

During the last century, synchronous outbursts in Pacific sardine populations (Japanese sardine *Sardinops melanostictus*), California and Peruvian

Sardinops sagax) were observed with approximate 60-year period thus inducing rise and fall of the extensive Japanese seaboards' regional economic evolution. Dramatic fluctuations of the Peruvian anchovy population induce significant changes in fish-meal production, one of the basic export products of Peru. Similarly, fluctuations in the reserves of Northern Pacific pollack, observed during the recent 50 years, were followed by serious changes in «surimi» (imitation crabmeat) production, which provides sufficient economic incentives for the fishing industries of several countries.

Already in the 1950s, concepts about relationships between climate processes and fluctuations in the population of commercial fishes were formulated by G.K. Izhevsky [1961; 1964]. He related fluctuations in the populations and hauls of Atlantic cod, herring and some other commercial fishes to multiyear eurhythmics of the solunar tidal forcing, variations in North-Atlantic Drift intensity, fluctuations in the heat delivery to the Arctic region, and the temperature variation in the 0–200 meter layer in the «Kola Meridian». In the recent fifty years an immense extent of new data was obtained, and understanding of the mechanisms of oceanic and climatic processes became more profound, hence Izhevsky's ideas are still useful [Elizarov, 2001].

In her famous monograph, T.F. Dementieva developed the ideas about dependence of long-period fluctuations of commercial fish population on climate changes [Dementieva, 1976].

The problem of climate change influences on the North Pacific fish capacity was considered in a series of works by V.P. Shuntov et al. [Shuntov, Vasil'kov, 1982; Shuntov, 1986, 1991, 2001]. Cushing [Cushing, 1982] and Laevastu [Laevastu, 1993] each wrote monographs devoted to finding a relationship between climate and fishery which each exerted a significant effect on the formation of ideas describing the reasons of fluctuations in the population of some commercial fishes, although the greater part of their results were derived from the data from only the North Atlantic. Since these reports were published, interests in global studies of the Earth climate have grown significantly and thus the volume of climatological data has also dramatically increased, while the geography of fishery zones were extended, and commercial catch statistics sequences have expanded.

The works by Lluch-Belda et al., Kawasaki and some other researchers [Lluch-Belda et al., 1989; 1992a, b; Kawasaki, 1992a, b; 1994; Schwartzlose et al., 1999], devoted to searching for the reasons of synchronous alterations of sardine and anchovy population increases in different regions, have attracted attention to the problem of possible existence of a global «climatic

signal» which synchronizes changes in ecosystems of different regions of the World Ocean.

Recently, 60–70 year repeating alterations of hemispherical and global climate were detected [Schlesinger, Ramankutty, 1994; Minobe, 1997, 1999, 2000]. Temperature sequences for the recent 1500 years, reconstructed from Greenland ice core samples, show domination of approximately 60-year periodicity of the climate fluctuations [Klyashtorin, Lyubushin, 2003; Klyashtorin, Lyubushin, 2005]. For the same period, similar (50–70 year) temperature periodicity was detected in the analysis of long-living tree annual growth rings in the Arctic region and California. Reconstruction of sardine and anchovy population fluctuations by analysis of scales in bottom sediments in Californian upwelling for the latest 1700 years has indicated their approximately 60-year periodicity [Baumgartner et al., 1992].

The role of climate as the main factor defining fluctuations in the populations of Pacific salmon and some other commercial species is shown in a set of recent works [Birman, 1985; Beamish, Bouillon, 1993; Jonsson, 1994; Klyashtorin, Smirnov, 1995; Klyashtorin, Sidorenkov, 1996; Klyashtorin, 2001; Chavez et al., 2003].

The main topic of this book is studying a relationship between cyclic e.g. more or less regularly repeating long-period climate changes and fish capacity / distribution and abundance changes. This requires demonstration of a relationship between repeating changes in the climate and fish capacity / distribution and abundance changes, as well as finding approaches to develop a model that successfully predicts possible fluctuations in the reserves of the main commercial species over the perspective of several decades.

Populations of the main commercial fish species that yield up to 40% of the world total fish landings are subject to long-period fluctuations inducing various fishery and economic events. More or less reliable relationships between climate variations and the fish capacity may be set using multiyear sequences of the population fluctuations of the largest commercial populations with annual landings that have reached over a million tons.

Time scale of the climate changes is two-three decades, and the spatial scale is several million square kilometers. There is to date no unified theory of the climate system of the Earth, and many climatological aspects are not also well elucidated. It is thus not our goal to discuss particular mechanisms of the climatic processes. In order to characterize long-period changes in the climate the results of intensive climatologic studies have been used, the so-called «climatic indices» with dynamics that show climate changes for many

decades, either global, hemispherical or regional. Our focus is on the practical and important question of the relationships between climate changes and the resulting productivity of oceanic ecosystems. Comparative data on the rate of climatic indices, dynamics of phyto- and zooplankton and commercial fishery populations in the productive zones of the ocean are considered. Analysis of the data on fluctuations of the climate and populations of some massive commercial fisheries during the latest 1500 years allows realistic conjugation of the climate and fisheries capacity fluctuations. Based on the results obtained, we provide a stochastic prognostic model of the fluctuations of climate and population for several of these large populations of commercial species for the prospect of several decades. The ideas about cyclic character of the climate and biota fluctuations allow modification of commercial operations, as we have described, and at which phase of the long-period cycle (fall or rise of the population) each of these commercial fisheries populations is in now, or will experience. This approach promotes feasible investments into long-term projections of commercial fleet or fish-processing enterprise management.

The results obtained clear up an old question under discussion about the reason for the long-period fluctuations of the resources of the main commercial species: climate or the large-scale fishery.

Note: Abbreviations are shown at the end of the book.

CHAPTER 1

ON CLIMATE REPEATING PATTERN

The term «climate» is defined as long-term statistically averaged weather indices. To smooth inevitable seasonal and annual variations, the averaging period should amount to decades. International meteorological conferences held in 1935 in Warsaw and in 1957 in Washington to determine characteristics of the modern climate recommended 30-year averaging periods [Monin, Shishkov, 2000].

Spatial parameter is the second important index for the climate estimation. To obtain statistically reliable climatic characteristics the Earth surface area used for the long-term analysis should be rather large. As shown by A.V. Kislov et al. [2000], the minimum area for data collection equals 1–3 mill. km^2.

Thus, the time scale of climate changes equals several decades and the spatial scale gives several million square kilometers. In actual practice, climatic variability is usually described by 10–30-year averaging for aquatic areas of million square kilometers.

SHORT-PERIOD TIME SERIES

Regular and reliable instrumental measurements of the surface layer air temperature were initiated about 150 years ago. The average temperature anomaly of the surface air layer (Global dT), averaged by all measurement points, is considered to be the most important index characterizing global long-period fluctuations of the Earths climate [Bell et al., 2001; Jones et al.,

2001]. It is this index considered to be the main characteristic of dynamics of the so-called global warming.

Fig. 1.1 shows dynamics of Global dT for the 140-year observation period and its annual fluctuations. Inter-year variations are rather large and should be smoothed in order to detect long-period behavior of Global dT fluctuations. For this purpose, a 13-year moving averaging is used

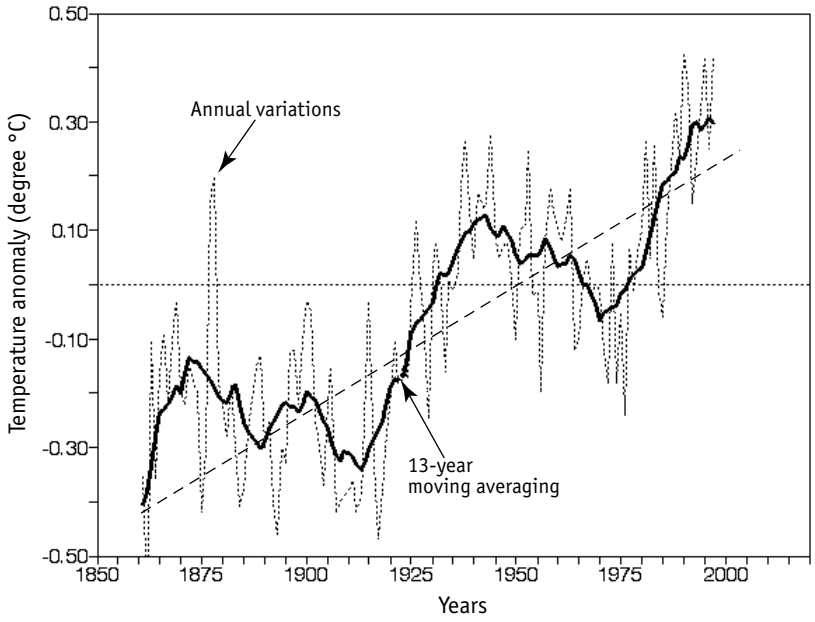

Fig. 1.1. Dynamics of the surface air Global temperature anomaly (Global dT) 1861–2000. Dotted line shows annual variations of Global dT, bold line is the same smoothed by 13-year moving averaging

As shown in Fig. 1.1, the increasing secular linear trend (about 0.06 °C per each 10 years; Sonechkin, 1998) at the background of interannual year Global dT variations is observed.

At the background of the secular linear trend, Global dT undergoes long-period, up to 60-year long, fluctuations. These fluctuations can be detected by detrending with the help of a standard statistical operation [Statgraphics, 1988]. After detrending, the long-period fluctuations of Global dT with the maxima at about 1870s, 1930s and, apparently, at 1990s are clearly observed (Fig. 1.2). Global dT detrending allows detection of 2.5 cycles of approximately 60-year Global dT fluctuations.

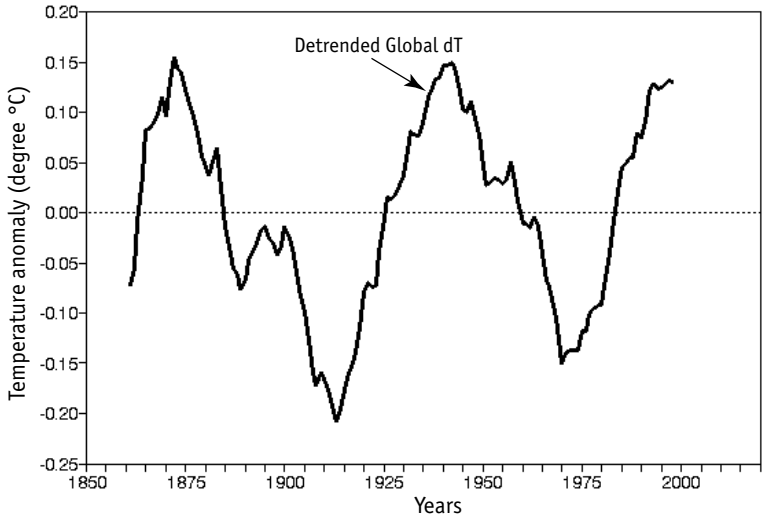

Fig. 1.2. Dynamics of detrended Global dT, smoothed by 13-years moving averaging

An approximately 60-year repeating pattern is also observed well from temperature anomaly dynamics in the circumpolar Arctic zone (Arctic dT) between 60 and 85° N. Detrended Global dT behavior compared with Arctic dT is shown in Fig. 1.3.

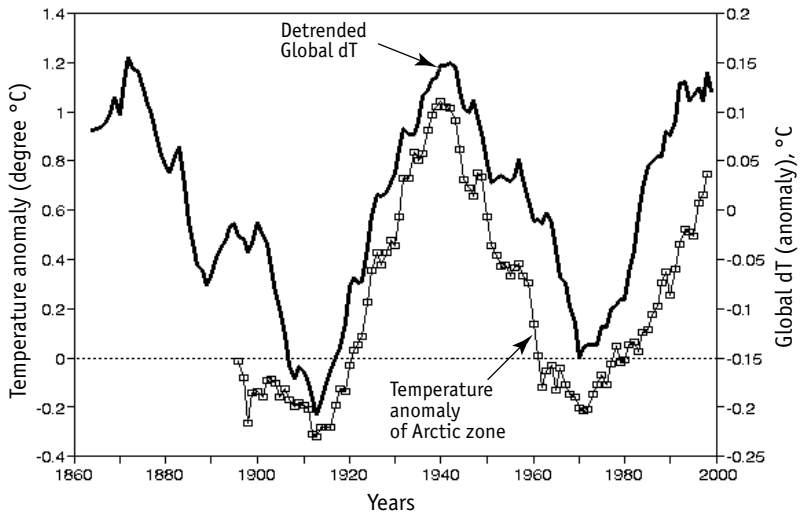

Fig. 1.3. Comparative dynamics of detrended Global dT (bold line) and temperature anomaly of Arctic circumpolar zone (Arctic dT). 60–85° N, (white squares) 13-year smoothing. Data from Alexandrov et al., 2003

The specific feature of the long-period temperature dynamics in the Arctic zone is the absence of secular, linearly increasing temperature trend observed for Global dT (see Fig. 1.1). Comparison of detrended Global dT and Arctic dT fluctuation dynamics demonstrates almost complete coincidence in behavior of these two indices during the last 100 years. This indicates that, actually, the Global dT linear increasing trend is not a global phenomenon. At the same time, approximate 60–70-year repeating pattern is observed for both Global dT and Arctic dT [Alekseev et al., 2000; Alekseev, 2003].

Another important climate index is Atmospheric Circulation Index (ACI), which characterizes periods of relative predominance of «zonal» or «meridional» air transfer by the hemisphere. This index is known as the Vangenheim-Girs Index and is calculated from the observations for direction of the air transfer in Atlantic-Eurasian region (30–80° N and 45–75° E) during the last 110 years [Vangenheim, 1940; Girs, 1971].

The Vangenheim-Girs classification is based on the multiyear repetition of air transfer directions, which is widely used in the works by Russian experts in meteorology and climatology. In accordance with this system, all observed fluctuations in the atmospheric circulation are classified by directions of air motion into three main types: meridional (C), western (W) and eastern (E) [Vangenheim, 1940].

Atmosphere circulation types, formulated by G.Ya. Vangenheim [1940]:

Type 1 — western (W) winter circulation.

> «The objective sign of this circulation are pronounced west-to-east air transfers. The external objective sign may be displacement of baric (pressure) formations with the east directed motion components».

Type 2 — eastern (E) winter circulation.

> «Eastern circulation occurs, when stable stationary anticyclones or anticyclones moving from E to W are formed in the middle latitudes. These anticyclones disturb normal west-east transfer. The signs of these processes are temporal termination of the west-east transfer and sometimes reversion of the transfer to the opposite direction (east-west)».

Type 3 — Central European meridional (C) circulation.

> «Arctic front is directed from north-west to south-east. In this direction cyclonic disturbances are moving. The objective signs of this type of circulation are cyclones moving from north-west to south-east. Then they regenerate on the polar front and move from south and south-west to north and north-east».

«The signs for recognizing the circulation type are quite objective. It is impossible to mix type W processes, when clearly expressed transfers from west to east

happen, with type E processes, when such processes are disturbed or changed to the opposite ones. On the other hand, due to strict geographical localization of C circulation (from north to south and from south to north — *L.K.*) they cannot be mixed with the circulation types W and E».

Each of the above-mentioned forms is determined by analyzing daily atmospheric pressure maps for Atlantic-Eurasian region. The direction of cyclonic and anticyclonic air mass transfers is elucidated by distribution of atmospheric pressure fields based on analysis of the general picture of the «atmospheric pressure topography» in the region.

However, there is some «asymmetry» in the Vangenheim-Girs system. If types E and W each marks an individual direction of the atmospheric transfer to the east or to the west, type C unites «meridional» transfers in the north (N) and south (S) directions and represents their sum (N + S). By analogy, an association of atmospheric transfers of east (E) and west (W) directions into one «zonal» type (W + E) is suggested.

Recurrence of meridional (N + S) and zonal (W + E) transfer are transformed as anomalies (deviation of the repetition of each shape from the long-term average). The sum of anomalies of all types per year equals zero: (N + S) + (W + E) = 0 and (N + S) = (W + E).

Thus far, for each transform 110 mean-year anomalies of their repetitions are accumulated. For characterization of long-period changes in circulation we use not a sequence of anomalies themselves, but the so-called «integral curve», obtained by sequenced summation of anomalies that represents a curve of accumulated frequencies (cumulative curve).

This index called Atmospheric Circulation Index (ACI) characterizes the long-period dynamics of zonal and longitudinal transfer processes in Atlantic-Eurasian region. Fig. 1.4 shows zonal and longitudinal ACI pattern for the latest 110 years.

As shown in Fig. 1.4, zonal and meridional ACI curves are antiphase, have no secular linear trend, and their fluctuations have approximately 60-year period. ACI dynamics characterizes the long-period behavior of atmospheric processes in North Atlantic. First of all, they should be compared with Arctic dT dynamics that reflect temperature variations in the latitudinal zone of 60–80° N. Fig. 1.5 shows full coincidence of Arctic dT and zonal ACI dynamics.

The comparison of zonal ACI and Global dT behaviors (Fig. 1.6) demonstrates their close affinity, although ACI curve precedes Global dT changes

by approximately 5 years. Thus, zonal ACI, the index regional by origin, may be considered as a climate index, which similar to Global dT reflects global changes in climate of the Earth.

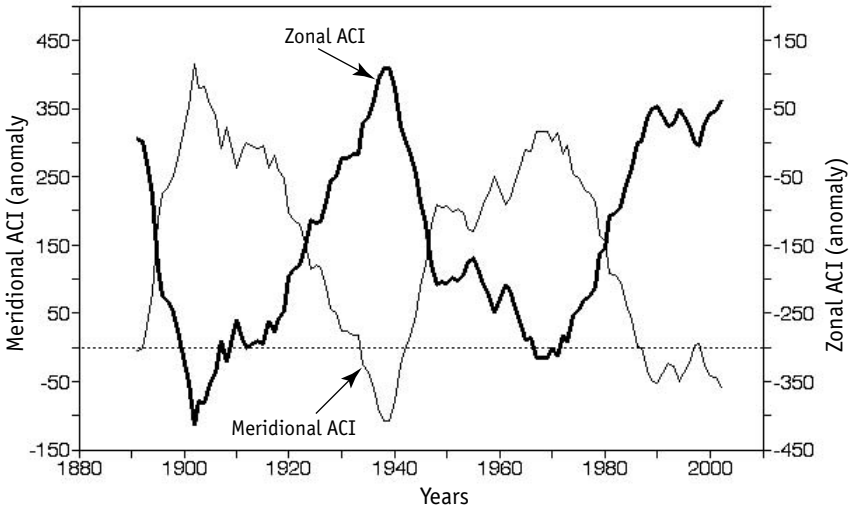

Fig. 1.4. Dynamics of zonal (bold line) and meridional (thin line) Atmospheric Circulation Index (ACI), 1891–2000. The data were kindly provided by Dr. V.V. Ivanov from Arcticand Antarctic Research Institute (AARI), St.-Petersburg

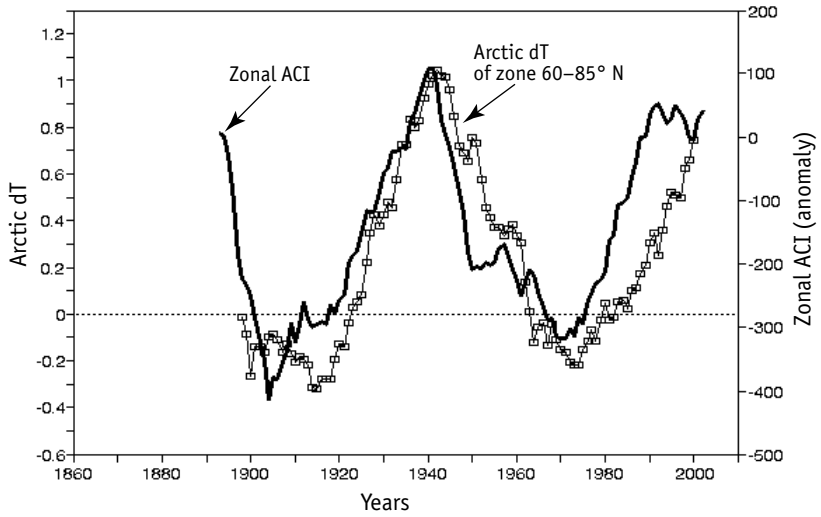

Fig. 1.5. Comparative dynamics of zonal ACI (bold line) and Arctic dT (white squares), smoothed by 13-year averaging, 1891–2000

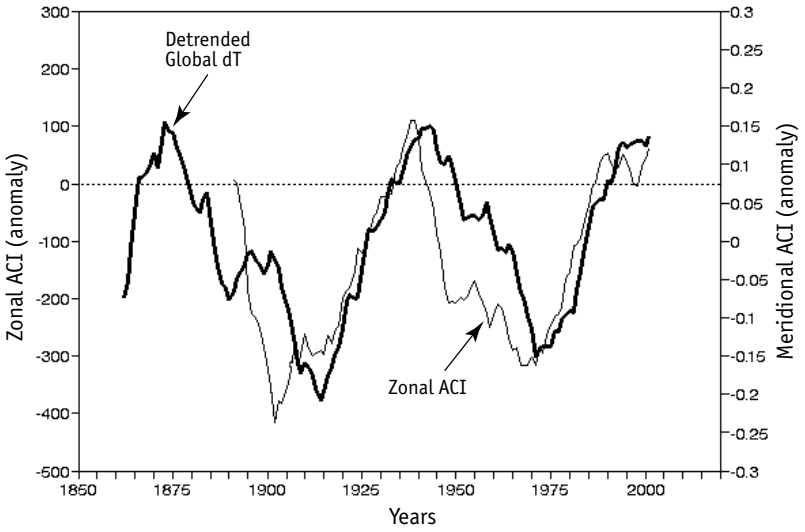

Fig. 1.6. Comparative dynamics of detrended Global dT (bold line) and zonal ACI (thin line), 1861–2000

In accordance with Global dT, zonal ACI increases in the periods of «warming», whereas decreases in the periods of «cooling». The comparison of zonal and longitudinal ACI fluctuation dynamics (see Fig. 1.4) shows that the dominance periods of each of these shift sign approximately every 30 years. These periods, called «zonal» and «meridional» climatic epochs, coincide with the periods of warm and cold epochs according to the long-period dynamics of Global dT fluctuations (see Figs. 1.5 and 1.6).

For separating climatic epochs by alteration of atmospheric circulation forms (see Fig. 1.4) and Global dT fluctuations (Fig. 1.6) only upper parts of the curves are used. The scheme in Fig. 1.7 clearly demonstrates alteration of warm (zonal) and cold (meridional) epochs with approximately 30-year repetition during the last 110 years. On this basis it is reasonable that the current warm or zonal climatic epoch, started in 1970s, will probably finish in the first decade of 2000s, and the subsequent cold epoch will last since 2010s till 2030s (Fig. 1.7).

The above-considered climatic indices were mainly obtained from observations in Atlantic region. In Pacific region two climate indices are widely used: Pacific Decadal Oscillation (PDO) and Aleutian Low Pressure Index (ALPI).

PDO characterizes the long-period temperature changes of Pacific Ocean surface in its northern part [Barnett et al., 1999; Hare, Mantua, 2000].

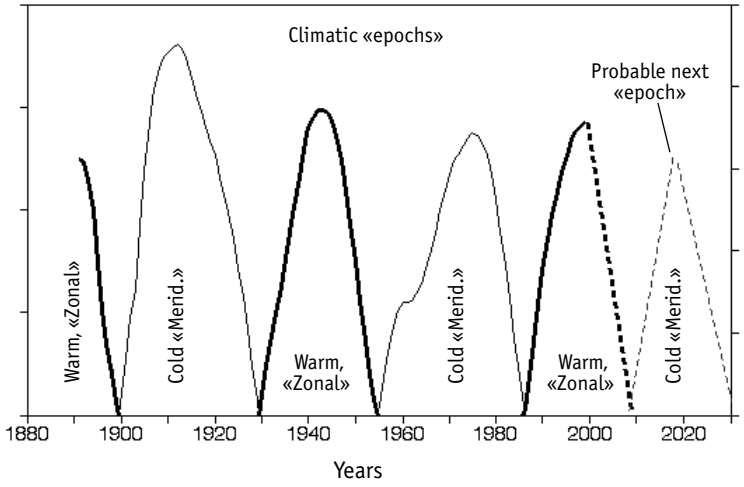

Fig. 1.7. Alteration of the warm (bold line) and cold (thin line) climatic epochs by fluctuations of the Global temperature anomaly (Global dT) and Atmospheric Circulation Index (ACI). Dashed thin line shows probable transfers into the next cold epoch

ALPI characterizes the long-period changes in the area of low atmospheric pressure in North Pacific (mill. km^2). It is considered as one of the main climate indices for this region [Beamish, Bouillon, 1993; Hare, Mantua, 2000].

Beside ALPI, the North Pacific Index (NPI) is also used, which characterizes the long-period changes of the atmospheric pressure in the entire water surface area of North Pacific [Trenberth, Hurell, 1995]. Dynamics of this index represents a mirror reflection of ALPI [Hare, Mantua, 2000].

Fig. 1.8 shows comparison of Atlantic, Pacific and global climatic indices behavior for the last 100 years. It is clear that PDO and ALPI dynamics is close to that of detrended Global dT, as well as to Arctic dT and zonal ACI. All curves have clear periods of both minima (1900s–1920s and 1960s–1970s) and maxima (1930s–1940s and 1980s–1990s). Note also that PDO and ALPI (as well as Arctic dT) virtually have not rising trend. Moreover, regional Pacific PDO and ALPI indices have definite differences from Global and Arctic dT. A maximum in the mid 1980s and an intermediate minimum in the mid 1990s are typical of PDO and ALPI, whereas in the middle 1990s Global dT and ACI curves each show the beginning of a maximum. Both global and regional climatic indices demonstrate general cyclic dynamics with approximately 60-year period.

Resemblance of the long-period dynamics of these main climatic indices indicates existence of a «global climatic signal» e.g. simultaneous development of climatic processes having approximately 60-year periodicity, observed, at least, for the whole northern hemisphere.

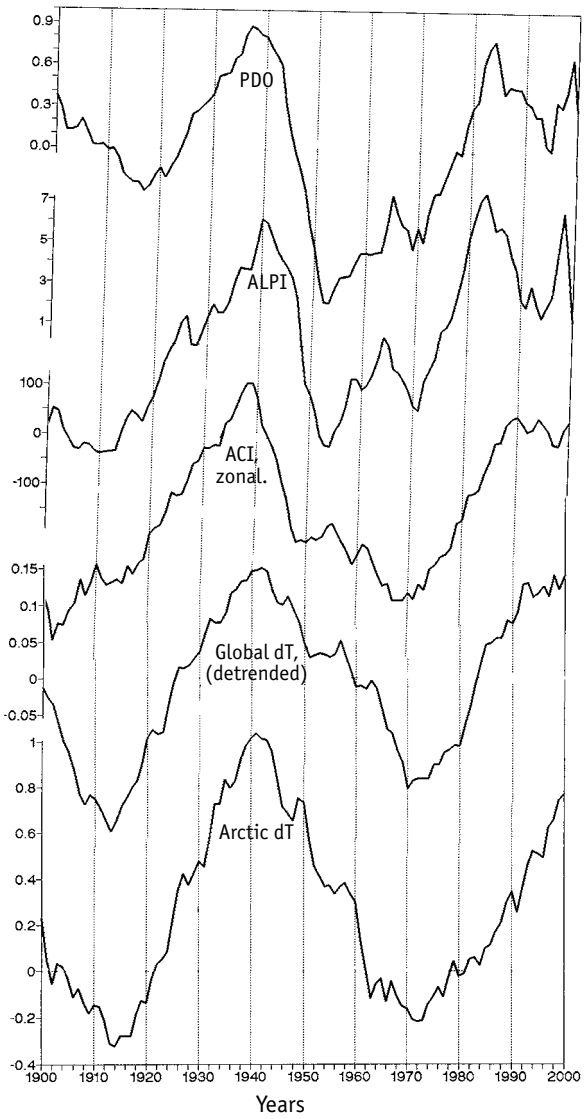

Fig. 1.8. Comparative dynamics of several climatic indices for 1900–2000: Pacific Decadal Oscillation (PDO), Aleutian Atmospheric Presssure Index (ALPI), zonal ACI, detrended Global dT and Arctic Temperature Anomaly (Arctic dT). Smoothed by 13-year moving averaging

The basic results indicate an approximately 60-year periodicity of climatic processes. These results are based on the analysis of relatively short observation periods, generally about 100 years, and the only longer empirical observation time series is that for Global dT, which comprise 140 years. Reliable detection of climatic processes requires analysis of much longer climatic data series, as long as several hundred or even thousands of years.

Such time series were obtained by reconstruction of paleotemperature from isotopic analysis of large glacier columns or analysis of annual growth rings of long-living trees.

LONG-TERM CLIMATIC TIME SERIES

Fig. 1.9 shows time series for temperature over the last 1500 years, reconstructed by the analysis of Greenland ice core samples and annual growth rings of the long-living trees: Arctic pine tree from Scandinavian Peninsula and North-California bristlecone pine tree.

After smoothing these annual temperature variations by 41-year moving averaging, multidecadal temperature fluctuation periodicity is detected with the help of spectral analysis methods.

Temperature fluctuations reconstructed by ^{18}O in the Greenland ice cores

Polar glaciers contain paleoclimatic information in the form of heavy oxygen isotope, ^{18}O, content in the ice [Dansgaard et al., 1975]. Isotope ^{18}O concentration is measured in parts per million in relation to its content in the so-called «standard oceanic water». As the air temperature increases, the relative number of water molecules with increased content of heavy oxygen isotope rises as their rate of evaporation from the ocean surface increases. Water vapors are transferred poleward by air flows to the North, and after their condensation above Greenland, the snow formed is gradually transformed to ice. Variations in ^{18}O content along the borehole in ice show air temperature fluctuations in the region at the moment of snowfall to ancient glacier surfaces.

In the central part of Greenland (at about 71° N) the conditions of snow accumulation and ice formation remained stable during several thousand

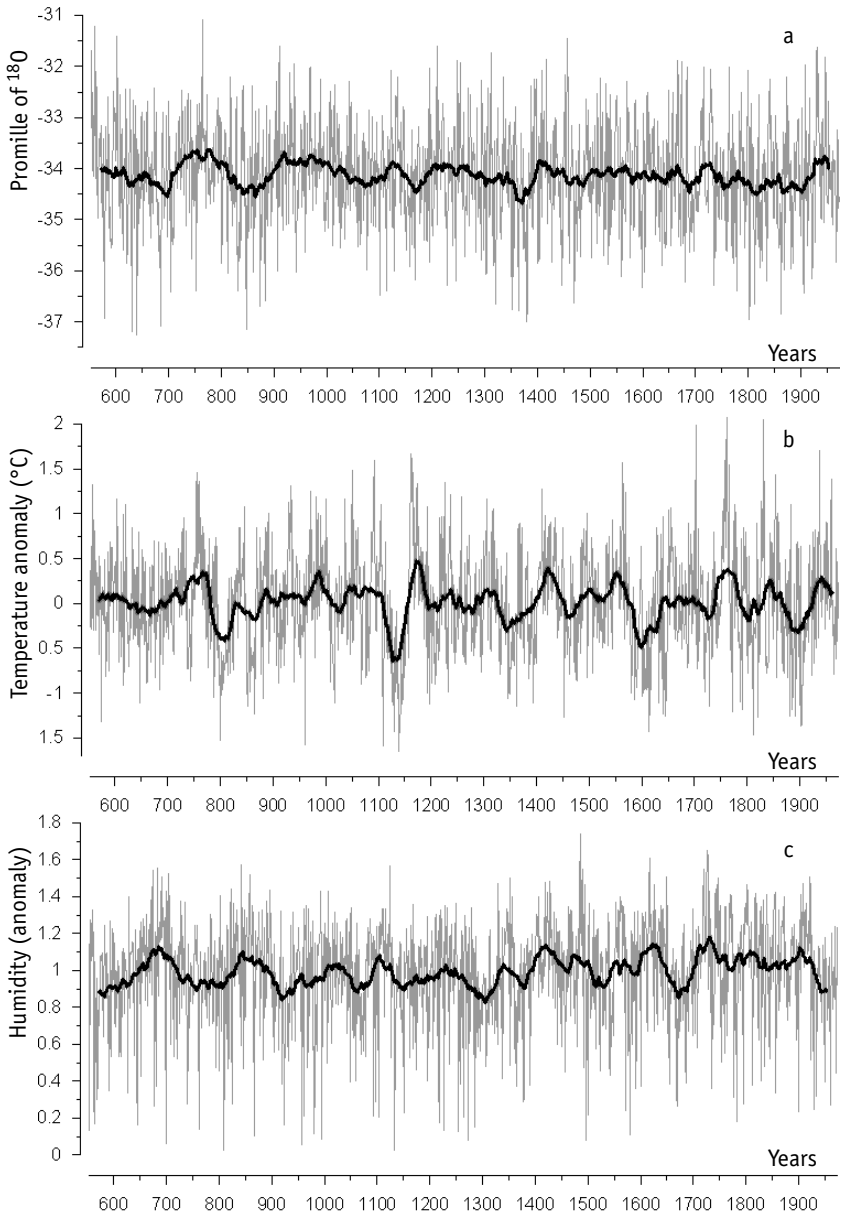

Fig. 1.9. Reconstructed temperature and humidity time series for 1500 years. Thin lines show annual data, bold lines give 41-year moving averaging by: *a* — Greenland ice cores, *b* — Arctic pine tree rings, *c* — California pine tree rings

years. «Nowhere else in the world is it possible to find a better combination of a reasonably high accumulation rate, simple ice flow patterns (which facilitates the calculation of the time scale), high ice thickness (which offers a detailed record, even at great depths) and meteorologically significant location (close to the main track of North Atlantic cyclones». [Dansgaard et. al., 1975]. Analysis of ^{18}O content in the ice core of more than 500 m in depth (with annual section thickness of 0.29 m) made it possible to reconstruct the mean annual air surface temperature for last 1423 years (from 552 to 1975).

Fig. 1.10 shows the full spectrum of temperature fluctuations from Greenland Ice core samples over almost 1500 years.

Of the greatest interest are fluctuations with «climatic» periodicities of 20 to 100 years. As the graphic shows, 19 and 54 year periodicities are most clearly expressed; the 160-year cycle is also clear.

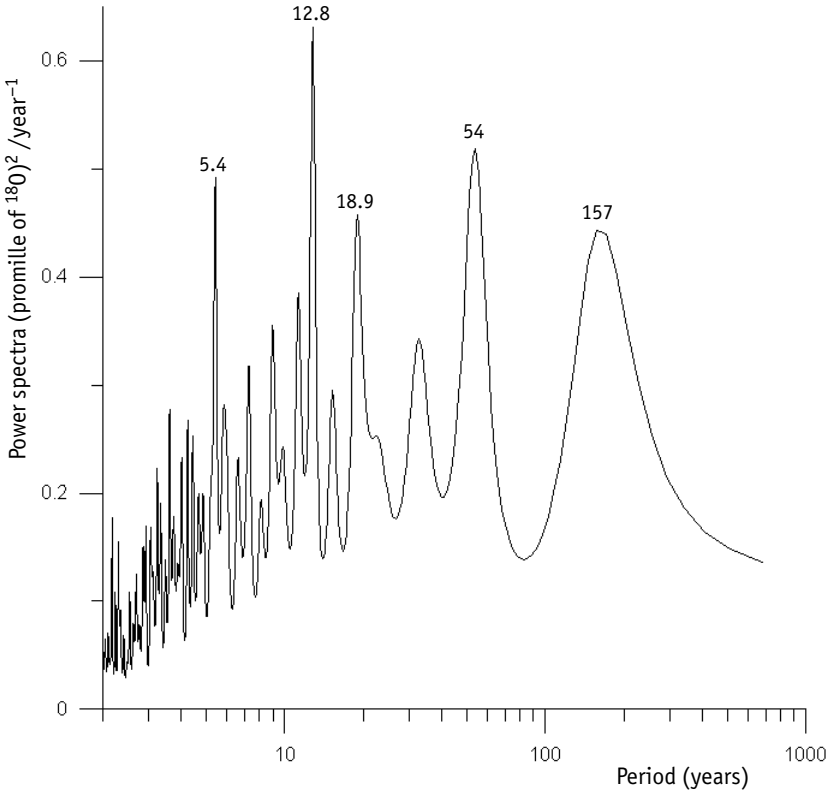

Fig. 1.10. Spectrum of periodical temperature fluctuations for 1423 years by Greenland ice core samples (logarithmic X-axis). Ordinate — spectral power. Abscissa — period, years

Temperature fluctuations for 1400 years (from 500th to 1900th) reconstructed by annual growth rings of pine tree (Pinus silvestris) in the North of Sweden

In Arctic regions trees grow in warm seasons only. This fact makes annual growth rings clear enough for reliable reconstruction of summer temperature. One of the most reliable long-period reconstructions was performed on growth rings of long-living pine tree from the North of Sweden [about 68° N; Briffa et al., 1990]. The full spectrum of temperature fluctuations is shown in Fig. 1.11.

Fig. 1.11 shows that 16.8-, 32-, 60- and 108-year periodicity are predominant. According to growth rings of Norway pine from Lofoten Islands, analysis of temperature fluctuations for the last 300 years yielded quite similar predominant periodicities: 17.5, 23 and 57 years [Ording, 1941; Ottestad,

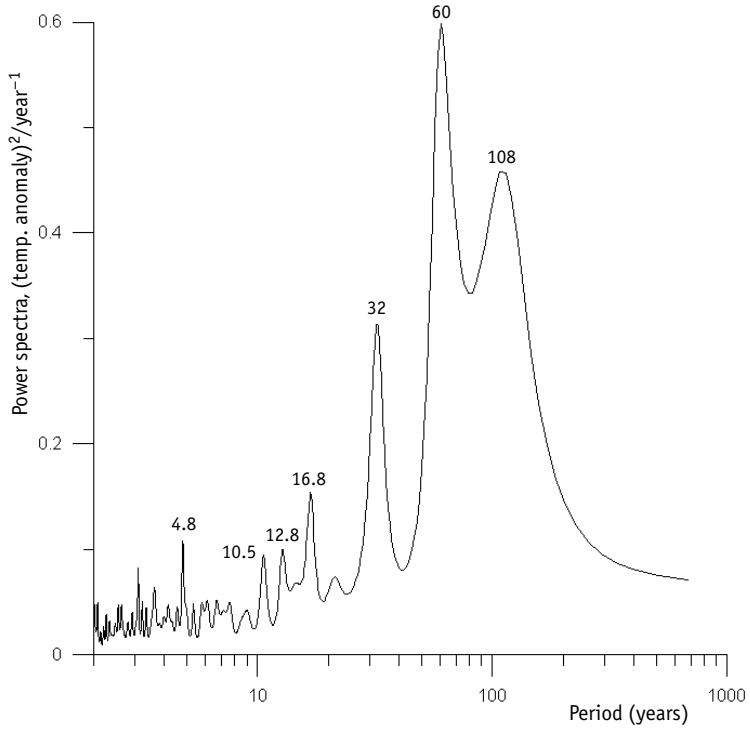

Fig. 1.11. Spectrum of periodical temperature fluctuations for 1400 years by the Arctic pine tree (*Pinus silvestris*) growth rings (logarithmic X-axis). Ordinate — spectral power. Abscissa— period, years

1942]. The periodicities most interesting for us are those of 57 and 60 years, which are very close from estimations of different authors.

Moisture / Aridity fluctuations for 1480 years (500^{th} to 1980^{th}) reconstructed by growth rings of North California bristlecone pine tree (Pinus aristata)

One of the longest climatic time series is the dendrochronology series (growth rings) changes for the oldest trees, the bristlecone pine, that grows at about 3000 meters above sea-level in the North Californian western ridges of the Great Basin. This year-ring series is almost 8000 years long (from 6000 A.C. until 1979 A.D.) that is called the Methuselah Walk Pilo (D. Graybill). The spectrum of final part (1500 years) of time series shown in

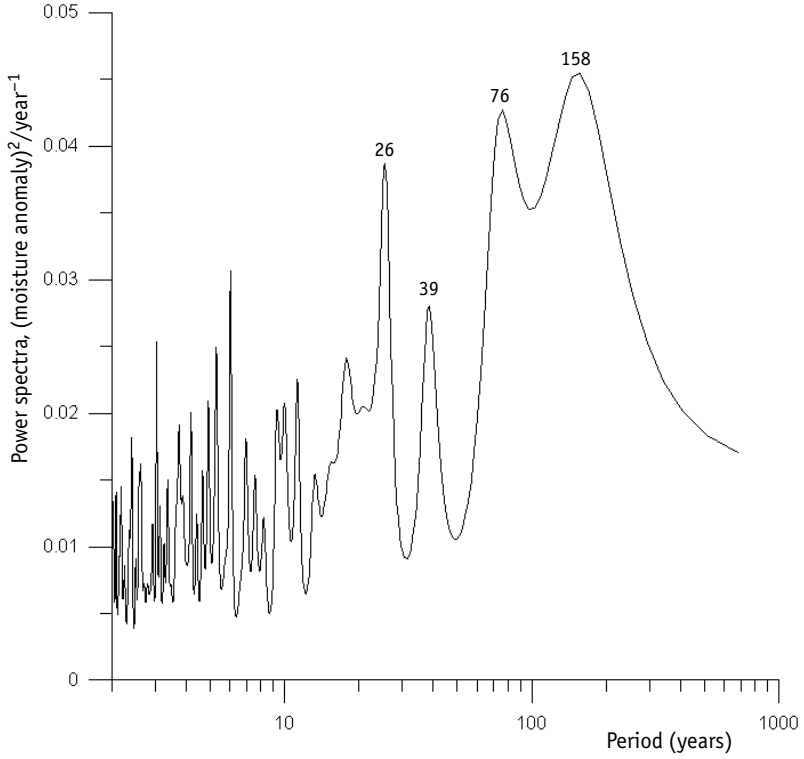

Fig. 1.12. Spectrum of periodical moisture fluctuations for 1500 years according to California bristlecone pine (*Pinus aristata*) tree growth rings (logarithmic X-axis). Ordinate — spectral intensity

Fig. 1.12 (http://www-personal.buseco. monash.edu.au/~hyndman/TSDL/ as well as http://www.ncdc.noaa. gov/paleo/treering.html).

Variations of the pine tree growth ring thickness depend on moisture content fluctuations reflecting droughts strength in the south of the North-American continent and, obliquely, fluctuations of the surface temperature of the entire Northern hemisphere. This known time series is the subject for detailed study, and its dynamics is similar to the 1500-year dendrochronology series of the North Scandinavian pine (*Pinus sylvestris L.)* tree and with the 10000-year series of bottom sediments from Lake Tingstede [Monin, Sonechkin, 2005].

Analysis of long-period time series spectra

Spectral analysis is used for detecting the most frequently repeating (predominant) periodical fluctuations of any index, for example, temperature or fish population abundance.

Relatively «high-frequency» regions of the spectra reflecting temperature fluctuations shorter than 20 years are not sufficient for detecting processes of «climatic» duration. Of the greatest interest for our ecologically significant estimation of climatic processes periodicity is the range of 20 to 100 years. Fig. 1.13 shows curves of predominant periodicities in the range of 20 to 100 years.

The spectrum of Greenland ice core samples (Fig. 1.13,*a*) shows predominance of a 54-year periodicity, the 32-year peak is less intensive. Spectrum of Arctic pine tree shows predominance of the 60-year peak, whereas the 32-year peak is lower (Fig. 1.13,*b*). The spectrum of California bristlecone pine (Fig. 1.13,*c*) shows predominance of the 76-year peak, whereas 26- and 39-year peaks are less intensive. These are somewhat longer than the periodicities obtained for ice core samples and Arctic pine tree. At the same time, the full time series of California bristelcone pine tree growth rings is about 8000 years, and that gives a possibility to track changes in periodicity of temperature fluctuations. Results of the spectral analysis of the entire 8000-year series shows predominance of the 55.4-year peak (Fig. 1.13,*d*). This spectral peak corresponds to predominant peaks (54 years) in the spectrum of ice core samples and is close to the 60-year periodicity for the spectrum of Arctic pine tree growth rings (Fig. 1.13,*b*).

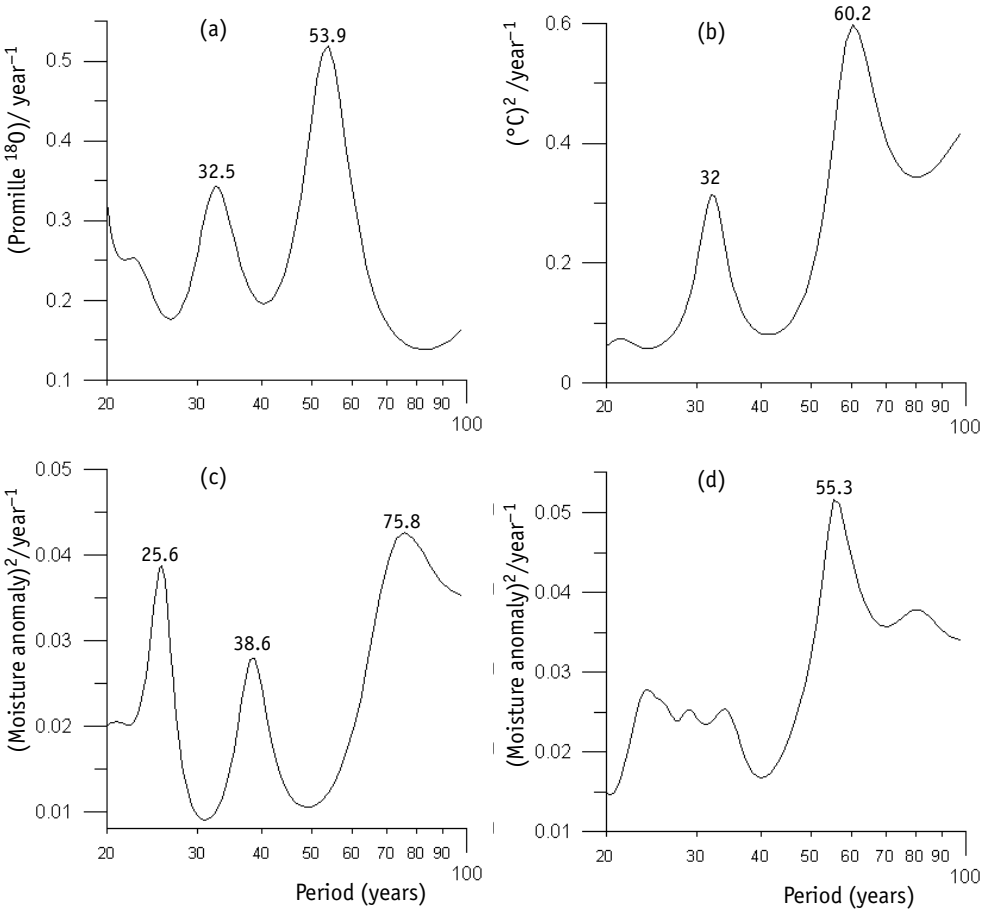

Fig. 1.13. Spectral density of the climatic periodicity maxima over the time range of 20–100 years: *a* — Greenland ice core samples, *b* — Arctic pine tree growth rings, *c* — California bristlecone pine tree growth rings, *d* — California bristlecone pine tree growth rings for the last 8000 years (logarithmic X-axis)

Fluctuations in populations of sardine and anchovy according to the data of fish scales analysis in bottom sediment layers of California upwelling

In recent decades data have been gathered that allow observation of fluctuations in sardines and anchovy populations during the recent 2000 years the in California coastal upwelling zone.

In anoxic basins of Pacific Ocean seabeds, particularly in the region of Southern California Bight upwelling, region fish scales residues are accumulated from the most abundant species, sardine (*Sardinops caerulea*) and anchovy (*Engraulis mordax*), observed in this region. No decomposition of organic residues (fish scales, in particular) happens due to stable anaerobic mode in these sediment basins.

Bottom sediment bore samples from this region demonstrate clear layered structure many meters deep. The lamina-based analysis of sardine and anchovy scales in the samples of sediments allowed reconstruction of population fluctuations for these species for 1700 years [Baumgartner et al., 1992]. Dynamics of reconstructed fluctuations of sardine and anchovy biomasses from this work are shown in Fig. 1.14.

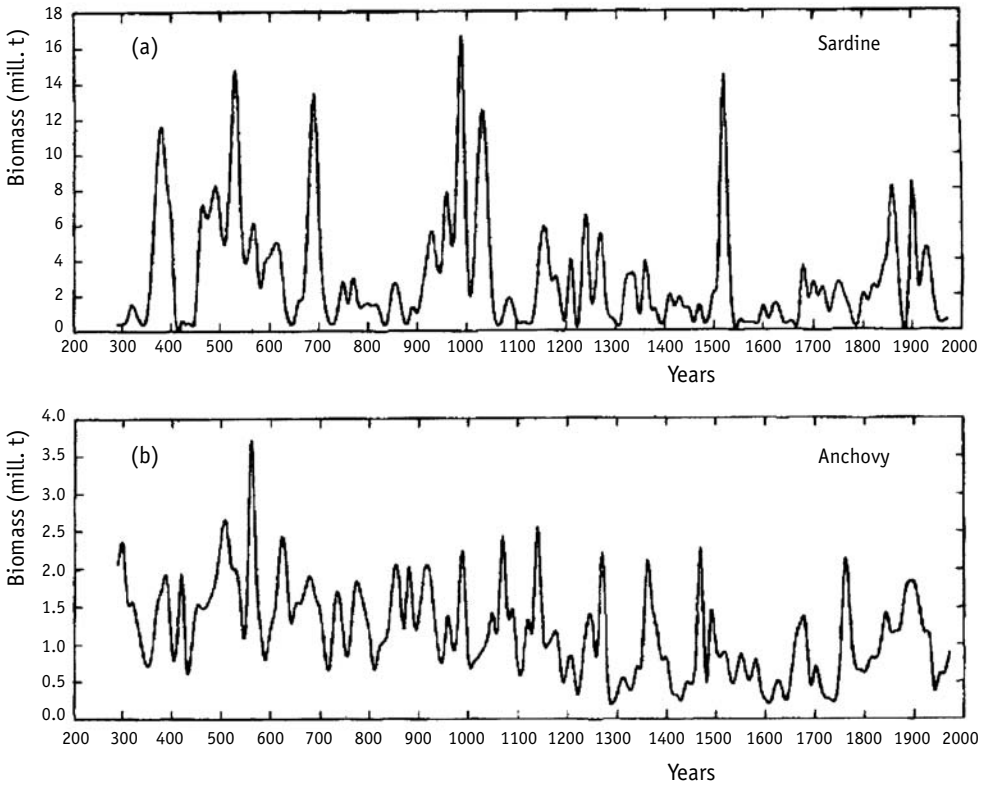

Fig. 1.14. Biomass fluctuations of (*a*) Californian sardine (*Sardinops cearulea*) and (*b*) anchovy (*Engraulis mordax*) reconstructed by the scale deposition in the sediment cores. Data from Baumgartner et al., 1992

Fig. 1.14 shows that within the 1700-year series the populations of both species fluctuated significantly: outbursts of the populations were followed by changes with periods of their almost complete disappearance. These fluctuations happened exclusively under the effect of natural (climatic) factors, i.e., without any effect of any fishery. Typically, modern fluctuations of sardine and anchovy populations in the 20th century, when they were intensively fished , demonstrated practically the same periods and amplitudes compared with the natural fluctuations during the last 2000 years [Baumgartner et al., 1992].

Fluctuation spectra of California sardine and anchovy populations during the recent 1700 years (Fig. 1.15) demonstrate well defined predominant peaks: 57 and 76 years for sardine and 57, 72, and 99 year for anchovy. This correlates well with the predominant spectra of climatic fluctuations during the last 1500 years according to ice core samples and tree growth rings.

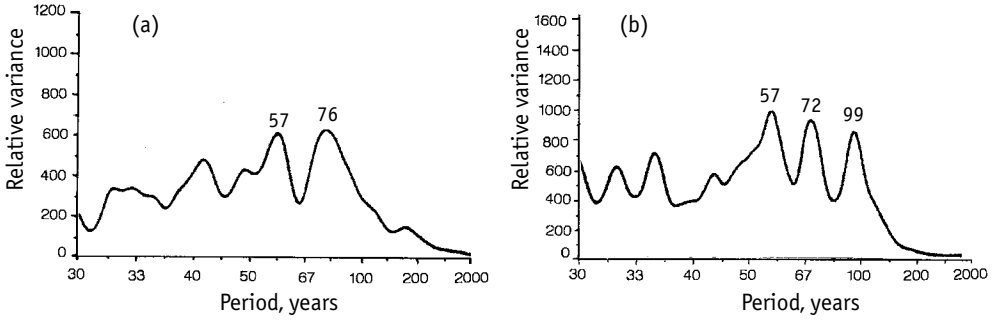

Fig. 1.15. Periodicity spectra of biomass fluctuation for (*a*) California sardine (*Sardinops cearulea*) and (*b*) anchovy (*Engraulis mordax*) reconstructed by the fish scale deposition in the sediment cores. Data from Baumgartner et al., 1992, slightly modified

Analysis of reconstructed and experimental spectra

To compare with the results of long time series analysis, the data of spectral analysis of relatively short series of Global dT from instrumental measurements and Atmospheric Circulation Index (ACI) (Vangenheim-Girs reference here!) with the predominant periodicity of 55 and 50 years, respectively, are shown in Fig. 1.16.

Table 1 presents general distribution of predominant periodicities of the above-considered time series.

Data in the Table shows that predominant periodicities for climatic and fish populations series correlate well, falling within the range of 54 to 76 years with the general average of 59.2 years. Data for California bristlecone pine

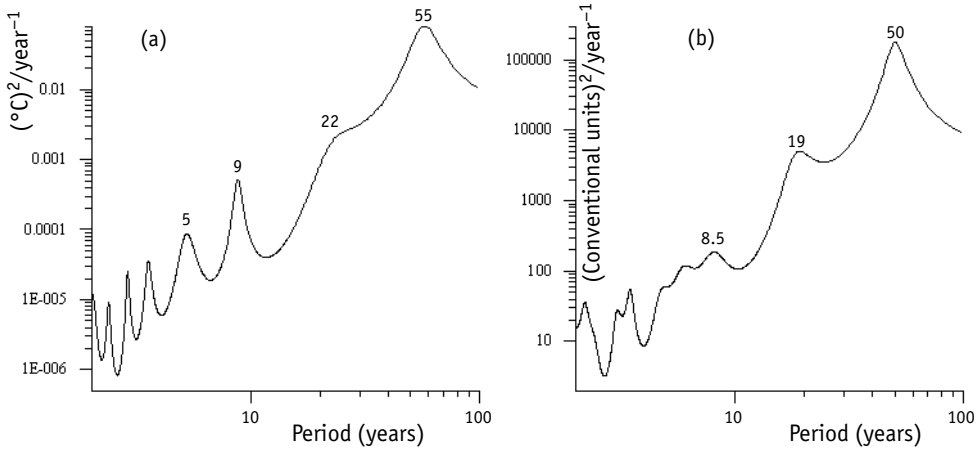

Fig. 1.16. Time series spectra of Global dT (*a*) for 140 years (instrumental measurements) and Atmospheric Circulation Index (ACI) (*b*) for 110 years (logarithmic X-axis, years)

Table 1. **Predominant periods of climatic fluctuations within the range of 20–100 years according to all data available**

Time series	Series length, years	Predominant peak, years	Secondary maxima, years
Ice core samples	1420 (552–1973)	54	32
Arctic pine tree	1480 (500–1980)	60	32
California bristlecone pine tree	1500 (479–1979)	76	32
California bristlecone pine tree	8000 (–6000–1979)	55.4	20–35
Sardine (sediment core samples)	1730 (270–1970)	57 and 76	56, 33
Anchovy (sediment core samples)	1730 (270–1970)	57	72, 99
Global dT	140 (1861–2001)	55	18.0
Atmospheric Circulation Index (ACI)	110 (1891–2001)	50	19.0

tree are slightly different from the general average, although a 55-year periodicity is definietely detected at the analysis of the 8000-year time series.

The most reliable data on long-period dynamics of the mean annual temperature are given by analysis of isotope ^{18}O content in Greenland ice core samples. Results shown in the Table show that for the last 1500 years the predominant periodicities of climate and biota fluctuations were around the 60-year average. Higher frequency (13–23 year) fluctuations are also of interest, however, reliable relationships between them and broad scale fish populations fluctuations cannot be detected.

The data obtained characterize the periodicity spectrum for each entire 1500-year series. However, understanding of the long-period climate fluctuations requires the knowledge how these predominant periodicities are distributed in time for the last millennia. These data may be obtained with the help Time-Frequency spectral Analysis (TFA).

TIME-FREQUENCY SPECTRAL ANALYSIS OF LONG-PERIOD CLIMATIC SERIES

Fig. 1.17 (see tinted insert) shows 3D relief diagrams of common logarithm development for intensities of the three long-term climatic time series. They are composed as follows. The time window of 600 counts (600 years) is shifted along the time series from the left to the right with 50-year time steps; for each location of the time window an intensity spectrum for the time series fragment, that occurred in each window, was estimated. The estimation was performed by the maximal entropy method with autoregression order 60. Thus, a dependence of the intensity spectrum estimation on two parameters was obtained: the frequency, as usual, and the time window location. This dependence may be visualized shaped as a 3D «mountain relief», where the ordinate is frequency and the abscissa is the right end of the time window location, and «by height» the common logarithm of the intensity spectrum is measured. The data are visualized by popular graphic software Surfer.

Diagrams of this type allow illustration of time-dependence of a selection of climatic series periodicities, shaped as 3D color pictures resembling landscapes of mountain chains aligned along the time scale (by abscissa). The height of «ridges» is defined by manifestation intensity e.g. by frequency of this periodicity, in accordance with the scale of periods (by the ordinate).

Moreover, the intensity of periodicity occurrence is demonstrated by colors: low intensity is blue through green to yellow, and high is from orange to red. White «peak tops» mark the highest frequency of this periodicity, for instance, 18.5-year periodicity (Fig. 1.17,*a*) or a maximum of 60–70-year periodicity (Fig. 1.17,*b*) at the end of the 20th century.

Tracking the height of «ridges» with time in Fig. 1.17, one may imagine how the intensity of one or another periodicity has been changing during the last 1000 years. The use of 3D diagrams provides a clear view that climatic fluctuations are cyclic, but the intensity of climatic cycles undergo significant changes with time.

Fig. 1.17,*a* shows, how the intensity of periodical temperature fluctuations (change their periodicity) with time from analysis of Greenland ice core samples. It is clearly observed that maxima of cyclic temperature fluctuations are distributed irregularly in time. The periodicity of 160 years is well expressed from the early 1200s until the late 1300s, and then disappeared. The 33-year periodicity is observed only between 1300s and 1700s, and then practically disappears, too. On the contrary, intensity of the 55-year periodicity continuously increased from 1500s and reached the maximum at the late 1990s.

Fig. 1.17,*b* shows time dynamics of the temperature periodicity, determined by the growth rings of Arctic pine tree from the North Sweden. It is clear that in the recent millennium 60–70 years was the predominant periodicity of temperature fluctuations. Its intensity was not so high in the period of 1750s until 1800s, but increased by the end of 1900s.

Fig. 1.17,*c* illustrates temporal dynamics of moisture/aridty fluctuations for California bristlecone pine tree data. Intensity of the mostly expressed periodicity of 65–75 years gradually increased from 1100s to their maximum at 1600s and is preserved at the level until the end of 1900s. The 25–27-year periodicity is observed only since the middle 1500s, and then its intensity gradually increased by the end of the 20th century. Periodicities of 18.5 and 12.5 years are detected only in the recent 300 years.

Note also that the data on the growth rings of trees characterize only summer moisture and related temperatures. The most reliable data on the mean-annual temperature are given by the analysis of heavy isotope ^{18}O content in Greenland ice core samples.

As observed from the plots, 55–70-year periodicity is expressed much more strongly relative to other periodicities. Hence, 55–70-year and other temperature periodicities are distributed irregularly in time for the entire

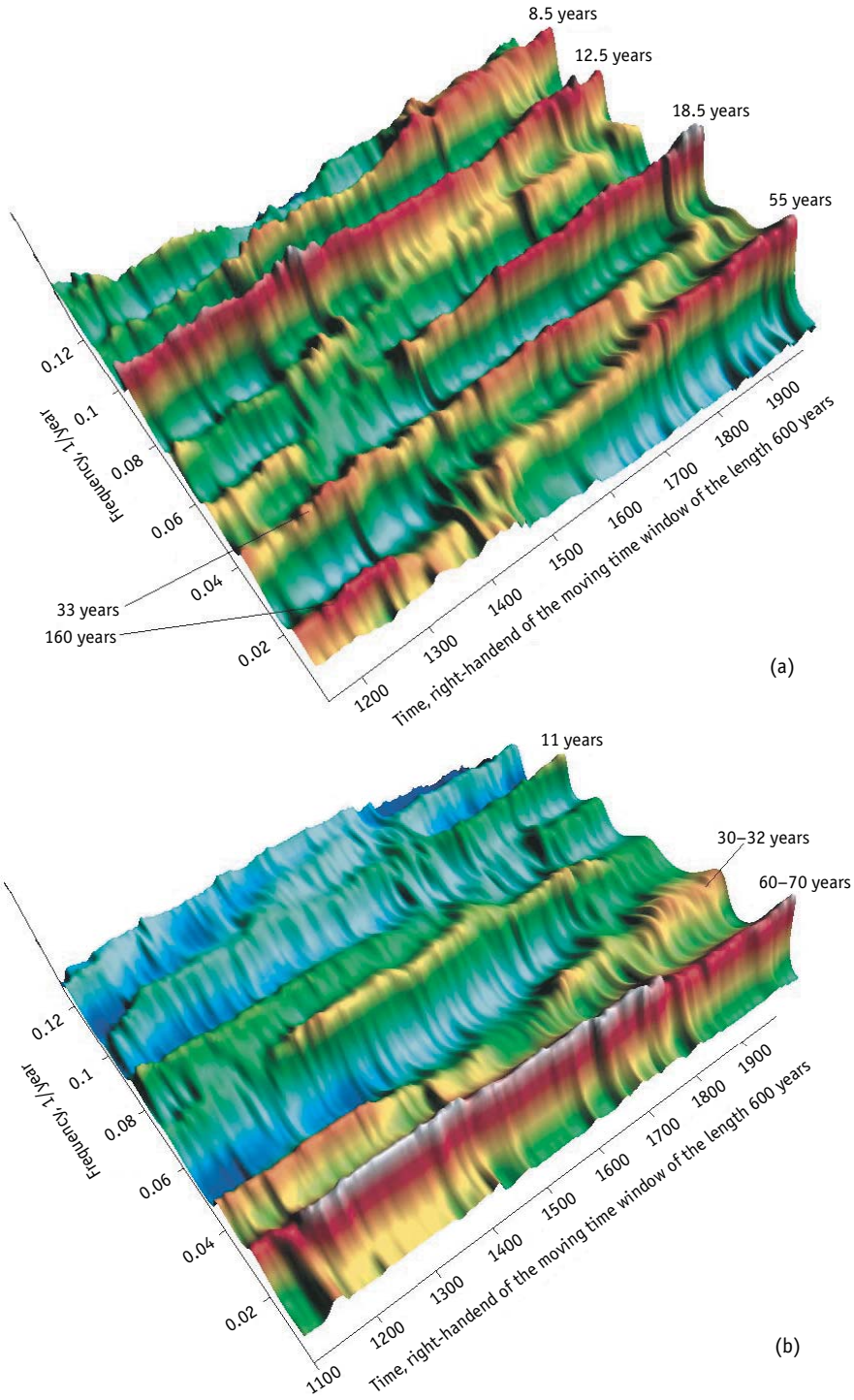
8.5 years
12.5 years
18.5 years
55 years
33 years
160 years
0.12
0.1
0.08
0.06
0.04
0.02
Frequency, 1/year
1200
1300
1400
1500
1600
1700
1800
1900
Time, right-handend of the moving time window of the length 600 years
(a)
11 years
30–32 years
60–70 years
0.12
0.1
0.08
0.06
0.04
0.02
Frequency, 1/year
1100
1200
1300
1400
1500
1600
1700
1800
1900
Time, right-handend of the moving time window of the length 600 years
(b)

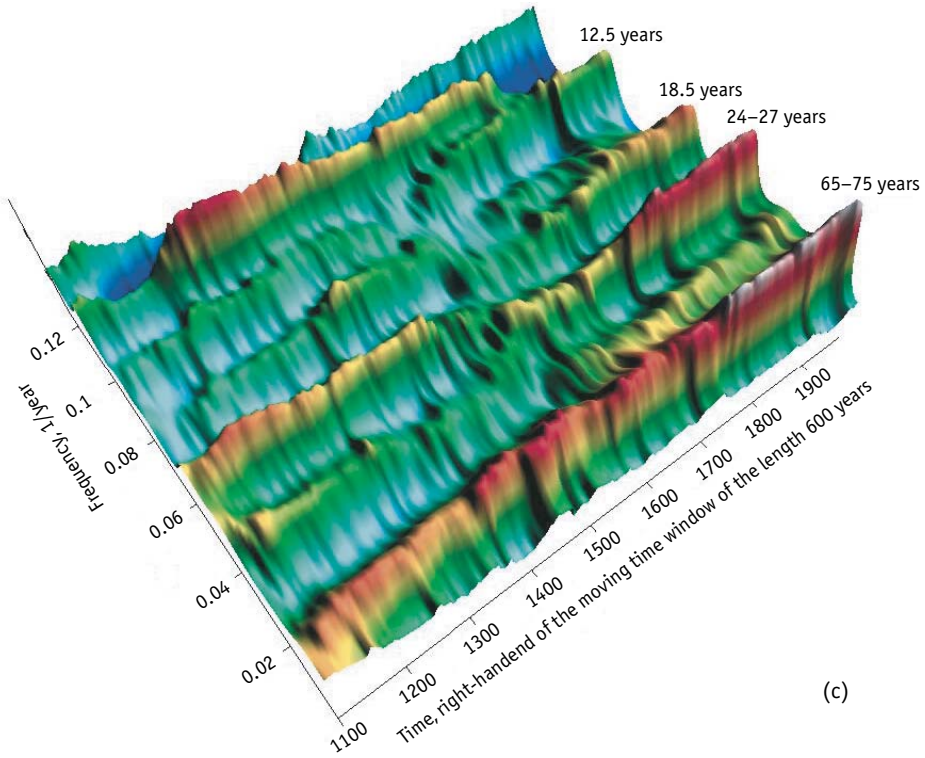

Fig. 1.17. Periodical temperature and humidity/aridity fluctuations intensity for 1500 years as analysed by: (*a*) Greenland ice core samples, (*b*) Arctic pine tree growth rings, and (*c*) California bristlecone pine tree growth rings (humidity / aridity). Left axis is frequency per year corresponded to the period of years: 0.02 — 50, 0.04 — 25, 0.06 — 16.6, 0.08 — 12.5, 0.1 — 10, and 0.12 — 8.3, respectively

1500-year time series. Typical feature of the 55–70-year periodicity is its intensity growth during the last 600–1000 years with a maximum at the end of the 20th century.

Although basic low-frequency peaks on the intensity spectrum correspond to 50–70 year periods, nevertheless, as observed from temperature reconstruction from Greenland ice core samples, longer periods of 100–200 years may exist.

Plots in Fig. 1.17 show that some periodical components occur, exist and then disappear, to reappear again having different predominant periods. There were also time intervals, when no clear monochromatic low-frequency components have existed. These time intervals may be defined as showing «low-frequency chaos».

This proper classification of climatic time series behavior may relate to the existence of time intervals with low and high predictability of the climate, see Chapter 7 for details. Here we specifically want to note that the existence of strong monochromatic components in the signal variations allows sharp increase of both efficiency and «hitting range» of the time series prediction due to the use of cyclical trends with the period of that monochromatic component (periodicity), which is predominant in the current period of time. If there were no predominant monochromatic components, this scheme of prediction is not valid, so we would then have to cope by using the usual prediction methods basied on correlations of neighboring values in the time series, which may be effective for 1–2 steps only e.g. the possibility of long-term prediction simply disappear.

In the context of such separation of the climate history into intervals of low and high predictability, it is of interest to overlook the evolution of intensity spectrum in the low-frequency range. The 8000-year time series of California bristlecone pine tree growth rings provides an opportunity to consider the change of intensity in the long-term climatic periodicities within a longer time period.

We have analyzed variability of the intensity spectrum for California bristlecone pine tree growth rings for 8000 years in the periodicity range of 40 to 200 years in a sliding time window 600 years long. For each location of this time window in the selected range a maximum of intensity spectrum logarithm was detected. The results are shown in Figs. 1.18 .

As observed from Fig. 1.18 plots, periodicity of low-frequency cycles varies significantly with time in the periods of 2000 to 1500 years. At the minimal level, periodicity of these cycles is sustained during 500–1000 years until the next period of growth, whereas at the maximal level it is maintained for only 200–500 years. Maxima on the curve correspond to time intervals of high potential predictability, and minima correspond to the periods of low predictability. However, this predictability is just potential; to make it real, we must make sure that the maximum value on this plot corresponds to occurrence of a signal localized by frequency (narrow band) rather than to steady increase of the intensity spectrum in the entire low-frequency range. In this case, prediction using a local cyclic trend can be applied.

For more accurate assessment of values of this increasing periodicity one has refer to TFA plots in Fig. 1.17. As all the plots clearly show, for the last 1000 years the periodicity of 50–70 years was predominant, and its recur-

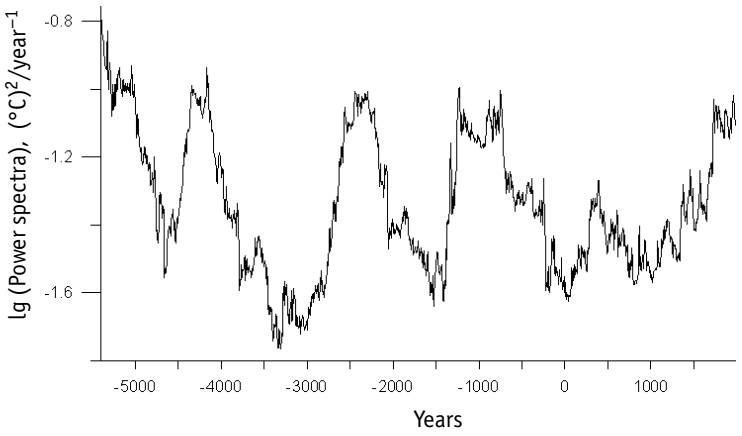

Fig. 1.18. Intensity spectrum variation for temperature (humidity/aridity) fluctuations, obtained from California bristlecone pine tree growth rings, in the frequency range of 0.025 to 0.005 year^{-1} (40–200 years) in the moving 600-year time window. Y-axis is intensity spectrum logarithm; X-axis is years at right end of the time window

rence steadily increased. As a consequence, for the long-period prediction of the climate fluctuations (for several decades ahead) it is reasonable to use the estimate of this cyclic trend (see Chapters 7 and 8).

Thus, by the end of the 20th century recurrence of the 50–70-year periodicity reached its regular maximum and will likely be sustained at this level, at least over the following century. This increases the reliability of perspective forecasts of long-period climate and biota dynamics.

Climate periodicity of about 50–70 years has been detected by various authors. Spectral analysis of temperature variability series in North America and Europe for the last 1000 years indicated predominance of cyclic temperature fluctuations within the range of 60 to 80 years and at 120 years [Shabalova, Weber, 1999]. In the work by Schlesinger and Ramankutty [Schlesinger, Ramankutty, 1994] predominance of 65–70-year periodicity of the global climate was demonstrated. Spectral analysis of the long-period dynamics of the ocean surface temperature and atmospheric pressure in North Pacific water area [Minobe, 1997, 1999, 2000] during the last century demonstrated predominant 50–70-year (and additional 20–30-year) periodicity of climatic indices PDO and ALPI. Similar data on the 50–70-year periodicity of ocean surface temperature fluctuations (PDO index) were obtained by Mantua and Hare [Mantua, Hare, 2002].

Comments in brief

Analysis of the three 1500-year long time series of reconstructed temperatures (and humidity/aridity) (Greenland, Scandinavia, California) indicate the predominant periodicity of climatic fluctuations during the last 1000 years equal about 60 years with the variation from 55 to 76 years. The second intensity spectral peak of periodicity occurs at 30–32 years. The existence of these climatic periodicities (50–70 and 30 years) is confirmed in by several authors [Schlesinger, Ramankutty, 1994; Minobe, 1997, 1999, 2000].

Temperature reconstruction by analyzing Greenland ice core samples for the last 1400 years characterize winter temperature, which practically determines fluctuations of the mean annual temperature. The predominant 55-year periodicity of the mean annual temperature detected by ice core samples is similar to periodicities of Global dT and ACI, instrumentally measured during the last 140 and 110 years, respectively.

For the last 1700 years, fluctuation periodicities of Californian sardine and anchovy populations approach climatic fluctuations falling within the range of 55–75 years. The intensity of 50–70-year periodicity have continuously increased during the last millenia and reached its maximum in the end of the 20^{th} century. Basing on the increasing dynamics of the 55–70-year periodicity intensity for the last 1000 years, it may be suggested that this periodicity will be preserved, at least over the next 100 years, and that likely increases reliability of the progressive prediction of the climate and biota dynamics in the current century.

CHAPTER 2

GLOBAL AND REGIONAL CLIMATE PERIODICITY

FEATURES OF ATMOSPHERIC CIRCULATION INDEX (ACI) DYNAMICS

Close affinity of zonal ACI and Global dT dynamics (see Chapter 1) indicates tight relationships between the planetary scaled fluctuations of atmospheric circulation and global temperature, and ACI may be a global climatic index. At the same time, significant differences between compared indices, ACI and Global dT, should be taken into account. The Global dT curve represents a series of anomalies, smoothed by moving averaging, and reflects real temperature fluctuations with time. In contrast, the ACI curve is the result of consequent summing of atmospheric transfer anomalies (AT anomalies), i.e. represents the curve of accumulated frequencies (cumulative sum values), the trend of which does not reflect the fact that real-time fluctuations of atmospheric transfer does occur simultaneously with the observed temperature fluctuations. To estimate the real connections between Global dT and ACI fluctuations, a curve of real-time anomalies of atmospheric transfer (AT anomalies) should be used rather than the integral (cumulative) ACI curve.

Fig. 2.1 shows dynamics of AT anomalies during the last century. Their high variability requires the smoothing of variations via moving averaging to determine the long-period trend of this index. Clearly, similar to ACI curve, the AT anomaly curve demonstrates quasi-periodical characteristics with the 50–60-year periodicity.

Real differences in dynamics of AT anomalies and zonal ACI during the last 100 years are shown in Fig. 2.2, where it is observed that the maxima

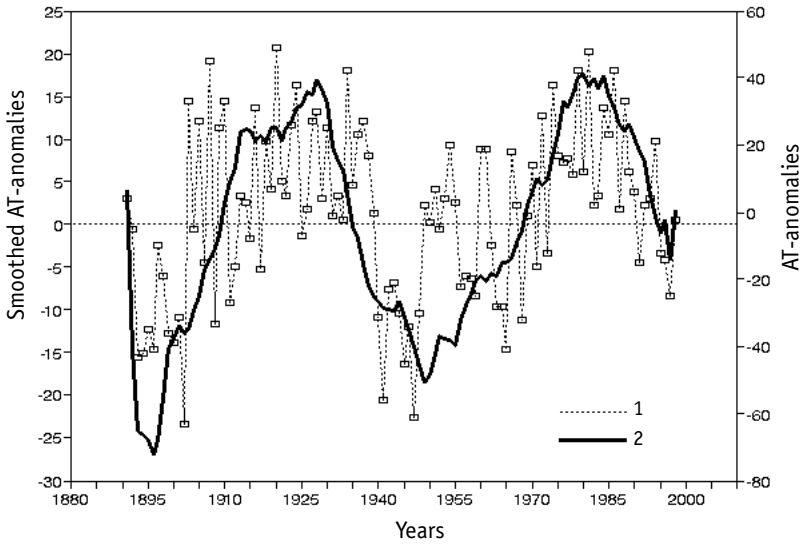

Fig. 2.1. Dynamics of the long-period variations of zonal atmospheric transfer anomalies (AT anomalies) for the period of 1891–2000: (*1*) average annual AT anomalies, (*2*) the same, with average annual anomaly values smoothed using 21-year moving averaging (see text for detail)

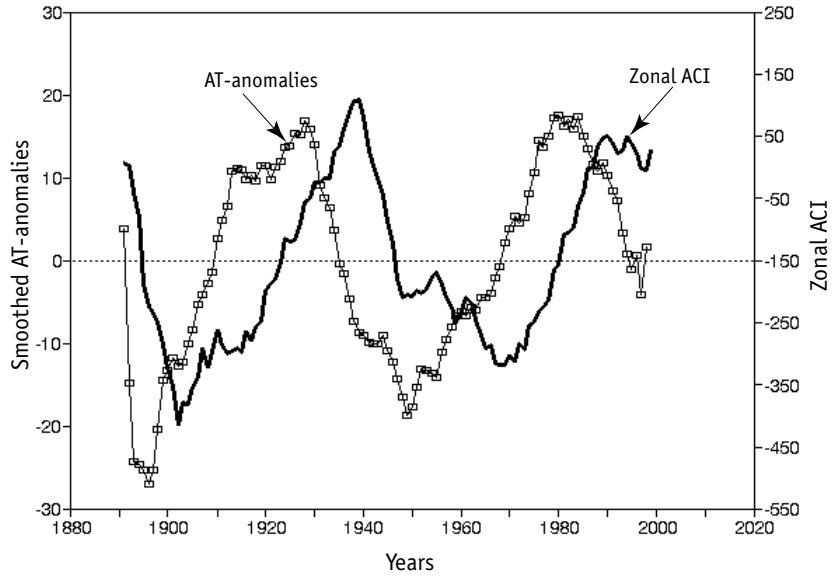

Fig. 2.2. Comparative long-period dynamics of zonal ACI (bold line) and smoothed AT anomalies (white squares) for the last century

of integral Vangenheim Girs (ACI) curve lag in relation to AT anomalies curve by 12–14 years.

As the AT anomalies curve is shifted ahead by 12 years (Fig. 2.3) it becomes almost coincident with the zonal ACI curve; hence, the correlation coefficient between these two indices increases from 0.06 to 0.9.

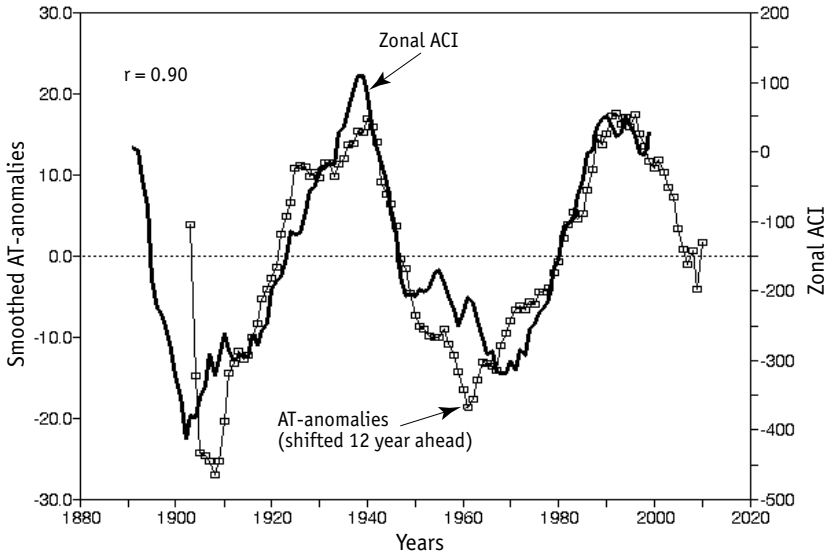

Fig. 2.3. Comparison dynamics of zonal ACI and smoothed AT anomalies shifted by 12 years ahead (to the right)

Of the highest interest is comparison of AT anomalies and Global dT trends, because this may illustrate a relationship between atmospheric circulation and temperature changes (Fig. 2.4). The curves have similar shape, but Global dT fluctuations lag by 16–20 years compared with AT anomalies. The AT anomalies curve shift by 18 years ahead leads to almost complete coincidence of both curves trends (Fig. 2.5). Hence, the correlation coefficient for these two indices increases from 0.09 to 0.9.

The analytical results confirm the cyclic character of AT anomalies and Global dT fluctuations with the period about 60 years, well-observed in the plots, and thus indicate the possibility of predicting a harmonic process. Fig. 2.5 shows that at AT anomalies curve shifts, it's right branch extends into to the future allowing approximate projections about the Global dT trend for the future 15–20 years. Based on these facts one may suggest that in the nearest future Global dT increase will decelerate and by 2015 reduce its value approximately to about 0.15. It should be taken into account that

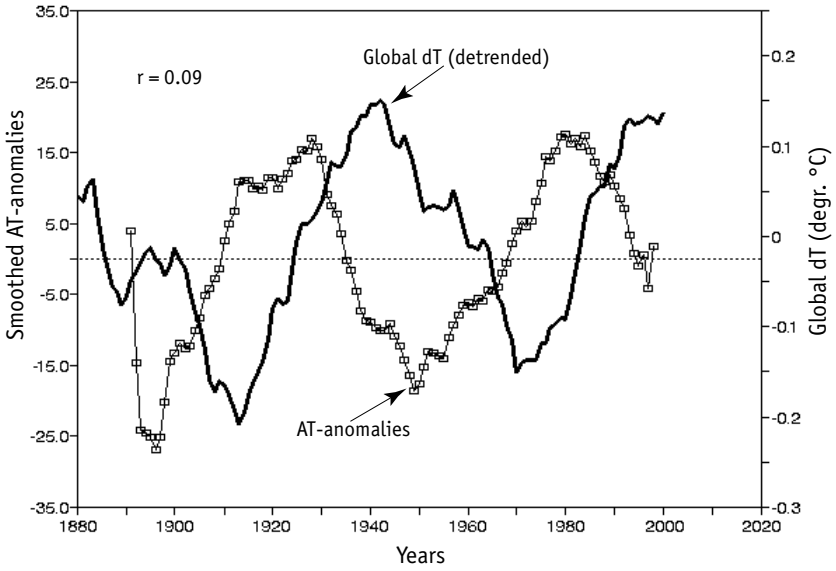

Fig. 2.4. Comparative dynamics of detrended Global dT (13-years smoothing, bold line) and zonal AT anomalies (21-year smoothing, white squares)

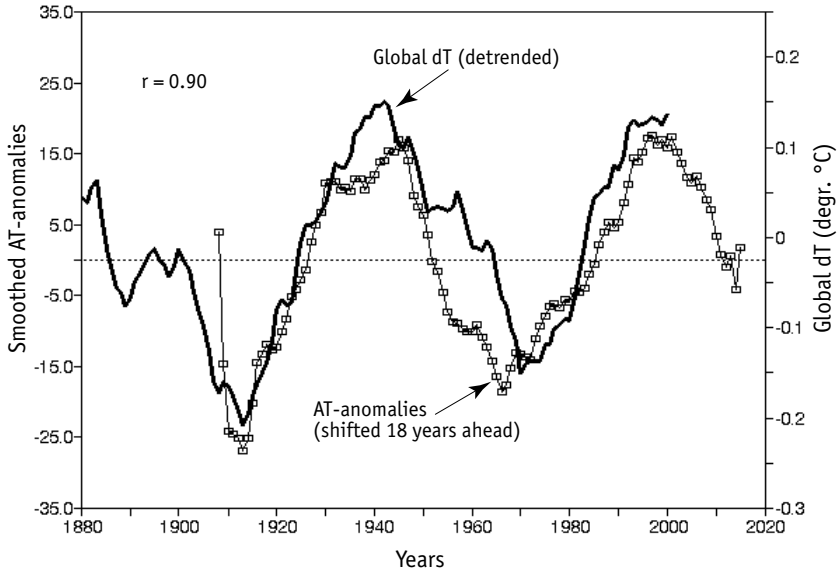

Fig. 2.5. The same as in Fig. 2.4, but with AT anomalies curve shifted by 18 years ahead (right)

Fig. 2.5 shows the detrended Global dT curve [Sonechkin, 1998]. If the increasing temperature trend is preserved, the expected decrease of Global dT by 2015 will be slightly lower, about 0.10. It is also quite clear that only a long-period temperature trend is projected rather than the values of significantly fluctuating mean annual temperatures.

Data on the long-period dynamics of AT anomalies were obtained for the Atlantic-Euro-Asian region and, in particular, the related Arctic region. Fig. 2.6 shows temperature anomaly trend in the zone from 60 to 85° N (Arctic dT) and AT anomalies curve trend, shifted forward 22 years. With respect to the shifting of the AT anomalies under the Arctic dT dynamics it can be seen that they are both are described by similar curves with approximately 60-year periodicity.

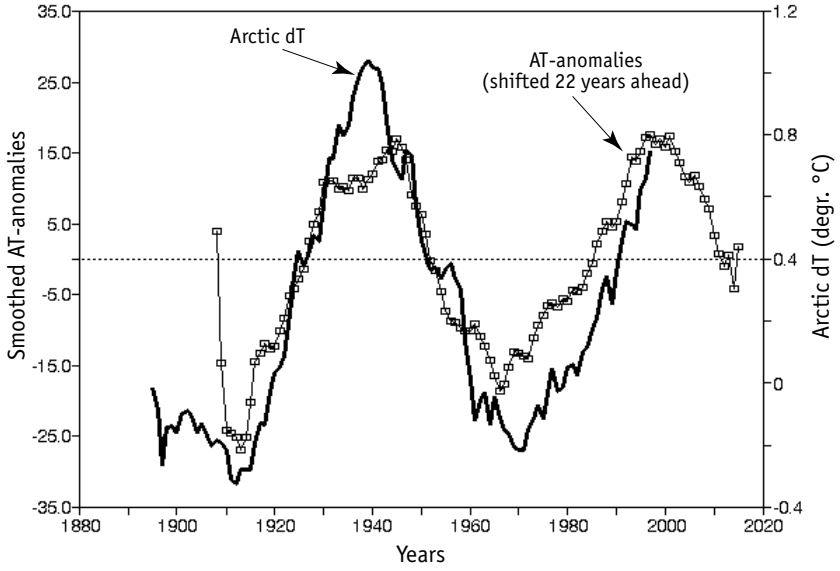

Fig. 2.6. Comparative dynamics of Arctic dT (13-years smoothing, bold line; data from Alexandrov et al. 2003) and zonal AT anomaly curve (white squares), shifted in time by 22 years ahead (to the right), (21-year smoothing)

Similarity in the shape of Global dT and AT anomalies curves also suggests that there is a relationship between changes in the atmospheric transfer and subsequent fluctuations of the global temperature, although the mechanism of this dependence in not clear yet. The ACI index may be used as a climatic index together with Global dT, Arctic dT, and indices characterizing atmospheric pressure fluctuations: ALPI and NPI.

Cyclic fluctuations of Balkhash lake volume

Balkhash lake is one of the larger lakes in the world, the volume of which during the last 120 years varied from 90 to 150 km^3. Similar to Aral Sea and Caspian Sea, the Balkhash watershed has no drain system, and about 80% of its water delivery is supplied by Ili river from mountain systems of Ala Tau and Tien Shan. The main delivery to this closed watershed system is supplied by snow and ice of highly located glaciers melting in summer [Abrosov, 1973].

The Ili river — Balkhash lake system represents a natural model of high mountain region water content fluctuations. Fig. 2.7 shows that long-period changes of Balkhash lake volume during the last 120 years are almost antiphase to Global dT (with the correlation coefficient r = 0.75) and demonstrates almost 60-year periodicity, which reflects fluctuations of the regional water content and Ili river flow.

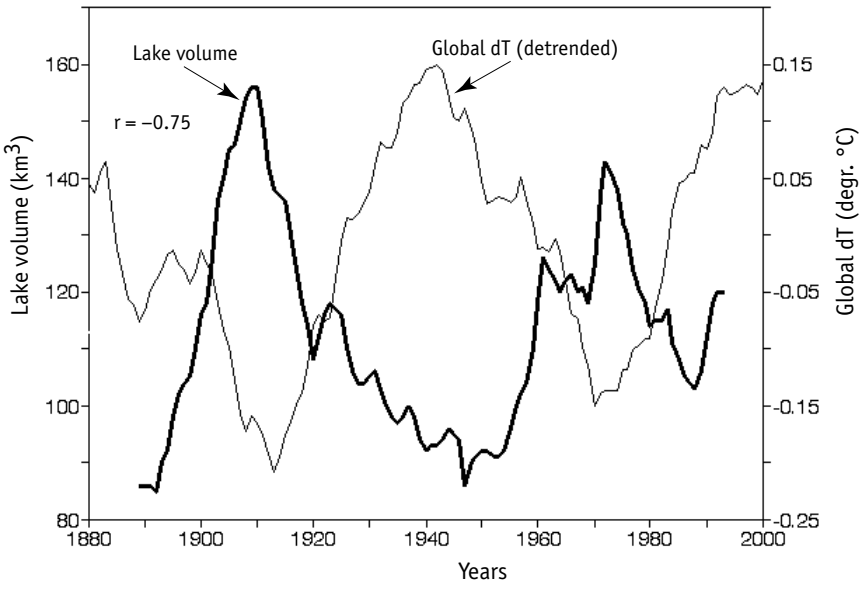

Fig. 2.7. Comparative dynamics of detrended Global dT (13-year smoothing) (thin line) and long-period fluctuations of Balkhash lake volume (bold line). Data from Shaporenko, 1993 with respect to Kapchagaisk reservoir filling, Ili river flow

Periodical increases of the lake volume are confined with in the so-called «cooling» periods, whereas diminution relate to periods of «warming». Cooling periods coincide with meridional ACI epochs. As compared dynamics

of Balkhash lake volume with meridional ACI trend (Fig. 2.8), a tight connection ($r = 0.75$) is observed. Slight delay of the lake volume fluctuations in relation to ACI trend can be observed. As the lake volume curve is shifted by 5 years to the future, the correlation coefficient increases to 0.82.

Based on alteration of approximately 30-year climatic warming and cooling epochs (see Chapter 1), one may suggest that in the following 10–15 years the reversal of the present warming epoch and predominance of zonal circulation will peak and reverse, similar to what was observed in 1940–1960s. Thus it may be expected that water content of the region and Balkhash lake volume will increase.

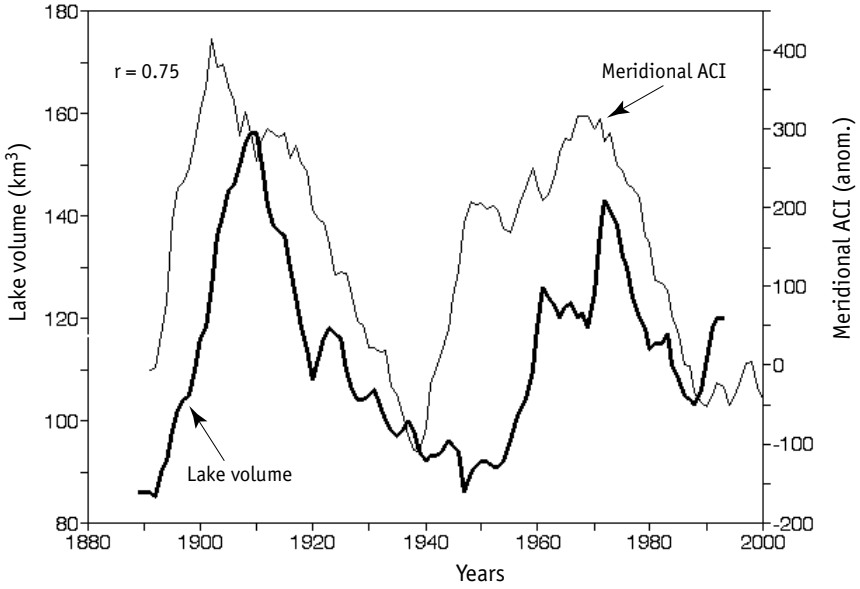

Fig. 2.8. Comparative dynamics of meridional ACI (13-year smoothing, thin line) and long-term fluctuations of Balkhash lake volume (bold line). Data from Shaporenko, 1993 with respect to Kapchagaisk reservoir filling, Ili river flow

Here we do not consider the direct fluctuation mechanisms of the high-mountain region water delivery and storage that provides drainage into Balkhash lake. The example of this large undrained lake clearly shows the role of longitudinal atmospheric transfer in the increase of the regional water flow and storage. Water to the lake inlet is delivered due to accumulation and subsequent melting of high-mountain glaciers. The records suggest that in cooling periods and at increasing meridional ACI periodicity the volume of high-mountain glaciers increases, whereas in the periods of warming and

zonal ACI predominance it decreases. Long-period fluctuations of Issyk Kul lake volume are similarly related to dynamics of the Tien Shan mountain system glaciers [Klige et al., 1998].

Aral Sea, another drainless water body, is fed by two large rivers whose flows depend the on high-mountain systems of Tien Shan and Pamir, may also be considered as an original analogue of the natural model of Balkhash lake. According to the Balkhash lake model, in the first 10–15 years of the 21st century one may suggest gradual increase of Amu-Daria and Syr-Daria flows and possible stabilization or even increase of the Aral Sea volume.

Cyclic nature of floods in Neva river estuary

The observations for maximal levels of Neva river, which cause floods in St.-Petersburg, were initiated more than 120 years ago [Pomeranets, 1999; Naidenov, Kozhevnikova, 2003]. The long-period dynamics of maximal levels of Neva river compared with Global dT trend are shown in Fig. 2.9. The smoothed curve of maximal Neva river levels for more than a hundred year period coincides with the detrended Global dT.

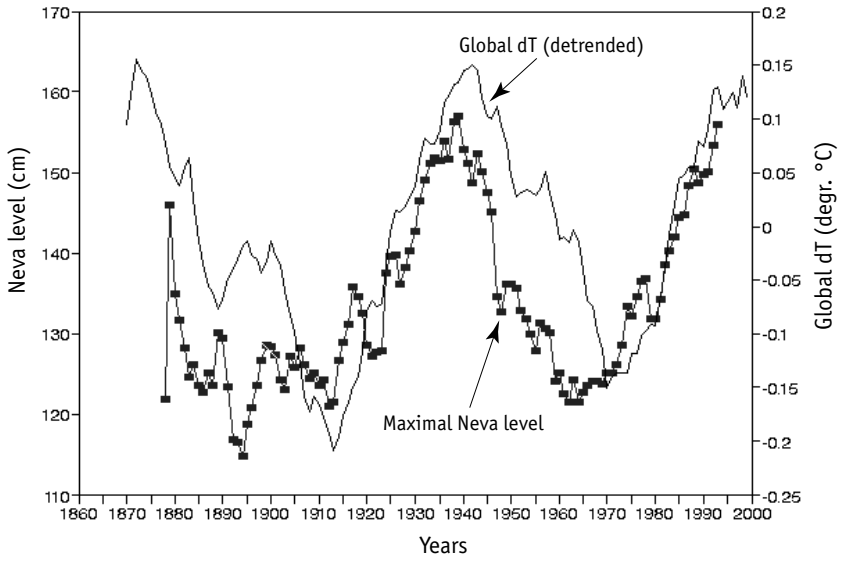

Fig. 2.9. Comparative dynamics of detrended Global dT (13-years smoothing, thin line) and maximum levels of Neva river (20-year smoothing, black squares). Data from Pomeranets [1999], Naidenov and Kozhevnikova [2003]

The comparison of maximal Neva river levels and Arctic dT dynamics (Fig. 2.10) shows their similarity and that both curves have no increasing secular trend.

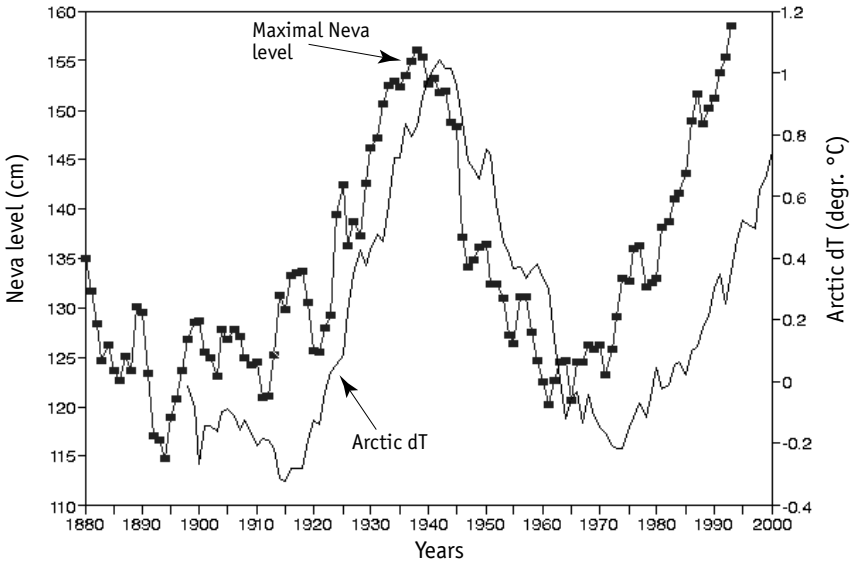

Fig. 2.10. Comparative dynamics of Arctic dT (13-years smoothing, thin line) and maximum water levels in Neva river (20-year smoothing, black squares). Data from Pomeranets [1999], Naidenov and Kozhevnikova [2003]

Fluctuations of the Neva river level are determined by atmospheric circulation features in the region. The motion of cyclones from North Baltic Sea to the south-west through the Gulf of Finland is accompanied by formation of a long wave pressure system, which enters the Neva estuary and produces surface winds that stave the river flow. The west wind accompanying the cyclone intensifies the level increase that leads to floods of various intensities up to catastrophic events [Pomeranets, 1993]. It is natural to suggest that ACI characterizing direction of air mass transfer in Atlantic region may be the long-term predictor of the conditions initiating floods (Fig. 2.11).

Fig. 2.11 shows close similarity of the curves of maximal levels and dynamics of zonal ACI. Maxima of both indices in the late 1930s and the late 1990s and minima in the late 1960s fully coincide. It is reasonable to state that that increase of zonal ACI periodicity characterizing predominance of the west-east air transfer increases probability of Neva river level rise. The belief of long-period cyclic dynamics of Global dT, Arctic dT and zonal ACI

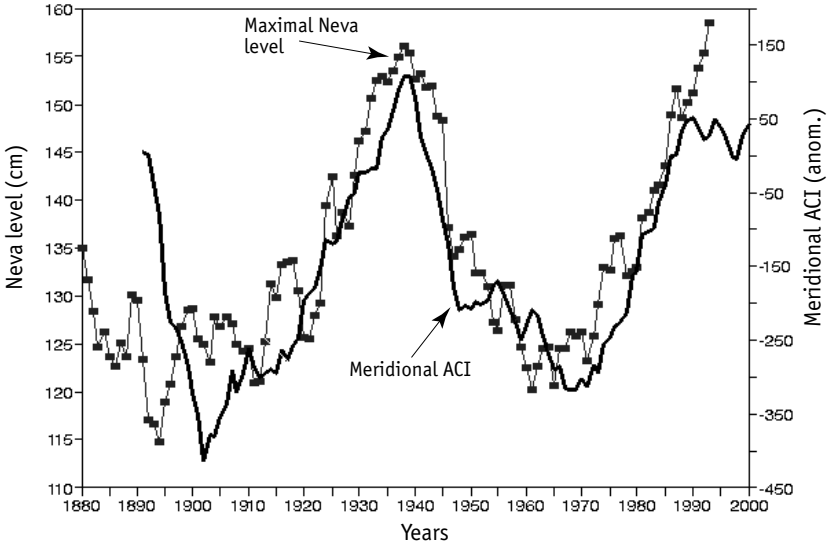

Fig. 2.11. Comparative dynamics of the fluctuations of zonal ACI (bold line) and maximum levels of Neva river (20-year smoothing, black squares). Data from Pomeranets [1999], Naidenov and Kozhevnikova [2003]

allows prediction of increasing (or decreasing) periods for the probability of catastrophic floods in St.-Petersburg.

Cyclic fluctuations of Oregon precipitation along the west coast of North America

At the west coast of the USA, in the Oregon state, observations for precipitation are available for over a century (Fig. 2.12). The long-period fluctuations of precipitation and Global dT are antiphase with approximate 60-year periodicity. The increase of precipitation occurs in the periods of cooling, whereas they decrease in the periods of warming.

The comparison of annual precipitation dynamics and longitudinal ACI for the 105-year period (Fig. 2.13) demonstrates complete coincidence of their curves. The data on dynamics of precipitation along the coast of Oregon state for the period of 1896–2001 again demonstrate approximately 60-year periodicity of global and regional climatic indices (detrended Global dT, Arctic dT, zonal and meridional ACI), but shows no secular increasing trend typical of Global dT.

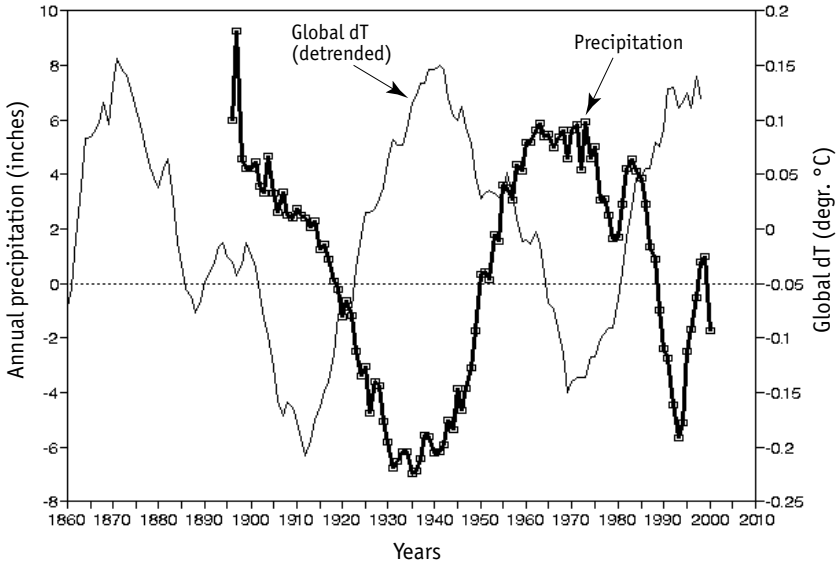

Fig. 2.12. Comparison of annual precipitation on the coast of Oregon (19-year smoothing, bold line) with detrended Global dT (13-years smoothing, thin line). Data from Taylor and Southards, 2002

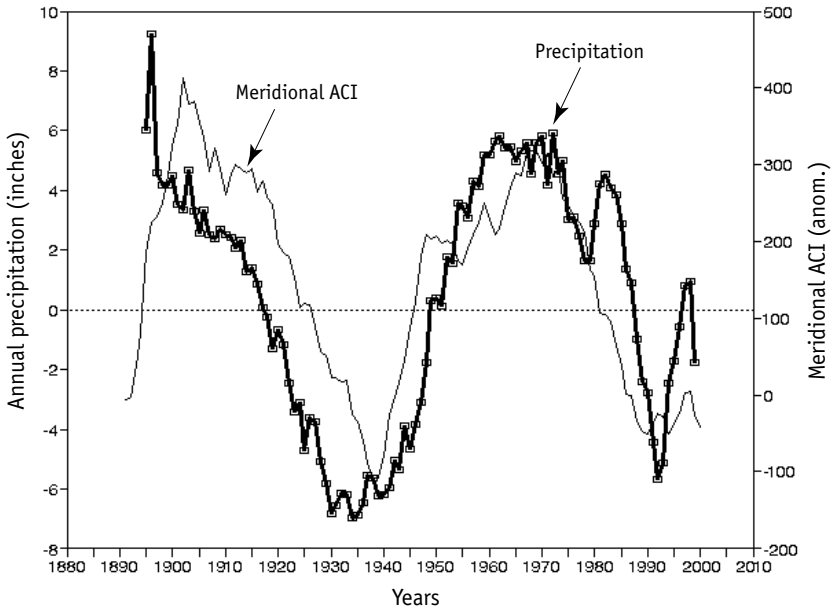

Fig. 2.13. Comparison of annual precipitation along the coast of Oregon state (19-year smoothing, bold line) and meridional ACI (thin line)

As the above examples show, the long-term fluctuations of Balkhash lake volume, flooding intensity in Neva river estuary, annual precipitation in Oregon state, and Atmospheric Circulation Index (ACI) occur simultaneously and demonstrate approximately 60-year periodicity. It may be suggested that simultaneity of the phenomena observed in different regions of the planet reflects generic global changes of atmospheric circulation and temperature. It is also typical that the above-considered curves of water regime, precipitation and atmospheric circulation fluctuations (including AT anomalies) have no increasing secular trend typical of Global dT.

Cyclic fluctuations of Barents Sea and Sea of Okhotsk ice cover

The time series of observations for the mean annual ice cover of Barents Sea (percent of the water area covered by ice) lasts almost a hundred years [Averkiev et al., 1997] that allows comparison of this index dynamics with Global dT. Instead of «ice cover», we will use the opposite value, called «water area free of ice» (ice-free water area). Fig. 2.14 shows that ice-free water area dynamics experiences long-term fluctuations and is close to Global dT, but delayed by a decade. Moreover, similar to Global dT, dynamics of water area free of ice demonstrates increasing secular linear trend (about 15% per century).

To compare multiyear fluctuations of the water area free of ice and Global dT, both detrended curves are shown in Fig. 2.15. Clearly, ice-free area dynamics is of about 60-year periodicity and virtually reproduces Global dT shape, delayed by almost a decade. This indicates inertia of the ice cover fluctuation. This process reflects a multiyear dynamics of heat accumulation and reduction by water masses. Shifting of the ice-free water area backward by 8 years back (Fig. 2.16) leads to its virtual coincidence with Global dT curve.

The long-term ice cover trend represents something like a chronicle of climatic fluctuations reflecting delivery of warm Atlantic waters to the region and Global dT fluctuations. The ice coverage of Barents Sea is one of the important indices for natural environmental condition dynamics in the region. The ice-free water area fluctuations are significant for the seasonal cycle of phyto- and zooplankton development, and for survival and growth of the

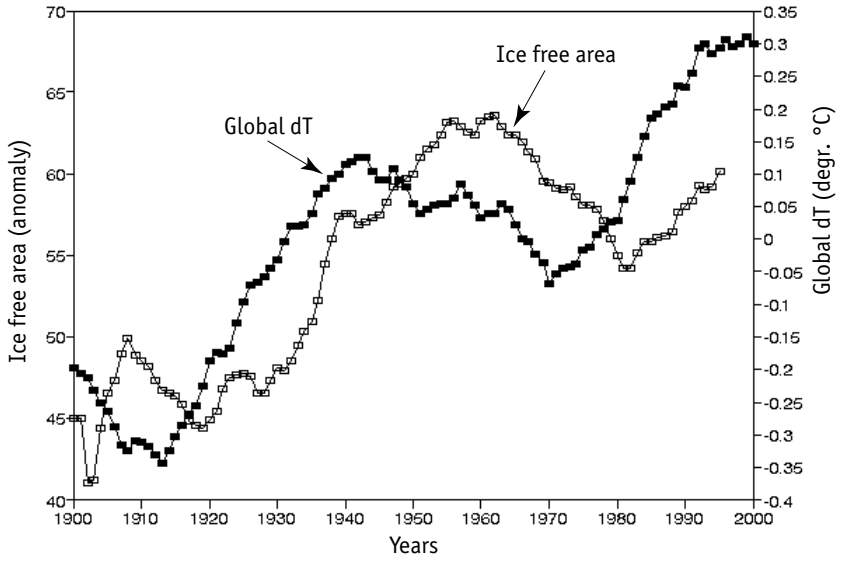

Fig. 2.14. Comparative dynamics of water area of Barents Sea free from ice (20-year smoothing, white squares) and Global dT (13-years smoothing, black squares). Data from Averkiev et al. 1997

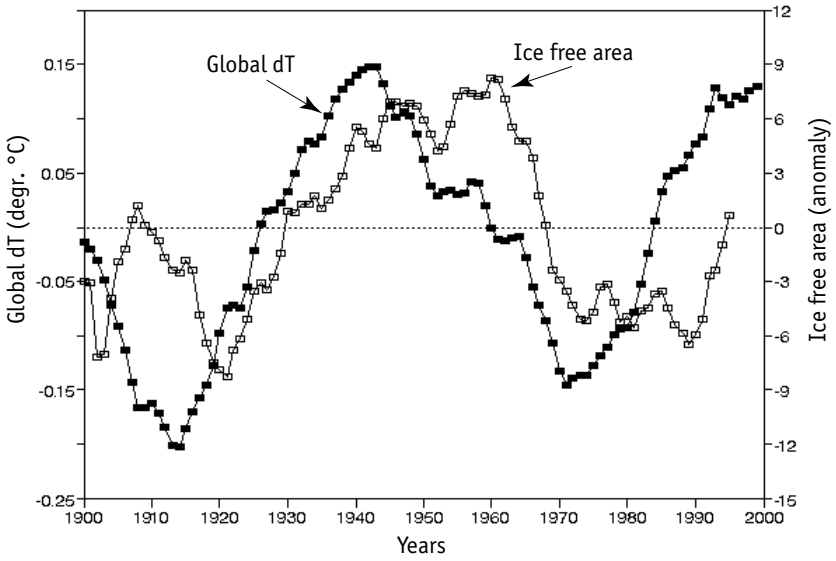

Fig. 2.15. Comparative dynamics of detrended Global dT (13-year moving averaging, dark squares) and detrended ice-free water area in Barents Sea (20-year smoothing, white squares)

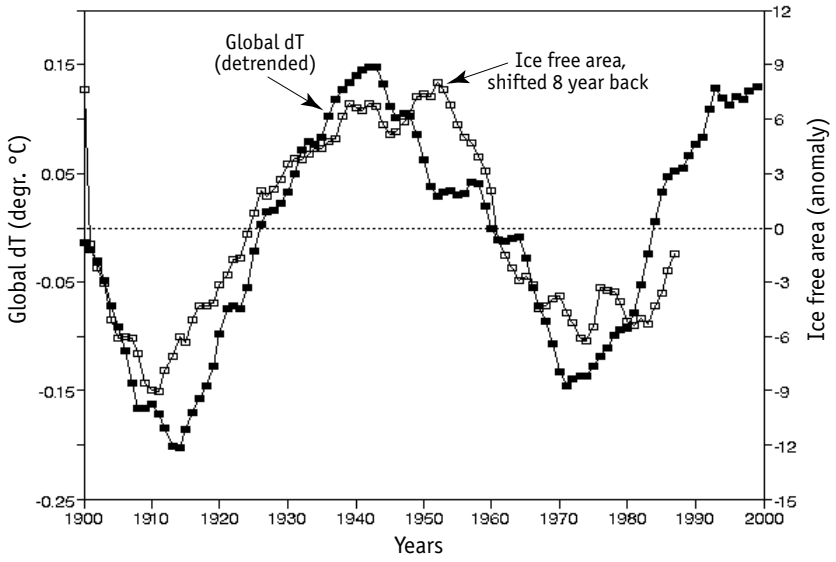

Fig. 2.16. The same as in Fig. 2.15 with the curve of ice-free water area shifted backward (left) by 8 years

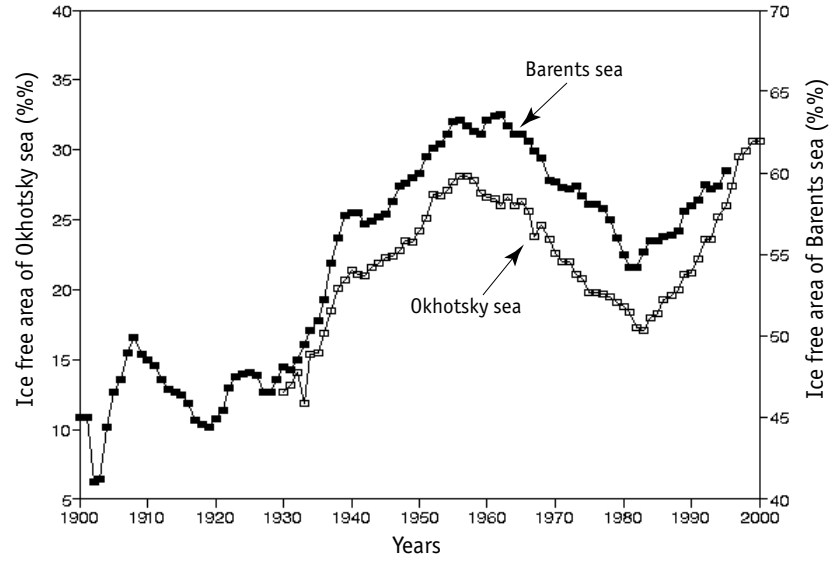

Fig. 2.17. Comparative dynamics for ice-free water areas in Barents Sea (dark squares) and Sea of Okhotsk (white squares) (20-years smoothing averaging). Sea of Okhotsk — data from Ustinova et al., 2002

fry of codfish, herring and other fish species. Approximately 60-year fluctuations of the ice coverage and the main climatic index, Global dT, are closely related and may serve for perspective forecasting dynamics of cod and herring stock population dynamics in Atlantic region. The examples of such use of the sea ice coverage index are shown in Chapter 3.

Beside Barents Sea, 50–60-year fluctuations of the sea ice coverage have been detected for Arctic seas of the Siberian shelf [Karklin et al, 2001], and for Sea of Okhotsk. Fig. 2.17 shows that ice-free water area curves for Barents Sea and Sea of Okhotsk are virtually coincident. This indicates simultaneity of the long-term fluctuations of the ice coverage in North Atlantic and North Pacific seas, which are determined by the long-term dynamics of Global dT.

North-Atlantic Oscillation and Arctic climate indices

Climatic changes in North Atlantic are closely related to long-term pressure fluctuations in the centers of action of the atmosphere Iceland minimum and Azores maximum. The difference in atmospheric pressure in these two regions is referred to as the North Atlantic Oscillation (NAO). This NAO index increases at diminution of the Iceland minimum and increase of the Azores maximum of atmospheric pressure, which is accompanied by western winds strengthening and increasing delivery of relatively warm Atlantic waters to North European seas. Simultaneously, cold air mass delivery to Labrador and West Greenland increases. Reduction of pressure difference between centers of action in the atmosphere (NAO reduction) causes lowering of western winds, reduced delivery of Atlantic water to European seas and cold air masses to Labrador and West Greenland. NAO increase causes warming, whereas its decrease causes cooling of the climate in Europe [Rogers, 1984; Alheit, Hagen, 1997; Smirnov et al., 1998].

In the western and eastern parts of North Atlantic simultaneous but opposite changes in climate indices occur [Smirnova, Smirnov, 2000]. The authors have analyzed the relationship between cod stock increases and NAO changes in Northwest and Northeast Atlantic and observed that the correlation coefficients between NAO dynamics and stock increase in the studied regions were opposite by sign, but their values have fallen within the range of (0.4 & 0.4), the coefficient of determination is thus $R^2 = 0.16$. To put it

differently, NAO is a useful index for assessment of the general tendency in climate changes and regional cod stock populations, but it explains less than 20% of observed population changes.

One of the latest studies of possible relationship between the Norwegian Sea cod population and NAO long-term fluctuations [Solow, 2002] showed that over the 26-year period (1946–1972) stock increase and NAO fluctuations occurred in opposite phase, whereas in the following 24 years (1972–1996) these indices were in phase.

From the 1960s until the mid 1990s in-phase dynamics of zooplankton population and NAO were observed, but after 1996 this tendency turned to the opposite phase [Reid et al., 1998]. These data indicate limitation of the NAO as a predictor for changes in productivity of North Atlantic ecosystem.

Therefore, of interest is comparison of long-term NAO dynamics and Global dT (Fig. 2.18). In the period of 1860–1930, fluctuations of these indices were oppositely phased, whereas from the late 1930s until the early 2000s the long-term changes of NAO are in phase with Global dT fluctuations.

An analogous situation is observed in the comparison of NAO index curve shape with temperature dynamics in the 0–200 meter layer by the Kola meridian (Fig. 2.19), as well as the temperature anomaly in the Arctic zone

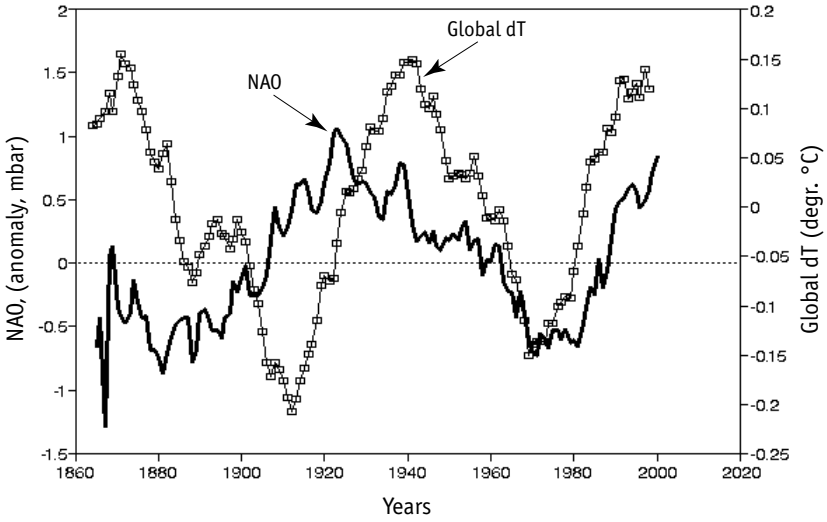

Fig. 2.18. Comparative dynamics of detrended Global dT (13-years smoothing, white squares) and average annual North Atlantic Oscillation index (NAO, 20-year smoothing, bold line) for 1860–2000. NAO series is developed by Turrel, 1995 and data from the site: www.cru.uea.uk/cru/data

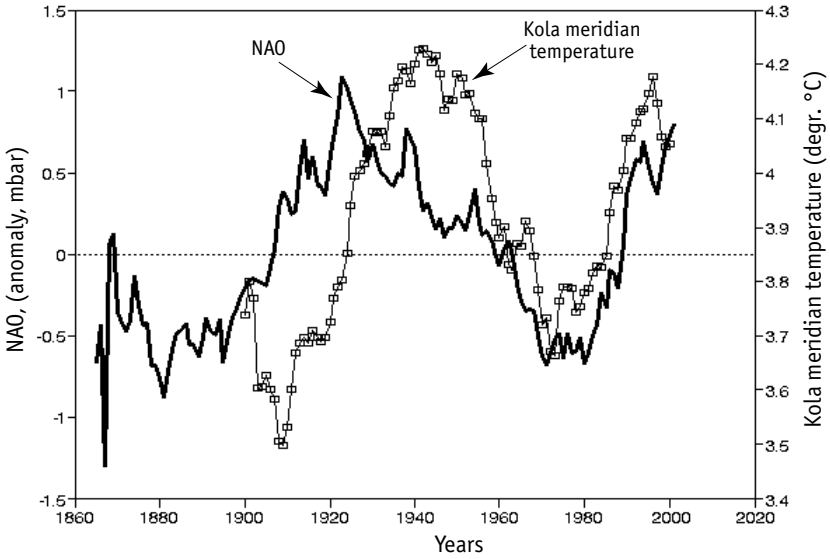

Fig. 2.19. Comparative dynamics of the average Kola meridian temperature in the water column 0–200 m (13-year smoothing, white squares) and the annual NAO (20-years smoothing, bold line) for the period of 1900–2000. NAO dynamics is developed by Turrel, 1995 and data from www.cru.uea.uk/cru/data, Kola meridian temperature from Yndestad, 2002

(Fig. 2.20). A typical feature of Arctic dT long-term dynamics is the detrending (see Fig. 2.12), which is atypical of Global dT [Sonechkin, 1998]. The average temperature in Arctic zone reached its maximum in the late 1930s into the early 1940s; in the period of 1950s–1960s a significant cooling occurred; and in 1970s–1990s a new warming trend was observed with a maximum in the early 2000s (Fig. 2.20). Long-term fluctuations of Arctic dT are considered as demonstration of a «low frequency» 60–80-year climate periodicity, which is presumably related to thermohaline circulation of the ocean [Alexeev, 2003].

Already during the first period of warming up in Arctic in 1920s–1940s, V.Yu. Vize [1937] and some time later B.L. Dzerdzeevsky [1943] and L.A. Wittels [1946] concluded that Arctic's warming up resulted from global increase of general atmospheric circulation, western atmospheric transfer and Atlantic water inflow to Arctic Ocean. Simultaneously, the reverse flow of waters from the Arctic Basin to Greenland Sea increases. Both in the 1930s and 1990s, a significant increase of temperature in Atlantic water layer occurred in the entire Arctic basin [Alexeev, 2003].

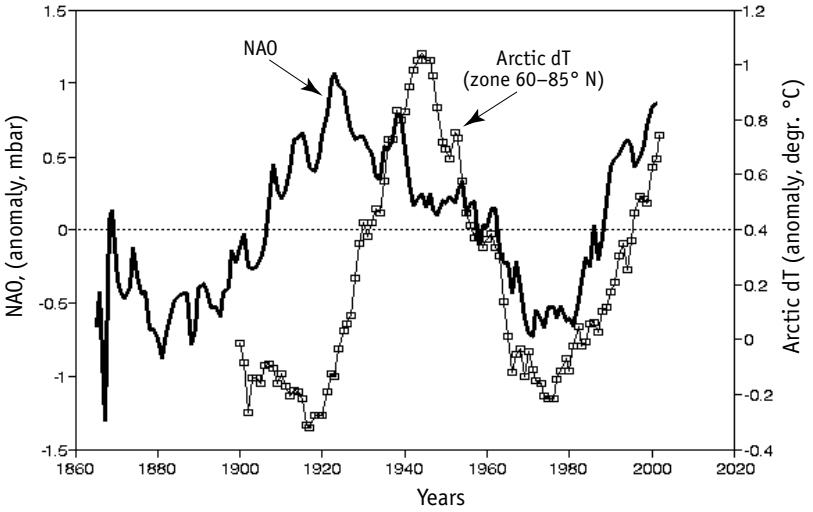

Fig. 2.20. Comparative dynamics of average annual NAO (20-years smoothing, bold line) and Arctic temperature anomaly (Arctic dT, white squares) for the period of 1900–2000 (13-years smoothing). NAO dynamics is developed by Turrel, 1995 and from www.cru.uea.uk/cru/data, Arctic dT data are from Alexandrov et al., 2003

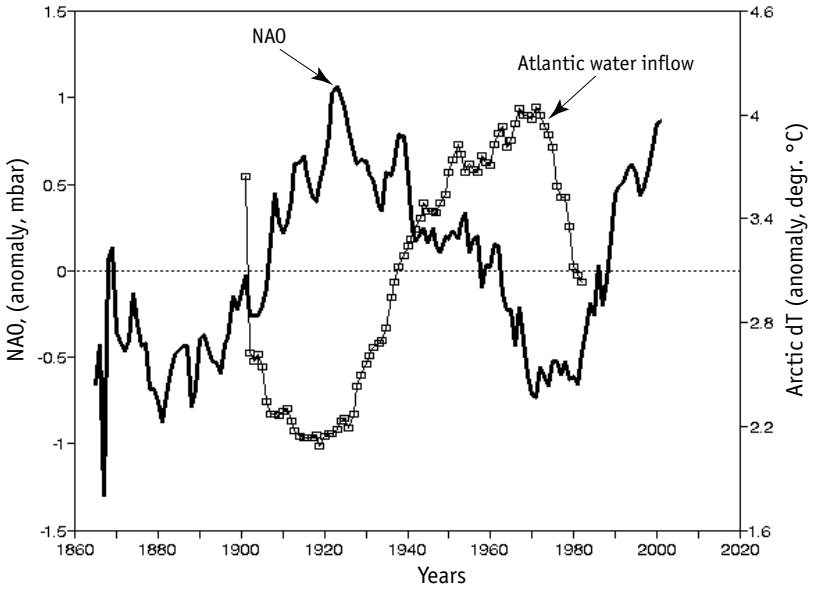

Fig. 2.21. Comparative dynamics of the average annual NAO (20-year smoothing, bold line) and Atlantic water inflow to Arctic through Faeroe-Shetland Strait (15-year smoothing, white squares) for 1900–1983. Data from Nikolaev and Alxeev, 1989. NAO dynamics is developed by Turrel, 1995 and data from www.cru.uea.uk/cru/data

However, a direct relationship of the long-term NAO dynamics and Atlantic water inflow is not exactly evident. Fig. 2.21 shows that dynamics of Atlantic water inflow and smoothed NAO index are virtually in the opposite phase.

We do not here discuss particular oceanographic mechanisms of heat transfer to the Arctic zone, however, the data shown indicate the need of further research to identify a relationship between heat delivery from Atlantic and NAO dynamics.

Cyclic changes of snow accumulation in Antarctica

The 50–60-year periodicity of snow accumulation during the recent 225 years was detected in the ice core studies from the Vostok Station in Antarctica. It is suggested that the accumulation is related to long-term fluctuations of cyclonic activity in the region [Ekaikin et al., 2002]. Over the recent 200 years, the authors did not observe any temperature rise of the Antarctic shield surface which, in turn, indicates the absence of a secular temperature trend typical of Global dT.

Quasi 50-year cycles are also displayed in fluctuations of Antarctic ice area, which is similar to the Arctic records, where such fluctuations have been observed for the ice coverage of Barents Sea [Karklin et al., 2001]. The results obtained correlate with the data on the existing of the 40–60-year longitudinal circulation cycle in the Southern Hemisphere [Enomoto, 1991].

Cyclic fluctuations of global temperature and the phenomenon of human-induced global warming

Global economic developments have a direct relationship with consumption and combustion of fossil fuels (oil, gas and coal) that results in emissions of the dominant fuel combustion products carbon dioxide and some other the so-called «greenhouse» gases to the atmosphere. There is a prevailing opinion that these substances prevent heat irradiation from the Earth to the space. Heath retained in the atmosphere increases temperature and

leads to global gradual rise of surface air temperature. This phenomenon was thus labeled «Global Warming».

Fig. 2.22 shows Global dT fluctuations over the the background of the world fuels consumption (WFC) increase during the last 140 years [Makarov, 1998]. Since the middle of the 19th century WFC is increasing at a rate of about 2.3% annually and is doubled every 30 years. Contrary to smoothly increasing WFC curve, compared with this secular increase trend, Global dT dynamics is subject to 50–60-year fluctuations with the maxima at the mid 1870s, the late 1930s and the late 1990s. In each «wave» of these fluctuations both ascending and descending parts of Global dT are observed. Table 2 shows comparison of Global dT and WFC fluctuations.

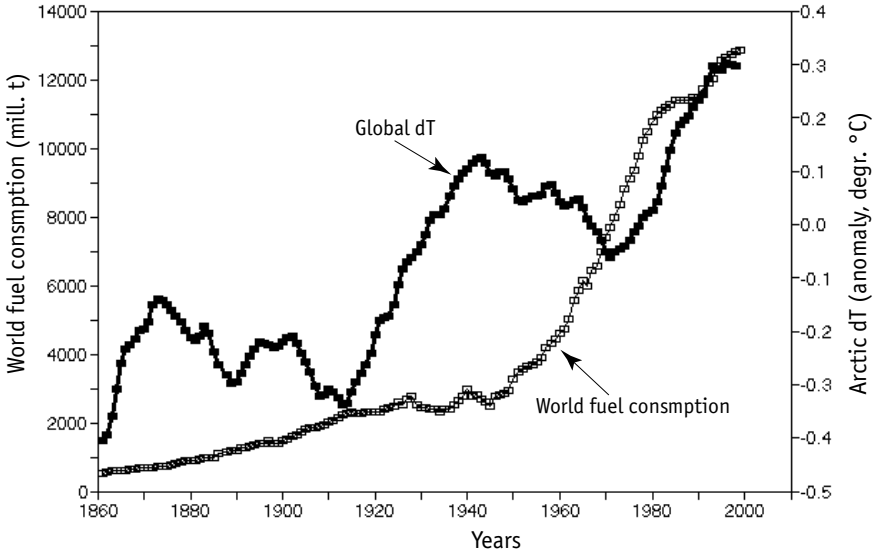

Fig. 2.22. Comparison of the Global temperature anomaly (Global dT, 13-year smoothing) (black squares) and world fuel consumption (WFC) (white squares) for 1860–2000. Data from Makarov, 1998

In the period of 1861–1875 a simultaneous increase of WFC and Global dT was observed, showing positive correlation ($r = 0.92$) of these processes. However, in the next period (1876–1915) WFC increase was accompanied by Global dT reduction rather than its increase, showing negative correlation ($r = -0.71$). In the period of 1910–1940 WFC increased very slowly and stopped growth in the period of 1920–1940 due to the world industrial crisis. However, in this period Global dT increased as much as by 0.4 °C — the re-

Table 2. **Correlation between Global dT and World Fuel Consumption (WFC) in different time periods of 1860–2000**

Global dT Fluctuation phase	Period, years	Correlation coefficient (r) between dT and WFC
Increase	1861–1875	+0.92
Decrease	1875–1910	–0.71
Increase	1910–1940	+0.28
Decrease	1940–1970	–0.88
Increase	1970–2000	+0.94
Decrease (?)	2000–2030	?

cord rate of Global dT increase for the entire 140-year period of instrumental measurements. In this period, correlation between WFC and Global dT is very low (r = 0.28). In the period of 1940–1970, WFC increased by 2.5 times, but Global dT decreased by 0.2C, and highly negative correlation (r = –0.88) was observed. The last 30-year period (1970–2000), corresponded to the phase of successive Global dT increase, a close positive correlation (r = 0.94) between WFC and Global dT is again observed.

As shown in Fig. 2.22 and Table 2, during the 140-year period under analysis, the background of monotonic WFC increase Global dT correlated either positively or negatively with WFC, changing sign every 20–30 years. Therefore, no direct correlation between WFC dynamics and Global dT is observed that provides no reason to conclude that WFC increase is the obvious reason for Global dT growth.

As shown by spectral analysis of temperature dynamics, based on Greenland ice core samples, 50–60-year periodicity of temperature fluctuations dominates over the recent 1500 years (see Chapter 1). For the more recent 140 years, the increasing linear trend with embedded 50–60-year fluctuations best describes the Global dT fluctuation dynamics. The results of analysis of even longer temperature time series (from 1500 to 8000 years) from ice core samples and tree growth rings were accepted and provided the initial data for development of a stochastic model of temperature fluctuations with predominant periodicity of about 60 years [Klyashtorin, Lyubushin, 2003; Klyashtorin, Lyubushin, 2005; see also Chapters 7 and 8]. Based on this model, which considers natural fluctuations of the global climate, Global dT fluctuations for the future 30 years have been predicted (Fig. 2.23). Accor-

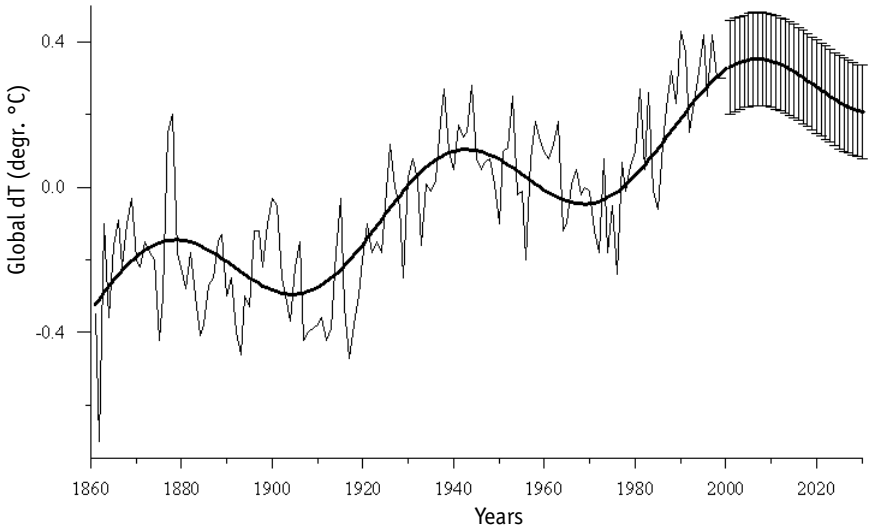

Fig. 2.23. Cyclic long-term fluctuations of Global dT (bold line), annual dT variations (thin lines), and modeled forecast of Global dT trend for 2000–2030 period with vertical sections of standard deviations

ding to this model, the maximal average of Global dT will occur within the next 5–10 years (~2005–2010), and then it will likely decrease by 0.1–0.15 into the 2020s. Similar conclusions regarding the future dynamics of Global dT are discussed in the paper by Datsenko et al. [2004].

CHAPTER 3

CLIMATE FLUCTUATION PERIODICITY AND MAJOR COMMERCIAL FISH POPULATIONS

The questions «how fishery statistics reflects the populations», and «whether catch dynamics may be used for assessing fluctuations of commercial stock populations», are not yet clear. Unfortunately, time series of major commercial fish catch statistics are usually shorter than 50 years, and reliable assessment methods for the populations, including acoustic survey methods, are only recently available for some fisheries.

Fig. 3.1 shows data on fluctuations of Japanese sardine (*Sardinops melanosticus)* commercial catches and estimates of annual recruitment to the stock by 2-year old fish, which initiate the commercial stock population [Wada, Jacobson, 1998]. Dynamics of the annual catches closely correlates with the recruitment (r = 0.93). An abrupt reduction of recruits began in 1987 due to climatic changes and hydrological changes that resulted in poorer juvenile growth conditions. Together these have induced reduced catches of Japanese sardine with some time shift (see Chapter 4). The previous outburst of this population in the 1920s–1940s was induced by natural mechanisms and characterized by close correlation between catches and sardine stock recruitment [Kawasaki, 1992a, b]. Over the 20th century population blooms of other sardine species occurred simultaneously with the Japanese sardine in the California, the Peru-Chile and the Benguela Upwelling Systems [Schwartzlose et al., 1999; Chavez et al., 2003].

The highest commercial catches of related coastal species reached 13 million metric tons of Peruvian anchoveta (*Engraulis ringens*). Assessments of fishery dynamics and anchovy biomass, including acoustic survey data, were implemented in 1950. This provided reliable data for comparison on dynamics of catches and the anchoveta population in the most productive region of

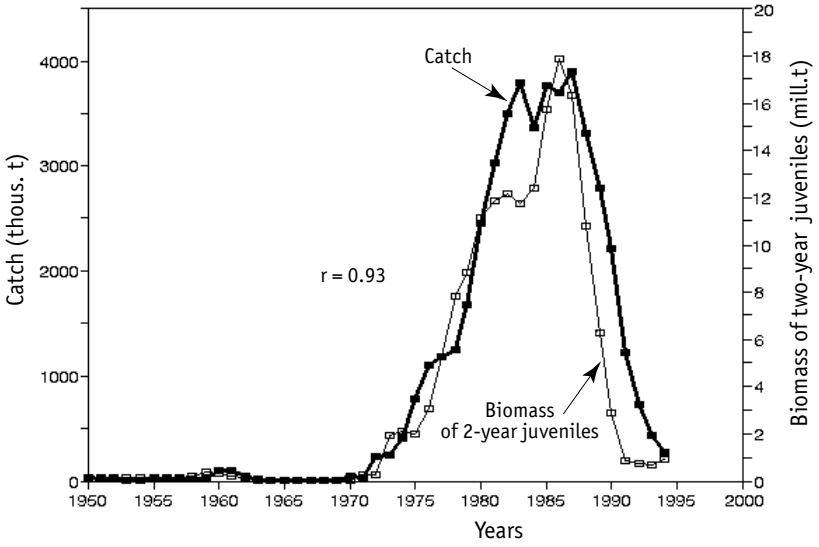

Fig. 3.1. Comparative dynamics of commercial catch (bold line) and recruitment (thin line) of Japanese sardine (*Sardinops melanosticus*) stock, 1950–1995. Data from Wada and Jacobson, 1998

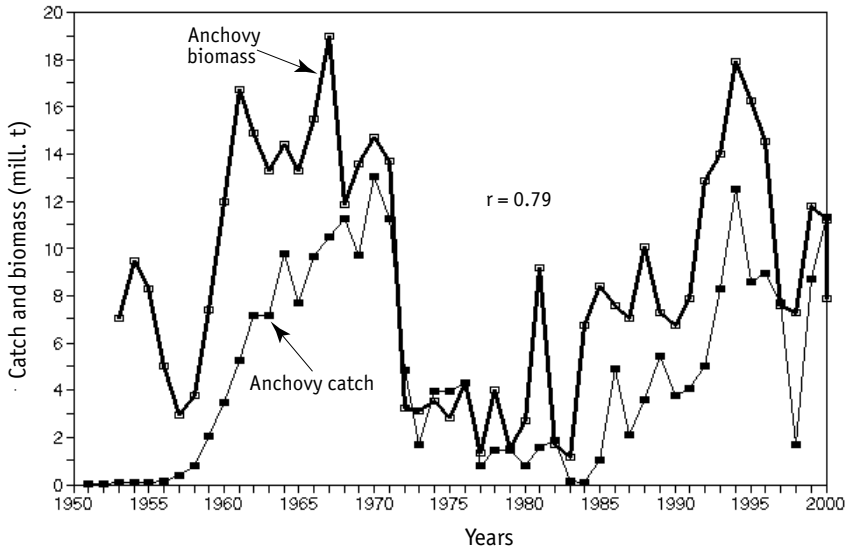

Fig. 3.2. Comparative dynamics of Peruvian anchoveta (*Engraulis ringens*) commercial catches (thin line) and biomass (bold line) 1952–2001

the World Ocean [Pauly et al., 1987; Ayon et al., 2004]. Fig. 3.2 shows comparative data on dynamics of Peruvian anchovy biomass and catches from 1950–2000. Over the 50-year period catches increased with the anchovy biomass (r = 0.79), but the fishery development was delayed in relation to dynamics of the population biomass increase. For more detail on fluctuation dynamics of Peruvian anchovy population, see Chapter 6.

Chilean jack mackerel (*Trachurus murphyi*) is one of the more productive species in the Southern Hemisphere. Its catches mostly comprising 3–6-year old fishes grew rapidly starting in the early 1970s, in 1996 reached almost 5 million metric tons, and then began an abrupt decrease. Data on correspondence of catches and recruitment of this species are scanty [Aranchibia et al., 1995; Konchina, Pavlov, 1999]. These works show data on the population of 2- and 5-year old jack mackerel, which provide the commercial stock. Fig. 3.3 shows dynamics of catches and Chilean jack mackerel stock recruiting with 5-year old fish.

Fig. 3.3 shows that in 1970–1993, mackerel catch fluctuations correspond to dynamics of 5+ fish biomass (r = 0.83), i.e. the catch curve generally reflects fluctuations in the population. This is also confirmed by dynamics

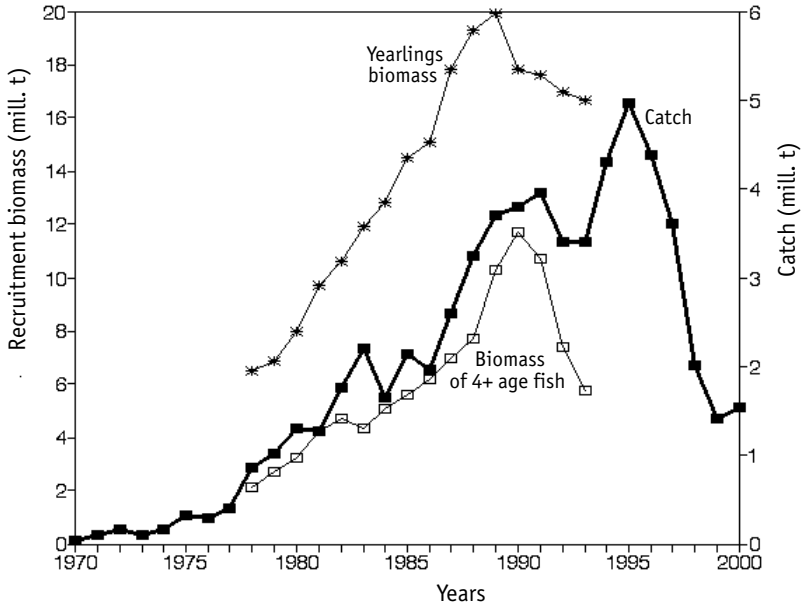

Fig. 3.3. Comparative dynamics of Chilean mackerel (*Trachurus murphyi*) stock recruitment (4+ age, white squares) and commercial catch (bold line). Data from Aranchibia et al., 1995

of 2+ fish biomass, not found in the commercial catch [Aranchibia et al., 1995]. Unfortunately, there are no data on mackerel stock recruitment in 1994–2000. The highest catches in 1995 and their decrease probably reflect delayed commercial activity despite the background of the population decrease, initiated in the early 1990s. Catch reduction in 1992 and 1993 was caused by decrease of both population and foreign fishery activity outside the Chilean economic zone.

Pollock (*Theragra chalcogramma*) is the most productive commercial species in the Northern Pacific. In the mid 1980s its catches approached 7 million metric tons. Up to 60% of total pollock catch is taken in the Bering Sea and about 20% in the Sea of Okhotsk. Fig. 3.4 shows the dynamics of commercial catches of pollock in the respective fishery regions according to assessments by O.A. Bulatov [Bulatov, 2003; Bulatov, 2003, 2004, 2005]. It is observed that biomass fluctuations of the pollock stock in Bering Sea correlate closely with the catch dynamics in the Bering Sea and the Total Pollock Catch in the Northern Pacific ($r = 0.83$).

Concerning dynamics of pollock catch in Sea of Okhotsk: in the first approximation it corresponds to that of Bering Sea, although catch minima are less well expressed. This may suggest that in this case catch dynamics corresponds to broad commercial resource biomass fluctuations.

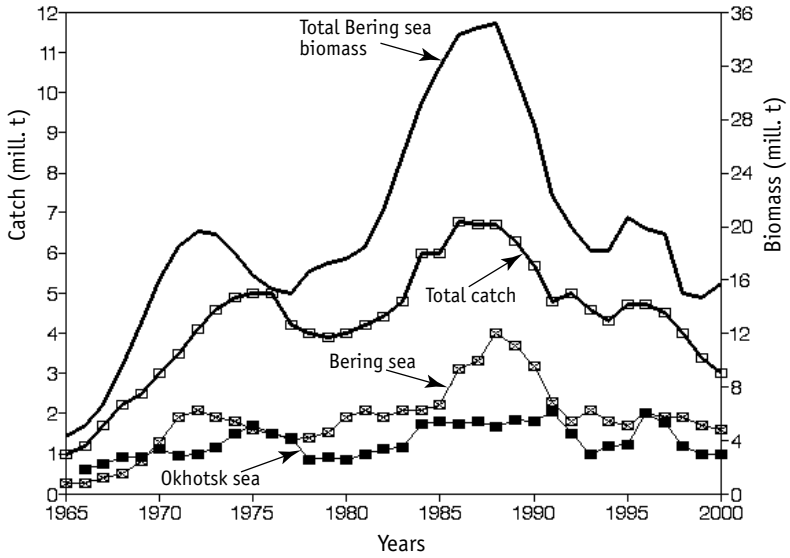

Fig. 3.4. Comparative dynamics of Alaska pollock (*Theragra chalcogramma*) catches and biomass in Bering Sea and Sea of Okhotsk in 1965–2000. Data from Bulatov, 2004

Pacific salmon species (seven spp.) provide up to 1 million metric tons of catches in the Northern Pacific. Almost a hundred years of catch statistics from fisheries and fish counts during upstream passage for spawning show that long-term fluctuations of Pacific salmon catches reflect fluctuation dynamics of their total population abundances [Klyashtorin, Smirnov, 1992; Beamish, Bouillon, 1993; Hare, Mantua, 2000]. Dynamics of Total Pacific Salmon Catch is presented in Fig. 3.5.

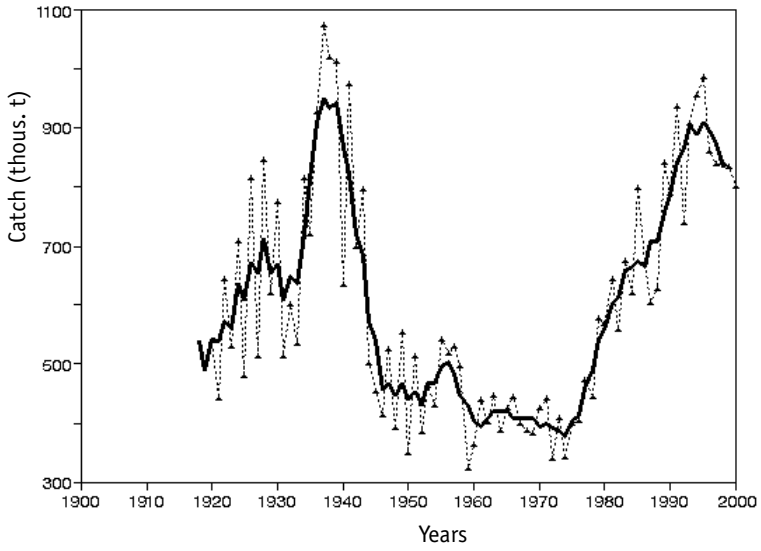

Fig. 3.5. Dynamics of Total Catches of all Pacific salmon from 1920–2000. Triangles and dotted line show annual catches, bold line shows total catches smoothed by 5-year moving averaging

The data above-provided show that catches in abundant populations of pelagic fishes, such as Peruvian anchoveta (up to 13 million tons catch), Japanese sardine (up to 5.2 million tons catch), pollock (up to 7 million tons catch), and Pacific salmon (up to 1 million tons catch), generally correspond to the abundance (biomass) dynamics of their commercial populations.

Unfortunately, there are mostly too-short time series of data available in the literature on the correspondence of mass commercial species catch to their specific populations. However, fluctuations of catches of these Pacific species are so extreme that there is no concern about their reflecting real fluctuations in the population [Lluch-Belda et al., 1989]. One may suggest that synchronous fluctuations of sardine (Peruvian, Californian, European,

and South-African) and anchovy (South-African and Japanese) catches correspond to the variations of their specificcommercial stock populations.

One particularly special, insightful regional case is the complex history of the large herring and cod population fisheries in the Northeastern Atlantic, about which the dependence of populations on climate changes are discussed below.

Dynamics of climatic indices and catches of the major commercial species of the North Atlantic region

Fig. 3.6 shows comparative dynamics of climatic indices and catches of the major commercial fish populations in the Northeast Atlantic. The upper four Climate Index data trends show that the dynamics of Arctic dT, Global dT (detrended), temperature by Kola meridian, and zonal ACI are rather close. Maxima of all the climatic indices fell within 1930s–1940s and 1980s–1990s, and their dynamics for the last 100 years had approximately 60-year periodicities.

The maximum (in the 1940s) and the minimum (in the 1970s) of spawning stock biomass for Atlantic spring-spawning herring (*Clupea harengus*) correlate well with the trends of global and regional climatic indices, whereas the spawning stock biomass increase in the 1980s–1990s corresponds with the rise of Global dT and Arctic dT, zonal ACI and temperature at the Kola meridian (Fig. 3.6).

Fig. 3.7 shows close correlation ($r = 0.95$) between spawning and commercial stock biomass fluctuations, i.e. dynamics of the spawning stock biomass rather accurately reflects changes in the general biomass of the commercial stock of herring and may be an index of its fluctuations.

Dynamics of commercial stock biomass (CSB) of North-East Arctic cod (*Gadus morhua*) also correlates with the changes of climatic indices — rising in the «warm epoch» with the peak in the early 1940s, and the decrease in the «cold epoch» in 1960s–1970s. However, codfish CSB decreases somewhat slower compared to climatic indices: its minimum is reached approximately 8–10 years later than the minimum of climatic indices. Fig. 3.8 shows that the CSB curve for North-East Arctic cod, shifted back by 8–10 years corresponds to dynamics of one of the major climatic indices of the region — the average temperature in the 0–200 m layer of the Kola meridian.

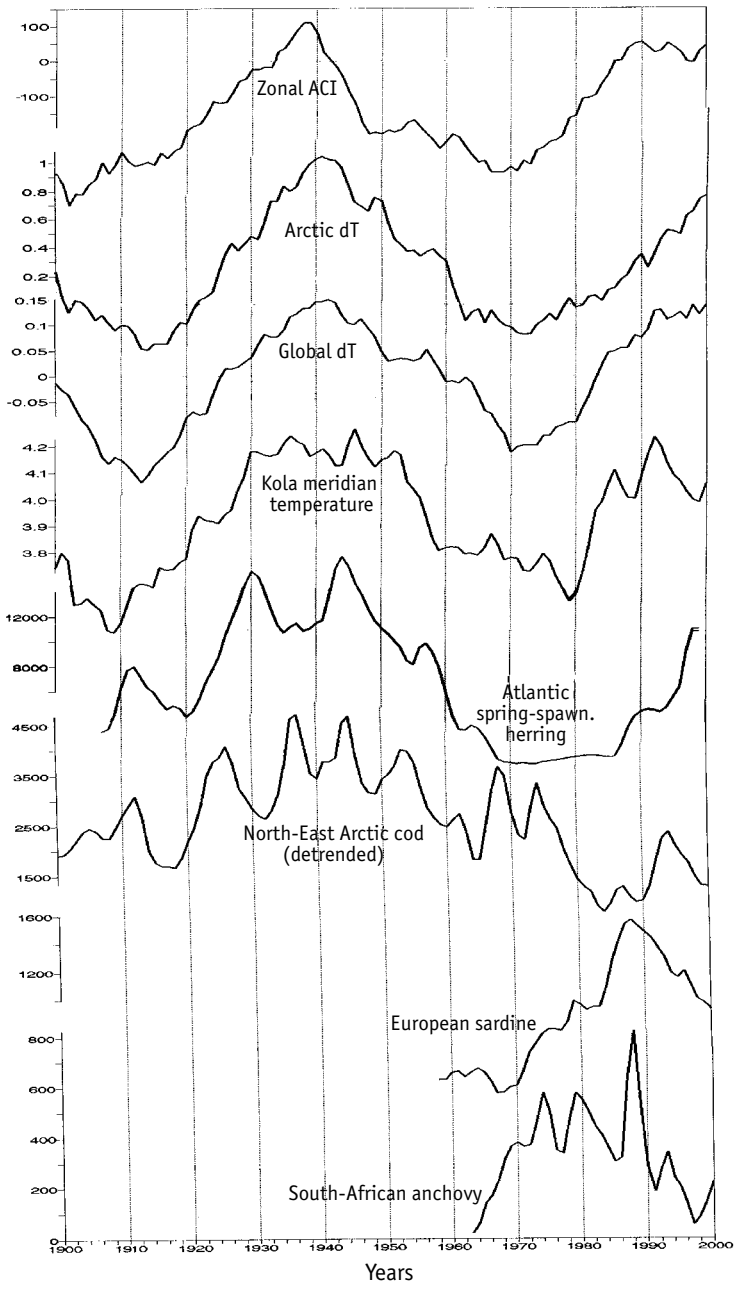

Fig. 3.6. Comparative dynamics of long-term changes of climatic indices and major commercial fish stocks in Atlantic. Atlantic spring-spawning herring — spawning stock biomass (explained in the text); North-East Arctic cod — commercial stock biomass [data from Hylen, 2002]

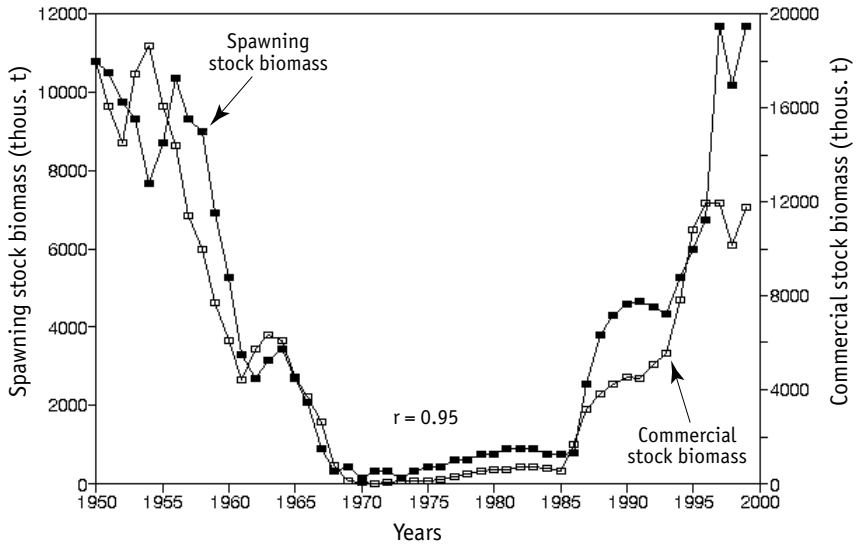

Fig. 3.7. Comparative dynamics of spawning stock biomass (dark squares) and commercial stock biomass (light squares) of Atlantic spring-spawning herring. Data from Toresen and Ostvedt, 2000; Borisov et al., 2001

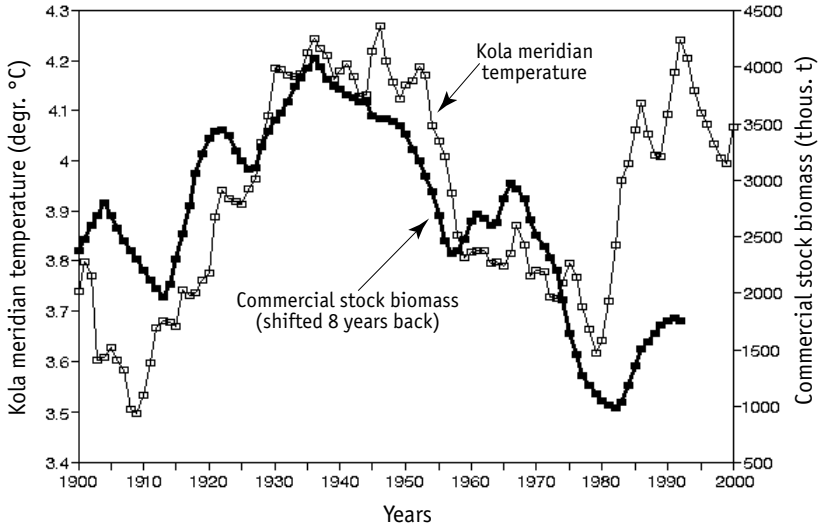

Fig. 3.8. Comparative dynamics of Kola Meridian Temperature (thin line) and Biomass of Commercial Stock of North-East Arctic cod (bold line) from 1900–2000. The Biomass curve is shifted back (to the left) by 8 years. Temperature and stock time series are smoothed by 13-year and 10-year moving averaging, respectively

Particular reasons for «delay» for codfish commercial stock biomass (CSB) dynamics in relation to climatic index trends are unclear, but its relation to dynamics of regional and global temperature, ice coverage of Barents Sea and Atlantic waters delivery to Arctic region are quite obvious. This problem is discussed in detail in Section 3.3.

Maxima of European sardine (*Sardina pilchardus*) and Southern-African anchovy (*Engraulis capensis*) catches are virtually coincident with development of the second «warm» climatic epoch of the 20th century (1980s–1990s).

Thus, dynamics of the largest commercial populations of Atlantic Basin regions demonstrate correspondence to approximately 60-year fluctuations of climatic indices. The details of relationships between climatic changes and dynamics of herring and codfish populations in Arctic region are discussed below.

Climate and fluctuations of herring and cod populations in the Northeastern Atlantic

Atlantic herring is the most abundant commercial species in the North Atlantic with the total production reaching ~4 million metric tons in the late 1960s. The major part of this catch was provided by Atlantic spring-spawning stock of herring, which is still providing 50–60% of the total herring landings in the Atlantic.

The North-East Arctic stock of cod is the second ranked fishery stock in Arctic region providing up to 30–40% of the cod catch in Atlantic. In the 1950s–1960s, catch of this cod stock exceeded 1 million tons, and at present it is 1/2–1/3 of the historical high levels.

Understanding of the reasons for long-term fluctuations of herring and cod populations in Arctic region is critical for ecologically sustainable catching and fishery management, especially for Russia and Norway. The state of Atlantic spring-spawning herring and North-East Arctic cod resources is the routine subject of discussion by experts from different countries who are trying to estimate the role of both fishing and natural conditions in the bloom–decline dynamics of populations of the major commercial fishes of North Atlantic [Toresen, Ostvedt, 2000; Godo, 2003].

Atlantic spring-spawning herring and climate fluctuations

Since the early 1900s until the 1930s–1940s the herring stock biomass increased, and then began decreasing, reaching its minimum in the 1970s (Fig. 3.9). Herring populations began decreasing during World War II (1939–1945) despite the relatively low intensity of the fishery. Later on, within the background of commercial stock population decreases, the herring fishery increased intensity with catches reaching 2 million tons by the late 1960s. This extremely intensive and uncontrolled fishery had negative effects on the stock population, however the role of the long-term decrease of the herring population is also important. In the 1980s, after the decline period, the herring population began increasing, and by the late 1990s catches again exceeded 1 million tons.

Time series of the fishery statistics for Atlantic spring-spawning herring exceeds 90 years that allows considering a question about a relationship between herring population fluctuations and climate changes.

Long-term fluctuations of the herring stocks are caused by population recruitment dynamics, particularly the 3+ aged fishes, which survive the period of high mortality and form the future commercial stocks. Fig. 3.10*a*, *b* shows

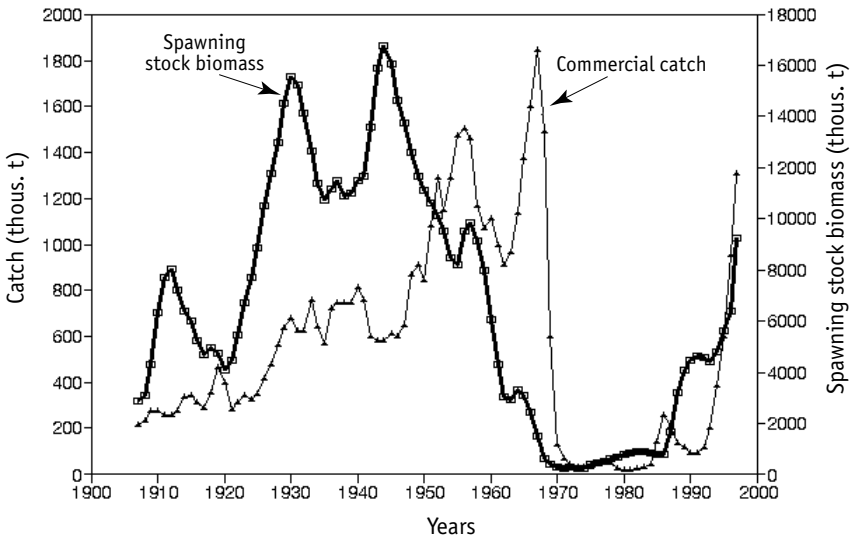

Fig. 3.9. Dynamics of spawning stock (bold line) and commercial catches (thin line) of Atlantic spring-spawning herring, 1907–1998. Introduction from Toresen and Ostvedt, 2000; Anon, 2000

the frequency of occurrence of high population herring generations compared with the climatic index Global dT. Fig. 3.10*a* shows that the 30 most abundant generations occurred during the first half of Global dT increase cycle (from 1910 until the early 1940s. In the second half of the cycle, within the background of Global dT decrease from the 1950s into the early

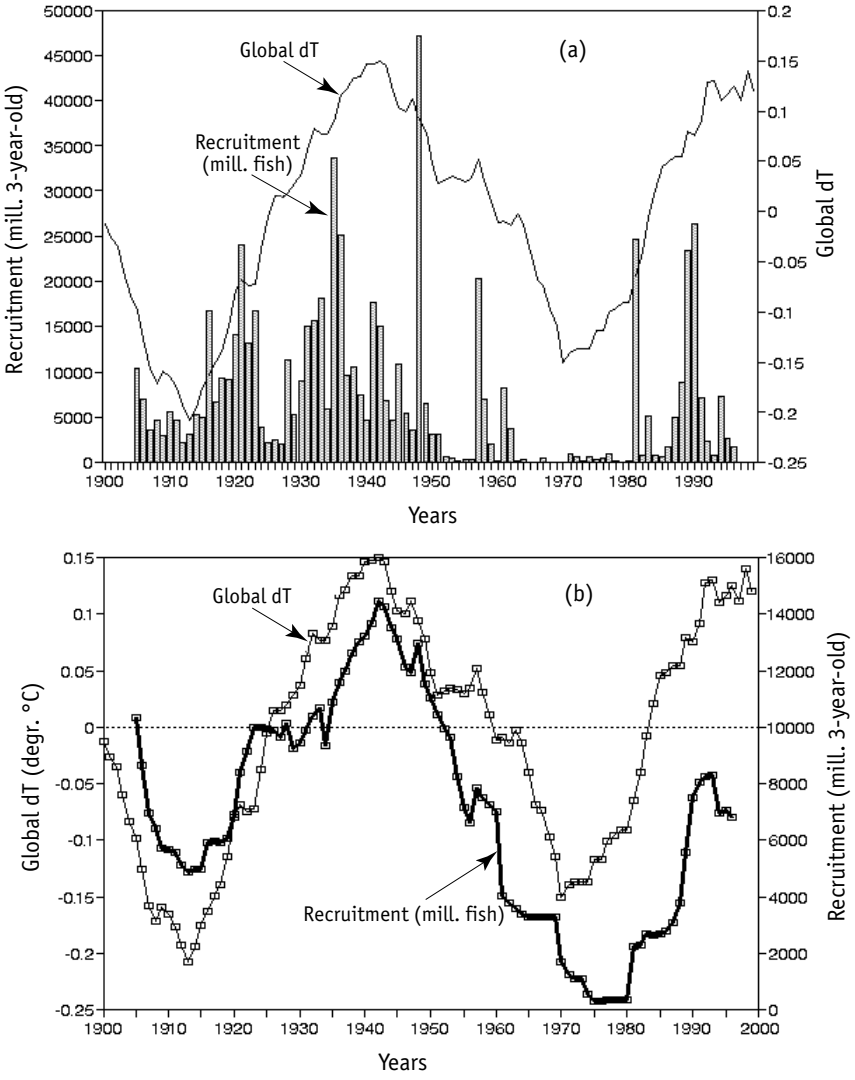

Fig. 3.10. Comparison of the recruitment dynamics of Atlantic spring-spawning herring stock (bold line) and detrended Global dT (thin line) in 1907–1998. *a* — annual number of recruits and Global dT, *b* — the same, but the recruitment time series are smoothed by 13-year moving averaging

1970s, the number of abundant generations was much lower, only 12, whereas during the almost 20-year long period of intensive cooling (1960s into the late 1970s) no abundant generations were observed. Following that period, abundant generations appeared starting at the beginning of new Global dT increase in the 1980s–1990s.

Herring population recruitments vary significantly with time (Fig. 3.10,*a*). This relates, in particular, to significant interannual fluctuations of regional and global temperatures (see Chapter 1). These interannual temperature oscillations are unpredictable and reflect the stochastic nature of heat transfer fluctuations in the atmosphere. However, temperature curves produced by moving-average smoothing allow separation of relatively «warm» or «cold» periods, within which the similar pattern of abundant generation occurrence increases or decreases is observed. Fig. 3.10,*b* shows similarity between long-term dynamics for herring recruitments and Global dT, the recruitment data being presented in a moving-average smoothed curve.

Fig. 3.11 shows close affinity of recruitment smoothed curve dynamics and herring spawning stock biomass. As shown above (Fig. 3.7), in the recent 50 years a close correlation ($r = 0.95$) between spawning and commercial resource abundance of herring is observed. This allows use of either the spawning resource curve or the smoothed recruitment curve as a population status index for herring commercial stocks.

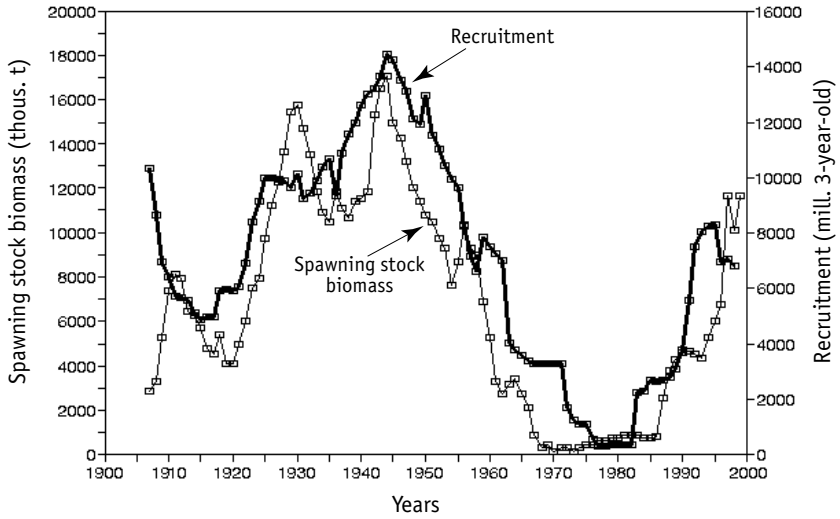

Fig. 3.11. Comparative dynamics of spawning stock biomass (thin line) and number of recruits (bold line) of Atlantic spring-spawning herring, smoothed by 13-year moving averaging, 1907–1998

Do dynamics of herring commercial stock population correlate with the Arctic region temperature curve? The comparison of air temperature changes in the zone between 60–85° N e.g. Arctic dT and Global dT for the last 100 years shows (Fig. 3.12) that Global dT and Arctic dT fluctuations happen synchronously. However, secular trends of these curves are different. Contrary to Global dT, Arctic dT has no increasing secular trend.

Fig. 3.13 Allows comparison of Arctic dT dynamics and detrended Global dT: both curves virtually coincide, both having 60-year periodicity. This provides the option to use either Arctic dT or detrended Global dT as a meaningful climatic index.

So far as concerns climatic changes in Northeastern Atlantic, air temperature in Iceland, Jan Mayen Island and Spitsbergen, as well as the average temperature in the 200-meter water column of the Kola meridian demonstrates dynamics close to the detrended Global dT (Fig. 3.14). All curves show a maxima at 1940s, minima in the 1970s, and rise again in the 1980s–1990s. The most serious difference between the Arctic dT curve and Global dT is that for the Arctic region in the recent 75 years no increasing temperature trend was observed [Alexeev et al., 2000; Alexandrov et al., 2003; Alexeev, 2003], i.e. not a sign of global warming is observed. In fact, the temperatures were higher in the mid 1940 and early 1950s than at present. The absence of an increasing trend is also typical of secular dynamics of the surface temperatures in Scandinavian countries [Nordklim data set, 2001].

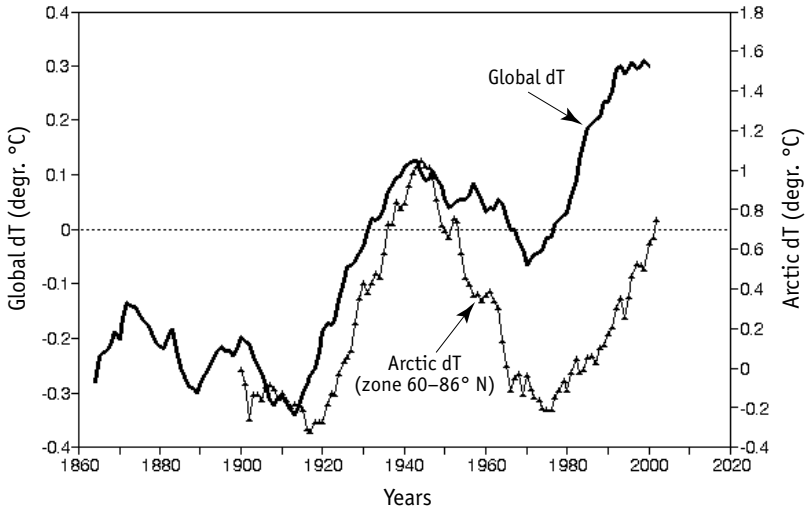

Fig. 3.12. Comparative dynamics of Global dT (bold line) and Arctic dT (triangles). Data from Alexandrov et al., 2003 (13-year moving averaging)

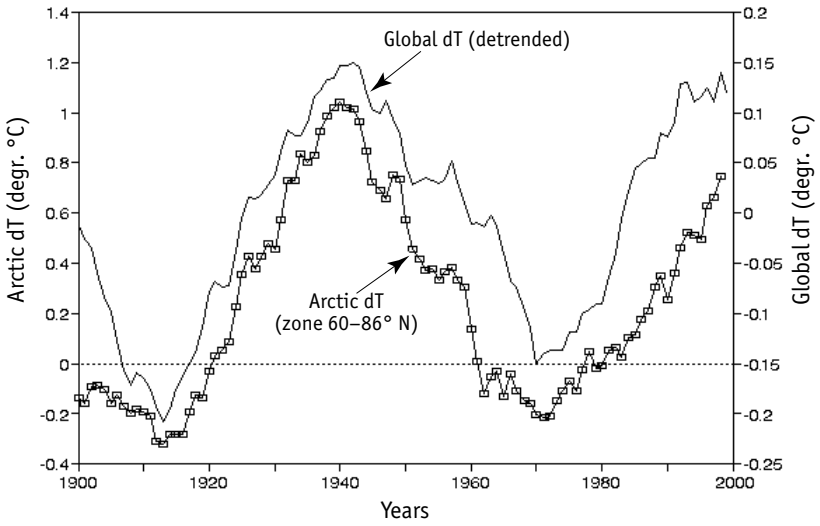

Fig. 3.13. Comparative dynamics of detrended Global dT (thin line) and Arctic dT (white squares). Data from Alexandrov et al., 2003 (13-year moving averaging)

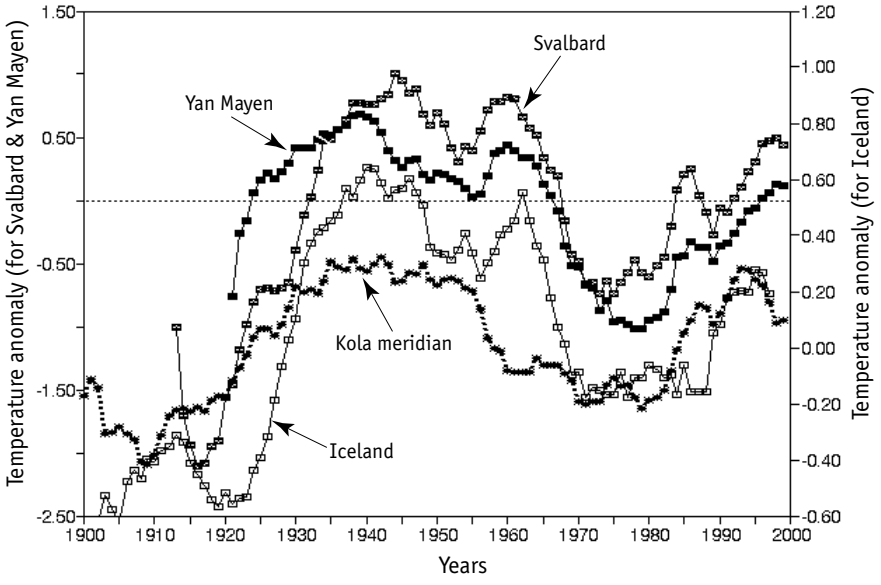

Fig. 3.14. Comparative dynamics of air surface temperature in Iceland, Jan Mayen Island and Spitsbergen and mean temperature in the 200-m water column by Kola meridian section for 1900–2000. Smoothed by 13-year moving averaging

The mean annual air temperature curve in the part of Russia north of Europe (Arkhangelsk, Naryan-Mar, Salekhard) from 1915–1990 also had no secular increasing trend, but demonstrated approximately 60-year periodicity with the maxima in 1930s and in the late 1990s, and a minimum in 1960s [Kryzhov, 2002]. The absence of secular increasing temperature trends in the Arctic region seems unexplainable from the point of view of the so-called global warming, which theoretically should be expressed much stronger in the Arctic region [Vinnikov, 1986].

The average temperature in the 200-meter water column along the Kola meridian is one of the most valuable climatic indices correlating with the Norwegian spring-spawning herring population. Fig. 3.15 shows that the dynamics of herring stock recruitment and the average temperature in the 200-meter water column along the Kola meridian [Bochkov, 1982; Yndestad, 2002] correlate well and demonstrate approximately 60-year periodicity. The correlation coefficient of spawning herring dynamics and smoothed Kola meridian temperature is 0.82 [Toresen, Ostvedt, 2000].

The Kola meridian average temperature is considered to be an indicator of climatic changes in Northeastern Atlantic, and used by many authors [Toresen, Ostvedt, 2000; Yndestad, 2002]. According to data by Seliverstov [1974], abundant generations of Atlantic spring-spawning herring occurred

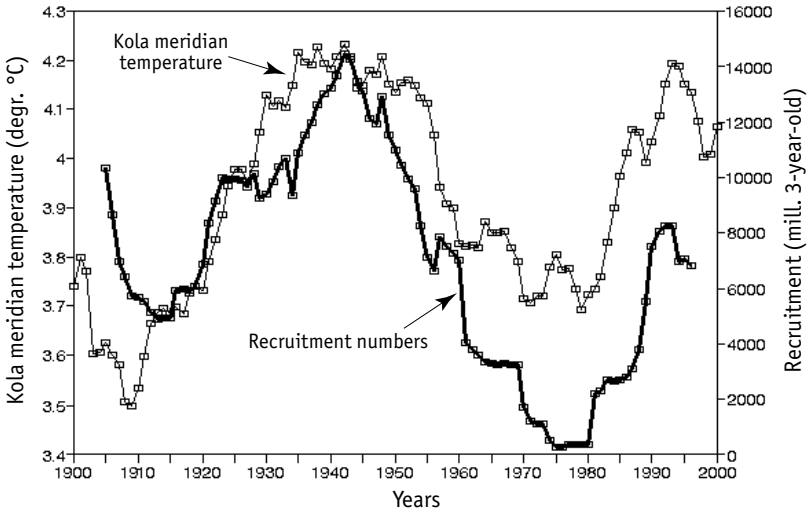

Fig. 3.15. Comparative dynamics of Atlantic spring-spawning herring recruitment (bold line) and average temperature in the 200-m water column along the Kola meridian (white squares) for the period of 1900–2000 (smoothed by 13-year moving averaging)

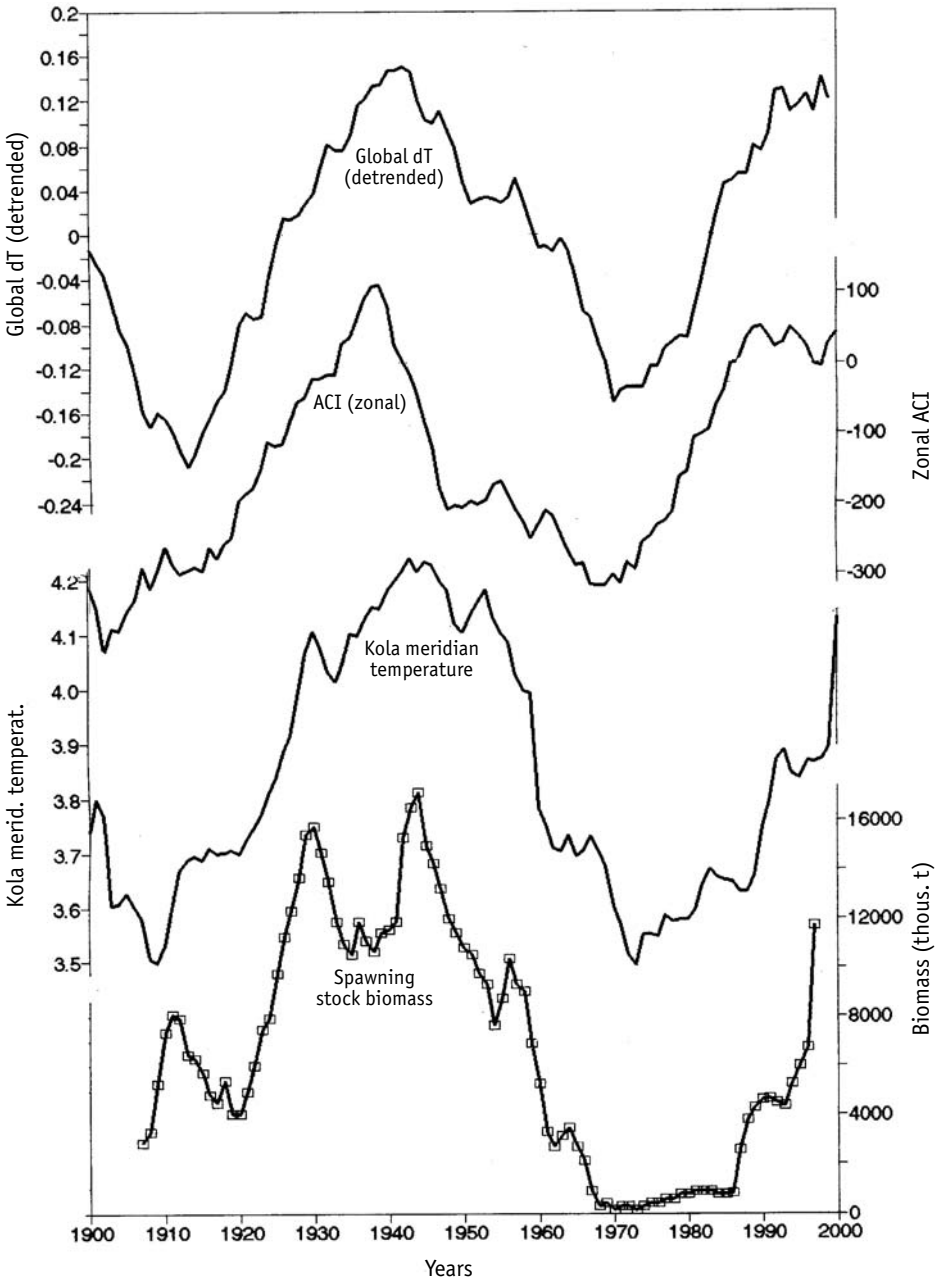

Fig. 3.16. Comparative dynamics of Global dT (detrended), zonal ACI, Kola meridian 0–200 m mean water column temperature and spawning stock biomass of Atlantic spring-spawning herring for the period from 1900–2000

in the warmest years only. These observations are confirmed by data that the greatest number of abundant herring generations fell within the period of the lowest ice coverage of Barents Sea (1930s–1950s) that corresponded with the maximum of «Arctic warming» [Yudanov, 1964]. Although the mechanism fundamental for temperature effect on herring population dynamics is not yet quite clear, the frequency of abundant generations significantly increases in periods of warming, which are clearly observed on smoothed Global dT curves and Kola meridian temperature curves.

Approximately 60-year periodicity of temperature and herring population fluctuations corresponds well with several global and climatic indices. Fig. 3.16 shows that dynamics of spawning herring biomass (and commercial stock biomass related to it) correlates with approximately 60-year fluctuations of climatic indices such as Global dT, zonal ACI and the average temperature by Kola meridian.

In the recent 50 years dynamics of total commercial stock of Atlantic spring-spawning herring corresponds with the Global dT curve (Fig. 3.17).

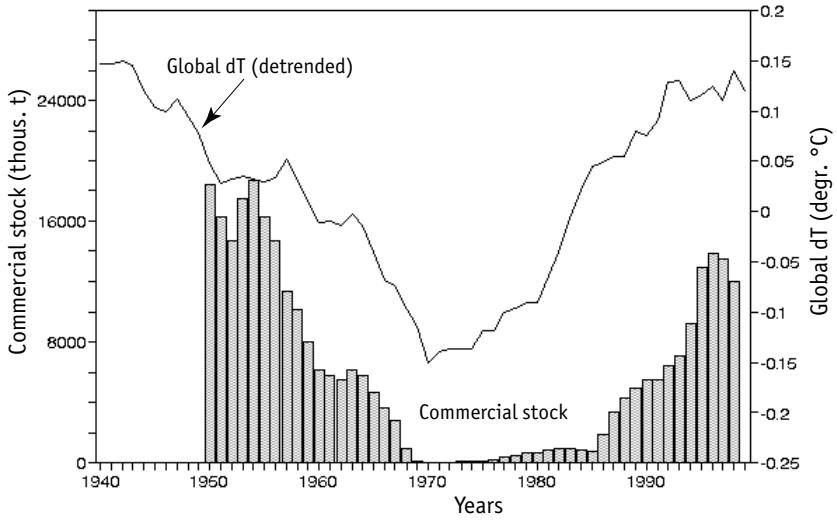

Fig. 3.17. Comparative dynamics of the detrended Global dT (thin line) and biomass of commercial stock of Atlantic spring-spawning herring (bars) for 1950–1998. Data from Krysov, 2000

Thus, changes of herring recruits' biomass and (commercial stock biomass) correlate with approximately 60-year fluctuations of climatic indices — Global dT, Arctic dT, the average temperature by Kola meridian, and air temperature in Arctic region of Atlantic.

North-East Arctic cod and climate fluctuations

North-East Arctic cod is one of the most well-studied cod populations in the Atlantic. Many studies have been devoted to analyses of relationships between this fish's population dynamics and climate fluctuations [Dragesund, 1971; Nakken, 1994; Rodionov, 1995; Boitsov et al., 1996; Hylen, 2002; Bondarenko et al., 2003; Godo, 2003]. Detection of these relationships is difficult given the background of the intensive fishing effort [Garrod, Shumacher, 1994].

One of the first attempts to relate the long-term dynamics of cod catches to climate fluctuations was made in the 1940s [Ottestad, 1942] using estimates of temperature changes for 200–300-year period using growth rings of spruce and pine tree from Lofoten Islands [Ording, 1941]. The following cycles of summer temperature fluctuations were observed using the growth rings: 57-, 23-, 17.5-, and 11-years dominate. Comparison of climatic fluctuation curves and large Lofoten cod catches for the period of 1884–1940 has shown that total dynamics of catches follows an approximately 50-year cycle, at the background of which ~20-year fluctuations are detected.

Some data series on the recruit (age 3+) population of North-East Arctic cod are available over 80 years [Dragesund, 1971; Anon, 2002; Hylen, 2002] and, similar to herring, allow the characterization of the periods of environmental conditions favorable for fry survival. Fig. 3.18,*a* shows distribution of abundant annual recruitment of the cod stock compared with Global dT dynamics. Fig. 3.18,*b* presents the same data, smoothed by moving averaging. One may see that the smoothed recruitment curve corresponds with Global dT dynamics with a lag of, approximately, 8 years.

We suggest that climatic indices of Arctic region: temperature of the Kola meridian, and air temperature in Iceland, Jan Mayen Island or Spitsbergen, will correlate well with the dynamics of North-East Arctic cod recruitment. Figs. 3.19 and 3.20 show that cod stock recruitment dynamics are somewhat better correlated with the dynamics of regional climatic indices (temperature of the Kola meridian and air temperature of Jan Mayen Island) than with Global dT.

Similarities and differences in dynamics of annual herring and cod recruitments are clearly observed by direct comparison. Fig. 3.21,*a* shows that smoothed recruitment curves of two species are similar, but with almost a decade lag for cod. Fig. 3.21,*b* shows the curve for cod shifted back by 8 years; in this case maxima and minima of both curves (in 1940s and 1970s, respec-

tively) are nearly coincident. This provides additional grounds for suggesting that for these two species similar dynamics driven by climate fluctuations are typical. However, fluctuations in the herring population happen almost synchronously with temperature index curves, whereas for cod population they are lagged by 8–10 years.

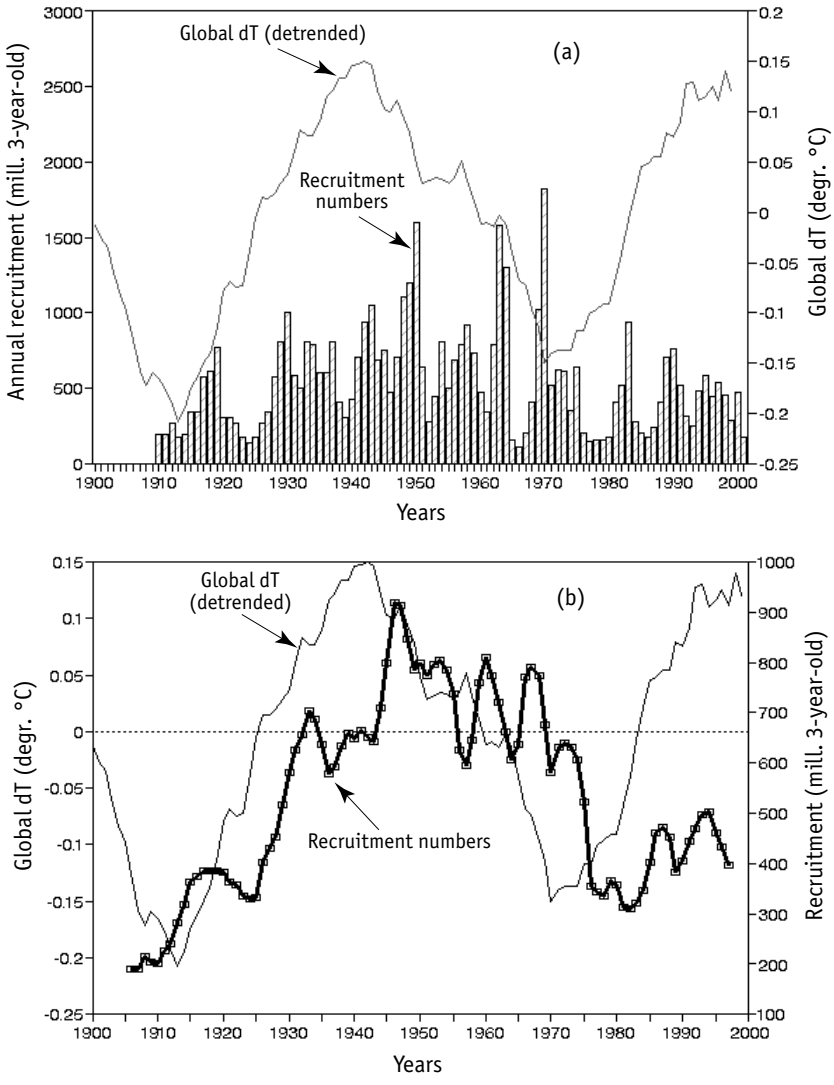

Fig. 3.18. Comparative dynamics of the North-East Arctic cod annual number of recruits (bars) and detrended Global dT (thin line) — (*a*); the same time series with recruitment smoothed by 10-year moving averaging (bold line) — (*b*)

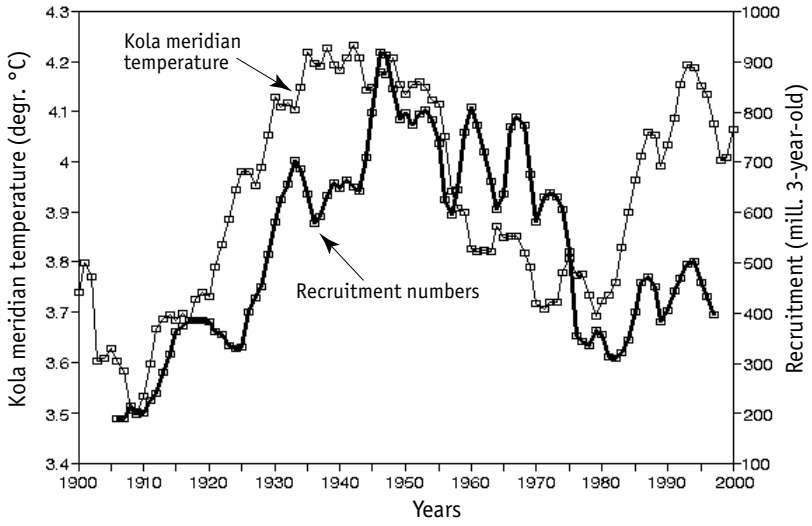

Fig. 3.19. Comparative dynamics of the Kola meridian section 0–200 m water column temperature (thin line) and North-East Arctic cod recruitment (bold line), smoothed by 10-year moving averaging

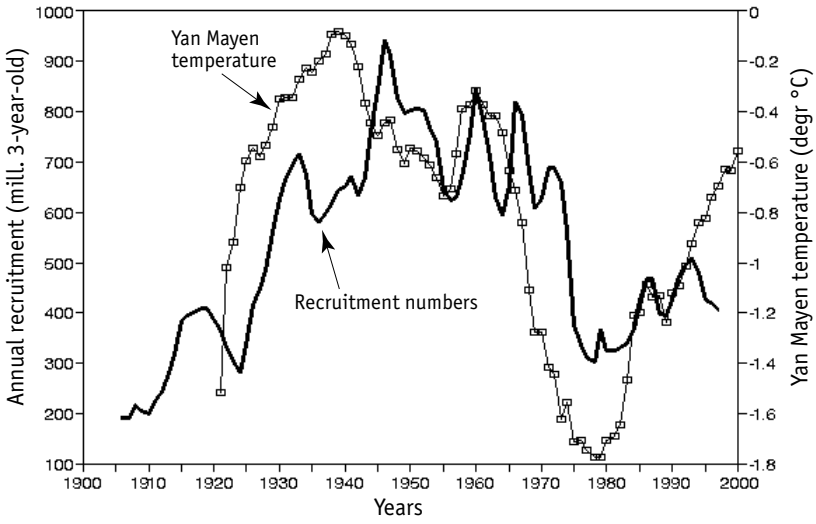

Fig. 3.20. Comparative dynamics of surface air temperature at Jan Mayen Island (thin line) and recruitment of the North-East Arctic cod commercial stock (bold line), smoothed by 10-year moving averaging

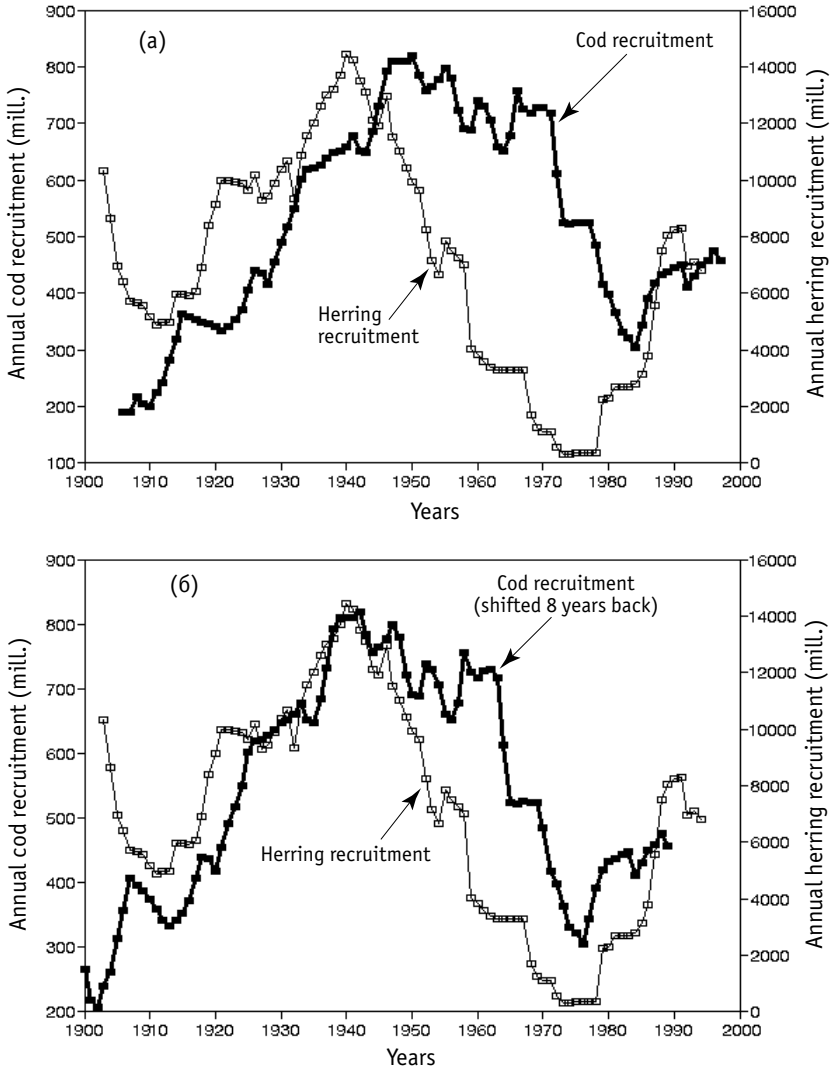

Fig. 3.21. Comparative dynamics of the smoothed time series of Norwegian spring-spawning herring and North-East Arctic cod recruitment: *a* — dynamics of both cod and herring recruitment smoothed by the 13-year moving averaging; *b* — the same dynamics with the curve for cod shifted back (left) by 8 years

Beside cod and herring, the effects of long-term temperature fluctuations were also observed for haddock (*Melanogrammus aeglifinus*) [Ponomarenko, 1973; Ellertsen et al., 1989; Ottersen et al., 1994]. North-East Arctic cod, Atlantic spring-spawning herring and Northeastern Arctic haddock breed vir-

tually in the same region. Larvae and juveniles of these species are affected by general natural and climatic factors, related to heat transfer from the Atlantic to the Arctic region. There is a reliable positive relationship between temperature fluctuations and fry growth rate for all three species, traced by 3 years old inclusively [Ottersen, Loeng, 2000].

Fig. 3.22 shows fluctuations of temperature along the Kola meridian and sizes of 0-year old juveniles of cod, herring and haddock. The coincidence between annual fluctuations of temperature by Kola meridian and changes in the lengths of larva of three main commercial species in the region is clear.

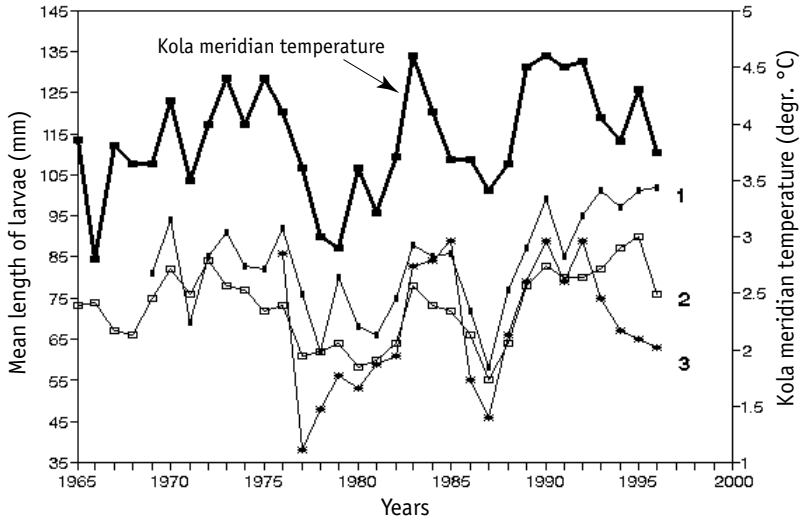

Fig. 3.22. Fluctuations of annual temperature in the 0–200-m water column along the Kola meridian (bold line) and body length of 0-year old haddock (*1*), cod (*2*) and herring (*3*) fry. Data from Ottersen and Loeng, 2000

Temperature rise causes two known effects: plankton production as food for larva increases; and physiological prerequisites for rapid food digestion and growth acceleration are created. In turn, this shortens time required for the early stages of larvae and juveniles development, when mortality is particularly high, and therefore juveniles survival significantly increases. It is suggested that this very effect is the main reason for occurrence of abundant generations of cod in Barents Sea in the so-called «warm years» [Aksnes, Blindheim, 1996].

The average temperature in 0–200-meter water column by Kola meridian characterizes fluctuations of the average temperature in the upper 200-me-

ter layer, but does not reflect the entire variability of all the environmental conditions in Arctic region. Temperature is not the unique index defining occurrence of abundant and lesser generations. There is an important effect on recruitment abundance caused by the presence of high plankton concentrations, wind and wave activity, as well as match or mismatch in time of a set of favorable environmental conditions and thus the appearance of new generations of herring and cod. To put it differently, the formation of pelagic fish population in the Arctic region the determining role is dominated by Cushing's «Match-Mismatch» mechanisms [Cushing, 1982].

The question about environmental condition effect on formation of cod generations and the stock abundance in Barents Sea was discussed in detail in an analytical report by I.Ya. Ponomarenko [1996]. Based on the analysis of a broad range of practical information sets, it has been shown that consideration of only temperature and hydrological conditions at the early stages of fish life yields no possibility for reliable forecasting of the generation abundance. Adequate relationships between the indices of environmental conditions and cod generation abundance in the year of their occurrence were preserved only for relatively short periods. At the same time, several factors have been identified as being favorable for recruitment of the stock that are related to thermal conditions and dynamics of waters in the region: the increase of the eastern branch of Norwegian stream flow rate; beginning time of biological spring; plankton biomass increases; acceleration of larval and juvenile growth; the features of juvenile distribution by the water area of the Barents Sea.

In the so-called «warm» years formation of abundant generations becomes more probable, but this potential is not always realized due to interannual changes of water thermal mode from «warm» to «cool». For example, if warming lasts 2–3 successive years, this promotes occurrence of several abundant generations and the subsequent growth of populations. More clearly, the probability of abundant recruitment to the commercial stock significantly increases with more stable favorable climatic conditions.

Figs. 3.10 and 3.18,*a* show that the abundance of annual recruitments of herring and cod stocks varies greatly between years. This is associated with the fact that interannual variations of both Global dT and Arctic dT are rather high. Interannual variations of both regional and Global temperature are practically unpredictable, reflecting the arbitrary (stochastic) type of heat- and wind-related processes occurring within the atmosphere. Smoothing by moving averaging of multiyear temperature series allows separation of rela-

tively warm periods, when frequency of years with positive deviations of temperature from the mean multiyear level increases, or relatively cold ones, when the frequency of negative deviations from the average increases. Similarities of smoothed temperature and recruitment abundance curves shows that stock population dynamics are also determined by frequency (periodicity) of occurrence of abundant or lean generations of herring, cod, and haddock.

As discussed in some works [Toresen, Ostvedt, 2000; Bondarenko et al., 2003], there are quite abundant annual classes of recruitments which may also appear in cold years. This indicates significance of oceanographic factors other than only temperature). Temperature increase promotes but does not guarantee formation of abundant recruitment.

It seems probable that consideration of the effects of a complex of factors related to climatic fluctuations, and monitoring of particular oceanographic characteristics known to affect populations of cod, herring and haddock generations would make for much easier forecasting of their population abundances.

On dependence of cod stock recruitment abundance on the spawning stock

The spawning stock biomass (SSB), which provides for occurrence of quite abundant generations, is considered as the key index for estimation of commercial cod stocks. This problem is discussed in several works [Garrod, 1967; Hylen, Dragesund, 1973; Ponomarenko, Yaragina, 1980; Ulltang, 1996], but optimal levels of «parent» cod stock biomasses are still not clear.

Comparison of cod stock recruitment dynamics and the spawning stock biomass (Fig. 3.23) shows that within the period from 1950–1970 SSB levels decreased to almost 1/5 (i.e. dropped to 80%), whereas the average recruitment decreased by only 20–30%. At the same time, in the periods of relatively low SSB fluctuations high fluctuations of cod stock recruitments were observed, inducing serious consideration that the effect of natural (climatic) factors are the main reasons for long-term fluctuations in the population.

To help resolve the question about the cod SSB relationship to resulting stock recruitments, in one study by I.Ya. Ponomarenko [1996] a 45-year time series was analyzed for fluctuations of these indices. The data were subdivided into 4 groups of recruitment abundances: very low, low, middle and

high. According to data of ICES working groups [Bondarenko et al., 2003] (Fig. 3.24), we have compared the average values of recruitments for each group with the corresponding SSB means.

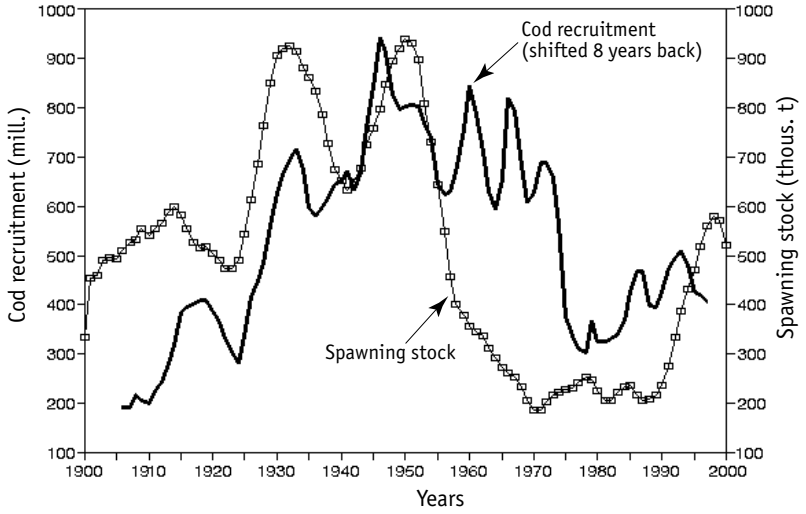

Fig. 3.23. Comparative dynamics of spawning stock (white squares) and recruitment (bold line) of North-East Arctic cod (10-year smoothing)

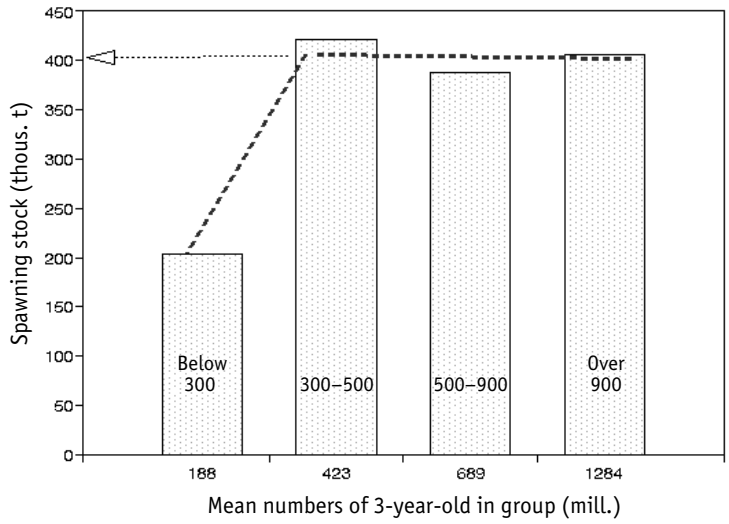

Fig. 3.24. Relationship between spawning stock levels and recruitments of North-East Arctic cod. Abscissa is the population of 3-year old recruits (millions), ordinate is spawning stock (thous. tons). Figures inside of the bars denote the range of recruit population, million species: below 300; 300–500; 500–900; over 900

Evaluation of the statistical validity of SSB differences by groups (Fig. 3.24) has shown the following. Differences between the group with very low recruitments (the first column) and the other three groups are statistically valid at the confidence level of 0.05. Differences between middle SSB and the other groups are uncertain. This means that occurrence of low, middle and high population recruitments ranged over 300–1300 million 3-year old fish is provided by a virtually equal level of the spawning stock biomas, about 400 thousand tons. Recently published work [Hylen, 2002] provides data on SSB fluctuations and North-East Arctic cod recruitments for a century. This allowed consideration of a relationship between SSB and cod stock recruitments on a much broader sample basis (Fig. 3.25).

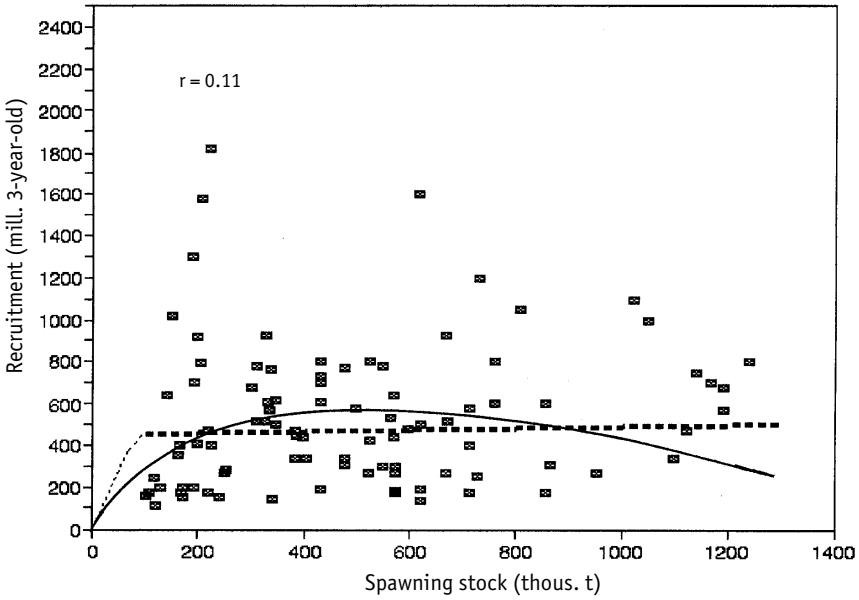

Fig. 3.25. Relationship between recruitment of North-East Arctic cod stock and spawning stock biomass. Dotted line from Beverton — Holt model, continuous line from Ricker's model. Introduction from Hylen, 2002, slightly modified. Abscissa — spawning stock (thousand tons), ordinate — recruitment (3-year old recruits, millions]

Based on actual observation data, the dependence between SSB and stock recruitment is very low (r = 0.11). The curve resulting from the Beverton–Holt model [Hylen, 2002] has no maximum and even demonstrates total absence of a relation between recruitments and SSB values in the range from 100 to 1200 thousand tons. The curve generated using the Ricker

model [Ricker, 1954] also demonstrates extremely low dependence of cod stock recruitment on the SSB level, and the right limb (in the range of large SSB) falls significantly below the measured points.

The use of the Ricker model does not cast more useful light upon determination of the relationship between recruitment and SSB value for cod stock. The results of regression analysis (Fig. 3.26) indicate virtual absence of a ny relationship between SSB and cod stock recruitments, and regression line is identical to the curve from the Beverton–Holt model (see Fig. 3.25). The dependence between SSB and recruitment «by Ricker» in the range of 200–1000 thousand tons falls within 95% confidence interval of the regression line, i.e. does not differ from it. According to the data in hand, the minimal SSB value is rather low, within the range of 100–200 thousand tons.

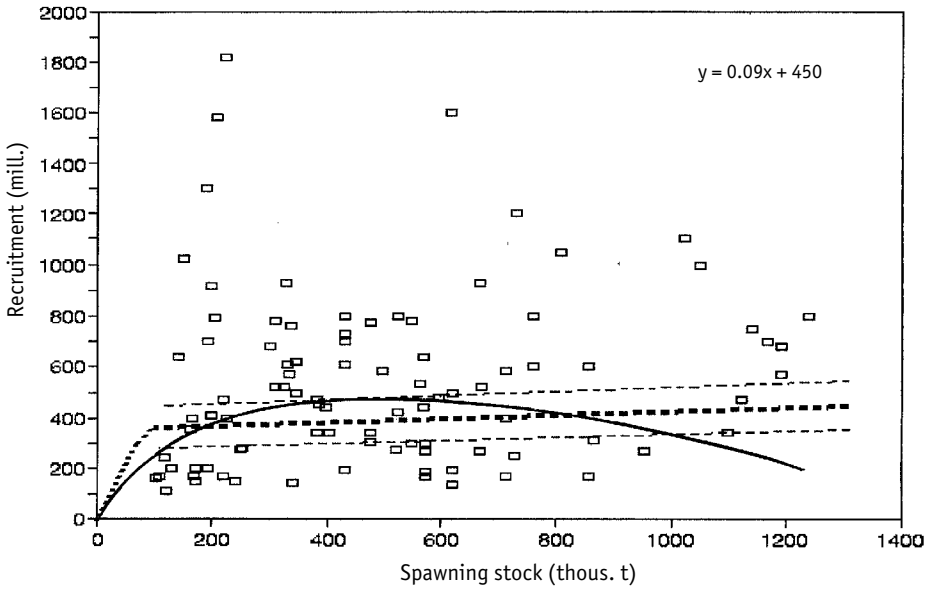

Fig. 3.26. Relationship between cod spawning stock biomass and recruitment for the period 1910–1996. Thick dotted line is the regression line; thin dashed lines denote 95% confidence interval; continuous line is the curve from Ricker model. Data from Hylen, 2002

In practice, the question about minimum SSB values that guarantees stable recruitment for a commercial stock cannot be resolved using only the statistical analysis of the SSB/R data, but also invokes biological, economic and environmental priorities [Garrod, Jones, 1974; Marshall et al., 1998]. For example, it has been shown that the frequency of occurrence of low abun-

dance generations of cod increases at SSB value below 400 thousand tons, and thus allows consideration that this value to be the minimal SSB level providing stable recruitment to the commercial cod stock [Jacobsen, 1996]. The assessment, made by the ICES working group, yielded optimal SSB values within the range of 500000–1000000 tons (on average, about 600000 tons), and a minimum value of 400000 tons. The revision of this assessment by Ulltang [1996] gave a higher value for the low, yet secure spawning resource of 500000 tons.

Dynamics of Atlantic waters inflow and herring and cod stock fluctuations

The occurrence of abundant generations of cod, herring and haddock in Arctic region is related to periods of increasing Atlantic waters passage through Faeroe-Shetland Strait. This is the strait through which the main mass of warm Atlantic water passes into the Arctic Ocean and then to the Norwegian and Barents Seas [Saetersdal, Loeng, 1987; Borisov, Elizarov, 1989].

Atlantic waters and heat delivery dynamics to the Arctic basin were analyzed for the 80-year period (1902–1983) in the monograph edited by Yu.V. Nikolaev and G.V. Alexeev [1989]. Unfortunately the measurement series was terminated several times, and to obtain more complete time series the missing values were generated by interpolation in accordance with their trends within plots from the mentioned monograph. Fig. 3.27 shows the smoothed dynamics of temperature and Atlantic water passage through Faeroe-Shetland Strait to the north. Smoothed curves of Atlantic water passage rates and temperatures within the 0–400 m layer coincide. Fig. 3.28 shows that smoothed dynamics of cod stock recruitment correlate well with dynamics of Atlantic water passage through Faeroe-Shetland Strait to Norwegian and Barents Seas.

The Atlantic spring-spawning herring population also depends upon thermal conditions of Arctic waters and, consequently, should correspond with the dynamics of Atlantic water passage rate. Fig. 3.29 shows that this is indeed so, but contrary to cod, SSB increase for herring proceeds with increasing phase of Atlantic water passage through Faeroe-Shetland Strait (1910–1940) and decreases — with decelerating water passage rates (1940–1970). The smoothed curve of herring stock recruitment (Fig. 3.30) demonstrates similar dynamics.

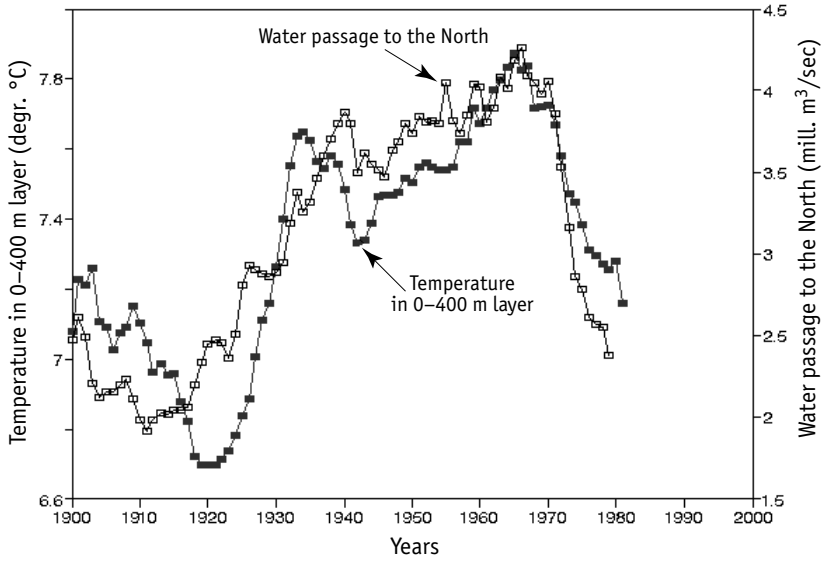

Fig. 3.27. Comparative dynamics of Atlantic water passage to the North (white squares) and mean temperature within the 0–400 m depth layer in Faeroe-Shetland strait (black squares) (10-year smoothing)

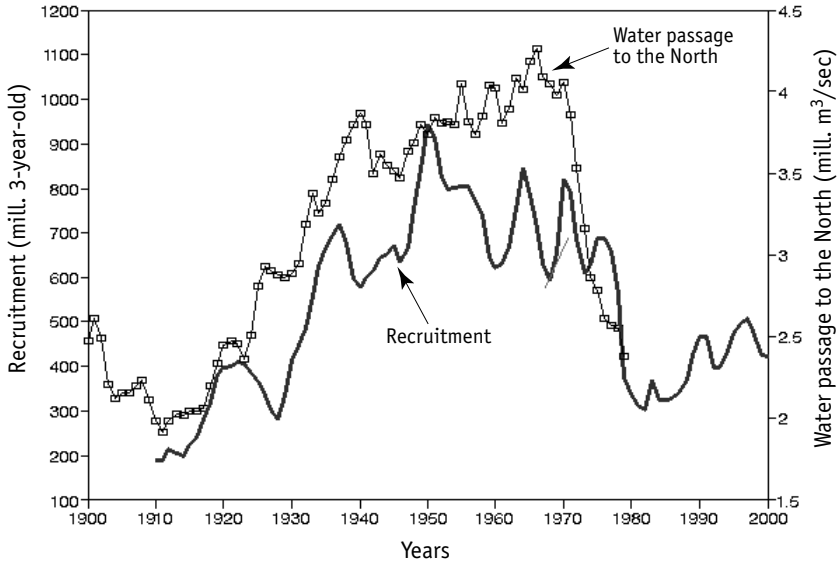

Fig. 3.28. Comparative dynamics of Atlantic water passage (thin line) to the North through Faeroe-Shetland Strait (10-year smoothing) and cod stock recruitment of North-East Arctic cod *Gadus morhua* (bold line) (10-year smoothing)

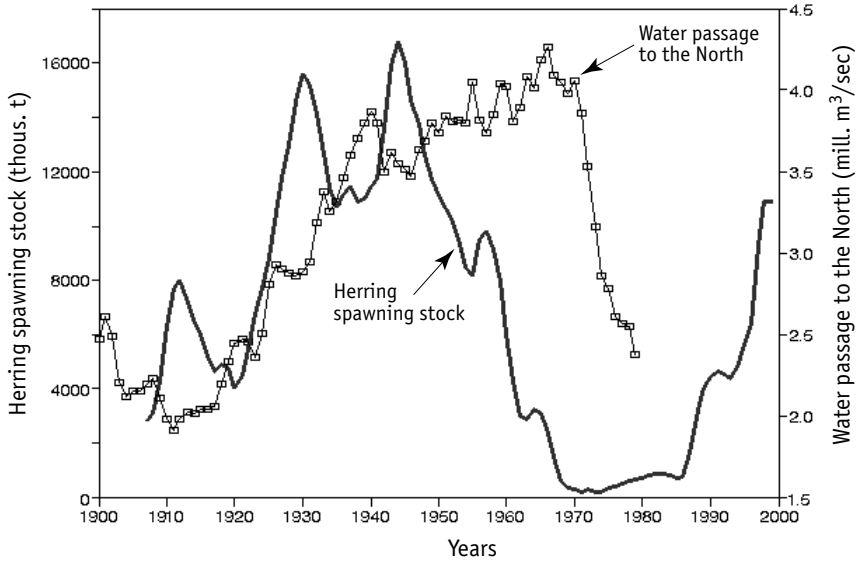

Fig. 3.29. Dynamics of Atlantic water passage to the North through the Faeroe-Shetland Strait (10-year smoothing, thin line) and spawning stock biomass of Atlantic spring-spawning herring *Clupea harengus* (13-year smoothing, bold line). Data from Toresen and Ostvedt, 2000

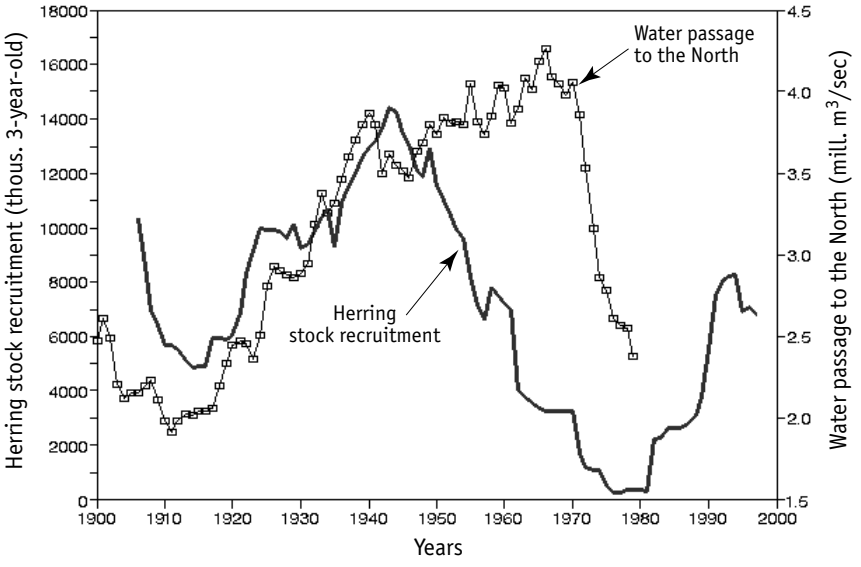

Fig. 3.30. Dynamics of Atlantic water passage to the North through the Faeroe-Shetland Strait (10-year smoothing, thin line) and recruitment of Atlantic spring-spawning herring (13-year smoothing, bold line)

Thus, the increase of herring population recruitment is related to the increasing flow phase of Atlantic water passage, whereas cod stock recruitment corresponds to general dynamics of Atlantic water passage into the Arctic basin. Differences in dynamics of herring and cod recruitments (see Fig. 3.21) are demonstrated by the 8–10 year delay of the cod recruitment curve compared with herring. These differences are, apparently, related to different responses of these species to Atlantic water inflow, although any specific mechanism causing the delay is unclear.

The average temperature in 0–200m layer within the Kola meridian reflects temperature conditions in the Norwegian Stream and its branch that spreads farthest to the East-Murmansk Stream. Comparison of the average temperature trend in 0–200 m layer within the Kola meridian with the average temperature in 0–400 m layer in the Faeroe-Shetland Strait (Fig. 3.31) shows that temperature within the Kola meridian increases in the phase with rapidly increasing Atlantic water passage during 1900–1930 and decreases with it during 1950–1960.

Unfortunately, since 1983 no regular measurements of rates and stream passage through the Faeroe-Shetland Strait were carried out. The long-term dynamics of cod and herring stocks may prove that Atlantic water inflow to

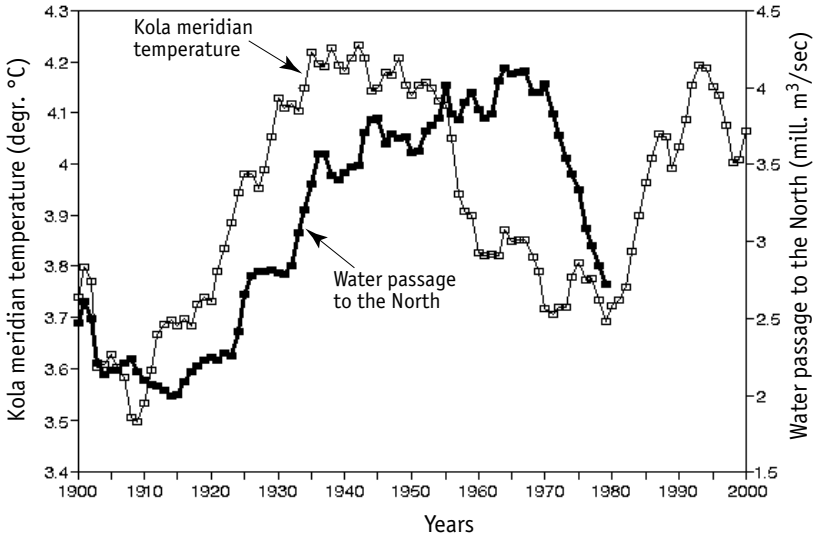

Fig. 3.31. Comparative dynamics of mean temperature in 0–200 m layer within the Kola meridian (thin line) and Atlantic water passage to the North through Faeroe-Shetland Strait (bold line) (13-year smoothing)

Arctic also demonstrates approximately 60–70-year fluctuations. Air temperature dynamics in Iceland, Jan Mayen Island and Spitsbergen are determined by heat delivery from Atlantic. Fig. 3.32 shows that air temperature change at Spitsbergen corresponds to long-term dynamics of Atlantic water inflow to Arctic basin.

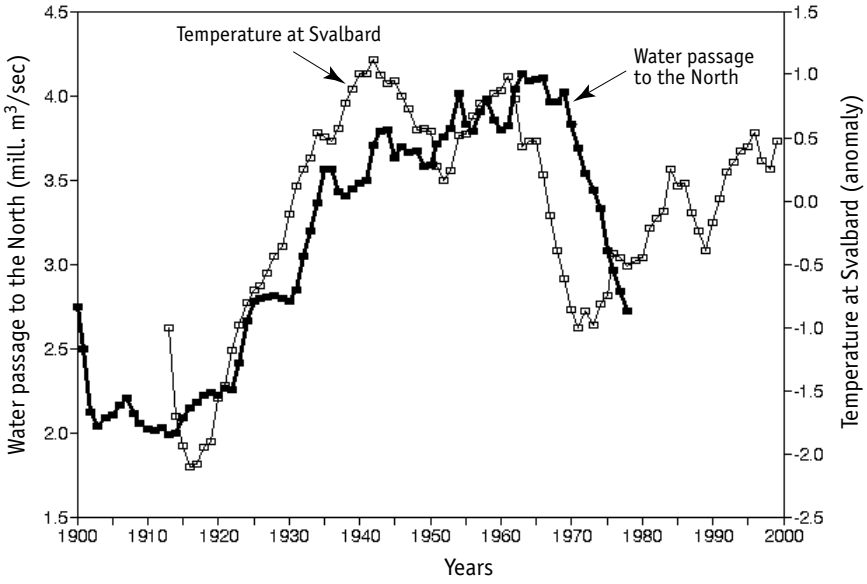

Fig. 3.32. Dynamics of Atlantic water passage to the North through Faeroe-Shetland Strait (bold line) and air surface temperature at Spitsbergen (thin line) (13-year smoothing)

Thus, dynamics of herring stock recruitment is closer to the Kola meridian temperature curve, whereas dynamics of cod stock recruitment is closer to smoothed curve of the Atlantic water inflow to Arctic basin and temperature trend in 0–400 m layer in Faeroe-Shetland Strait.

Cod stock and ice regime fluctuations in Arctic region

The long-term fluctuations of the ice coverage of Arctic seas are one of the most important natural factors affecting the cod commercial stock population. Time of the spring ice retreat depends on the long-term changes in the climate of the region and causes direct effect on the development of phyto-

and zooplankton, the forage base for larvae of cod, herring, and other commercial fishes.

The fluctuations of Barents Sea ice coverage for almost 100 years are described in Chapter 2. As shown, the long-term fluctuations of the ice-free water area [Averkiev et al., 1997] correlate with the dynamics of Global dT with approximately a decade delay (see Fig. 2.15,*a*). As the ice-free water area curve is shifted back by 8 years (see Fig. 2.15,*b*), it virtually coincides with Global dT. Ice-free water area dynamics delay relative to this temperature curve is most likely caused by the relative inertness of thermal processes in the ocean-atmosphere system in Arctic basin.

Resembling the Global dT curve, the curve of ice-free water area demonstrates a secular increasing trend, about 0.3% per year. During the same time, the previously discussed curves of multiyear herring and cod recruitment dynamics have no increasing secular trend, and their fluctuations are reflected by long-term oscillations in accordance with the detrended Arctic dT or Global dT rather than by absolute changes of temperature.

Comparison of the ice-free water area dynamics and the North-East Arctic cod stock recruitments (Fig. 3.33) shows that both curves correlate

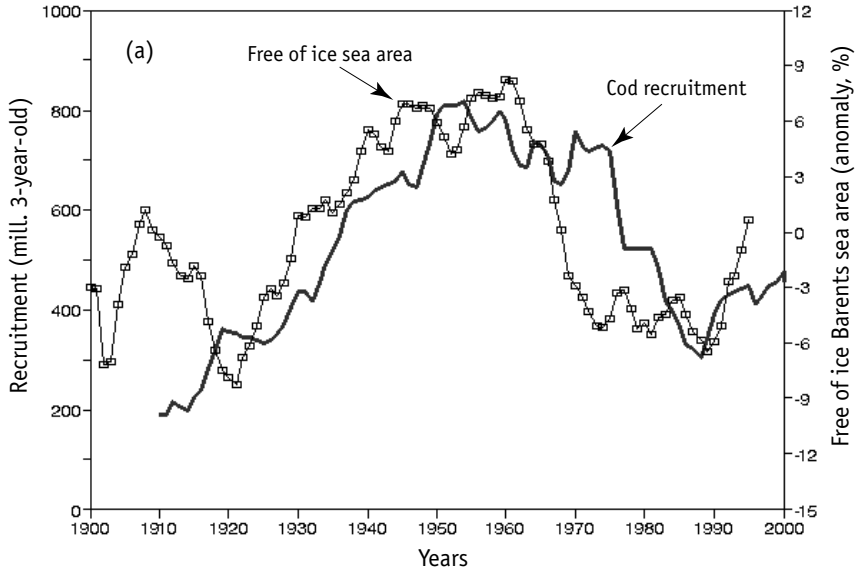

Fig. 3.33. Comparative dynamics of cod (3+, *Gadus morhua*) stock recruitments, (bold line, 10-year smoothing) and detrended ice coverage of Barents sea (thin line) (*a*). See p. 88

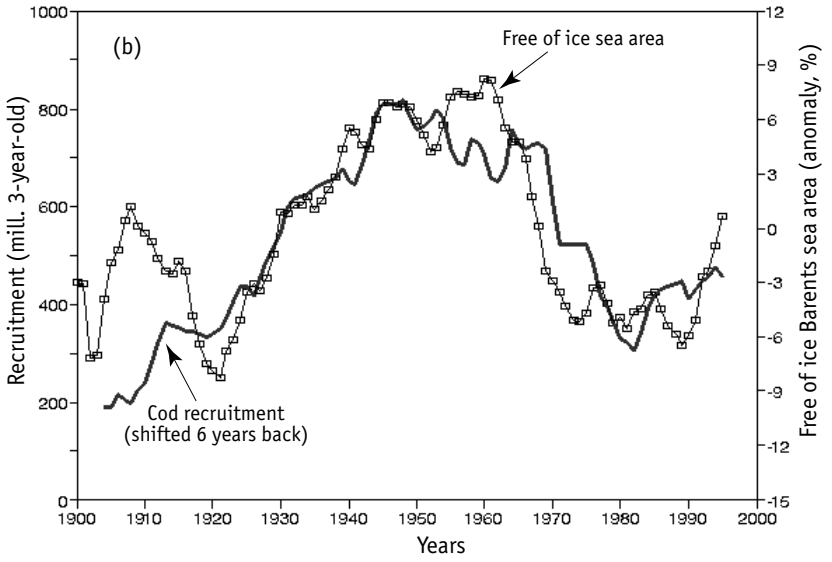

Fig. 3.33. Comparative dynamics of cod (3+, *Gadus morhua*) stock recruitment curve shifted by 6 years back (left) (*b*), (13-year smoothing). See p. 87

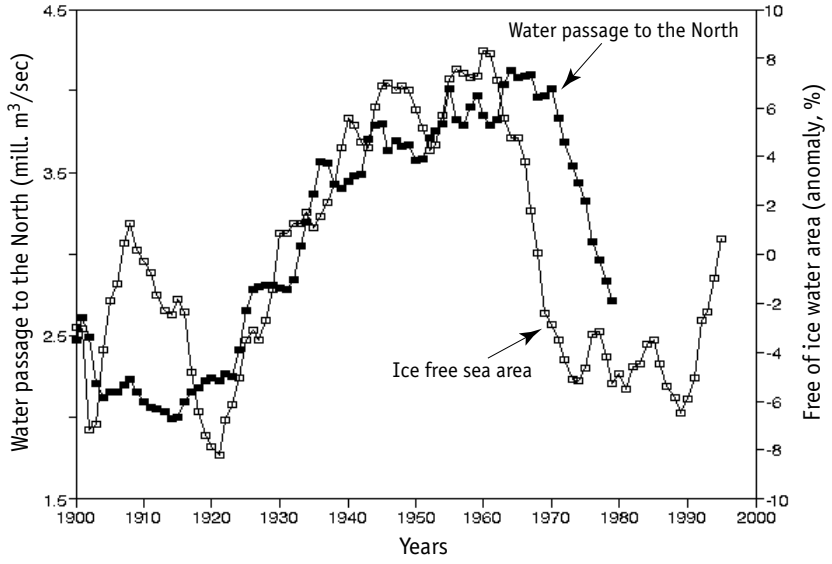

Fig. 3.34. Comparative dynamics of Atlantic water inflow to Arctic region through Faeroe-Shetland Strait (dark squares) and ice-free water area of Barents Sea (light squares), 13-year smoothing

quite well, but that recruitment is lagged by 5–6 years (Fig. 3.33,*a*). Shifting the Recruitment curve 6 years earlier (Fig. 3.33,*b*) leads to its virtually full coincidence with the ice-free water area curve.

The main source of heat delivered to Arctic basin is warm water inflow from North-Atlantic Stream through Faeroe-Shetland Strait [Nikolaev, Alexeev, 1989]. It is reasonable that ice coverage dynamics in the Barents Sea must correlate with the incoming volume of water from Atlantic. Fig. 3.34 shows total correspondence of ice-free water area dynamics in Barents Sea to water and heat delivery from Atlantic to Arctic region.

Hence, the above data show that the long-term induces such as Global dT, Arctic dT, the mean temperature in the 0–200 m water layer within the Kola meridian, Atlantic water delivery to Arctic basin and ice-free water area dynamics in Barents Sea (with respect to time shifts) correlate well with each other and can be used to characterize climatic changes in the region.

Forecasting of herring and cod population fluctuations in Arctic region

Based on the analysis of predominant periodicity of climate and biota (Chapter 1), a stochastic model for prospective forecasting of some commercial fish stock fluctuation dynamics has been offered [Klyashtorin, Lyubushin, 2005], see Chapters 7 and 8. The model is based on the analysis of extended data showing that over the recent thousand years 50–70-year cyclic changes of temperature were predominant. Similar periodicity was predominant over the 140-year period of instrumental observations and will likely be preserved for at least the next hundred years (see Chapters 1 and 2).

Fig. 3.35 shows the comparative dynamics of detrended Global dT cyclic fluctuations and the Atlantic spring-spawning herring stock, obtained from this model. It may be suggested that the herring population will reach a maximum during the first decade of the century, after which it will begin gradually decrease to a minimum in the mid 2020s.

As concerns forecasting of the prospective North-East Arctic cod population, it is suggested that its changes will occur similarly, with approximate 10-year delay relative to herring stock recruitment dynamics. It should be

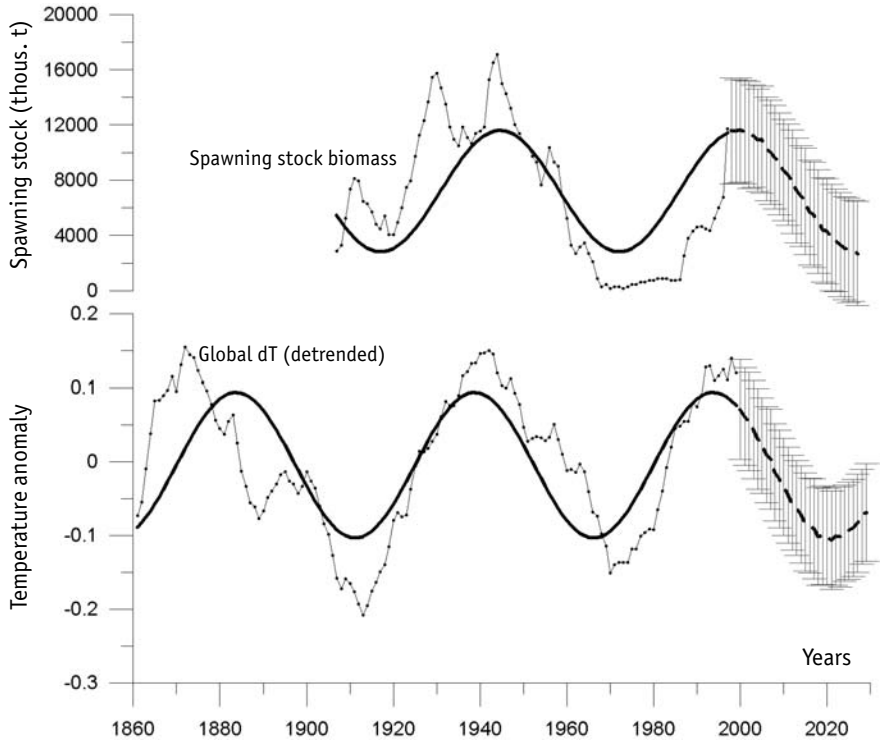

Fig. 3.35. Cyclic dynamics of detrended Global dT (lower curve), Atlantic spring-spawning herring *Clupea harengus* stock biomass (upper curve), 60-years harmonics (bold line). Modeled predictive trend for the 21th century is marked with vertical hatches

taken into account that the smoothed cod population numbers will show approximately 10-year fluctuations within the background of changes related to climate.

Dynamics of climatic indices and catches of the major commercial fish in Pacific region

Fig. 3.36 shows dynamics of climatic index and catch changes for abundant commercial species in Pacific region. Clearly, population outbursts of Pacific salmon, Japanese and Californian sardines that occured within the periods of 1920s–1940s and 1970s–1990s corresponded to the rises of Glo-

bal dT, zonal ACI and regional Pacific climatic indices PDO and ALPI (for index definitions refer to Chapter 1). Catch and climatic index fluctuations proceed almost synchronously, with approximately 60-year periodicity.

As regards other major fishery species with shorter series of catch statistics, according to observations [Serra, 1983], a substantial increase of the Peruvian sardine population was observed during the 1920s– 1940s period e.g. simultaneously with the population outbursts of Japanese and Californian sardines [Elizarov et al., 1989]. Over the period of 1970–2000, the Chilean Jack mackerel population outburst also occurred synchronously with fluctuations of climatic indices and populations of other commercial species (Fig. 3.36). This suggests that long-term fluctuations of the population of these species are related to dynamics of climatic indices for Pacific region.

Two periods of increased fish productivity, 1920–1930 and 1970–2000, are significant given the number commercial species involved and the magnitudes of catches. In the first period, the maximum summed total catches of Japanese sardine, Pacific salmon and Californian sardine reached 4.8 million tons. In the second period these three species were added by pollock, Peruvian sardine and Chilean Jack mackerel. Total maximum catch of these six species reached 22 million tons. The comparison of total catch dynamics for major commercial species in Pacific region (except for Peruvian anchovy) (Fig. 3.37) shows that the catch maxima during the periods of 1920–1950 and 1970–2000 are observed during the phase of Global dT rise rather than at its peak. Deceleration of the catch rise and then its decline is initiated at the deceleration phase of Global dT rise and stops with the onset of the Global dT decrease phase.

However, the dynamics of catches of various species within the same climatic period are not completely identical. As shown in Fig. 3.38, catch maxima of Alaska pollock, Japanese, Californian and Peruvian sardines virtually coincide, falling within 1988–1990, whereas the catch maxima of Pacific salmon and Chilean Jack mackerel are observed almost 10 years later. Full synchrony of fluctuations, given the differences in biology and duration of the lifecycle of the species, is not unexpected. It is of greater importance that catch increase and decrease cycles for these species occur within the same climatic epoch (1970–2000) with the maximum in the mid to late 1990s.

Time series of catch statistics for the above described major commercial species are rather short. This does not allow analysis of the correspondence between fluctuations of catches and changes in climatic indices for all relevant species. For salmon, Japanese and Californian sardines such correla-

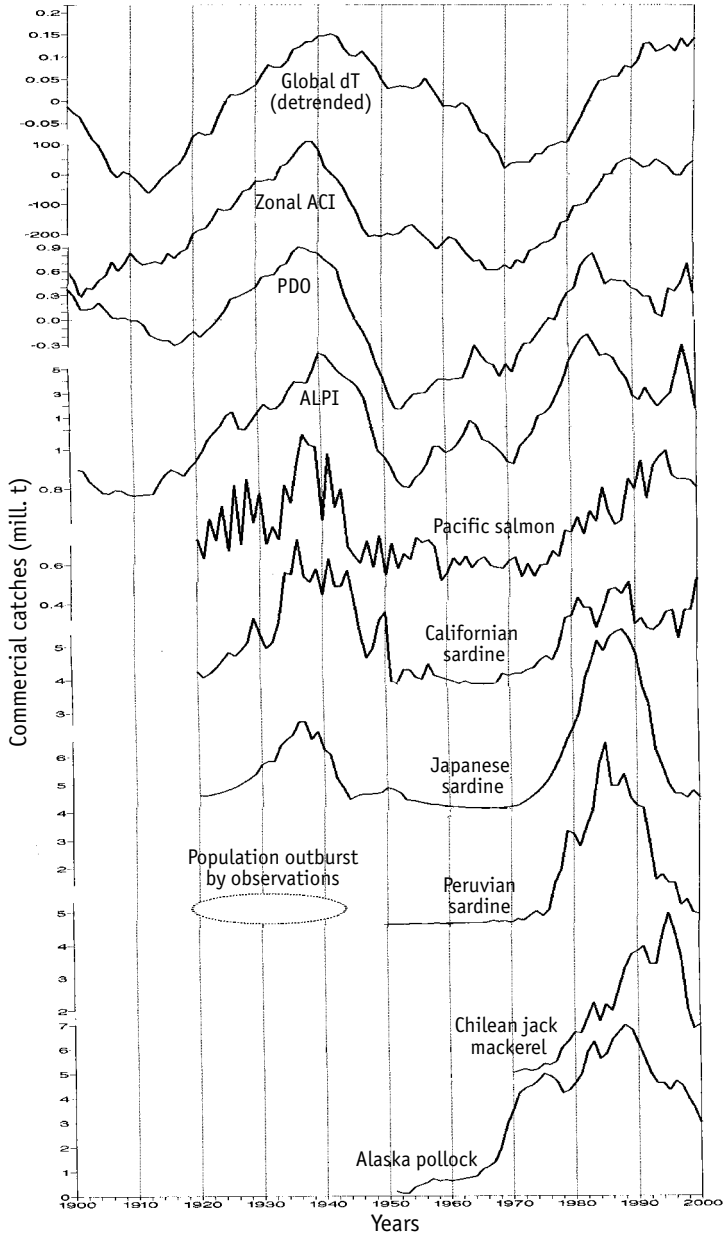

Fig. 3.36. Comparative dynamics of climatic indices and commercial catches of major Pacific commercial species (without anchovies). Climatic indices: Global dT (detrended), Pacific Decadal Oscillation (PDO), Aleutian Low Pressure Index (ALPI), zonal Atmospheric Circulation Index (ACI). Commercial catches (from up to low): Pacific salmon, Californian sardine, Japanese sardine, Peruvian sardine, Chilean Jack mackerel, and Alaska pollock

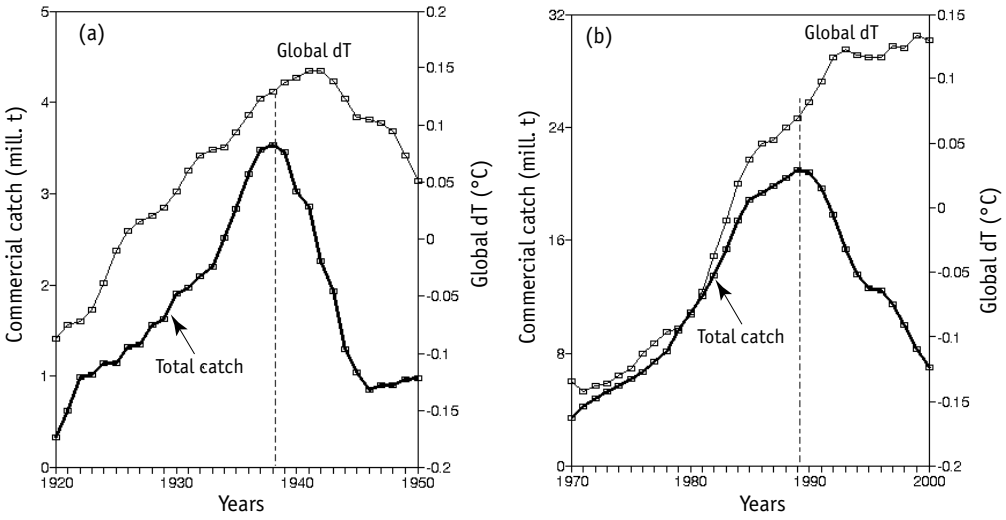

Fig. 3.37. Comparative dynamics of commercial catches of major Pacific commercial species (except for Peruvian anchovy) and Global dT: *a* — total commercial catch for period of 1920–1950 (Pacific salmon, Californian sardine, Japanese sardine); *b* — total catch for the period of 1970–2000 (Pacific salmon, Japanese sardine, Californian and Peruvian sardines, Chilean Jack mackerel, and Alaska pollock). Vertical dotted line indicates the catch maximum

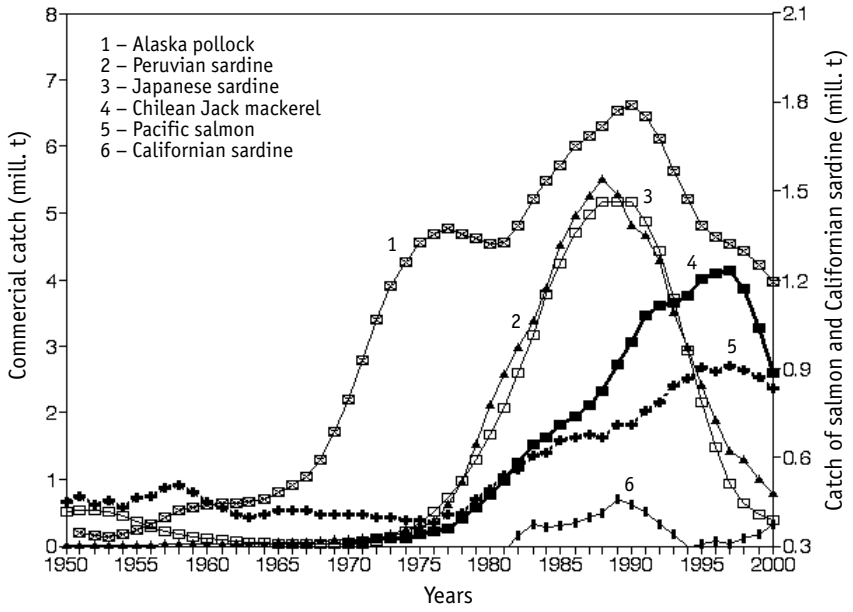

Fig. 3.38. Comparative dynamics of catches of major Pacific commercial species (except for Peruvian anchovy) in the period of 1950–2000, (5-year smoothing)

tions were observed since 1920s and only since 1950s for Peruvian sardine, and are confirmed by data from fishery-related observations, obtained within the 1920s–1940s period. For Alaska pollock and Chilean Jack mackerel, there is only a single observed cycle of catch fluctuations available, which does, however, correspond with both the dynamics of catches of other species and the approximately 60-year climate fluctuations.

Japanese chronicles provide information on the long-term increases of Japanese sardine population over almost 400 years. During the periods of growth, fluctuations of Japanese sardine resource populations promoted people's influx to fisheries settlements, whereas people left these settlements during the periods of sardine catch decrease [Kawasaki, 1994]. Fig. 3.39 shows that the periodicity of Japanese sardine population outbursts correspond to approximately 50–60-year cyclic temperature fluctuations according to analysis of Greenland ice core data and instrumental measurements (see Chapter 1).

Approximately 60-year periodicity of Californian sardine population outbursts over the last 1500 years was demonstrated in the work by Baumgartner et al. [1992], see Chapter 1.

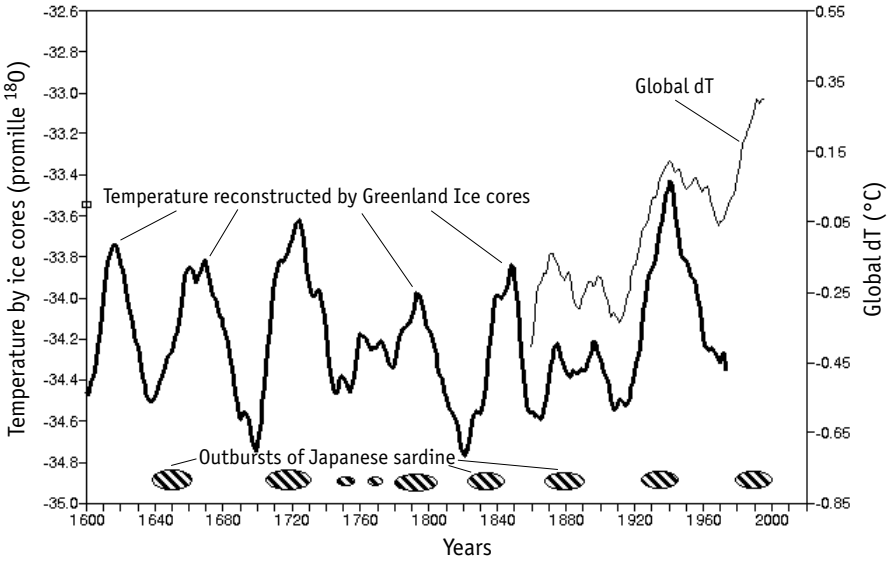

Fig. 3.39. Cyclic temperature fluctuations and outbursts of Japanese sardine over the last 400 year (1640–1880) from the data derived from Japanese chronicles and the commercial statistics available beginning in the period of 1920–1998. The bold line is temperature reconstructed by Greenland ice cores (13-year smoothing), the thin line is the Global dT, ellipses show sardine outbursts

Data showing approximately 60-year cyclic fluctuations of Pacific salmon productivity are referred to in previous studies by various authors [Klyashtorin, Smirnov, 1992; Beamish, Bouillon, 1993; Klyashtorin, Smirnov, 1995].

Correspondence between climate fluctuations and long-term dynamics of populations is also observed for North Pacific pinnipeds, such as fur seals (*Callorhinus ursinus*) and sea lions (*Eumetopias jubatus*) [Vladimirov, 1997, 2002]. It has been shown that long-term fluctuations in the population of pinnipeds relate to the large-scale climatic changes, with the Global dT and ACI dynamics, in particular.

Ice regime and pollock biomass dynamics in the Berings Sea

For Bering Sea ecosystems, dynamics of the ice regime, time of ice cover retreat in spring and ice-free water area are of the major importance.

Analysis of the multiyear dynamics of Berings Sea ice coverage have shown that due to increasing Global dT the southern ice border was moved northward by 2 degrees of latitude during the period of 1972–1993 [Willie-Echeverria, Wooster, 1998]. The populations of Alaska pollock (*Theragra chalcogramma*) and polar cod (*Boreogadus saida*) moved northward simultaneously. Dynamics of ice-free seawater area and temperature of the ocean surface (PDO index) are shown in Fig. 3.40,*a*. Clearly, the ice-free seawater area increases with the average temperature of the ocean surface (PDO) with a 8–10-year lag. Shifting of the «ice» curve back by 8 years shows virtually complete coincidence with PDO curve (Fig. 3.40,*b*).

One may suggest that fluctuations of Alaska pollock, the major commercial species in the Bering Sea, are related to the changes in temperature and ice-free water area. Comparison of pollock biomass dynamics and Pacific decadal PDO fluctuations (i.e. the average temperature of the ocean surface) demonstrates a rather high correlation (Fig. 3.41). At the same time, comparison of the pollock biomass and ice-free seawater area of Bering Sea, has shown that the changes of the latter (Fig. 3.42) are delayed by approximately 10 years.

Comparison of Figs. 3.41 and 3.42 suggest the major role of temperature changes in the Bering Sea region e.g. long-term dynamics of PDO index characterizing the mean temperature of the ocean surface. It seems possible that the ice situation affects dynamics of pollock population, however, indi-

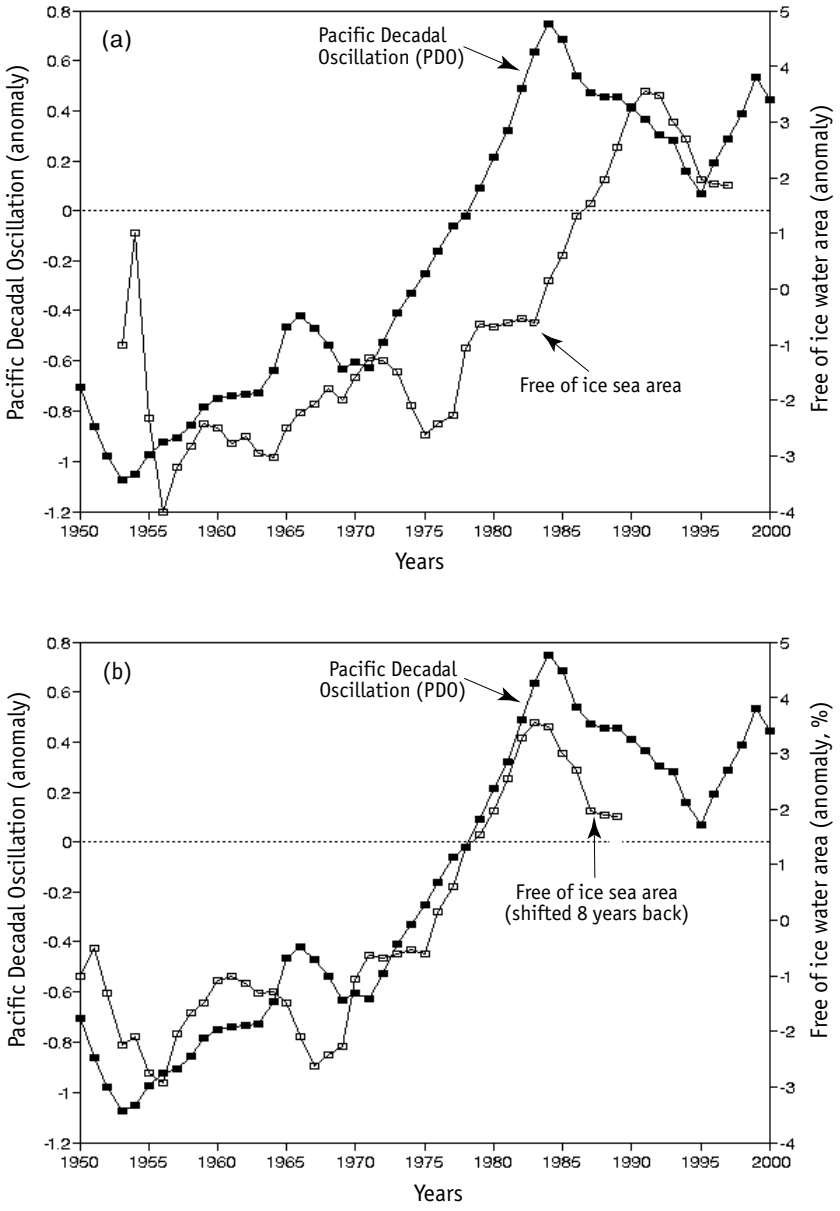

Fig. 3.40. Comparative dynamics of ice-free seawater area (*a*) of Berings Sea (light squares) and Pacific Decadal Oscillation (PDO) (dark squares) for the period of 1955–1995 (15-year smoothing); the same with the ice-free seawater area curve shifted back (to the left) by 8 years (*b*). Data from Ponomarev et al., 1999; Niebauer, 1999

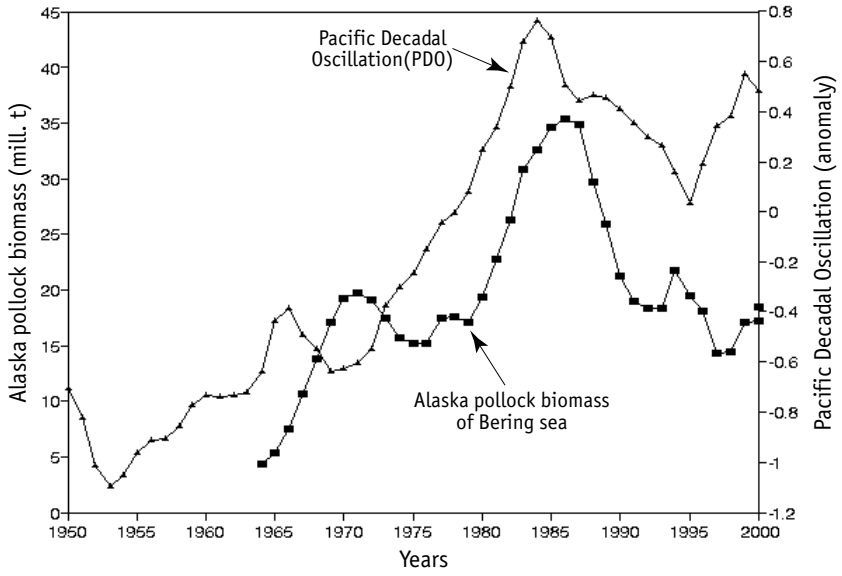

Fig. 3.41. Comparative dynamics of Pacific Decadal Oscillation index (PDO, triangles), (15-year smoothing) and Bering Sea Alaska pollock biomass (dark squares) (3-year smoothing). Data from Bulatov, 2003; Bulatov, 2004

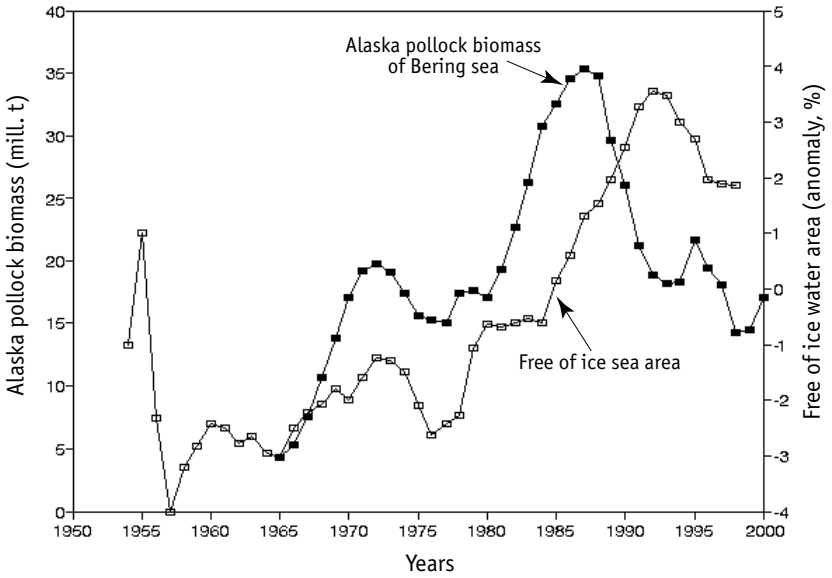

Fig. 3.42. Comparative dynamics of Alaska pollock biomass (dark squares, 3-year smoothing) and ice-free area in Bering Sea (light squares, 5-year smoothing)

rectly, via temperature change. One may suggest that the pollock biomass increases during climatic warming periods is a result of direct effects of temperature on acceleration of fry development and growth, ice-free seawater area increases, earlier development of zooplankton, and prolongation of the region's algal vegetation season.

CLIMATE AND FLUCTUATIONS IN POPULATION OF PACIFIC SALMON

Due to reliable multiyear commercial fishery statistics, long-term changes in catches of Pacific salmon may provide good indicators of ecosystem and climatic changes in the North Pacific [Beamish, Bouillon, 1993; Hare, Mantua, 2000; Ueda et al., 2001].

By 90% Pacific salmon catches comprise three major species: pink salmon (*Oncorhynchus gorbuscha*, 37%), dog salmon (*O. keta*, 33%), and sockeye salmon (*O. nerka*, 20%). Statistics of salmon catches during the recent 80 years (Fig. 3.43) were added to data on Japanese catches in the Russian Far East territory for the period of 1930–1943. During these years, the summed average catches of pink salmon and dog salmon in Japanese concessions within the Russian Far East reached 200 thousand tons [Klyashtorin, Smirnov, 1992].

Fig. 3.43 shows that dynamics of total catches of salmon correspond with Global dT fluctuations: catch increased in the 1920s–1930s (with the maximum above 1 million tons), decrease in the 1950s–1960s, and a rise in 1970s–1990s also reaching the 1 million tons level. In the late 1990s a reduction of catches was observed, which by the early 2000s was 20% below the mid-1990 high. The scheme of long-term salmon catch fluctuations in the 20th century can be represented as double waved change of their population, with a rise during the 1920s–1940s, a decrease in the 1950s–1960s and a new rise during the 1970s–1990s.

The increase of Pacific salmon catches in the 19th century was observed during the 1870s–1880s, indicated by data on dynamics of salmon catches in Japan [Kaeriyama, 1989; Klyashtorin, Smirnov, 1992; Beamish, Bouillon, 1993]. Over the last 130 years fluctuations in the overall Pacific salmon population had a periodicity of 55–65 years, with maxima in the late 1870s, early 1940s, and late 1990s.

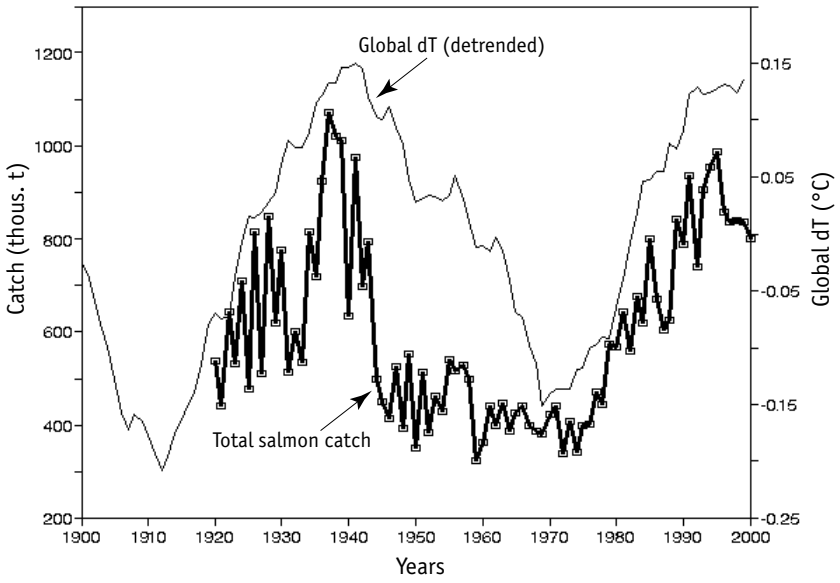

Fig. 3.43. Long-term dynamics of total Pacific salmon catch (bold line) and detrended Global dT (thin line)

Dynamics of total salmon catches resemble curves of both global and Pacific climatic indices [Klyashtorin, 1997, 1998a, 2001]. Oceanic foraging areas of American and Asian salmon significantly overlap, and, after yearling migration to the ocean, both stocks are apparently affected by the same climatic processes. Catch dynamics of Asian and American salmon catches are generally similar, but have specific regional features (Fig. 3.44). An abrupt (almost by 500 thousand tons) decrease in Asian salmon catches in the period of 1943–1950 is explained by almost full cessation of the Japanese salmon fishery after the World War II. The dashed line in Fig. 3.44 shows probable curve of Asian catches in the hypothetical case of continuation of the pre-WWII Japanese fishery catch contribution.

In the 20th century, the first maximum of American salmon population occured during the period of 1934–1938, whereas Asian salmon population reached its maximum in the early to mid 1940s (see the curve of probable trend of Asian salmon catches in Fig. 3.44). The second peak of American salmon population was observed in 1994–1996. Asian salmon population increased in 1998–2000. This may suggest that changes in population (and catches) of American salmon precede those of Asian stocks by 6–8 years. This hypothesis should be clarified in the near future. Despite the various

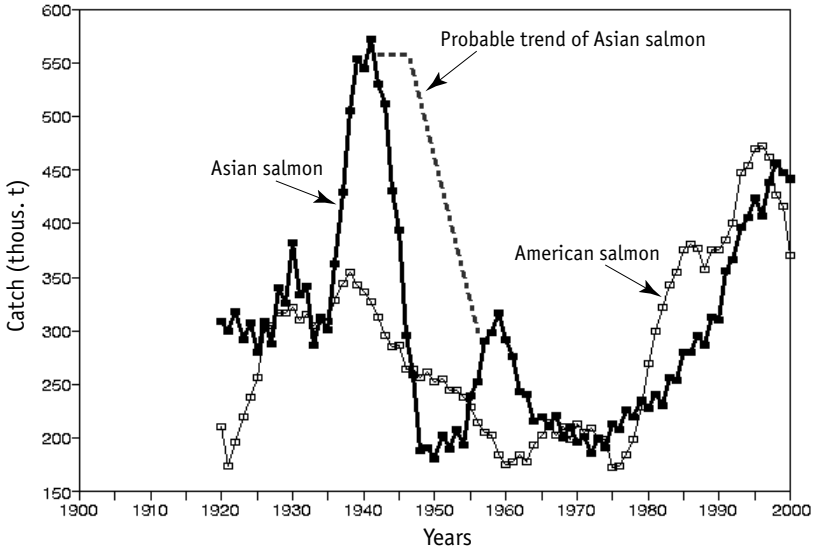

Fig. 3.44. Comparative dynamics of total catch of Pacific, American (white squares) and Asian (bold line) salmon. Dashed line represents a probable trend of Asian salmon catch adjusted collapse of Japanese salmon fisheries in the period of 1943–1950

features of salmon catch dynamics near each of the continents, long-term fluctuations in the populations of both Asian and American salmon occur almost synchronously and correspond well with the dynamics of long-term detrended Global dT fluctuations.

Salmon are not the most abundant species that utilize non-commercial resources (mainly plankton), distributed in the North Pacific Ocean. The long-term fluctuations of salmon catches coincide with those of Japanese and Californian sardines, as well as some other abundant commercial species which together contribute to the Pacific Ocean total catch, today exceeding 20 million tons [Klyashtorin, 1998a, 2001]. Dynamics of salmon and Japanese sardine catches are rather close, but maxima of sardine catches precede salmon catch maxima by approximately 10 years (Fig. 3.45). Almost synchronous fluctuations of fish productivity of sardines, salmon and other major commercial species of North Pacific are, apparently, related to the long-term climate fluctuations [Klyashtorin, Smirnov, 1995; Klyashtorin, 1998b].

Another feature of the latter «wave» of Pacific salmon population during the period of 1970–2000 is the increase of artificially reproduced salmon, from which catches within the period of 1980–1990 equaled 250 thousand tons e.g. about one forth of total salmon catch. Almost 80% of this amount

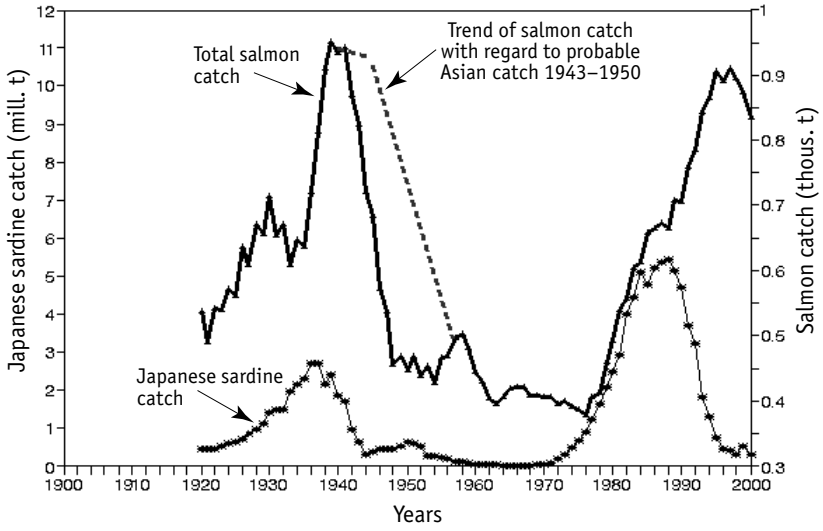

Fig. 3.45. Long-term dynamics of total catches of Pacific salmon (bold line) and Japanese sardine (asterisks) (5-year smoothing). Dashed line represents probable catch trend, corrected for collapse of Japanese salmon fisheries in the period of 1943–1950

is chum salmon, produced in the salmon hatcheries of Japan. Meanwhile, in the recent 50 years, naturally reproduced salmon catches (mostly of Asian stocks) have decreased by 250 thousand tons, i.e. a major portion of «wild» salmon were substituted by «farm raised» ones. Almost a half-century history of artificial reproduction of chum salmon in Japan may be considered as a large-scale ecological experiment, which allows relevant judgements about fluctuations of Pacific salmon population related to the climate changes [Ueda et al., 2001; Mayama, Ishida, 2003].

Dynamics of chum salmon fry yield from Japanese salmon farms and commercial return of farm fish are shown in Fig. 3.46. In the period of 1960–1980 chum salmon juveniles releases increased from 300 thousand to 2 billion individuals and, simultaneously, catches increased from 7 to 100 thousand tons. In the period of 1980 to 2001 the quantity of juveniles produced was virtually constant (about 2 billions). During this period, commercial returns increased continuously until 1996 (88 million individuals), then began decreasing, despite the same level of juveniles releases, and landings decreased by almost 40% by 2001.

The objective index for salmon survival, which is independent of the yield, is the index of commercial return (percentage of adult fish return as

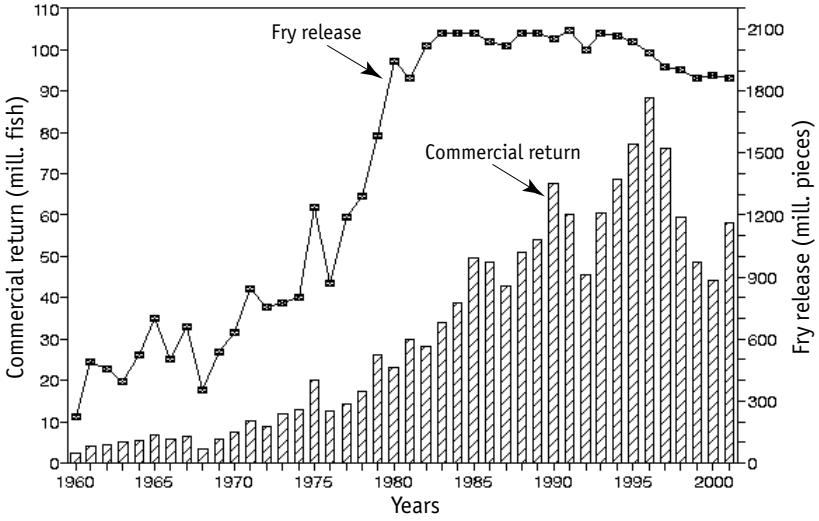

Fig. 3.46. Comparative dynamics of dog salmon fry release from Japanese salmon hatcheries (dark squares) and total number of adult fishes in commercial landings (bars). Data from Mayama and Ishida, 2003

compared with the juveniles releases). Dynamics of the commercial return are shown in Fig. 3.47. Since the mid 1960s, commercial return continuously increased, indicating an improvement of salmon survival in the ocean.

After 1980 the fry production was stabilized at the level of 2 billion individuals. within the 1980–2001period, changes in the Japanese dog salmon population, within the background of virtually unchanged quantity of the juveniles releases, occured as shown using the fluctuations in the commercial return index, that reflects changes in the natural conditions of the ocean that either increase or decrease survival of the salmon fry. Fig. 3.47 shows that the commercial return index reached its maximum in 1996, but decreased over the next 5 years by about 40%. In this relation, total return (and catch) of Japanese chum salmon also decreased by approximately 40%. The inflection of commercial return index curve is observed in 1996, indicating that deterioration of conditions supporting salmon survival in the ocean, related to changes in climatic conditions, occured in the mid 1990s.

This change of commercial return index does not indicate particular reasons for survivability changes. However, it is known that the salmon population is mainly determined by juveniles mortality during its early period of marine life [Karpenko, 1998]. As shown by multiyear studies of Japanese dog salmon fry survival in the early marine period [Mayama, Ishida, 2003],

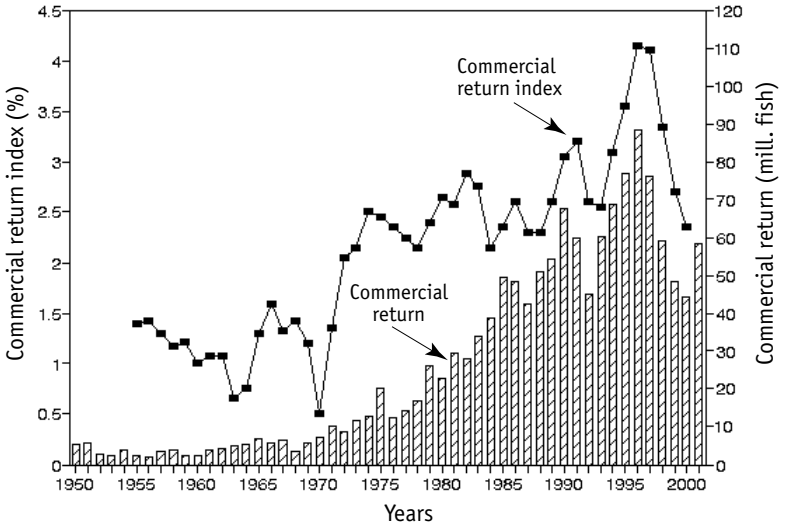

Fig. 3.47. Dynamics of chum salmon commercial return index (black squares) and total number of adult fishes in commercial return (bars). Data from Kaeriyama, 1989; Kaeriyama, Urawa, 1992; Kaeriyama, 1998; Mayama, Ishida, 2003

increasing the quantity of chum salmon juveniles from fish hatcheries into the sea substantially increases their density in the nearshore zone, and that decreases their growth rate. As shown in some studies [Mayama, Ishida, 2003; Starovoitov, 2003], dog salmon yearlings migrating from the shore of Japan into the ocean accumulate in the northern area of the Sea of Okhotsk and then move into oceanic foraging areas through the middle Kuril straits. This early period of life is critical for survival of 0+ dog salmon and significantly depends upon forage abundance, temperature, oceanographic conditions in the region, and as well, predator abundances. Unfortunately, there are no available data on the effect of hydrological conditions on the early life history survival. However, similar to changes in Japanese sardine population, long-term dynamics of Japanese chum salmon population may be another index of climatic changes in the region.

Population abundance and salmon growth in the ocean

In 1996, catches of hatchery-produced Japanese chum salmon reached 280 thousand tons which was an order of magnitude greater than historical maximum catch of chum salmon in Japan during 1870–1880 [Kaeriyama,

1989, 1999]. Such a high increase of chum salmon population owing to Japanese fish hatcheries raises questions about possible limitations of forage resources in the open sea for feeding chum and other salmon species, as well as about increasing competition for forage in the feeding areas of the ocean [Mayama, Ishida, 2003].

Multiyear observations of Japanese chum salmon growth show that as the commercial resource population increased, the length and individual weight of returning mature fish decreased. During the period of 1963–1989, simultaneously with the fish growth deceleration the average age increased from 3.8 to 4.5 years [Kaeriyama, 1998]. This might be a consequence of the so-called «density-dependent» control, i.e. limitation of salmon growth rate due to their population increase per unit oceanic foraging area. It is also of high practical interest how forage carrying capacity of these areas limit eventual salmon culture breeding potentials.

Fig. 3.48 shows dynamics of Japanese chum salmon length changes for the three major age groups in catches for the 43-year period (1953–1995). The average individual length of fish slowly increased during 27 years in the period of 1953–1980, then the growth rate began rapidly decreasing until 1987 and after that stabilized at the lower level.

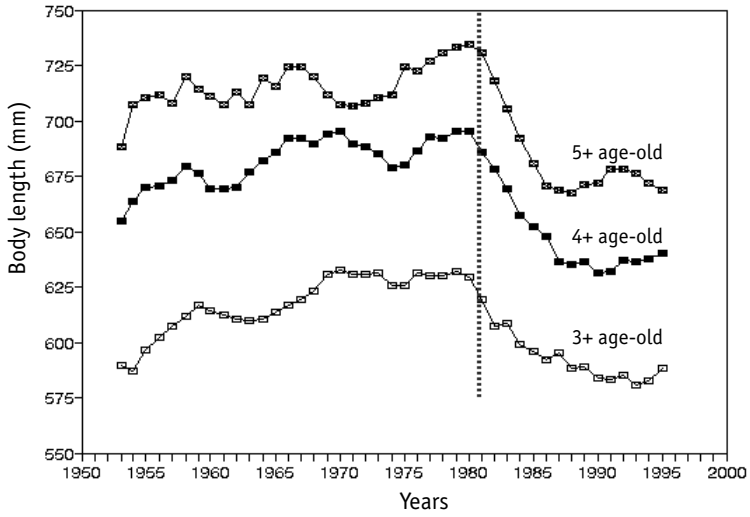

Fig. 3.48. Body length dynamics of adult chum salmon (*Oncorhynchus keta*) in three major commercial age groups (3+, 4+, 5+) for the 43-year period of 1953–1995 (5-year smoothing). Vertical dotted line shows the onset boundary of growth rate deceleration. Data from Kaeriyama, 1998

The same data is presented in Fig. 3.49 in the form of relative body length changes show close dynamics of the fish growth for all three age groups. As chum salmon population increased from 3.5 to 25 million individuals, their body length did not decrease, but slightly increased. While as the resource population increased from 20 to 40 million individuals (1980–1987), the average body length of fish decreased by 8%, whereas the weight decreased by 12% [Kaeriyama, 1998]. Further increase of the stock population from 40 to 80 million individuals (1987–1996) was not accompanied by a growth rate decrease. Thus in the period of 1953–1996 the growth of Japanese chum salmon decreased only during the 1980–1987period.

A decrease of individual fish body weight causes an approximately 12% biomass loss within the commercial resource. This occurred within the background of increasing population abundance from 20 to 70 million individuals, with the resulting increase of the commercial resource biomass by almost 300%. Thus, 10–12% potential losses of the biomass due to deceleration of individual fish growth rates are overlain by an increasing total biomass of

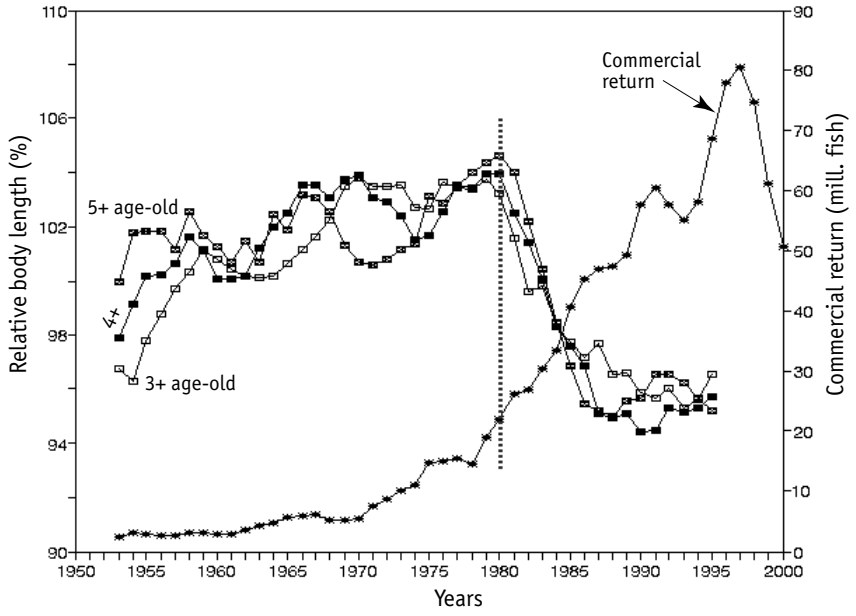

Fig. 3.49. Comparative dynamics of the relative change of body length (% of average) for three age groups of chum salmon and number of individuals in the commercial return (asterisks) for the period of 1953–1995 (5-year smoothing). Vertical dotted line shows boundary of growth deceleration. Data from Kaeriyama, 1998

salmon by almost 3 times. The effect of some individual body weight decrease during a significant increase of the commercial resource population of chum salmon is quite real and may be explained by a significant expansion of the foraging area and the resulting increase in energy costs due to the expanded searching effort and related energy requirements.

Commonly, the effect of chum salmon growth deceleration is approximated by linear equations [Kaeriyama, 1998; Helle, Hoffman, 1998], but intrinsically this process is far from linearity. Fig. 3.50 shows dynamics of mature chum salmon average body length with respect to commercial stock population. At the initial stage of the stock population increase the length of fish gradually increases. Reduction of chum salmon growth rate was observed at the stock population increase from 20 to 40 million individuals. As the population numbers exceeded 40 million, the chum salmon growth rate stabilized at a level close to that in 1950s, when the stock population equaled only 3–5 million individuals.

Given the background of the resource population increase, reduction of the chum salmon growth rate is considered to be a sign of change in forage

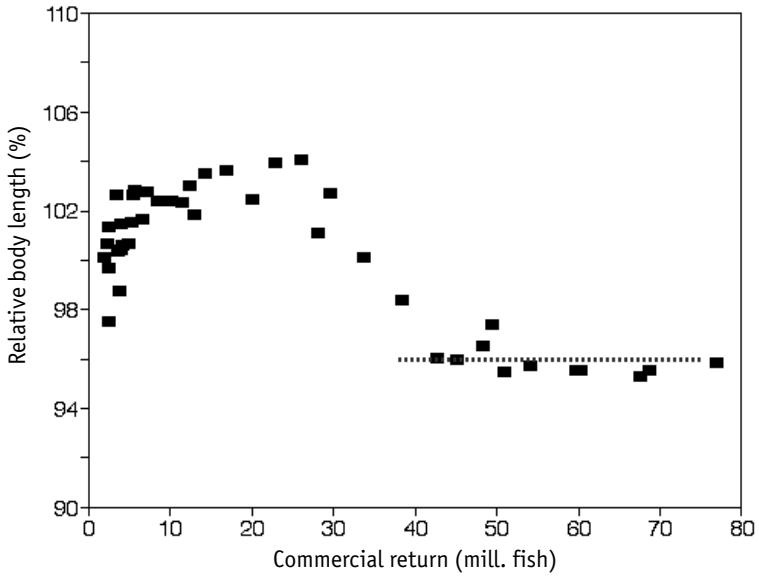

Fig. 3.50. Dynamics of body length (ordinate) (change in % from average) for three age groups of chum salmon in relation to total number of fish in commercial return (abscissa) for the period from 1953–1995, (5-year smoothing). Dotted line shows a trend of change in length of chum salmon at stock population numbers increase from 40 to 80 million. Data from Kaeriyama, 1998

abundance patterns within the current ecosystem [Kaeriyama, 1998]. The main components of salmon forage species (chum salmon, in particular) are macroplankton, small squids and myctophids [Brodeur, 1988]. As the forage species concentration decreases or as the stock population increases, the search area (the foraging area) increases and energy consumption for obtaining food may significantly increase, causing the observed growth rate deceleration.

The phenomenon of individual growth deceleration with increasing population was observed in several salmon species [Ishida et al., 1993; Ricker, 1995; Bigler et al., 1996], for instance, for Amur river, Sakhalin and Kamchatka pink salmon. The body length and weight of pink salmon decrease in the years of abundant populations, whereas they increase in the lower abundance years, with the difference in weights attained at size varying by 35–40% [Semko, 1937; Pravdin, 1940; Gritsenko, 2002].

A decrease of individual size of fish is clearly detected within the fluctuations of the Japanese sardine population abundance (Fig. 3.51): curves of catches reflecting population abundance and length-at-age of sardines are of virtually opposite phase. The observed decrease of mean sardine body length from 21 cm in 1960s to 18 cm in 1980 corresponds to a weight decrease of 35%. Over this period, total catch of Japanese sardines increased

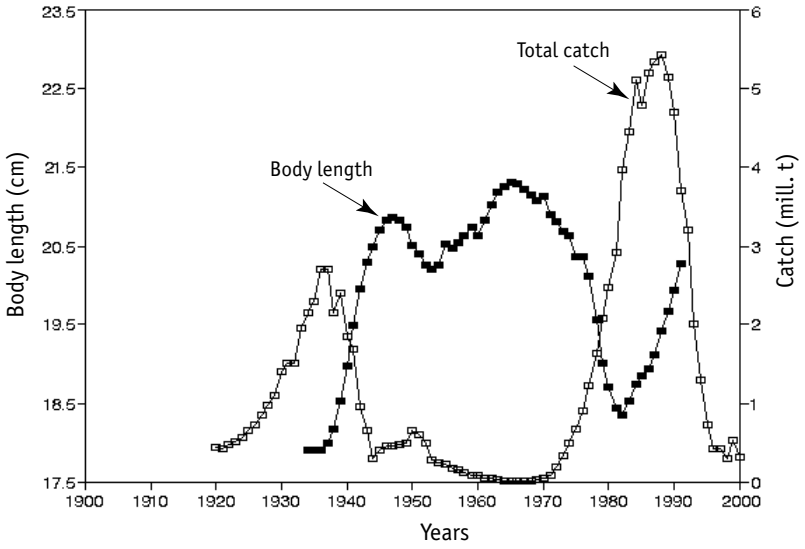

Fig. 3.51. Comparative dynamics of Japanese sardine body length (dark squares) and sardine commercial catch (light squares) for the period of 1920–2000 (5-year smoothing). Data from Kawasaki and Omori, 1995

to 5.4 million tons, which is approximately 350 times higher than the early levels. To put it differently, enlargement of total biomass of the sardine population exceeds potential losses of biomass due to individual body weight decrease of fish by almost three orders of magnitude (1000 times). In this period the foraging area of Japanese sardines increased by more than an order of magnitude. As with salmon, energy consumption due to expanded foraging area may cause a decrease of individual weight and size-at-age of fish.

The comparison of food requirements of salmon, a predominant species within the upper pelagic zone, with zooplankton production in oceanic foraging areas has shown a significant excess of available forage resources, [Pearcy et al., 1996, 1999]: salmon consume only 0.04–0.15% of the entire annual production of zooplankton in the oceanic foraging areas [Brodeur et al., 1999]. Analysis of trophic structures of the oceanic ecosystems show that the fish associated with the pelagic zone (including salmon) utilize less than 0.5% of the primary production [Shuntov, 2001; Dulepova, 2002]. The proportional role of salmon in total forage consumption of nekton species is less than 1–2%, and their role as consumers in the pelagic zone is negligible [Temnykh et al., 2004; Shuntov, Temnykh, 2004]. However, these estimations neglect direct dependence of the overall salmon production on the trophic dynamics within oceanic foraging areas. Yet it is the dynamic seasonal and spatial variations in distribution and accessibility of the forage items that may promote situations when the feeding factor may become sufficient explanation for the varying salmon production [Pearcy et al., 1999].

Climate and dynamics of local salmon populations

Salmon typically return to their freshwater reproduction habitats (homing). This helps clear up questions about relationships between climate changes and the long-term changes in salmon population of some regions — and local populations. There are unique data available on the dynamics of sockeye salmon from within the Bristol Bay. The world's largest stock of sockeye salmon reproduces in this region. This stock provides up to 50% of the total yield of this salmon species, and over 50% of Alaska's sockeye salmon catch. The greatest river-lake systems are located here, in which sockeye salmon breed, the resulting fry grow, and from where juvenile migration to the ocean begins. Eventually multimillion individual mature sockeye salmon return to restart the cycle.

For nearly half of a century the number of salmon caught and those that returned for spawning upstream were counted for every lake system. This unique statistical information was provided by Doctor Lowell Fair [Fair, 2003], the lead specialist of the «Bristol Bay Salmon» project. As shown, there is a direct relationship between total sockeye salmon approach and the number of fish in commercial catches (Fig. 3.52) and high correlation index (0.91) (Fig. 3.53).

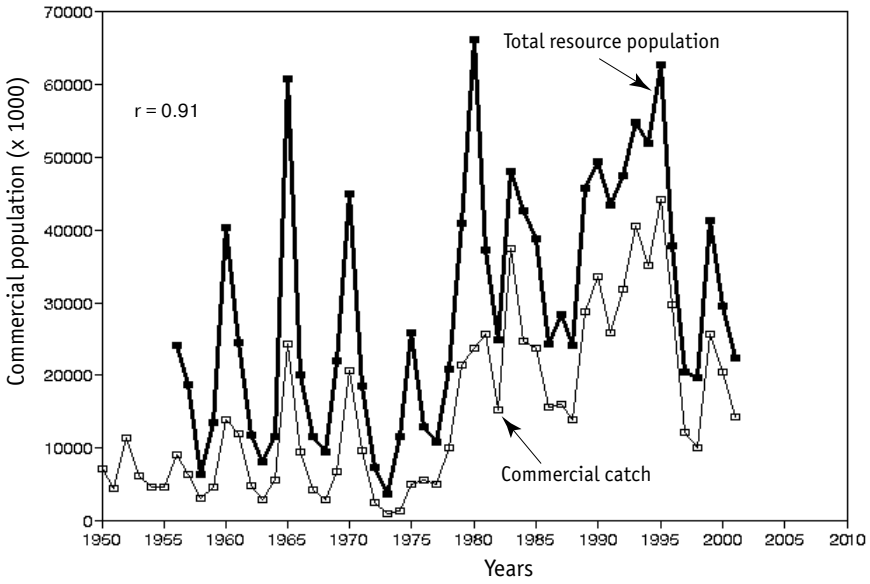

Fig. 3.52. Changes in commercial resource population (bold line) and catch (thin line) of Bristol Bay sockeye salmon *(Oncorhynchus nerka*, million individuals) in the period of the mid1950s into the early 2000s

The figure shows that fishery, on average, removes about 55% of total approaching salmon population. As observed, commercial catches of sockeye salmon reliably reflect dynamics of the population and may be used for the comparison with climatic index curves.

Sockeye salmon spawning and fry feeding occurs in 11 river-lake systems of the Bristol Bay system, whereas 90% of total catch is obtained from only 5 of these. The most productive system is Kvichak lake, which provides 40% of total catches. Egegik lake yields about 30% of the total catch, and three relatively small lakes [Naknek, Ugashik and Wood] yield another 20%. Populations of the latter three lakes have similar dynamics and may be classified into a single group. The dynamics of sockeye salmon populations of

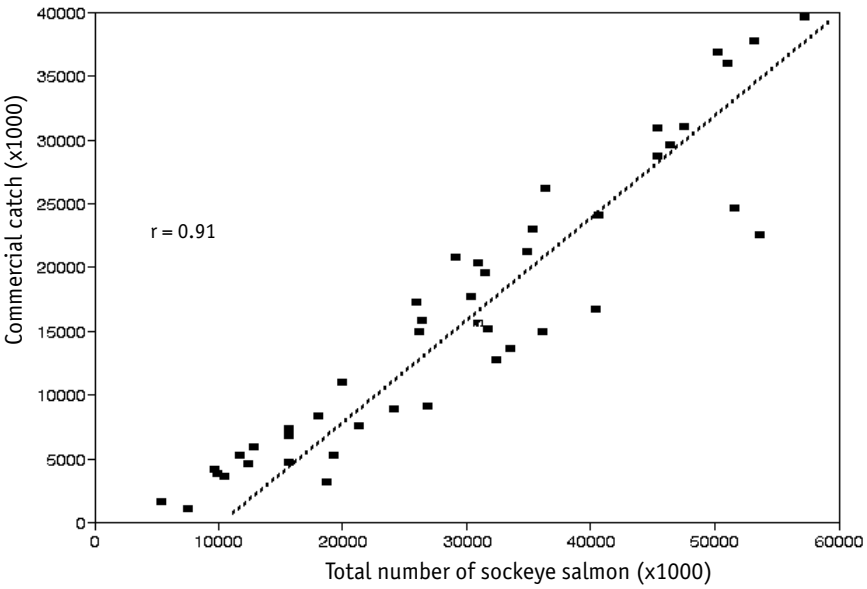

Fig. 3.53. Relationship between commercial catch and total number of sockeye salmon in commercial stock of Bristol Bay for the period of the mid 1950s into the early 2000s. Abscissa is the total number of fish in commercial stock. Ordinate is the commercial catch (thousand fish)

these 5 major river-lake systems is shown in Fig. 3.54. Sockeye salmon population in Kvichak lake has 3 maxima, three small lakes have 2 maxima, and Egegik lake exhibits 1 maximum. Every large population of sockeye salmon from Bristol Bay has its own long-term dynamics, but the general tendency for a catch increase is observed: from 20 thousand tons in 1950s to 120 thousand tons in the mid 1990s. The decrease of abundance in the late 1990s is characteristic of all these populations.

How do dynamics of the populations of the main lake systems correlate with our primary climatic index (Global dT) curve? Fig. 3.55 shows that dynamics of sockeye salmon populations in these lakes (except for the Egegik lake system) show low correlations with Global dT trend). The most productive population of Kvichak lake does not correlate with the Global dT curve.

Yet, the dynamics of the total sockeye salmon catches in Bristol Bay (Fig. 3.56) generally correlates with Global dT. Changes of sockeye salmon in southwest Alaska also follow the tendency of sockeye salmon increase in the period of 1970s–1990s, and correlates with Global dT dynamics. Note that total correlation between catch curves and Global dT curves is observed in only the mid 1990s, when the sockeye salmon population began decreas-

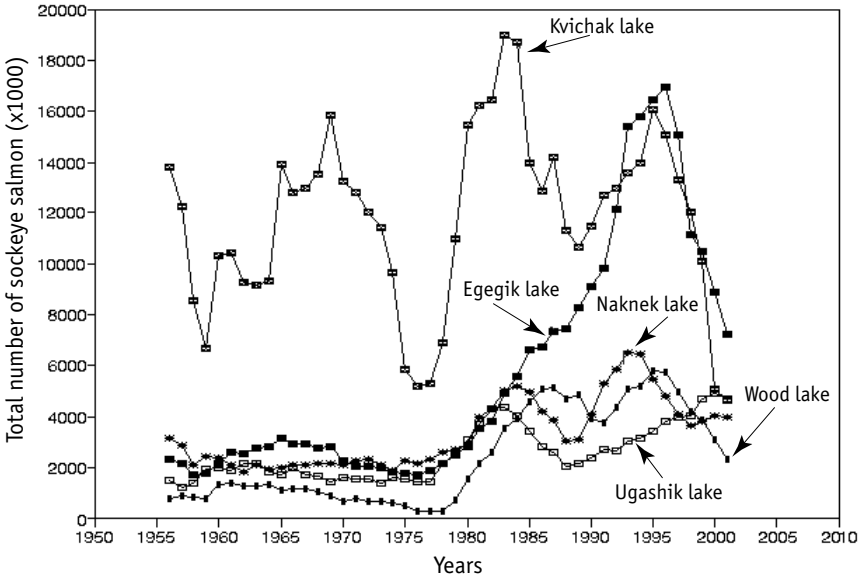

Fig. 3.54. Dynamics of major sockeye salmon (*Oncorhynchus nerka*) populations of Bristol Bay zone (5-year smoothing) in the period of 1955–2000

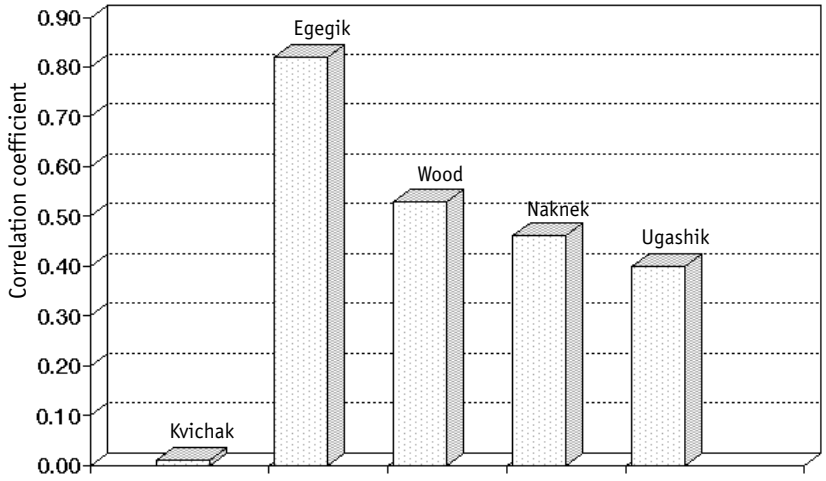

Fig. 3.55. Correlation between dynamics of sockeye salmon populations of the 5 main river-lake systems of the Bristol Bay area and Global dT for the period of 1950–2000

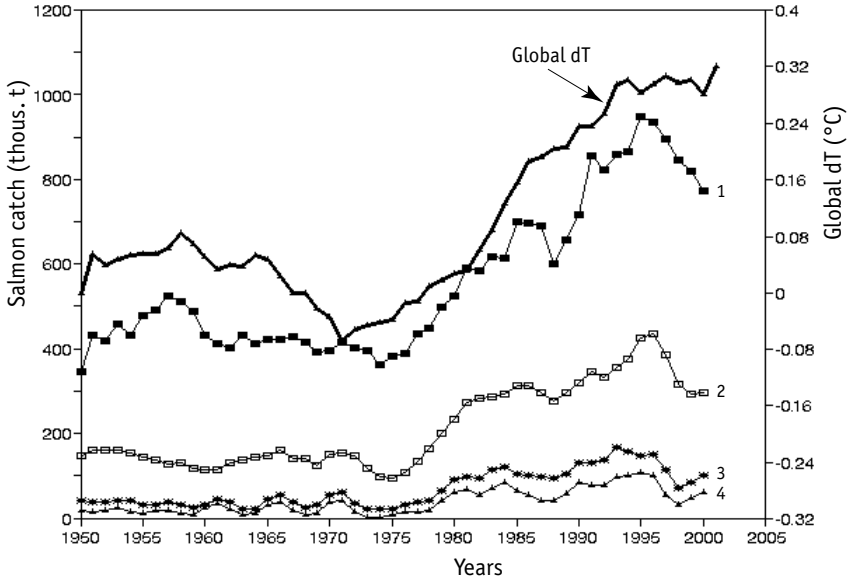

Fig. 3.56. Comparative dynamics of Global dT (bold line) and salmon catch of different regions of the North Pacific in the period of 1950–2000. *1* — total Pacific salmon catch; *2* — total salmon catch in the USA; *3* — sockeye salmon catch in the USA; *4* — Bristol Bay sockeye salmon catch

ing, whereas the Global dT curve has shown only a slight deceleration of temperature increase.

Fig. 3.57 shows correlation between the Global dT curve and salmon catches in different North Pacific regions. The correlation index increases with enlarging of compared regions equaling 0.70 for sockeye salmon in Bristol Bay; 0.78 for sockeye salmon catches in Alaska and the USA; 0.84 for total salmon catches in the USA; and 0.91 for total salmon catches in North Pacific. As observed from these data, dynamics of local salmon populations have their own specific features and do not always correlate with global climatic indices, Global dT, for example. However, as the compared regions are enlarged, similarity of relationships between climate changes and long-term dynamics of salmon population increases significantly, and reaches a maximum for the larger integrated regions, such as the total North Pacific.

The long-term ACI dynamics, which characterizes predominance of the zonal or longitudinal (meridional) direction of atmospheric mass transfer, correlate closely with the Global dT and provides another unique index of global climate changes. Fig. 3.58 shows that dynamics of some sockeye

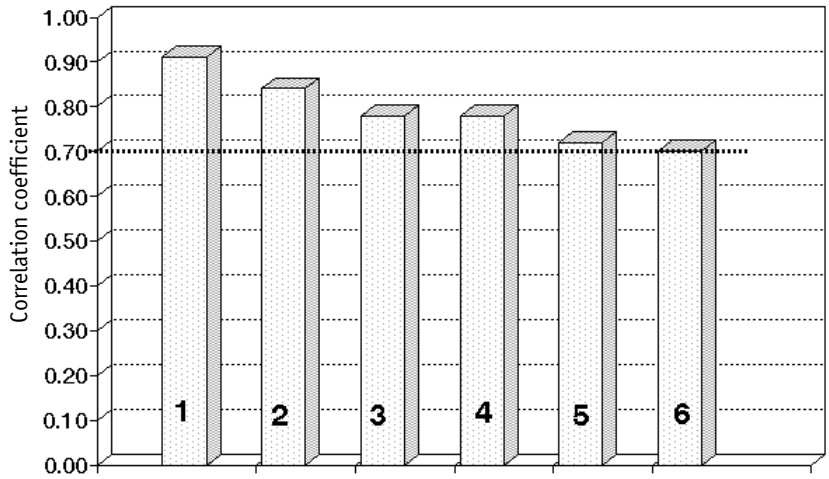

Fig. 3.57. Correlation between dynamics of Global dT, Pacific salmon and sockeye salmon commercial catch in different North Pacific regions in the period of 1950– 2000. The dotted line marks the level of correlation index equal to 0.7. *1* — total Pacific salmon catch ; *2* — total US Pacific salmon catch; *3* — total US sockeye salmon catch; *4* — Alaska sockeye salmon catch; *5* — Southeast Alaska sockeye salmon catch; *6* — Bristol Bay sockeye salmon catch. Bold dotted line shows the level of correlation coefficient equal 0.7

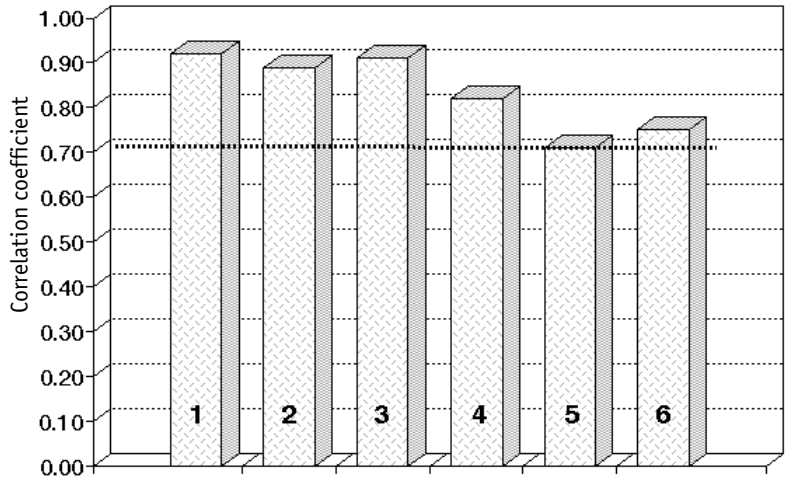

Fig. 3.58. Correlation between dynamics of the zonal ACI, Pacific salmon and sockeye salmon catches in different regions of the North Pacific within the period of 1950–2000. Notations are the same as for Fig. 3.57

salmon stock populations correlate with ACI even better than with Global dT. Closeness of relationship between ACI and sockeye salmon catches increases with the size of compared region: the correlation coefficient between ACI, sockeye salmon catches in the USA and salmon catches in North Pacific reaches 0.91.

To illustrate climate changes in the North Pacific, regional climatic indices, such as the PDO and ALPI are used [Beamish, Bouillon, 1993; Mantua et al., 1997; Hare, Mantua, 2000]. The PDO characterizes the long-term fluctuations of the average surface temperature in the North Pacific [Mantua, Hare, 2002], and ALPI gives the zonal area (in million km^2) with decreased air pressure with the center located above the Aleutian region. This index is considered to be one of the main climate forming factors for the North Pacific [Beamish et al., 1999; Hare, Mantua, 2000]. One may suggest that dynamics of Alaska's sockeye salmon population show better correlation with regional climatic indices rather than global ones. However, these indices were defined by these correlations with regional salmon production.

Fig. 3.59 shows that over the last 50 years the dynamics of total salmon catches in the USA and the PDO had similar long-term tendencies, although

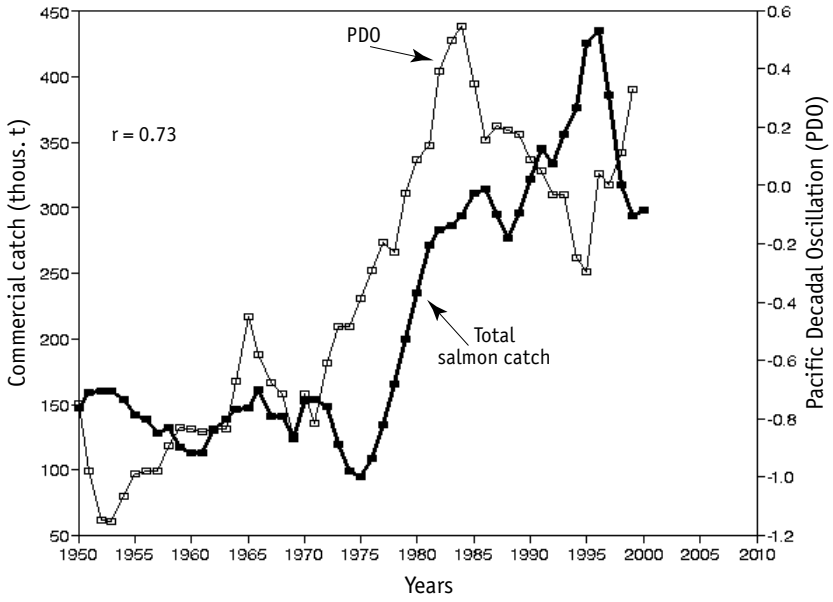

Fig. 3.59. Comparative dynamics of Pacific Decadal Oscillation (PDO) (white squares) and total Pacific salmon catch in the USA (bold line) in the period of 1950–2000

the relationship between catches and PDO is somewhat lower (r = 0.73) compared with Global dT (0.82) or ACI (0.89), see Figs. 3.57 and 3.58.

A correlation between total Pacific salmon catch in the USA and ALPI is also much lower (r = 0.70) compared with Global dT (r = 0.91) and ACI (r = 0.92) (see Figs. 3.57 and 3.58).

These data characterize a relationship between dynamics of salmon populations and climate changes for the 50-year period of observations. However, curves in Figs. 3.59 and 3.60 show that the trends of compared indices significantly change with time. Since 1980s, ALPI and PDO are in opposite phase with the dynamics of salmon catches. Fig. 3.61 shows that over the period of 1950–2000 dynamics of US Total Salmon catches and the Global dT, ALPI and PDO curves correlate rather well. In the latest half of this period (1975–2000) comparison of climatic indices and catches shows rather high correlation between Global dT and salmon catches (r = 0.81), whereas a relationship between PDO and ALPI is almost negligible. Over the latest period of 1985–2000, the correlation between salmon catches and Global dT decreased, still remaining positive (r = 0.58), whereas the correlation between dynamics of salmon catches and PDO and ALPI curves became

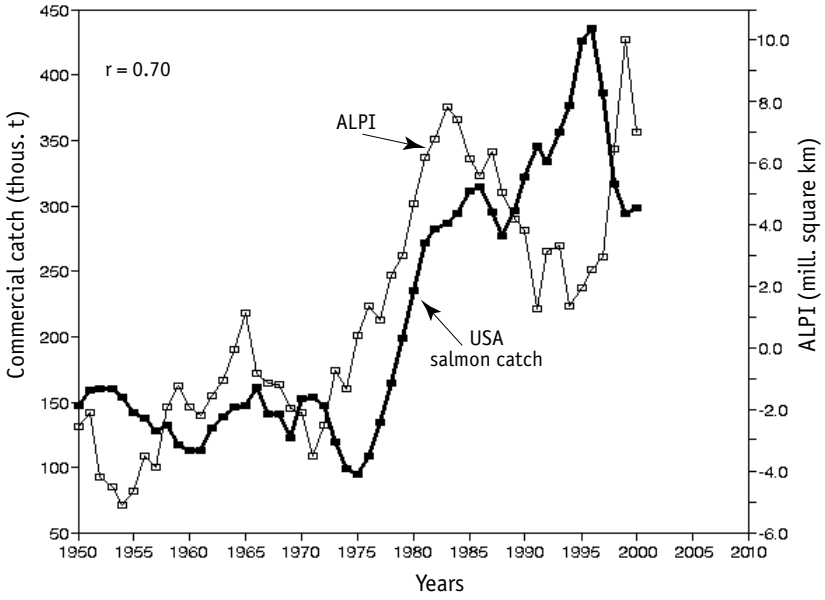

Fig. 3.60. Comparative the dynamics of Aleutian Low Pressure Index (ALPI) (white squares) and total Pacific salmon catch in the USA (bold line) for the period of 1950–2000

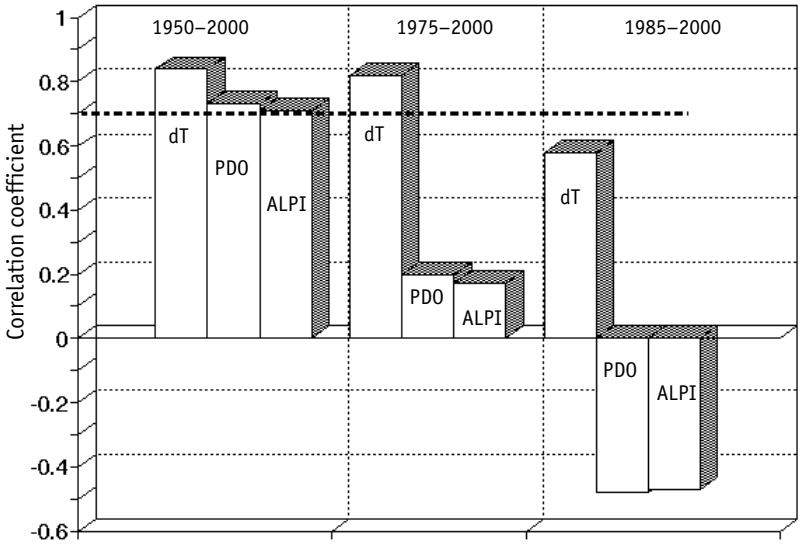

Fig. 3.61. Correlation between dynamics of total American salmon catch and the Global dT, PDO and ALPI over the recent 50, 25 and 15 years for the period of 1950–2000. Dotted line shows the level of the correlation index equal 0.7

negative ($r = –0.54$ and $r = –0.47$, respectively). As observed, the long-term changes in American and all Pacific salmon populations show better correlation with dynamics of global (Global dT or ACI) rather than regional climatic indices of the North Pacific (PDO and ALPI).

Similar dependencies are also observed for pink salmon of Alaska and the Eastern Kamchatka. Fig. 3.62 shows catch curves over the recent 50 years. Clearly, the long-term dynamics of Alaska's chum salmon and sockeye salmon and pink salmon of the Eastern Kamchatka are in good agreement. This shows also that in large regions different salmon species demonstrate similar dynamics.

Therefore, local populations of salmon demonstrate specific unique features within their population dynamics, not always correlating well with global climatic index trends. Total catches in the regions comprise catches from local and subregional commercial stocks. When these data are combined, the closeness between climate changes and the dynamics of salmon populations increases significantly, reaching higher statistical confidence levels for large regions of Asian and American coasts. These data correspond with considering «climate» as a long-term process, which affects regions about million square kilometers in size.

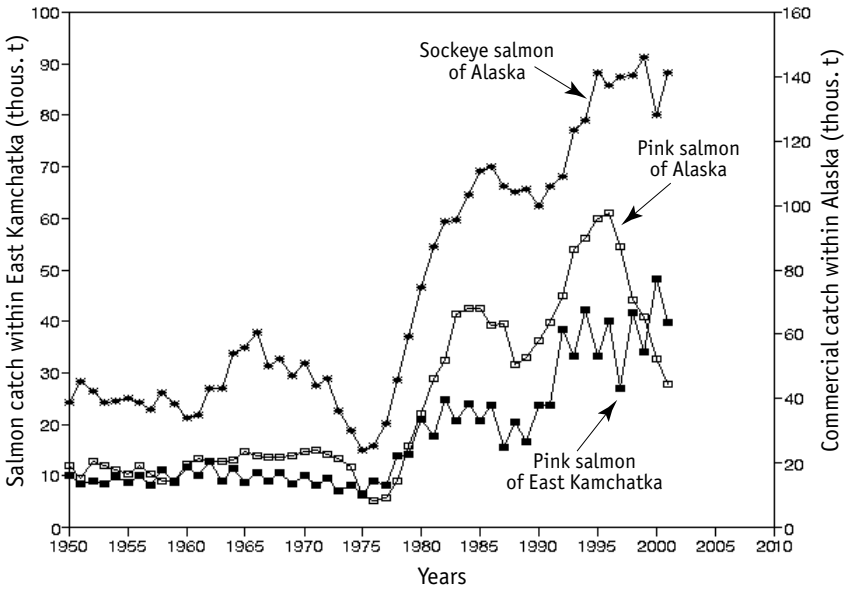

Fig. 3.62. Comparative dynamics of commercial catches of the Eastern Kamchatka pink salmon (dark squares), Alaska's pink salmon (asterisks) and Alaska's chum salmon (white squares) (5-year smoothing) in the period of 1950–2000

The long-term changes in Pacific salmon populations correlates better with global dynamics (Global dT or ACI) than with the more «local» climatic indices of the North Pacific (PDO and ALPI).

CHAPTER 4

CONDITIONS FOR DEVELOPMENT OF ABUNDANT POPULATIONS

The data presented in the previous chapters show that long-term fluctuations of the largest commercial fish populations are related to climate changes. Development of abundant generations depends upon an entire complex of hydrobiologic and oceanographic conditions, providing for both high larval survival and ultimately the formation of a subsequent generation that endured the early life history period with the highest natural mortality and their recruitment into the commercial resource. Answers to the question(s) about what particular changes of the environment limit populations of anchovy, sardines, herring and other commercial species are somewhat paradoxical: all of them are complex. As per Lasker [1985] the question can be formulated differently: what are the dominant factors limiting population of Clupeiformes and other major pelagic fish species? This question is followed by many others: what is the life stage of fishes critical for successful recruitment to the fished population? What are particular mechanisms of limiting factors effecting these fish? Does our knowledge about fluctuations of oceanographic conditions and biology of major resource species allow prediction of the likely development of either abundant or small generations?

Despite the significant progress in the knowledge about the ocean, few dependable answers can be given to these simple questions. Below, in brief, are the dominant hypotheses about abundant generation developments for pelagic fish.

BAKUN'S «TRIAD» HYPOTHESIS

The so-called Bakun «Oceanic triad» [Bakun, 1996] generalizes and considers three main oceanographic processes providing the favorable conditions for spawning, survival and growth of pelagic fish larval and juveniles.

«Enrichment» of the upper layers of the pelagic zone with nutrient transport into the euphotic zone is a result of upwelling activities, tidal and wind mixing of the upper layer. In the layer enriched with nutrients first come advantages to phytoplankton, zooplankton and then pelagic fish.

«Concentration» of plankton and drifting fish larval are observed in the convergence zones and at the borders of frontal zones in the upper mixed layer of the ocean. An increase of forage plankton biomass in these concentration zones reduces energy consumption of the feeding fish, accelerates their growth and increases the survival rate of larval. After hatching, pelagic fish larval are small, have only small yolk sacs, and are virtually incapable of active swimming. High concentrations of small planktonic forage organisms is one of the required conditions for larval survival and growth.

«Retention» is the third component of the Bakun triad, characterized by oceanographic conditions which prevent larval drift out of the zones with optimal forage conditions, outside of which the mortality levels sharply increase. Wind speed, direction and current drifts that retain larval in the shelf zone are considered to be required factors, promoting development of abundant population.

Bakun's triad hypothesis is based on the analytical results of observations regarding the many processes occurring in upwelling zones. Hence, a situation favorable for development of abundant generation implies simultaneous presence of all three triad elements; as only their combination enhances the probability of abundant generation occurrence. Unfortunately, this approach is not completely clear. For example, alteration of alternative periods of anchovy and sardine population outbursts in large upwellings indicates the existence of not yet known conditions providing preferential increase of population(s) of one of these species over the other.

«Optimal environmental window» hypothesis

This hypothesis is based on the observations for dynamics of oceanographic conditions and populations of anchovy and sardines in the large upwelling zones [Cury, Roy, 1989]. The basic concept is that the dependence of recruitment populations on upwelling intensity is very nonlinear. The best conditions for larval survival and development of abundant anchovy and sardine populations are somewhat middle upwelling intensities (Fig. 4.1) rather than its high or low values.

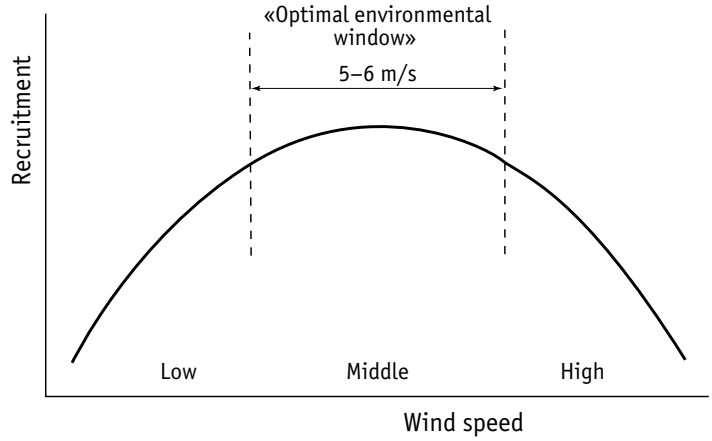

Fig. 4.1. «Optimal environmental window» chart. Data from Cury and Roy, 1989

Considering the change of recruitment at the background of gradual wind speed increase in the upwelling zone (Fig. 4.1), it increases at first. However, with further increase of the wind speed the population growth is slowed, and reaches its maximum at the optimal wind speed of 5–6 m/s. Further increase of the wind speed and upwelling intensity create unfavorable conditions for larval survival and a resulting decrease of the recruitment value. The wind speed range of 5–6 m/s, corresponded to the average upwelling intensities and high recruitment values, was thus labeled the «optimal environmental window».

Apparently, limitation of the wind speed and upwelling intensity reduces larval transport from more favorable coastal environment away into the open sea, where their mortality significantly increases [Parrish et al., 1981, 2000]. Also, excessive development of turbulent mixing is prevented, which dis-

rupts the supportive local aggregates of small plankton required for successful larval transition to their more mobile active feeding stage [Lasker, 1978; Owen, 1981].

On the other hand, too low wind speed and resulting lower upwelling levels do not provide nutrient transport to the surface, hindering both phyto- and zooplankton development, and define a minimal level of vertical turbulence promoting larval survival. Successful larval transition to the active feeding stage requires an intermediate level of turbulence, which regulates the frequency of encounter of the larval and their particulate microplankton forage above the critical level, but not disrupting the structure of the upper ocean layer favorable for their survival [Rothschild, Osborn, 1988]. As shown, this mechanism is critical for sardine, anchovy, cod [Sundby et al., 1994, Sundby, 1997], herring [Fiksen et al., 1998], pollock [Megrey, Hinckley, 2001], and some other species of pelagic fishes.

LASKER'S HYPOTHESIS OF «STABLE OCEAN»

Basing on multiannual observations for dynamics of sardine and anchovy populations in the Californian upwelling region, Lasker [Lasker, 1978] has formulated ideas about conditions for development of abundant generations of these species. According to Lasker, microplankton comprising unicellular flagellate algae and copepod nauplii required for initiation of active feeding by anchovy larval is irregularly distributed in the upper oceanic layer, forming patches, and often occurring as microlayers. It is in these microlayers that increased concentrations of anchovy and their best survival are observed. This layered structure is stable at low turbulence, but is disrupted by storms or strong winds, which cause intensive mixing of the surface layer. Simultaneously, anchovy larval survival decreases that then decreases recruitment into the commercial resource. It has been found that formation of patches and microlayers of increased forage organism concentrations require a minimum 5-day stable zero-wind weather situation. These periods of the so-called «calm ocean» that promote high survival of larvae were named «Lasker windows». It is shown that interannual variations of anchovy larval mortality variations in the Californian upwelling correlate with the periodicity of 5–6 day periods of relatively calm weather («calm sea»). In this case,

according to different assessments, the wind speeds varied from 5 to 10 m/s with those speed assessments at 5 m/s being predominant [Peterman, Bradford, 1987].

Contrary to Bakun's hypothesis of «oceanic triad» considering favorable effect of «concentration» and «retaining» forage organisms and drifting larvae within frontal zones and convergences, the «Lasker window» hypothesis indicates importance of the passive microlayer structure formation in the upper ocean layer with minimal turbulent mixing. In fact, both hypotheses consider the same process — feeding particles and larval concentration increase in the upper layer — as one of the main prerequisites for increasing larval survival and development of abundant generations.

Comparison of «Lasker window», «optimal environmental window» and Bakun's «oceanic triad» hypotheses indicates significant overlap of the concepts upon which they are based.

CUSHING'S «MATCH/MISMATCH» HYPOTHESIS

Based on the multiannual studies in the North Atlantic, Cushing (I969, 1971, 1980, 1990) formulated the underlying reasons for development of abundant recruitment of herring, cod, and other fish with drifting pelagic eggs. Due to the short vegetative season of phyto- and zooplankton development in the northern region, favorable conditions for high survival and growth of fish larvae are rather short-term. Ultimately, their survival, thus breeding success, depends on the massive occurrence of copepod nauplii (the main forage of larvae during transition to active feeding) coinciding with the hatched larvae. When these events coincide, survival of larvae and probability of a subsequent abundant generation development increases, or in the opposite situation, recruitment decreases.

Temperature strictly determines the rate of development of both eggs and larval and the plankton that directly affect fish population recruitment.

Optimal vertical turbulence in the surface layer significantly accelerates zooplankton reproduction and promotes high survival of larvae. In contrast, high intensity wind mixing (regular spring storms, for example) destroys the oceans' upper layer structure and negatively affects survival of larvae, and thus the population recruitment.

Similar to the «Lasker window» or «optimal environmental window» hypotheses, the concept of Cushing's «match–mismatch» is based on the idea of an initial ecological «window» of optimal environmental requirement for abundant generation development.

The above hypotheses do not present all possible mechanisms that can result in high population variabilities. For instance, as recently reported, mesoscale anticyclone circulation systems as large as several dozens to hundred kilometers with lifetimes of 50–100 days form regularly in the Californian Current. Owing to centripetal component of these circular streams, formations of high concentrations of phyto- and zooplankton occur within these dynamic features, and as well, increased survival of sardine larvae is observed [Smith, 2000; Logerwell, Smith, 2001]. These observations suggest that generally a high population recruitment of Californian sardine depends on the frequency of occurrence of such mesoscale circulation patterns, which, in turn, is determined by the periodicity of various types of atmospheric circulation. An abundant generation develops as a result of many natural factor, the combination of which provides high survival of larvae and creates other prerequisites for subsequent population increases. Sustained conditions beyond only that are favorable for growth and survival of the fry are required that are supportive of their gradual development and ultimate recruitment to commercial stocks.

The examples of direct applications of Cushing's approaches to forecasting of the cod stock recruitment show that seasonal, annual and spatial variations of primary production, zooplankton biomass, population fecundity rate, temperature, and the upper layer stratification may be taken into account and simulated on the basis of accessible meteorological and biological data. However, such simulations may not predict well the development of an abundant or, a poor year class — or observed stock recruitment [Brander et al., 2001].

Formation of abundant year classes result from arbitrary matches of the time of massive larval transitions to mobile foraging stages with the periods of high microzooplankton population abundance (for example, early copepod stages), relatively stable surface layer of the ocean, and optimal vertical turbulence that increase probability of larval encounter rates with the forage particles.

Every year and in every region, survival of cod larvae is determined by «match–mismatch» between the processes of plankton development and larval drift, but the multiplicity of environmental variations makes either high

or low survival of fish prior to their recruitment of the commercial stock virtually unpredictable.

Comments in brief

The above hypotheses indicate prerequisites of successful breeding of some major pelagic fish species, but do not provide prediction of abundant generations. They also do not clarify the questions about which particular complexes of conditions promote the predominance of either sardine or anchovy in the larger upwelling zones.

Apparently, the long-term fluctuations of fish productivity relate to the fact that an increase or decrease in frequency of conditions that correspond with definite types of meteorological and hydrologic processes that either promote or limit survival of the fry, and the subsequent growth and survival to the developmental phase of their entry into the commercial stock [Brander et al., 2001; Brander, 2003].

CHAPTER 5

POSSIBLE REASONS FOR POPULATION FLUCTUATIONS IN MAJOR COMMERCIAL FISH SPECIES

Relationships between fluctuations in the large commercial populations and total productivity of ecosystems, from the lower components (phytoplankton and the primary production) up into fish productivity, have been discussed for a long time [Cushing, 1982]. Partly, these ideas reflect the views on a «cascade» of productivity levels known for terrestrial ecosystems, where generally the stages of energy transfer may be traced rather certainly from soil nutrients to plants and then to animals.

Alterations of blooms of sardine and anchovy populations in several ocean upwelling zones result in oscillation amplitudes of commercial catches from very low levels up to many million tons per year and provide enlightening examples of fish productivity fluctuations. The general opinion is that these alternating outbursts of sardine and anchovy populations are determined by periodical fluctuations of biological productivity of ecosystems [Kawasaki, 1994]. In turn, it is suggested that total productivity fluctuations are determined by periodicity of climatic and related oceanographic changes that have favorable (or unfavorable) effects on primary production and phytoplankton development, then the changes in species specific zooplankton production lead to fluctuations in anchovy, sardine and other planktivorous fish populations [Kawasaki, Omori, 1995; Brodeur, Ware, 1995].

This point of view does not completely explain the phenomena observed. For example, if sardine population outbursts or diminutions are the direct consequence of increasing or decreasing total productivity of the area, population outbursts of the alternative species — anchovies — should also be accompanied by the same significant and synchronous increases of phyto-

and zooplankton quantities. Hence, it is unclear why some periods of biological productivity increase cause anchovy population outbursts and others cause increase of sardine population.

On the trophic status of sardines and anchovies

Two alternative species anchovies and sardines — determine the long-term fluctuations of fish biomass in the most productive regions of the World Ocean. Extremely high oscillations in populations of these species are related to their phytoplankton feeding capabilities, i.e. to use the first trophic level and thus transfer energy and substance directly from primary producers to fish [Ryther, 1969; Longhurst, 1971; Walsh, 1981]. Anchovies and sardines use a «filter» type of feeding, which is interpreted as a specific mechanism for capturing and eating small cellular phytoplankton [Kawasaki, 1992a, b]. However, how long anchovies and sardines maintain the capability for predominantly phytoplankton feeding has long been debated [Cushing, 1978; James, 1988]. Analysis of foraging of the principle commercial fishes within the Peruvian upwelling region [Konchina, 1991; Konchina, 1991] has shown that mature anchovies (anchoveta) and sardines mostly feed on zooplankton, not phytoplankton.

The study of anchoveta and sardine feeding during their life cycle has shown [Muck, 1989] that an early stage of transition to active feeding, as most (80%) anchoveta larvae at 2–3 mm generally feed on phytoplankton (dinoflagellates]. However, the role of the latter in the forage of larvae rapidly decreases with their growth, and the complete transition to zooplankton feeding occurs when larvae attain the length of 4 mm. Mature stage anchoveta forage consists exclusively of zooplankton, with a preference for macrozooplankton.

The proportion of phytoplankton (dinoflagellates) in the diet of sardine larvae is lower than for anchoveta (about 20% vs 80%) and rapidly decreases with their growth. As reaching 5 mm size, sardine larvae transition to 100% zooplankton forage, consuming mostly smaller forms. The assessment of phytoplankton energy contribution to feeding larvae should also take into account that their calorific content is about 4 times lower than that of zooplankton. For early sardine larvae, the dinoflagellate contribution is not

as high as 20%, and thus yields only about 5% of the total calorific content of their diet.

The digestive tracts of sardines and anchovies consist of a well developed stomach and a short intestine (which does not exceed the body length). That is absolutely atypical of herbivorous fishes, which have very long intestine and poorly developed stomach [Pauly et al., 1989; Mann, Lazier, 1996]. Recent studies of sardine and anchovy feeding within the Benguela upwelling have shown that sardine and anchovy juveniles and mature fishes almost exclusively consume zooplankton [van der Lingen, 2002]. Hence, anchovies prefer microzooplankton, while sardines prefer small forms of zooplankton.

Estimation of the part of the primary production transiting to the anchoveta biomass in the Peruvian upwelling has shown that even during the period of the maximum anchoveta population, when their biomass reached 15–20 million tons, only 2–3% of primary production are converted to the anchoveta biomass [Chavez et al., 1989]. As the biomass was reduced to 2–3 million tons, the efficiency of the primary production conversion into fish decreased to only 0.2–0.4%. These estimations are 5–10 times lower than those obtained previously under a supposition that anchoveta feed exclusively on phytoplankton [Walsh, 1981].

The long-term fluctuations of the primary productivity (and phytoplankton, respectively) themselves may not be the reason for anchovy and sardine population outbursts. One may suggest that changes in anchovy and sardine populations depend on dynamics of the second trophic level, which is zooplankton. To clear up these questions one must work with rather long time series of the dynamics of primary production, zooplankton biomass, anchovy and sardine biomasses in the most highly productive regions of the ocean.

Humboldt Current

Within the Humboldt Current anchoveta catches attained 13 million tons, and cathes of sardine 6 million tons. This region is of special interest for revealing a relationship between climate changes and the fish productivity. The primary part of this Current adjacent to Peruvian coast (between 4 and 14° S) is the most highly productive. The secondary part is adjacent to the southern coast of Peru and the northern coast of Chile (15–25° S).

The entire region has been investigated rather well, and comprehensive data on dynamics of primary production, zooplankton biomass, and both anchoveta and sardine catches during the period of 1953–1985 are published in two fundamental documents [Pauly, Tsukayama (eds.), 1987; Pauly et al. (eds.), 1989]. Time series of the primary production changes (Fig. 5.1) were obtai-ned using dynamics of nitrates efflux with transport of bottom water into the euphotic zone due to upwelling activity. The estimate was adjusted by direct measurements of the primary production using the radioactive carbon method [Chavez, Barber, 1987; Chavez et al., 1989].

Fig. 5.1 shows that dynamics of upwelling intensity and long-term changes in the primary production correlate rather well. This is clear, because the potential level of primary production is determined by nitrate delivery to the euphotic zone which, in turn, is directly related to the upwelling intensity. During the 33-year period, both indices show approximately 10-year oscillations. Bakun and Mendelsson [1989] have noted an increase of the average intensity of the current upwelling and primary production by approximately 25% during the 35-year period (1953–1987).

The comparison of dynamics of the primary production with total biomass of anchovies and sardines (Fig. 5.2) shows that during the 35-year

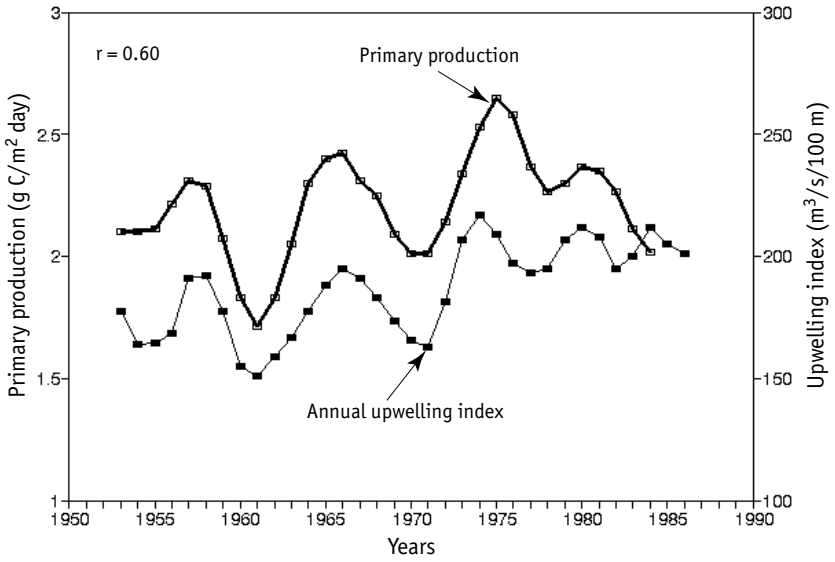

Fig. 5.1. Dynamics of the coastal annual upwelling index (lower curve) and primary production in the Peruvian upwelling region (4–14° S) (upper curve) during the period of 1953–1987 (3-year smoothing). Data from Bakun and Mendelsson, 1989; Chavez et al., 1989

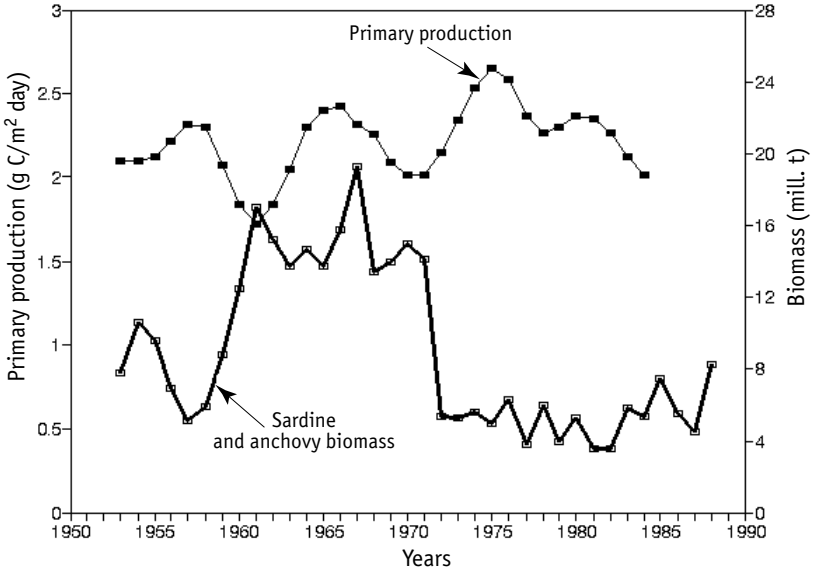

Fig. 5.2. Dynamics of the primary production (dark squares, 3-year smoothing) and total biomass of Peruvian anchoveta and sardine (bold line) in the Peruvian upwelling region (4–14° S) during the period of 1953–1989. Data from Chavez et al., 1989

observation period the biomass fluctuations of these major commercial species occur independently of the primary production level.

Since long-term fluctuations of anchoveta biomass (and catches) in the Peruvian upwelling system occur independently of the primary production levels, of greatest interest is the determination of possible relationships between zooplankton dynamics and the changes in primary production and fish productivity. Fig. 5.3 shows that dynamics of the primary production (in parallel with the plankton biomass) and the zooplankton biomass are rather different. The most significant differences in dynamics of phyto- and zooplankton were observed during the 1970s–1980s, when the level of the primary production remained practically constant, and zooplankton biomass has 4-fold decreased as compared to levels in the 1960s [Carrasco, Lozano, 1989; Muck, 1989]. Therefore, no direct relationship between the primary production level and the zooplankton biomass has been observed.

Until very recently, we have had only the 24-year (1964–1987) series of simultaneously measured anchoveta and zooplankton biomasses in the area of the Peruvian upwelling [Chavez et al., 1989]. As additional data on the changes of these values until 2001 became available [Ayon et al., 2004], it

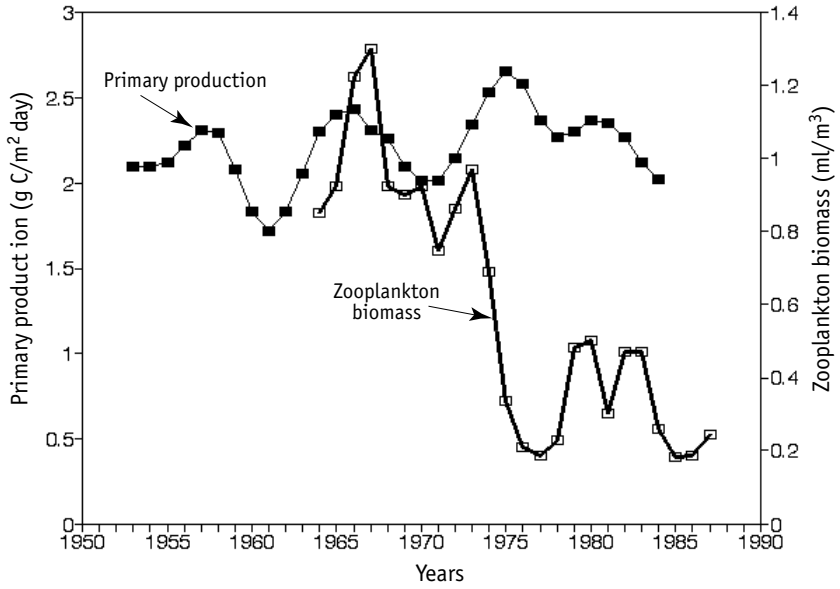

Fig. 5.3. Dynamics of primary production (dark squares, 3-year smoothing) and zooplankton biomass (bold line) in the Peruvian upwelling region (4–14° S). Data from Chavez et al., 1989

became possible to compare the 37-year time series during the period of 1964–2001 (Fig. 5.4). According to the relationship between zooplankton and anchoveta biomass, the entire 37-year period of observations can be divided into two parts: during the period of 1964–1982, these indices correlated rather well ($r = 0.71$) with each other, whereas during the period of 1983–2001 the relation between changes in zooplankton and anchoveta biomasses was rather low ($r = 0.32$).

The anchoveta biomass reached the peak levels of almost 20 million tons while the same-time zooplankton biomasses differ by 4–6X. Based on the previous data for the period of 1964–1987 it was suggested that changes in anchoveta biomass and catches correlate with zooplankton biomass oscillations [Alheit, Niquen, 2004], however, no such a conclusion can be made as based on the more complete database. For the period of 1964–2001, comparison of dynamics of these indices shows the absence of any explanatory relationship between them ($r = 0.51$, $p < 0.01$). It is also typical that when strong El Niños occurred in 1982–1983 and in 1997–1998, these caused abrupt decreases of anchoveta biomass, but virtually did not affect the zooplankton biomass. Thus we conclude that in the most highly productive

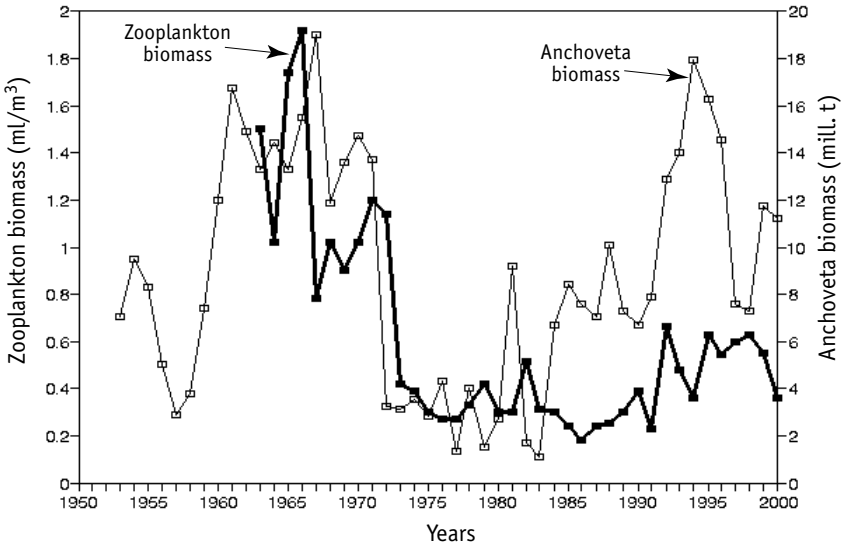

Fig. 5.4. Dynamics of zooplankton (bold line) and anchoveta biomasses (white squares) in the Peruvian upwelling zone (4–14° S) during the period of 1953–2002. Data from Chavez et al., 1989 and Ayon et al., 2004

region of the World Ocean no reliable relationship exists between changes in zooplankton biomass and fish productivity.

Questions about direct effects of upwelling intensity on the long-term dynamics of fish biomass are discussed in the work by Mendelsson and Mendo [Mendelsson, Mendo, 1987] based on analysis of a 33-year time series. It has been found that dynamics of the upwelling intensity and turbulent mixing index do not correlate with the dynamics of Peruvian anchoveta population. The authors have also shown that no effect of the so-called «Lasker's window» e.g. in the 4–5-day period of a «calm ocean» promoting high survivability of pelagic fish larvae [Lasker, 1981a, b] has been detected in the region. According to the hypothesis of «optimal environmental window» [Cury, Roy, 1989; see Chapter 4] the relationship between sardine and anchoveta biomass changes and the upwelling intensity is significantly nonlinear. Population outbursts of these species occur at similar average values of upwelling intensity within the rather narrow range of the wind speed: from 5 to 6 m/s. Outside these borders of the wind-driven activity (optimal upwelling intensity) the recruitment to populations of anchovies and sardines decrease [Cury et al., 1995]. Fig. 5.5 shows the comparative dynamics of anchoveta biomass and upwelling intensity in the Peruvian region.

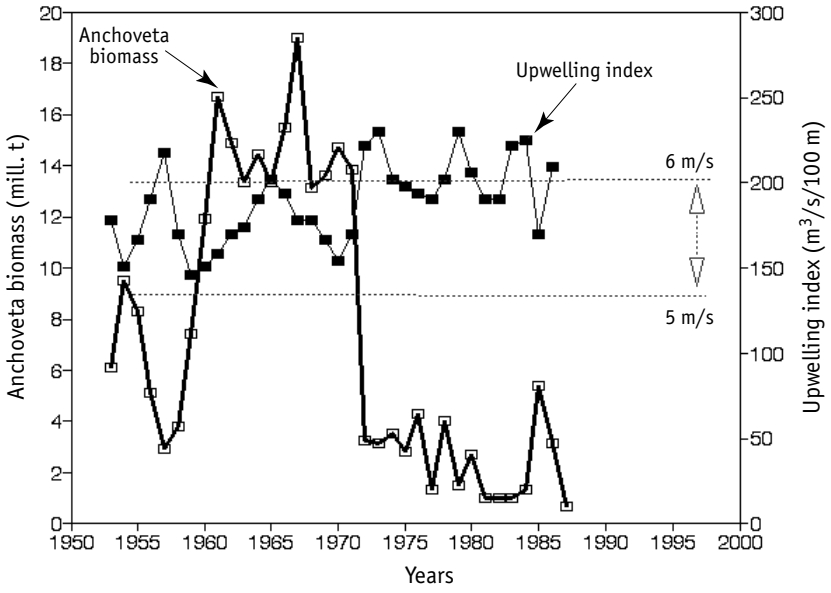

Fig. 5.5. Dynamics of anchoveta biomass (bold line) and coastal upwelling index (dark squares) in the Peruvian upwelling region (4–14° S) during the period of 1953–1985. Dotted lines show optimal boundaries of the upwelling index characterized by average wind speed within the range of 5 to 6 m/s. Annual upwelling index were taken from Bakun and Mendelsson, 1989

Fig. 5.5 shows that the highest anchoveta biomasses are observed at the upwelling intensity of about 150 m^3/s per 100 m which is equal to the wind speed of 5 m/s. The wind speed exceeding 6 m/s and the upwelling index exceeding 200 m^3/s per 100 m is accompanied by a significant decrease of the anchoveta biomass. Even relatively minor excursion beyond the upper border of the mentioned diapason causes 5–8-fold decrease of the anchoveta biomass.

During the 15-year period from 1971–1987, after each strong El Niño the upwelling intensity indices (and wind speeds) rose above the range optimal for successful anchoveta reproduction, and resulting catches were low, yielding about 2 million tons, on average. Unfortunately, measurements of the upwelling activity in the region of 4–14° S are limited to only near coastal data.

Sardine is the second most abundant pelagic fish species caught in this region. During the period of 1975–1987 sardine catches in the Peruvian region increased sharply, when the coastal upwelling intensity was below the optimal range for anchoveta. Hence, the level of zooplankton biomass

remained low, and the anchoveta population was minimal [Schwartzlose et al., 1999]. The strongest El Niño, which diminished the anchoveta biomass to the lowest level within the recent 50 years, has not caused any negative effect on the sardine catches. This clearly indicates differences in the responses of anchovies and sardines to environmental changes. The questions about particular effects of changes in the atmospheric circulation, wind activity, upwelling intensity, and turbulent mixing on the long-term dynamics of the fish biomass in the Peruvian upwelling region will require additional studies and analyses of longer-term time series of observations [Muck, 1989].

In the other highly productive part of the Humboldt Current zone, located south of the Peruvian upwelling (in the range of 15–25° S) yields catches up to 53% sardines and 16% anchoveta of the total. In this zone, the upwelling activity was measured from 1981 until 2000 [Norton et al., 2001].

The anchoveta habitat is virtually identical to the 50-mile coastal zone affected by the coastal upwelling, whereas the area of sardine breeding and feeding is located as far as 70–150 miles from the coast, in the far weaker upwelling of the open ocean. Contrary to the Peruvian upwelling, for the area of southern Peru — northern Chile the data are available for both coastal and oceanic upwelling zones [Norton et al., 2001]. This allows consideration of the relationships between measurements of the anchoveta and sardine populations and the upwelling dynamics in their respective habitat areas. Fig. 5.6 shows the long-term dynamics of the coastal upwelling and anchoveta catches in the southern Peru — northern Chile area.

In 1980–1987, the increase of upwelling intensity to 300 m^3/s per 100 m of the coastline was accompanied by decrease in anchoveta catches. Contrarily, during the period of 1987–1996, the decrease of upwelling intensity to the values close to the optimal level (150 m^3/s per 100 m) demonstrated simultaneous sharp increase of the population and increase in anchoveta catches to 2.5 million tons. As in the Peruvian upwelling, changes in anchoveta catches occur according to the hypothesis of the «optimal environmental window».

Fig. 5.7 shows dynamics of sardine catches compared with the changes of oceanic upwelling intensity. During the period of 1980–1987, the highest sardine catches (2–3 million tons) were observed at the upwelling intensity which was close to the optimal level of 150 m^3/s per 100 m, and decreased with the upwelling intensity diminution to 100 m^3/s per 100 m. At the same time, during the period of 1995–2000 the return of the upwelling index to optimal values did not yield any increase in the sardine population. This may

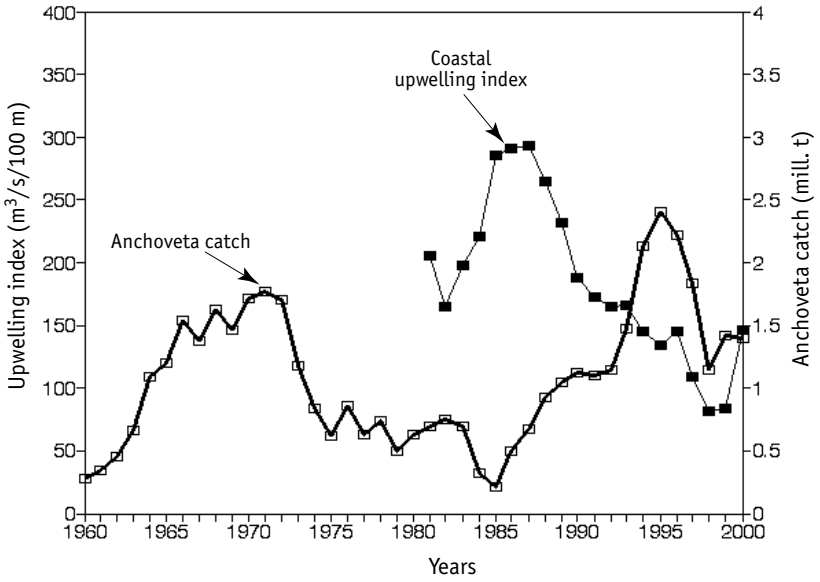

Fig. 5.6. Dynamics of anchoveta catch (bold line) and coastal upwelling index (dark squares) in the southern Peru — northern Chile region (15–25° S). Annual upwelling index was taken from Norton et al., 2001

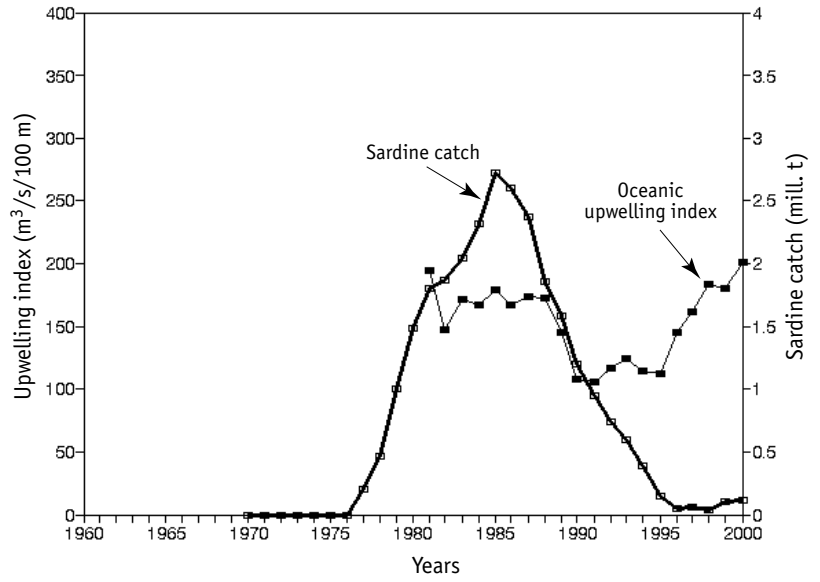

Fig. 5.7. Dynamics of Peruvian sardine catch (bold line) and oceanic upwelling index (dark squares) in the southern Peru — northern Chile region (15–25° S). Annual upwelling index for the region of 15–24° S was taken from Norton et al., 2001

indicate that dynamics of the sardine population depends on both upwelling intensity (i.e. the «optimal environmental window») and some other unknown causes.

Comments in brief

The primary production level in the Humboldt Current zone is determined by the rate of deep water lifting due to upwelling effect. The intensity of the latter depends on periodicity and speed of southern winds. No clear relationship between dynamics of the primary production, zooplankton, and fish productivity has been observed.

The anchoveta population outbursts are observed in the optimal intensity periods (about 150 m^3/s per 100 m) of the coastal upwelling, whereas sardine population outbursts do not always coincide with the periods of optimal upwelling values.

According to the «optimal environmental window» concept, both primary commercial species should simultaneously increase their population. In fact, this does not occur, and alteration of outbursts on anchoveta and sardine populations indicates a unique complex of optimal environmental conditions for the each species. The optimal upwelling intensity level may be considered as low as just a single among the group of conditions required for population outburst of each species.

California upwelling

The dynamics of catches of the major commercial species — sardine (*Sardinops caerula*) and anchovy (*Engraulis mordax*) — in the California Current upwelling zone is well documented (Fig. 5.8). During the period of the 1930s–1940s sardine provided high catches (around 700000 tons), but in the mid 1950s they decreased by ~90%. The anchoveta biomass began increasing in 1960s, attaining maximum catches in the early 1980s. After that they abruptly decreased, and by 1990 the anchovy fishery was halted.

From the early 1950s until the early 1990s, rather detailed plankton surveys were performed in the California Current [McGowan, 1995; Roemich, McGowan, 1995]. This allowed comparison of the long-term dynamics of zooplankton and fish biomasses within the region (Fig. 5.9). It can be seen that dynamics of catches and zooplankton in the region are significantly dif-

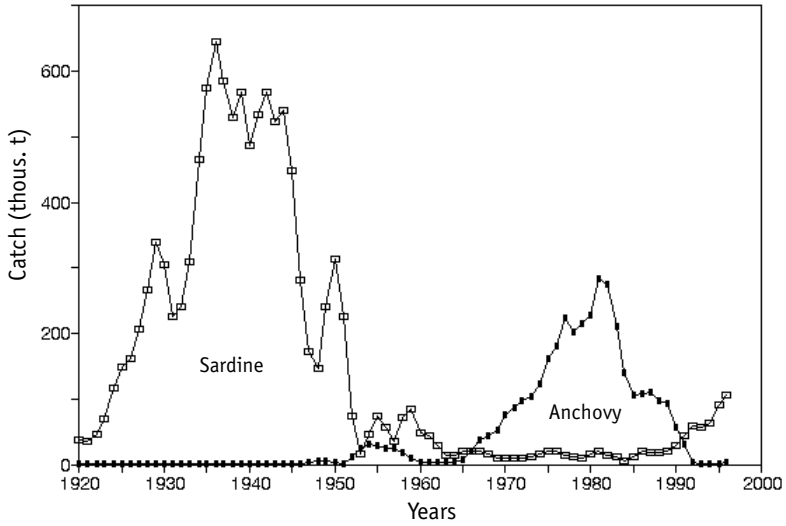

Fig. 5.8. Pacific sardine *Sardinops caerulea* (white squares) and anchovy *Engraulis mordax* (dark squares) catches in the California Current zone (3-year smoothing) during the period of 1920–1996

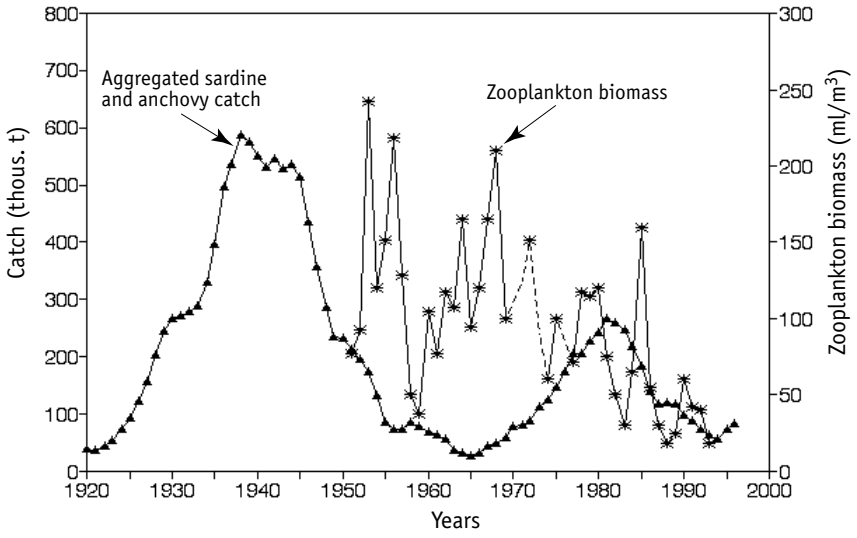

Fig. 5.9. Comparative dynamics of aggregated Pacific sardine and anchovy catches (triangles) (5-year smoothing) and zooplankton biomass (asterisks) in the of California Current region. Dashed line shows the interpolated probable trend of the zooplankton dynamics. Data from Roemich and McGowan, 1995

ferent. With the backdrop of the general tendency to decrease the observation periods, the zooplankton biomass shows significant fluctuations; the highest values relate to the period of the lowest fishery catches obtained in 1960s–1970s. That the catch dynamics of fish catches and zooplankton biomass are out of phase is suggested; however, due to the incomplete zooplankton sampling series, consideration of any relationship between the dynamics of the fish population abundance and zooplankton biomass is statistically unreliable.

Catches of California sardine decreased by almost an order of magnitude from late 1930s until the mid 1950s. During this period, the intensity of fishing activity remained virtually unchanged. Therefore, the sardine fishery output reflects changes in the population abundance, which in turn was considered as a response to the change of habitat conditions [Murphy, 1961].

So far as concerns oceanographic factors affecting dynamics of catches in the region, data analysis by Cushing [Cushing, 1995] show that during the period of high population of sardines in the late 1930s the wind strength was significantly lower. According to the authors' point of view, the subsequent collapse of the sardine population, occurred in the mid 1940s, is related to increasing wind activity in the region. At the same time, as shown in Fig. 5.10, the upwelling index decreased in this period. Unfortunately, the time series of measurements of the wind activity and upwelling intensity in the region started in 1946 and included only the period of rapid decrease of the sardine population. The available data do not permit determination of any direct relationship between dynamics of sardine population and the upwelling index changes.

The outburst of the anchovy population occurred in the 1970s–1980s is also related to the long-term dynamics of the upwelling intensity [Cury et al., 1995]. According to modern concepts, survivability of anchovy larvae and recruitment population to the commercial stock have nonlinear dependences upon the upwelling intensity: the optimal survival of larvae is observed at the average values of the upwelling intensity (about 150 m^3/s per 100 m), which corresponds with concept af the «optimal environmental window» [Cury et al., 1989].

During the period of the 1970s into the early 1980s, anchovy catches in the central part of the California Current (between 30 and 33° N) increased continuously up to the maximum of 310000 tons, landed in 1981. Only two years afterward the catch decreased by 70%, and after 1990 the anchovy fishery was practically halted. Fig. 5.10 shows the mean-year dynamics of

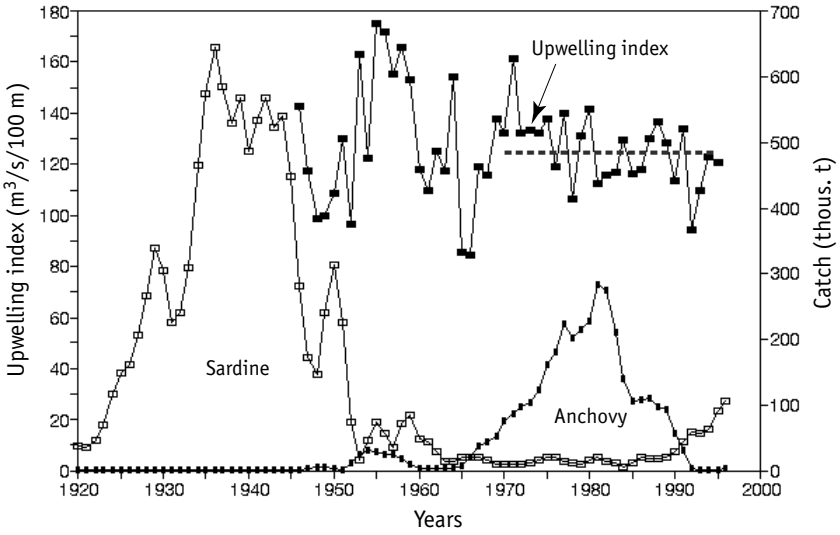

Fig. 5.10. Dynamics of the annual upwelling index (dark squares) in central part of California Current (27–33° N) and sardine (white squares) and anchovy (small black squares) catches during the period of 1920–1996. Dotted line shows the average upwelling index during the period of 1970–1995 taken from the data of Schwing et al. [1996]

the upwelling intensity in the central part of the California Current compared with dynamics of sardine and anchovy catches.

During the period of 1968–1992, the average upwelling index was rather stable, which equaled about 126 m^3/s per 100 m of the coastline. In the first half of the period (1968–1980) the anchovy catches increased by 5X, and in the second half (1981–1992) they decreased by more than 5X. Apparently, long-term fluctuations of the anchovy population may not be explained only by the concept on optimal upwelling intensities.

Thus, despite relative knowledge about the region, particular reasons of long-term fluctuations and alterations of sardine and anchovy population outbursts in the California upwelling region remain unclear. Reliable relationships between the long-term dynamics of zooplankton and sardine and anchovy productivity in the California upwelling region have not been observed.

KUROSHIO-OYASHIO REGION

The Kuroshio region is one of the most productive and relatively well-studied zones of the North Pacific. In this zone systematic measurements have been performed over more than 40 years of plankton biomass [Odate, 1994; Shugimoto, Tadokoro, 1997, 1998] along with comprehensive studies of development features of the recent Japanese sardine population outburst [Kawasaki, 1992a, b, 1994; Nakata et al., 1994; Watanabe et al., 1995; Oozeki, 1999].

Commercial catches in the region comprise two main components: Japanese sardine (*Sardinops melanosticus*) providing catches of 5.4 million tons as it's maximum, and a group of pelagic fishes, which includes Japanese mackerel (*Scomber japonicus*), Japanese horse-mackerel (*Trachurus japonicus*), Pacific saury (*Cololabis saira*), and Pacific anchovy (*Engraulis japonicus*), providing total catches of about 2 million tons at their maximum [Kawasaki, 1992a, b]. The breeding and feeding area of these species includes the Kuroshio-Oyashio system, and the feeding area of sardine also includes the Kuroshio extension, well into the western North Pacific. Therefore, dynamics of the fish productivity should be compared with the multiyear changes of the plankton biomass within the entire North Pacific region neighboring the Kuroshio-Oyashio zone (Fig. 5.11). In the north, in the Oyashio zone, the zooplankton biomass is 3–5 times greater than in the Kuroshio zones and the transition zone between them. Dynamics of zooplankton biomass in the Oyashio zone has as rather well expressed maximum in the early 1970s, whereas the long-term dynamics of zooplankton in the Kuroshio and transition zones are weak. In fact, total changes in zooplankton biomass of the entire Kuroshio-Oyashio region is dominated by dynamics of zooplankton in the Oyashio zone ($r = 0.92$).

The dynamics of chlorophyll-*a* concentration, which reflect development of phytoplankton, and dynamics of zooplankton biomass in the Kuroshio-Oyashio region and western and central zones of the North Pacific are shown in Figs. 5.12 and 5.13 [data from Shugimoto, Tadokoro, 1997, 1998; Tadokoro, 2001]. Fig. 5.12 shows that chlorophyll dynamics in these two regions are quite similar ($r = 0.86$) and demonstrate 2–3-fold increase during the period of 1950s into the early 1970s followed by the decrease into the 1990s. The long-term zooplankton changes in the central zone of the North Pacific and in the Kuroshio-Oyashio region (Fig. 5.13) are similar to the changes in chlorophyll-*a* concentration (Fig. 5.12). From the early 1950s until the mid

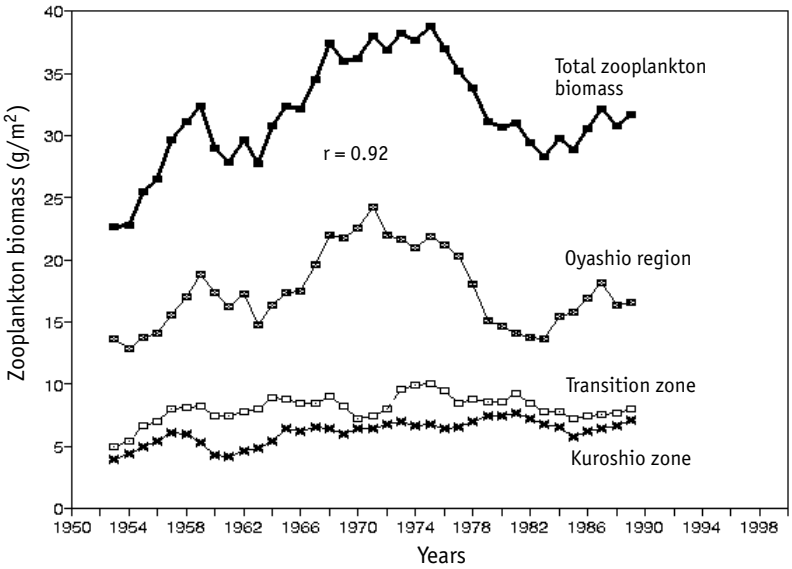

Fig. 5.11. Comparative dynamics of zooplankton biomass in different parts of the Kuroshio-Oyashio region during the period of 1953–1989. The bold line shows total zooplankton biomass, crossed squares — zooplankton of Oyashio region, white squares — zooplankton of the transition zone, black cross — zooplankton of the Kuroshio zone. Data from Odate, 1994

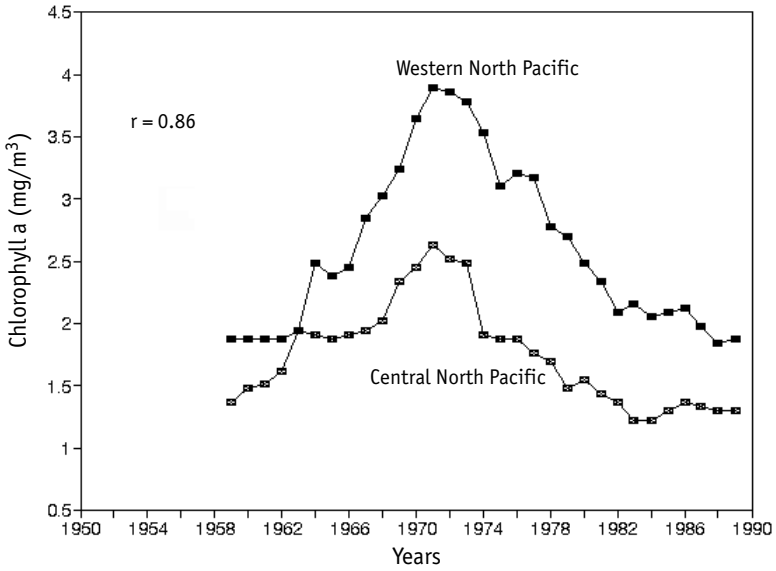

Fig. 5.12. Long-term dynamics of chlorophyll-*a* in the upper 30-m layer of central (crossed squares) and western (dark squares) North Pacific during the period of 1960–1998. Data from Tadokoro, 2001

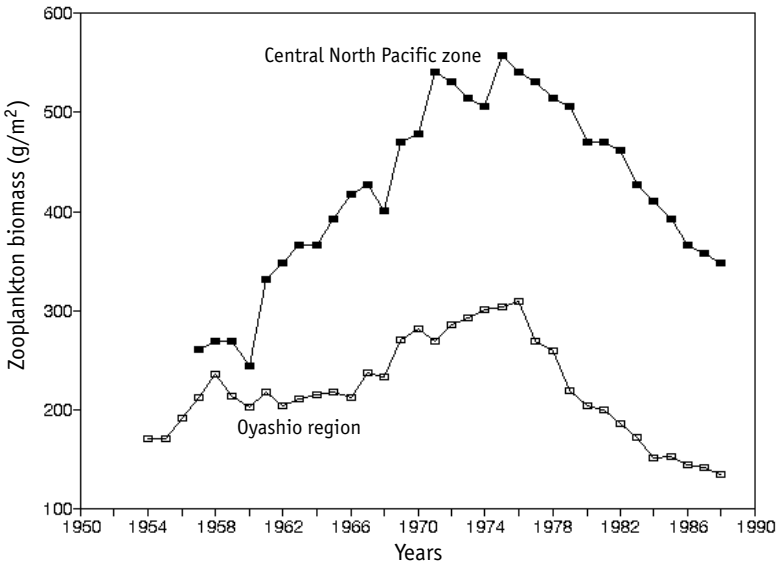

Fig. 5.13. Dynamics of zooplankton biomass in the central North Pacific zone (dark squares) and Oyashio region (white squares), 10-year smoothing. Data from Shugimoto and Tadokoro, 1997; Tadokoro, 2001

1970s, in these two regions the zooplankton biomass increased by 2–3X, and afterwards began decreasing [Shugimoto, 2001, 2002]. The long-term dynamics of zooplankton in the western zone of the North Pacific is similar to that in the central part of the North Pacific [Shugimoto, Tadokoro, 1997]. Thus, according to the available data all three regions considered (Kuroshio-Oyashio, central and western zones of the North Pacific) exhibit similar dynamics of both phyto- and zooplankton with the maximum in the mid 1970s.

The long-term dynamics of total fishery catch for the five dominant species in the Kuroshio-Oyashio region for the 36-year period (1953–1989) are shown in Fig. 5.14. An almost 5-fold increase of commercial catches observed during the period of 1975–1985 occurred within the background of a somewhat steady zooplankton biomass in the Kuroshio-Oyashio system, as well as in the northwestern and central areas of the North Pacific. Maximum catches (about 7 million tons) were observed in the mid and late 1980s, with 80% of the peak catch comprising the most productive species e.g. Japanese sardine.

The dynamics of Japanese sardine catches are significantly different from the oscillations of the total catches of other planktivorous fish species in the Kuroshio-Oyashio system. Contrary to the sardine having maximum catches

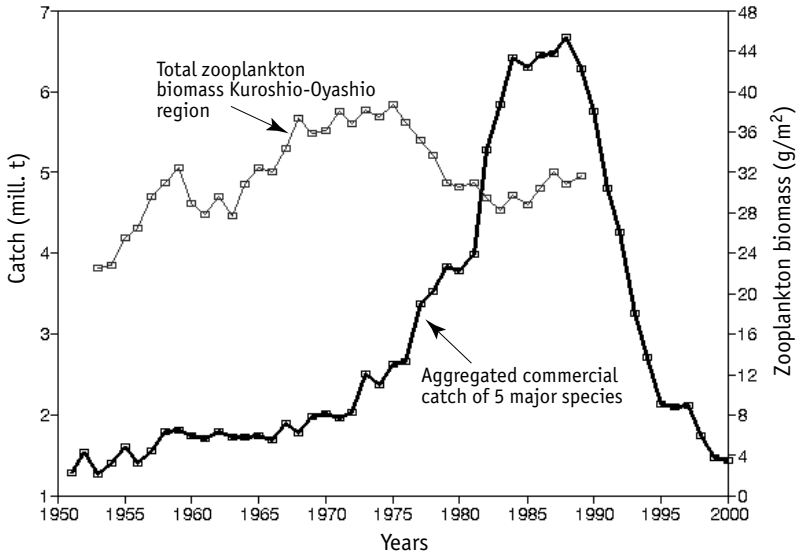

Fig. 5.14. Dynamics of zooplankton biomass (white squares) and aggregated commercial catch of 5 major commercial species: Japanese sardine, Japanese mackerel, Japanese horse mackerel, saury and Japanese anchovy (bold line) in the Kuroshio-Oyashio region

in the late 1980s, maximum catches of planktivorous fishes (except for Japanese sardine) were observed in the early 1970s (Fig. 5.15). Total catch for the four planktivorous fish species of the region (Japanese mackerel, Pacific saury, Japanese horse mackerel, and Japanese anchovy) closely correlate with the dynamics of zooplankton biomass ($r = 0.92$). However, this close correlation is generally generated due to only one species, which is Japanese mackerel (Fig. 5.16), whereas changes in catches of Pacific saury, Japanese horse mackerel, and Japanese anchovy exhibit low correlations with the dynamics of zooplankton.

The dynamics of the sardine catches are in opposite phase with the dynamics of zooplankton abundances (Fig. 5.17), although the correlation coefficient is low ($r = –0.33$) due to variability of the plankton data.

Amplitudes of oscillations of zooplankton biomass and sardine catch during the period of 1960s into the late 1980s are significantly different. During that time, the zooplankton biomass decreased by approximately 25% (from 22 to 17 g/m^2), whereas sardine catches increased from several thousand tons in the 1960s to 5.4 million tons in the mid 1980s, i.e. by approximately a thousand X. The scope of changes in the fish productivity and zoo-

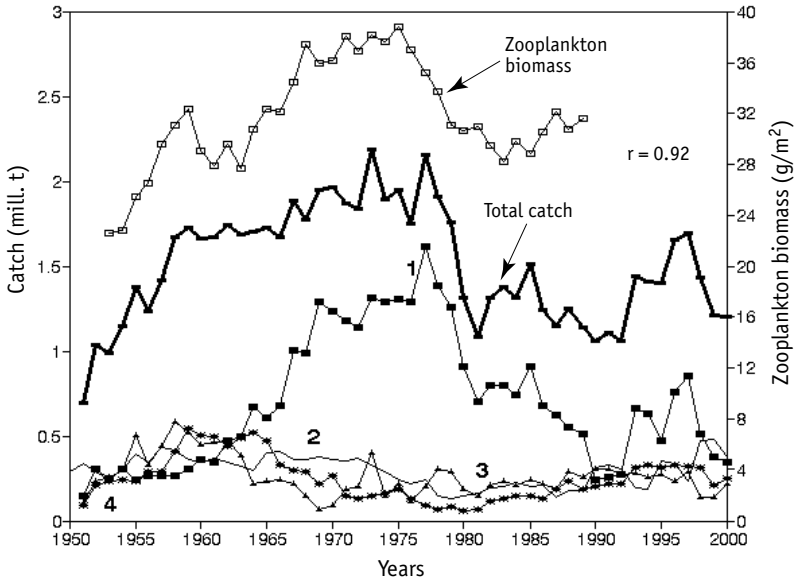

Fig. 5.15. Comparative dynamics of zooplankton biomass (white squares) and commercial catches of the major commercial species in the Kuroshio-Oyashio region (except for Japanese sardine). *1* — Japanese mackerel, *2* — Pacific saury, *3* — Japanese horse mackerel, *4* — Japanese anchovy. Bold line shows the aggregated commercial catch in the Kuroshio-Oyashio region

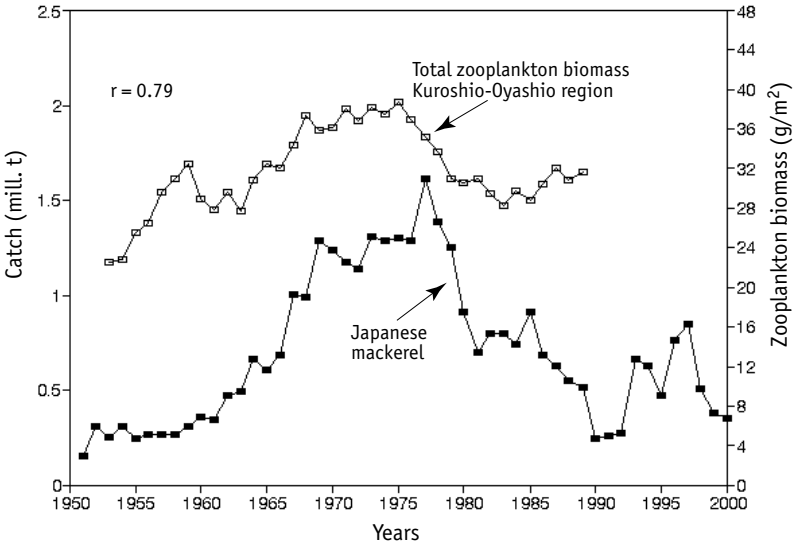

Fig. 5.16. Comparative dynamics of Japanese mackerel commercial catch (dark squares) and zooplankton biomass (white squares) in the Kuroshio-Oyashio region during the period of 1950–1986

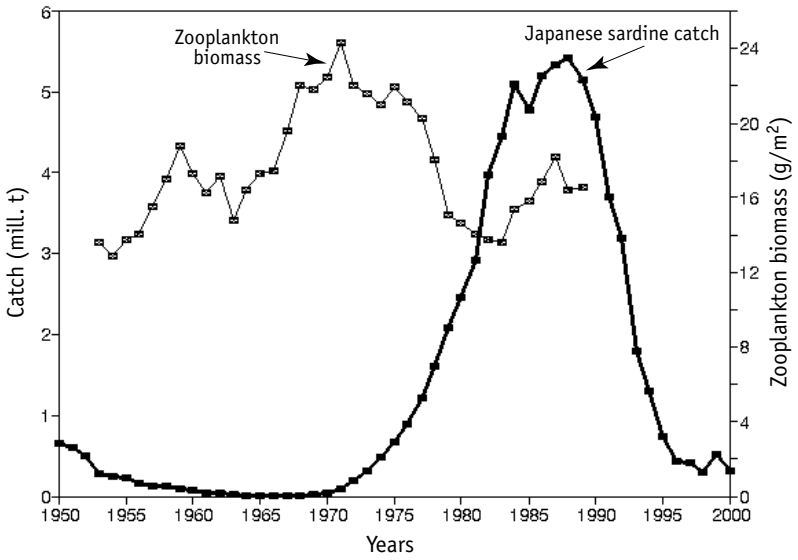

Fig. 5.17. Comparative dynamics of zooplankton biomass (crossed squares) and Japanese sardine catch (dark squares) in the Kuroshio-Oyashio region during the period of 1950–1989

plankton are incomparable. This indicates the independence of large-scale outbursts of sardine population and zooplankton biomass changes.

The most rapid increase of sardine population, during the period of 1975–1985, coincided with the decrease of zooplankton biomass in the region. Contrary to other planktivorous fish species in the Kuroshio-Oyashio system, the outburst of sardine population during the 1970s–1980s was accompanied by expansion of its feeding area to the east by as far as 20° (to 165° W). In this period, the sardine feeding area increased by about an order of magnitude and included both the Kuroshio-Oyashio system and a significant area of the western North Pacific out to the Dateline. High production of sardines was the result of their feeding in the ocean area to the east and northeast of Japan, outside the Kuroshio-Oyashio system itself.

In the 1990s, the rapid decrease of sardine population and catches resulted from the abrupt decrease of the reproductive population. As suggested [Shugimoto, 2002], this relates to weakening of southern interventions of the cold Oyashio Current in to the intermediate confluence zone of the Kuroshio and Oyashio Currents. This led to a decrease of zooplankton biomass, and thus the abrupt decrease of sardine larval survivability, and subsequent decrease of recruitment to the adult population.

Fig. 5.18 shows dynamics of the long-term changes of the ocean surface temperature in the confluence zone of the cold Oyashio Current and the relatively warm Kuroshio Current [Wada & Oozeki, 1999; Qiu, 2002]. Clearly, the beginning of sardine population outburst coincides with the temperature anomaly transition from positive to negative values in the early 1970s. Hence, a sharp increase of sardine population occurred at the more negative temperature anomalies in this mixing zone. Conversely, the beginning of sardine population decrease in the second half of the 1980s coincides with the anomaly transition to positive (warmer) values.

It is of interest that during the period of the 1970s–1990s temperature decrease in the Kuroshio-Oyashio mixing zone occurred while the Global dT and PDO index increased, the latter characterizing the average surface temperature of the North Pacific. Apparently, a temperature decrease in the Kuroshio-Oyashio mixing zone reflects strengthening of cold Oyashio Current. This creates favorable forage conditions for Japanese sardine larval survival and development of abundant generations within the mixing zone. Vice versa, the Oyashio Current weakening is accompanied by increasing tempera-

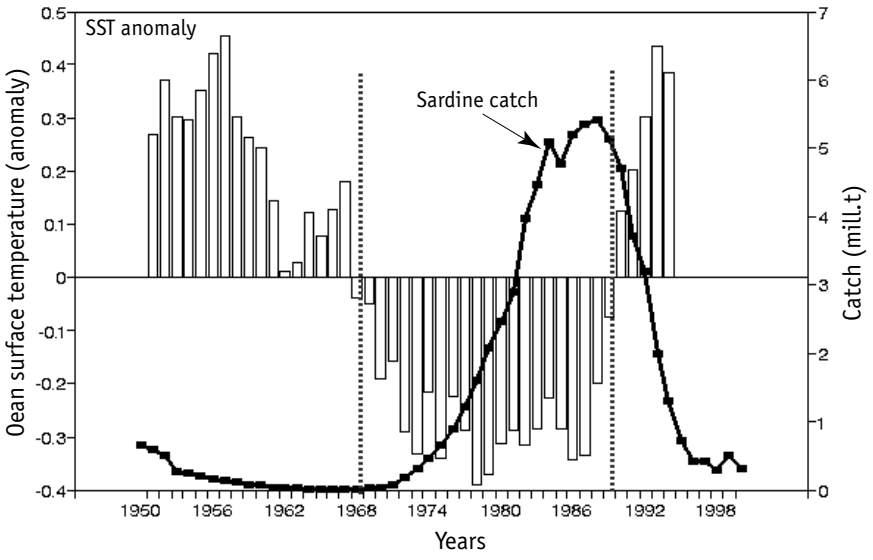

Fig. 5.18. Comparative dynamics of total Japanese sardine catch (dark squares) and the ocean surface temperature anomaly (bars) in the Kuroshio-Oyashio mixing zone (30–35° N and 130–180° E). Vertical dotted lines show temporal boundaries of the negative sea surface temperature anomaly. Data from Wada and Oozeki, 1999

ture of the mixing zone and deterioration of the forage conditions for early stage drifting sardine larvae.

Data shown in Fig. 5.18 allow, as a first approximation, estimation of the periodicity of long-term temperature fluctuations in the mixing zone. The time between the temperature maximum in the mid 1950s and the minimum in the early 1980s is about 25–30 years. One may suggest that the total fluctuation period is estimated as 50–60 years. This correlates with the fishery statistics data for sardine catches for the recent 80 years and with historical evidence of an approximate 60-year periodicity of Japanese sardine population outbursts for the recent 400 years [Kawasaki, 1994; Klyashtorin, 2001].

The long-term changes of atmospheric circulation in the West Pacific during the sharp increase of Japanese sardine population during the 1970s–1980s was accompanied by increased wind forcing, the higher frequency of Oyashio Current incursions to the south, and the temperature decrease in the mixing zone [Qiu, 2002]. Apparently, the latter is related to total strengthening of atmospheric circulation in the North Pacific, affected by the expansion of the Aleutian Low atmospheric pressure area. The latter caused the increase of both the Oyashio Current rate and cold water delivery to the mixing zone [Yasuda et al., 1999; Tadokoro, 2001].

The analysis of long-term dynamics of atmospheric pressure and wind activity dynamics in the North Pacific allowed estimation of the major current discharge in the region for the 20-year period of 1966–1986 [Schwing, 1998]. From the mid- 1970s until the mid- 1980s the wind activity, upwelling intensity and turbulent mixing of the upper layer increased significantly. Total discharge of the currents to the north increased by almost 7 times. That led to the increase of the western reverse current in the sub-Arctic circulation and influx of relatively cool waters of the Oyashio Current, delivered from the north-east to the zone of mixing with the Kuroshio Current. Therefore, changes in the atmospheric circulation and dynamics of oceanic water, general for the entire North Pacific, affect hydrology and fish productivity of particular regions. In an empirical model of Japanese sardine biomass fluctuations [Noto, Yasuda, 2003], changes of the spring-summer temperature in the Kuroshio-Oyashio mixing zone is considered to be the dominant factor determining the long-term fluctuations in the sardine biomass. According to the model, control of the population density, or abundance, is relatively insignificant.

On the fishery effect on Japanese sardine population and catches

Between 1970 and 1988, Japanese sardine catches increased by three hundred times, from 17000 tons to 5.4 million tons. Within 11 years (1981–1991) the average annual catches equaled about 4 million tons; catches decreased at a rate of 400–500 thousand tons annually during the period of 1989–2000, and finally, fell to ~300000 tons.

Such a dramatic decrease of the catches is routinely explained by suggesting overexploitation due to excessive fishing effort. In such cases, a decrease of the commercial stock and rapid decreases of catch are usually accompanied by the significant decrease of the spawning stock population and thus the amount of eggs spawned. The first expectation is that overexploitation results in disappearance of older fishes from the catch [Gulland, 1982]. However, the proportion of older Japanese sardines has not decreased, as many would expect, but actually began increasing. Moreover, the number of spawned eggs and post first-feeding larvae remained stably high [Watanabe et al., 1995; Wada, Jacobson, 1998], see Fig 5.19.

Fig. 5.19 shows that the number of spawned eggs and post first-feeding larvae remains virtually unchanged or even increased by 1992. At the

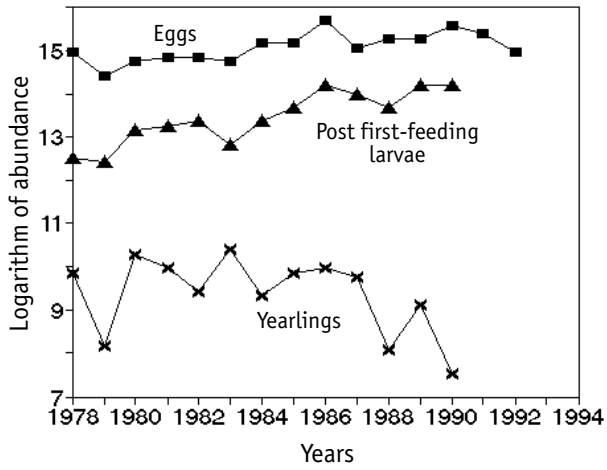

Fig. 5.19. Changes in abundance of eggs (dark squares), post first-feeding larvae (triangles) and age 1+ recruitment (crosses) in the Doto region, which is the main foraging area for sardine juveniles in the Oyashio region. Ordinate is the logarithm of abundance. Data from Watanabe et al., 1995

same time, from 1986 the number of age 1+ fishes representing future stock recruitment began decreasing rapidly, and by 1990 it had declined by over 99%.

High population numbers of spawning sardine and the amount of spawned eggs do not guarantee the occurrence of abundant generations. The key condition for the occurrence of a successful recruitment generation is the successful drifting of the larvae from the spawning zone at the northern area of Honshu Island to the northeast into the Kuroshio-Oyashio zone, where an abundant forage base has developed, and then onward into the forage area in the ocean northeast from Hokkaido Island [Wada, Oozeki, 1999; Yasuda et al., 1999; Oozeki, Nakata, 2002]. As described earlier, the occurrence of abundant generations of sardine are related to the long-term shifts of Kuroshio and Oyashio Currents borders from the south to the north and back. High survival of larvae and juveniles was observed during the 1970s–1980s, when increased Kuroshio meandering was observed. Low survival was observed in the years when meandering of the current was weak [Nakata et al., 1994]. Despite the multiyear monitoring of the Kuroshio Current, specific oceanographic and hydrobiologic mechanisms that determine sardine population outbursts are not yet entirely clear [Oozeki, 1999].

Given these observations, despite the extremely high level of the sardine fishery, the «expected» signs of population overexploitation were not observed. The main reason for the recent Japanese sardine fishery decrease is related to changes of hydrologic and hydrobiological situations that occurred in the late 1980s. These deteriorated the conditions necessary for larval sardine survival, decreasing the recruitment population, and subsequently, resulted in the decreases in both the commercial resource population and sardine catch.

Japanese anchovy and Japanese flying squid

The Japanese flying squid (*Todarodes pacificus*) fishery area approaches the Kuroshio zone from the southwest. Total catch of the Japanese flying squid in this area approaches 750000 tons. Oscillations of the catch in the south Sea of Japan and East China Sea during the 34-year period from 1965–1998 are closely related to dynamics of the zooplankton biomass (r = 0.82–0.86)

[Kang et al., 2002]. Before the 1980s the zooplankton biomass and squid catches increased slowly, but since the mid 1980s their growth appeared much more rapid. It has been suggested that this growth was basically regulated by the macrozooplankton biomass. Comparison of total catches of Japanese flying squid [Sakurai et al., 2000] and dynamics of zooplankton in the Kuroshio system is shown in Fig. 5.20. Although the time series for zooplankton is rather short, one may consider that in the first approximation the trends of both curves are rather close.

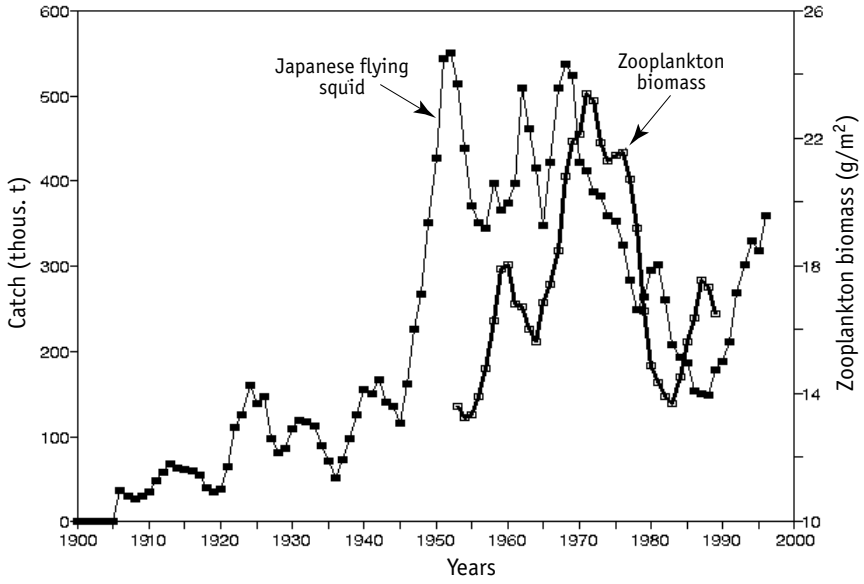

Fig. 5.20. The dynamics of Japanese flying squid (*Todarodes pacificus*) commercial catch (dark squares) and zooplankton biomass (bold line) in the Oyashio region. Data from Odate, 1994

Comparison of Japanese flying squid and Japanese anchovy catches (Fig. 5.21) show that the dynamics of the catches of both commercial species correlate closely ($r = 0.78$), which, along with the concepts regarding their feeding preferences for macrozooplankton, may provide indirect evidence of corresponding changes in the zooplankton biomass and squid population.

There are no data on the zooplankton dynamics in the Kuroshio-Oyashio system available from the period of 1990–2000. However, judging from the increasing anchovy and Japanese flying squid population, we suggest

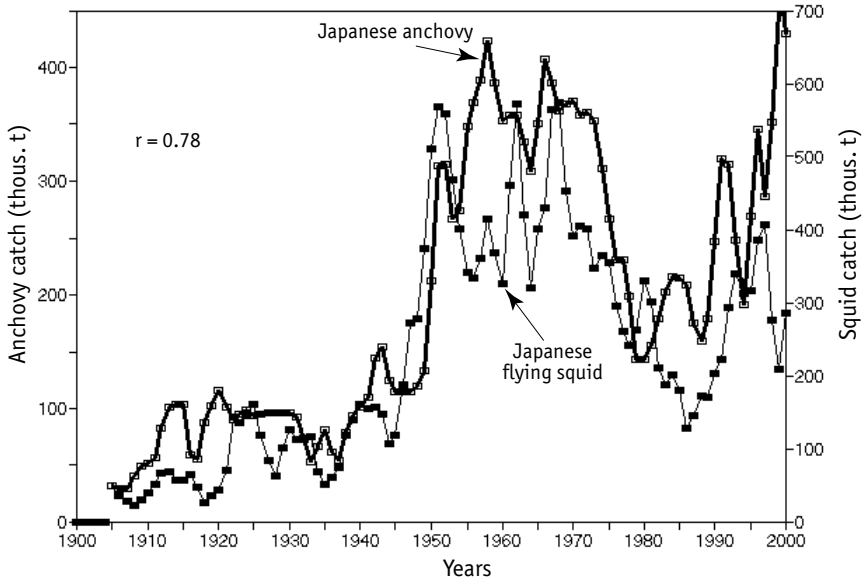

Fig. 5.21. Comparative catch dynamics of Japanese anchovy (bold line) and Japanese flying squid (dark squares) during the period of 1905–2000

that over the recent decade in the Kuroshio-Oyashio zone and neighboring part of the western North Pacific, there was likely an increase in zooplankton biomass.

Comments in brief

In the Kuroshio-Oyashio region, the northwest and central areas of the North Pacific, long-term phytoplankton (using proxy of chlorophyll-*a*) and zooplankton fluctuations show similar dynamics, with their maxima in the mid- 1970s.

The dynamics of total fish productivity in the Kuroshio-Oyashio region (including Japanese sardine) with the maximum in the mid 1980s is almost in opposite phase with that of phyto- and zooplankton. Japanese mackerel is the only species for which catches closely correlate with the zooplankton dynamics.

During the period of the 1970s–1980s, the outburst of the Japanese sardine, the most productive fish population, occurred with the background of the descending zooplankton biomass for the northwestern and central parts of the North Pacific, with the simultaneous expansion of the forage area of the sardines by more than an order of magnitude.

The dynamics of the Japanese sardine population depends on both long-term changes in the zooplankton biomass in the region and oceanic conditions in the Kuroshio-Oyashio convergence mixing zone. These conditions determine the relative survival of sardine larvae during their critical first-feeding period, as well as their further general growth and maturation, thus determining the recruitment to the commercial resource population. Formation of favorable conditions is related to the increase of frequency of the Oyashio Current incursions into the zone of mixing with Kuroshio Current which is, apparently, determined by large-scale general fluctuations of the atmospheric circulation over the entire North Pacific — with the periodicity of 50–60 years.

Northeastern Pacific and Gulf of Alaska

From the early 1960s until the late 1980s the zooplankton biomass virtually doubled in the entire Gulf of Alaska (area of over 4 million sq. km). During this period, the biomasses of salmon, sea bream and squid also increased by approximately 2X [Brodeur, Ware, 1992, 1995]. Since 1970s, total nekton biomass was increasing and reached its maximum in the mid 1980s. These authors relate fish biomass increase in this region (pollock and salmon, in particular) to general increase of the ecosystem productivity: owing to winter wind mixing concentration of nutrients in the euphotic layer, primary production and zooplankton biomass increased.

According to these data, changes in fish and zooplankton productivity in Gulf of Alaska are in positive phase. However, in most regions of the North Pacific the increase of fish productivity in the recent 30 years was in opposite phase with dynamics of the zooplankton biomass. The long-term changes in the zooplankton biomass in Gulf of Alaska are in similar phase with the California Current region [McGowan, 1995] and other regions of the North Pacific [Shugimoto, Tadokoro, 1997, 1998; Tadokoro, 2001; Shugimoto, 2002].

Thus, we see that during the recent 30–40 years, according to the features of the long-term dynamics of phyto- and zooplankton in the northeastern areas of the Pacific and Gulf of Alaska, these regions are different from the rest of the North Pacific. At the same time, the fish productivity in this region changed in phase with the many changes that occurred around the entire North Pacific zone.

SOUTH-BENGUELA UPWELLING

Plankton collections in the South-Benguela upwelling region along the western coast of the South Africa (from Cape Columbine to Saint Helena Bay) were performed routinely over the 46 year period of 1951–1996 [Verheye et al., 1998; Verheye, Richardson, 1998]. This allows comparison of the long-term changes in the zooplankton biomass and fish productivity in this region. Fig. 5.22 shows dynamics of total sardine (*Sardinops ocellatus*) and anchovy (*Engraulis japonicus capensis*) catches and long-period changes of zooplankton in the region.

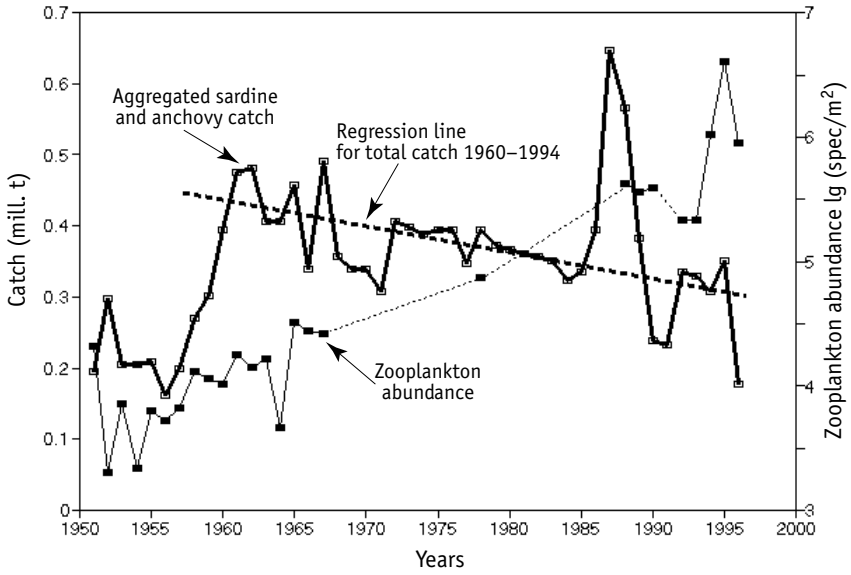

Fig. 5.22. Dynamics of zooplankton abundance (dark squares, logarithmic scale, right axis) and aggregated catch of sardine (*Sardinops ocellata*) and anchovy (*Engraulis japonicus capensis*) (bold line) in the South Benguela region. Data from Verheye and Richardson, 1998

Over all 46 years of observation, the total sardine and anchovy catches varied from 200000 to 600000 tons. For various reasons, during the period of 1960–1994, there was a decrease of total fish productivity by approximately 25% in the region (from 400000 to 300000 tons, on average). During this period, the zooplankton population increased by more than two orders of magnitude. The plankton population increase was accompanied by a decrease in the proportion of macroplankton and increased proportion of

small copepods [Verheye, Richardson, 1998]. Even taking into account these circumstances, the fundamental changes in the fish productivity of the region compared with the increase of zooplankton population, in the first approximation, was accepted as being constant. The long-term relationship between zooplankton and fish productivity approaches the opposite phase (negative relationship) although the level of correlation is low (r = –0.47) [Cury et al., 2000].

During the period of the 1950s into the mid- 1980s, the dynamics of the coastal upwelling activity in the region correlates with the trend of logarithmic increase of the zooplankton population abundance [Verheye, Richardson, 1998]. During the period of low upwelling intensity (up to 1970s) the sardine population increased, whereas during the period of relatively high intensity (1970s–1980s) anchovy catches increased. From the perspective of these authors, the long-term increase of the zooplankton population in the South Benguela upwelling reflects simultaneous action on the so-called «top-down control» mechanisms, i.e. fish grazing of zooplankton, and the «bottom-up control», i.e. the change of total ecosystem levels of zooplankton, starting from the primary production level. Unfortunately, these explanations provide no clear pathway to understanding of real-world ways that energy transfers take place between different trophic levels in these ecosystems.

A RELATIONSHIP BETWEEN ZOOPLANKTON DYNAMICS AND CLIMATIC CHANGES

As mentioned above, data on the long-term changes in the zooplankton biomass are very scanty. First of all, this is determined by the difficulties of implementation of such investigations, which require continuous measurements of oceanographic and biological characteristics at the same locations over two or three decades.

One of the longest observational series for the dynamics of zooplankton development was performed over 44 years (1954–1998) at the so-called «Station P» in the western part of the North Pacific [Mackas, Tsuda, 1999], (Fig. 5.23). During the period of «cooling» beginning in the late 1950s, the calendar date of the maximum spring-summer zooplankton population bloom gradually shifted from the end of May to a later time. By the mid 1970s, at the minimum of Global dT (and PDO index), the delay in peak bloom time

was over 40 days. Therefore, the maximum of zooplankton development occurred in early July. During the warming period since the mid 1970s, the peak of the zooplankton bloom was observed earlier and earlier. By the late 1990s, it occurred in late May, almost 60 days earlier than in the mid 1970s. Thus, the occurrence of the zooplankton development peak shifts in parallel to Global dT changes. In the entire northeastern Pacific, including the «Station P» region, the zooplankton biomass gradually increased from the middle of the century, and reached its maximum by 1960s–1970s, i.e. at the middle of the «cooling» period [Shugimoto, Tadokoro, 1997; Tadokoro, 2001].

These latter publications show that the surface temperature increase of the Atlantic Ocean was accompanied by shifting of calendar times of phytoplankton «blooming» in the North Sea to earlier times (almost by 3 weeks), and the maximum of the zooplankton bloom shifted by almost 2 weeks compared with those in the 1950s–1960s [Edwards, Richardson, 2004]. Hence, in the warming period of 1970s–1990s temperature increased in the Arctic part of Atlantic, whereas in the southern part it decreased. Generally, the her-

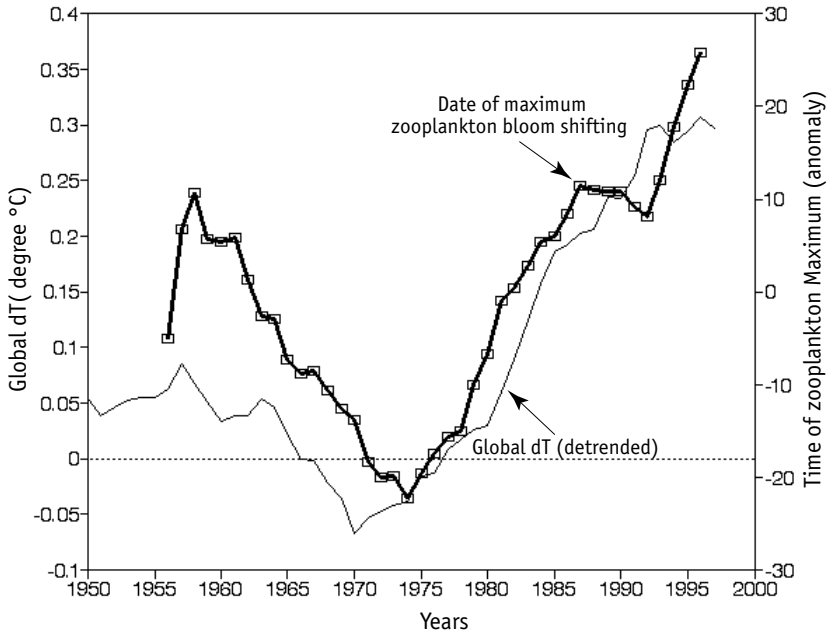

Fig. 5.23. Long-term changes during the period of the spring-summer zooplankton bloom maximum at the «Station P» (5-year smoothing). Data from Mackas et al., 1998; Mackas and Tsuda, 1999. Thin line shows Global dT; white squares show times of zooplankton maximum abundance (anomaly)

bivorous zooplankton population followed the same patterns related to temperature. Direct consequences of the effect of these changes on the fish productivity are not clear. However, noticeable shifts of calendar dates of seasonal maxima for phyto- and zooplankton development must affect the functioning of the entire pelagic ecosystem [Richardson, Schoeman, 2004].

The early ice retreat in the northern part of the Barents Sea is accompanied by delayed development of phyto- and zooplankton, but leads to the formation of high copepods biomasses. Conversely, later ice retreat is accompanied by early development of phyto- and zooplankton, and low copepod biomass. An additional factor affecting the plankton development is the surface layer mixing mode determined by the frequency of storm ocurrences, current intensities and existence of summer stratification zones [Ladd et al., 2002].

Thus, the long-term climatic changes determine the periods of phytoplankton development, the duration of the vegetation season and zooplankton productivity that affects both total productivity of the ecosystem and the frequency of recurrence of favorable conditions that support abundant generations of pollock, cod, herring and other commercial species [Hunt, 2003].

Comments in brief

The above data show that the long-term fluctuations in Peruvian anchoveta (*Engraulis ringens*) population do not correlate with the dynamics of zooplankton. Other species considered, as per the Japanese sardine (*Sardinops melanosticus*), Peruvian sardine (*S. sagax*), California anchovy (*Engraulis mordax*), demonstrate opposite phase or weakly correlated fluctuations between zooplankton biomass and abundances of their populations. A reliable relationship between the long-period fluctuations of zooplankton and fish biomass could not really be determined due to the high variability and erratic sampling of the plankton data. Therefore, any comparison is limited to trend estimations.

Opposite phase, but weakly correlated relationships between dynamics of zooplankton and fish productivity (with the correlation indices in the range of 0.2–0.4) were observed in the ecosystem of Guinea upwelling, the Kuroshio-Oyashio region, and in the California Current [Cury et al., 2000]. Back in 1961, when analyzing the effect of fishery on the California sardine population during the period of its outburst and decrease in 1930s–1960s, Murphy [1961] had concluded that there is no reliable correlation between

the long-term dynamics of zooplankton biomass and the sardine population, and that the principle controller of sardine population dynamics is oceanographic conditions changes.

The comparative analysis of catch dynamics of the major commercial fish species in the North Sea and the zooplankton population was performed using the data from the continious plankton recorders obtained during the period from 1948 to 1998 [Reid et al., 2000]. Changes in catches of the most productive species, herring (*Clupea harengus*), correlated positively with the long-term dynamics of copepods, whereas catch dynamics of mackerel (*Scomber scombrus*) were weakly anti-phase to the total *Calanus* copepod abundance estimates. A relationship between dynamics of age 1+ cod population in the North Sea and the zooplankton abundance index was found [Beaugrand et al., 2003], although correlation coefficients are, again, rather low (ranged within 0.5–0.6). However, the abundance of zooplankton is considered to be one of the possible reasons for *Gadidae* population abundance dynamics observed during the 1960s to the 1980s in the North Sea.

During the period from 1955 to 1987, the long-term changes in the populations of phyto- and zooplankton, and herring in the North Atlantic and the North Sea were coherent : the maximum level of their abundance indices was observed in the 1950s, and the minimum in the 1970s [Aebisher et al., 1990]. Generally, the trends of these biological abundance indices correlated with the dynamics of the western wind periodicity within the same period. The authors suggest that the long-term changes in the plankton and herring population are related to climate changes.

Cushing [1995] analyzed dependencies between dynamics of zooplankton, wind activity and the recruitment to commercial fish stocks over 30–40 years in the North Atlantic, the Kuroshio-Oyashio region, California Current, and Peruvian upwelling. The recruitment trend of Atlantic herring and cod, California sardine, mackerel and Peruvian anchoveta stocks demonstrated both positive and negative correlation with zooplankton dynamics and the wind activity index. In conclusion the author states that «The relationship between zooplankton population and recruitment is still unclear, but whatever the nature of the relation between zooplankton dynamics and the fish population would be, climatic factors may play an important role» [Cushing, 1995, p. 22].

When considering the opposite phase changes of the zooplankton and fish biomass, commonly discussed is the so-called «top-down control», i.e. the decrease of zooplankton populations due to active grazing by fishes.

However, it should be taken into account that as fish biomass increases, a decreasing zooplankton population should somehow simultaneously increase its production rate to support the increasing fish population. For example, the increase of Japanese sardine biomass by several orders of magnitude would require corresponding (by several orders of magnitude) increase of zooplankton production, despite zooplankton biomass decreases, which is simply unrealistic. Apparently, this basic local imbalance is compensated by the significant increase of the sardine forage area out into the adjacent ocean.

Significant oscillations of planktivorous fish populations in the ocean apparently cause only weak effects within the food chains, and the so-called «top-down control», observed in oligotrophic fresh water bodies, is not really observed in oceanic ecosystems [Steele, 1998]. The long-term changes in the populations of Gadidae in the North Sea have occurred with the background of significant plankton biomass oscillations, which does not support the general concepts about trophic cascades, which include phytoplankton, zooplankton and fishes. [Steele, Collie, 2005, in press]. Abrupt changes in the Georges Bank populations of commercial fish species have been practically independent of the zooplankton population [Sherman et al., 1998].

The examples above of the long-term fluctuation dependence of the major pelagic fish population abundances on zooplankton production or biomass are contradictory and allow no unambiguous conclusions.

When estimating feeding relations within pelagic communities, one should focus on the value of planktonic association and production rather than on biomass or population. Hence, it should be taken into account that copepods do not always comprise the major portion of zooplankton biomass, but they are particular species, which yield up to 80% production of the planktonic association [Shuntov, 2001]. The conceptual basis from which assumes fluctuations of fish productivity in ecosystems are primarily due to the «cascade» formation: primary production (phytoplankton) > zooplankton > fish, are not confirmed for the majority of productive ocean regions [Shuntov, 2001]. The concept of trophic cascades arose from investigations carried out in oligotrophic lakes with very simple trophic chains: phytoplankton > zooplankton > fishes-plankton feeders. Food chains in oceans are much more complicated, multistage, and demonstrate inapplicability of the «cascade» concept ideas to them [Steele, Collie, 2005, in press].

In marine ecosystems, the number of intermediate trophic components that progress between the primary production, zooplankton and highest tro-

phic level comprise more numerous trophic levels than those of fresh water trophic systems. Moreover, within the planktonic association, trophic relations represent a complex network, in which, figuratively speaking, «all eat all», and almost 90% of energy of the oceanic planktonic association is consumed within itself. Oceanic planktonic associations represent multispecies systems with multiple relationships between many population components. Although oceanic trophic systems is rather complex, each has two main components: carnivorous and herbivorous zooplankton [Shuntov, 2001; Dulepova, 2002]. Among species of carnivorous zooplankton, the main role is played by chaetognaths (*Chaetognatae*), in particular, the widespread species *Sagitta elegans*. For example, in the North Sea this species, is the main planktonic predator, and directly effects the structure and dynamics of the various component zooplankton populations, and is thus the key factor for the long-term dynamics of the entire zooplanktonic association. In turn, changes in *Sagitta* populations are related to the effects of hydrological and climatic factors [Clark et al., 2003].

Due to these oceanic ecosystems' complex operation, given this multistage system of cross-forage relationships, the role of fish species as consumers in such systems do not appear to be predominant. Zooplankton consumption by nekton (fishes, squids, etc.) is at least an order of magnitude lower than that by carnivorous plankton, and overall, fishes consume less than 10% of zooplankton production [Shuntov, 2001].

At present, there is no general opinion on the effective energy transfer between the different trophic levels in ocean ecosystems. The suggestion for the approximately 10% efficiency of energy transfer between different trophic levels was formulated long ago [Slobodkin, 1960]. However, later estimates of this index were much lower, yielding 1 to 5% [Pomeroy, 1979]. These measured indices of energy transformation were much lower. For example, in the Peruvian upwelling system, with the anchoveta population biomass at its maximum, only about 2–3% of the primary production are diverted into anchoveta, whereas at its minimal population this index decreases by an order of magnitude to 0.2–0.3% [Chavez et al., 1989]. From 0.2 to 0.3% of the primary production is converted to biomass of commercial fishes of the Sea of Okhotsk and Bering Sea, and for the entire North Pacific region production of commercial fishes apparently does not exceed 0.5% of the primary production. At the same time, high seasonal production of zooplankton, comprising small copepods, may determine the local survival of larvae and juveniles of pelagic fishes in the critical periods of their life

cycle, promoting, or not, occurrences of abundant recruitment generations [Dulepova, 2002].

Thus, the dependence between zooplankton dynamics as a trophic unit between phytoplankton (the primary production) and fish production is still uncertain. High levels of the primary production, alone, do not guarantee high levels of zooplankton development and subsequent fish production. Fluctuations in the populations of the major commercial species in the upwelling zones and other highly productive areas of the ocean depend on naturally occurring sequences of conditions that eventually support abundant recruitment. The periods of outbursts (or decreases) of major pelagic fish populations correspond to periodicities of favorable (or unfavorable) meteorological, hydrological, and hydrobiological conditions. Clearly, the highest amplitudes of fish productivity fluctuations are observed in the most productive areas of the ocean, where potentials for anchovies, sardine and other pelagic fishes population outbursts are rather high.

CHAPTER 6

DYNAMICS OF ANCHOVY POPULATIONS IN THE PACIFIC REGION

PERUVIAN ANCHOVETA

Peruvian anchoveta (*Engraulis ringens*) is the most abundant and productive species in the Pacific region; biomass of its population reaches 20 million tons and catches reach 13 million tons (Fig. 6.1). In a first approximation, oscillations of catches correspond with the population biomass changes of this species. Although in 1950s–1960s fishery development was some-

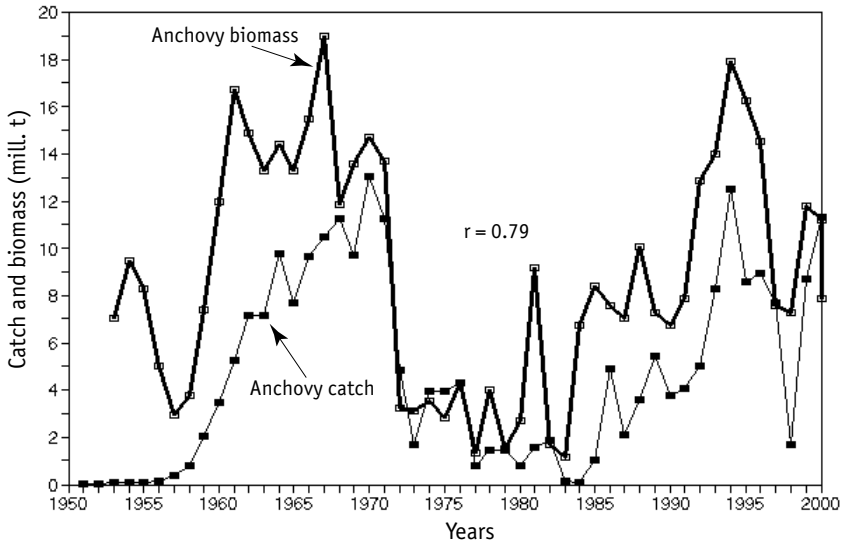

Fig. 6.1. Dynamics of biomass (bold line) and commercial catch (dark squares) of Peruvian anchoveta *Engraulis ringens* during the periods of 1953–1982 and 1983–2001. Data from Pauly et al., 1987 and Ayon et al., 2004

what delayed relative to biomass changes, generally the dynamics of anchoveta catches and biomass correlate rather closely ($r = 0.79$).

Peruvian anchoveta experience catastrophic oscillations of their populations due to conditions resulting from strong El Niños that occur every 8–12 years (Fig. 6.2) [Mysak, 1986]. For example, as a result of the strong El Niño of 1956–1957, the population biomass abruptly decreased, but within 2 years it increased to 12 million tons, and after another year to 17 million tons. The next decrease of the anchoveta biomass (to 3 million tons) occurred due to the strong El Niño of 1971–1972. The population began regenerating, and by 1980 reached a biomass over 9 million tons. The El Niño of 1982–1983, one of the strongest in the 20th century, induced the anchoveta biomass decrease to the observational minimum of 1 million tons, and the catches decreased to 0.1 million tons. However, after one year the biomass increased to 7 million tons, and after 2 more years attained 8.5 million tons. By 1994, the anchoveta biomass reached 18 million tons, but the El Niño of 1997–1998, the second strongest of the century, induced the anchoveta biomass decrease to 7 million tons, and catches decreased to 1.7 million tons. Only one year afterward the biomass returned to 12 million tons, and the catches increased to 9 million tons.

The ability of anchoveta population to recuperate its abundance after strong El Niños is amazing. This was observed during the period of 1955–

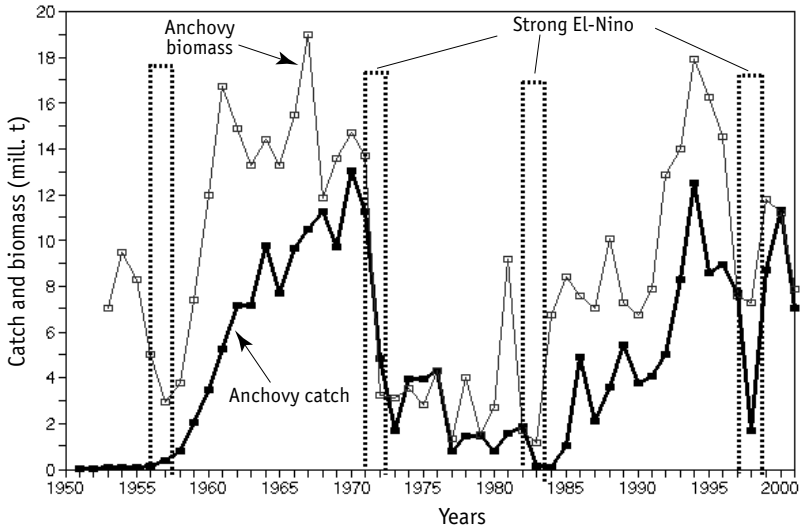

Fig. 6.2. Comparative dynamics of Peruvian anchoveta *Engraulis ringens* biomass (white squares), anchovy catch (bold line) and strong El Niño events (bars) in the period of 1950–2000

1970 and since the mid 1990s. Yet, during the mid 20 years of the period 1973–1992 no such capability was observed. It is notable that during this 20 year period there was a sharp expansion of the Peru-Chilean sardine (*Sardinops sagax*) population, which by 1985 attained its maximum biomass level, providing catch of 6.5 million tons (Fig. 6.3). Figs. 6.2 and 6.3 show that strong El Niños do not have any deleterious effect on the sardine population or its catches.

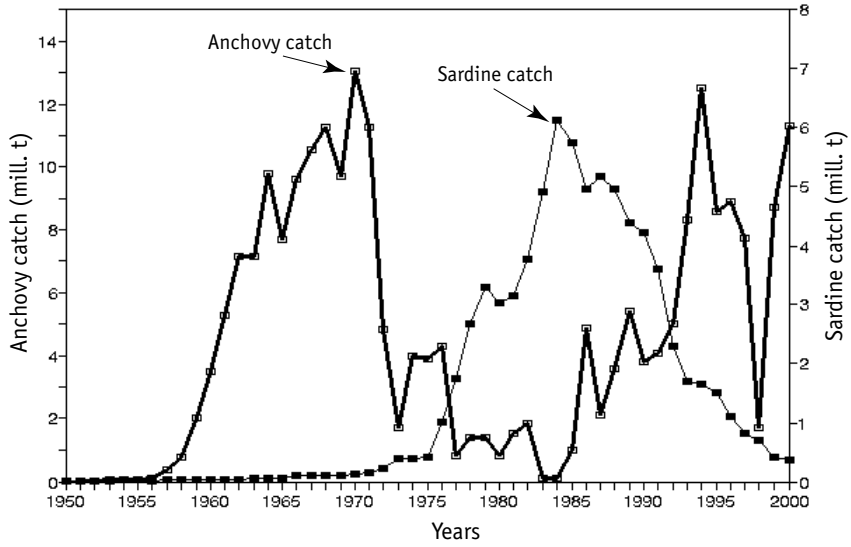

Fig. 6.3. Opposite phase dynamics of the Peruvian anchoveta (bold line) and Peru-Chilean sardine (dark squares) commercial catches during the 1950–2000 period

Catastrophic reductions of the anchoveta population caused by strong El Niños may be considered as an original model of unregulated fishing process, which leads to an abrupt decrease of the commercial resource. Almost complete elimination of the anchoveta population, induced by strong El Niños, caused no irreversible loss of the commercial resource: in environmentally favorable periods the anchoveta population was restored within the life of one generation and provided catch growth up to 7–10 million tons.

A question about probable reasons for alternative oscillations of anchovy and sardine population in the Humboldt Current is discussed in a recent publication [Alheit, Niquen, 2004]. The authors suggest that the main reason reformation of the regional ecosystem and replacement of the predominant species is alteration of so-called «cold» and «warm» periods, which last several decades. According to these concepts, in the cold period there are bio-

mass increases of relatively large copepods and euphauziids, which are the preferred forage of anchoveta, that induces growth of their population. Conversely, during the warm period the biomass of small zooplankton increased, which are the preferred forage sources for sardine, and this provides the prerequisites for the growth of its population. Unfortunately, the concepts about the leading role of these structural changes of planktonic association in alteration of anchovy and sardine populations are based on relatively short time series of only about 50 years.

It is also suggested that during the periods of cooling the main anchoveta predators (horse mackerel and chub mackerel) migrate to warmer more offshore parts of the region. and that reduces predation pressure on the coastal upwelling associated anchovy population. This perspective is not entirely persuasive, because even catastrophic consequences of strong El Niños cause no general long-term effects on the anchovy reproduction.

There is an additional theory: that temperature increases have a negative effect on anchoveta reproduction [Muck, 1989]; however, the author does not consider this mechanism to be the principal reason for long-term fluctuations of anchoveta population. Unfortunately, there are still no clear opinions in this work about the mechanisms behind the long-term alternative oscillations in sardine and anchovy populations within this most productive region of the World Ocean. The principal factor that causes ecosystem reformation and the changes of predominant commercial species is thought to be long-term alterations of ocean temperatures in the Humboldt Current [Yanez et al., 2001; Alheit, Niquen, 2004].

The durations of cold and warm climatic epochs are several decades. Within, this decadal scale background, the very strong El Niños that occur every 8–12 years apparently only have short-term influences on the dynamics of the anchoveta population, although these events perturb perspective of these long-term general ecosystem fluctuations.

Given that the time series of Humboldt anchoveta biomass measurements and fisheries catch statistics are rather short (~50 years), analysis of long-term fluctuations of the anchoveta population becomes complicated. The results of the anchoveta population reconstruction for the last 100 years via analysis of fish scales in the bottom sediments core samples from the Peruvian upwelling region [Baumgartner et al., 1999, cited from Schwartzlose et al., 1999] helps to clarify this question.

No sharp oscillations caused by strong El Niños can be seen in the reconstructed anchovy population curve (Fig. 6.4).

The period between maxima of the anchoveta population is about 65 years. That value corresponds with the average periodicity of fluctuations of Global dT, two Pacific climatic indices, PDO and ALPI, and with the predominant 60–70-year periodicity of anchovy and sardine biomass fluctuations in the Southern California upwelling region for the last 1700 years [Baumgartner et al., 1992].

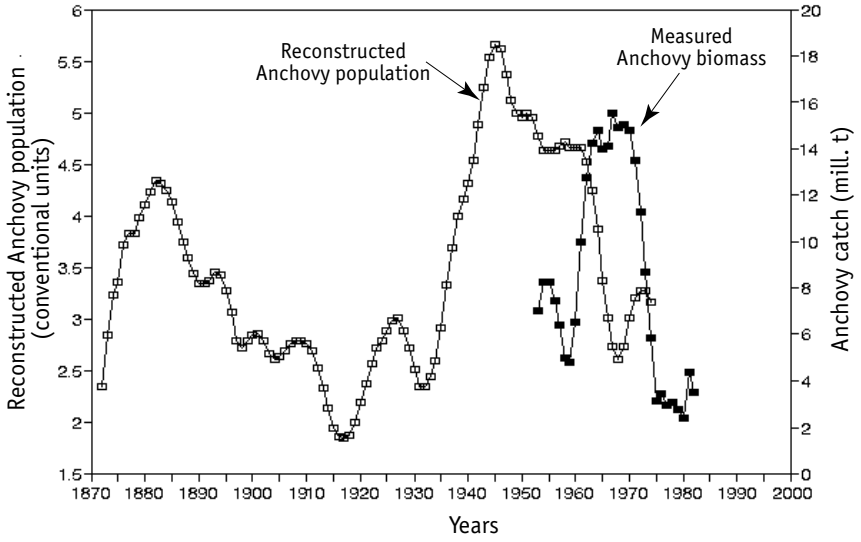

Fig. 6.4. Comparative dynamics of measured Peruvian anchoveta biomass (dark squares) and anchovy population reconstructed from bottom sediment core analysis (white squares, 4-year smoothing]

Fig. 6.4 shows deviations between observed and reconstructed data. For example, the reconstructed curve shows the population maxima from the 1940s into the 1950s, whereas according to measurement and fishery data the peak of anchoveta biomass occurred in the mid 1960s. These deviations are most likely related to difficulties in exact dating of the sediments and the absence of bottom sediment stratification in the Peruvian upwelling. Such laminated structure is typical of bottom sediment cores in the Southern California upwelling region [Baumgartner et al., 1999, cited by Schwartzlose et al., 1999].

Yet, data on the anchoveta population biomass obtained on the basis of direct acoustic measurements [Johannesson, Vilchez, 1980] and the method of virtual populations (VPA) — utilizing data including that from the slowly

evolving fishery that only began in the early 1950s) both show a maximum at about 1965 [Pauly et al., 1987; Ayon et al., 2004]. Given the more frequent and stronger El Niño occurrences in 1968, 72, 76, and the strong 1982 event — the decline of the anchoveta during the late 1960s into the mid 1980s would be more attributable to these than long-term climatic forces [Sharp, 1992]. It seems more acceptable to align two curves (measured and reconstructed from sediments) using the curve of the measured biomass as actually observed data. For alignment of the observed and the reconstructed curves, the latter should be shifted forward by approximately 15 years (Fig. 6.5).

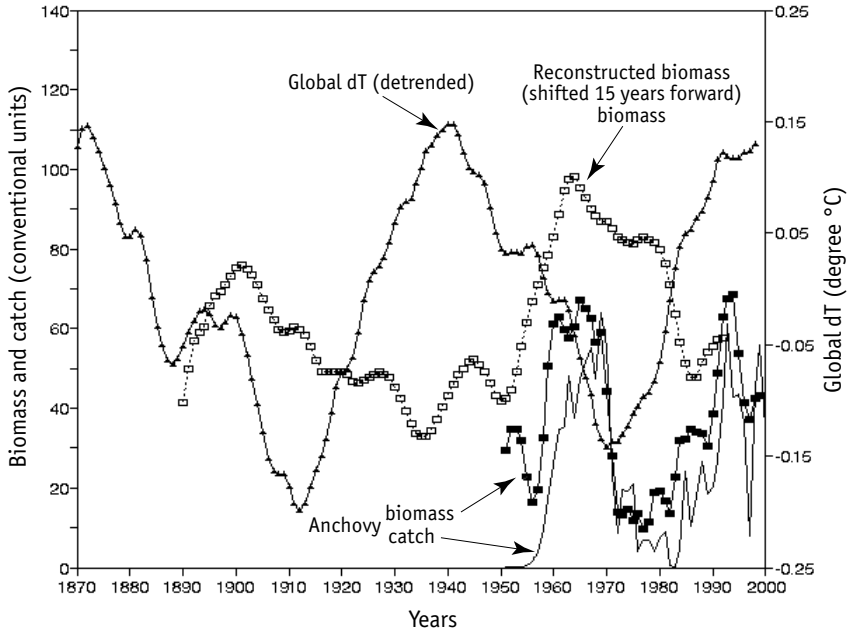

Fig. 6.5. The comparison of trends for reconstructed population of Peruvian anchoveta *Engraulis ringens* (white squares), measured biomass (dark squares) and catch (thin line), and detrended Global dT (triangles, 4-year smoothing). The curve of reconstructed anchoveta population is shifted by 15 years forward (to the right). See text for details

Fig. 6.5 shows the curve of detrended Global dT demonstrating alteration of approximately 30-year warm and cold periods. It may be seen that according to measurements and reconstructed data, the periods of Peruvian anchovy biomass increase correlate with the cool periods of 1890s–1920s and 1950s–1970s. Hence, the maxima of anchovy biomass approach the ini-

tial phase of cool, when Global dT is decreased, rather than its middle part. As shown in Chapter 1, the cool periods are in good agreement with the predominance periods of meridional atmospheric circulation (meridional ACI) (Fig. 6.6).

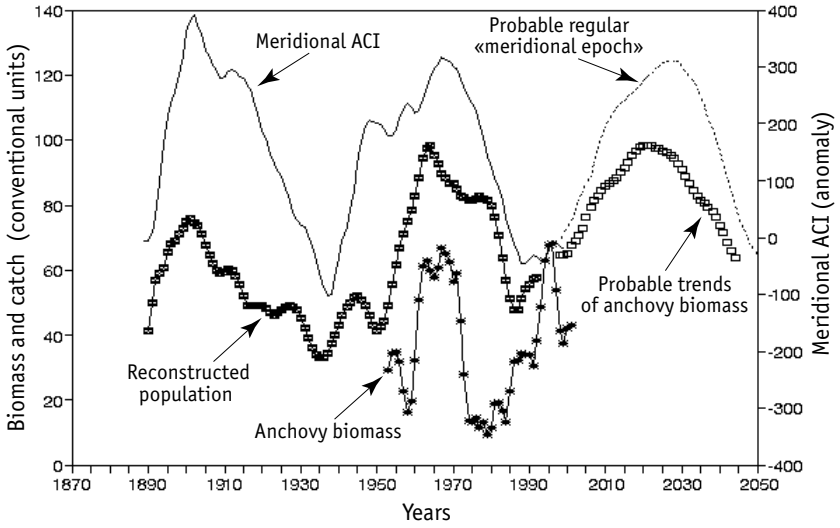

Fig. 6.6. Dynamics of reconstructed Peruvian anchoveta *Engraulis ringens* biomass (crossed squares), shifted by 15 years forward (right), meridional ACI (thin line), measured Peruvian anchoveta biomass (asterisks), and probable trends of anchovy population (white squares) and ACI (dotted line) before the period 2030s–2040s (4-years smoothing)

Fig. 6.6 shows that the maxima of measured and reconstructed curves, shifted by 15 years biomass of anchoveta population correspond well with the periods of meridional ACI predominance. This indicates conformity between the long-term fluctuations of anchovy biomass and the approximately 60-year periodicity of Global dT and ACI, although regional features of anchovy dynamics and the effect of strong El Niños must be taken into account. Despite these, characterstics the long-term changes in the anchovy population may be approximated to the future based on the data on cyclic alteration of 25–30-year climatic epochs (see Chapter 1). According to the prognostic trend (Fig. 6.6), the Peruvian anchoveta population will increase into the early 2020s, after which it will begin to decrease. The prognostic trend characterizes only the general direction of changes of the Humboldt anchoveta population, which is routinely perturbed by strong El Niños.

COMPARATIVE DYNAMICS OF ANCHOVY CATCHES IN THE PACIFIC REGION

Two more anchovy species inhabit the Pacific regions: Japan (*Engraulis japonicus*) and California (*E. mordax*). Catches of the first species yield maxima up to 2 million tons, for the second they reach 0.7 million tons. These values are much lower than the levels of Peruvian anchoveta catches, but also allow consideration of relationships between their population fluctuations and dynamics of climatic indices.

Catch statistics from the Japanese anchovy fishery include over 80 years of data. During the recent 15 years anchovy catches abruptly increased due to increasing power of fishing fleets of North Korea and China. During the period of 1990–1998 the catches from North Korea and China increased by 6X and 25X, respectively, and total catch of Japanese anchovy reached 2 million tons. Contrary to these other countries, since the 1950s the anchovy fishery in Japan remained at a more or less stable level (with oscillations within 10–15%) and was based on relatively constant number of fishing vessels and fishing fleet capacity [Korelsky, 1996]. It may be suggested that dynamics of Japanese anchovy catches reflect better the long-term changes in its population rather than total catch of this species [Schwartzlose et al., 1999].

The long-term dynamics of Japanese anchovy catch compared with that of Japanese sardine is shown in Fig. 6.7. It is observed from this Figure that the amount of anchovy catch changes in opposite phase with fluctuations in Japanese sardine catches.

When comparing catch dynamics of the three anchovy populations in the Pacific region (Fig. 6.8), it is clear that the maximum Japanese anchovy catch was observed in 1960s, and minimum in 1980s, which virtually correlates with dynamics of Peruvian anchovy. However, the trend of California anchovy catch is practically in opposite phase to the changes in catches of both Japanese and Peruvian anchovies. California anchovy population began increasing in the cool period in 1960s, reached its maximum in 1980, and then abruptly decreased. At that time the population of alternative species, which is sardine, in the oceanic zone of the California Current did not actually increase, but began increasing in the internal area of the Gulf of California, where it reached its maximum in the 1990s, and expanded into the California Current and recolonized the northwest Pacific over the following decade [Bennett et al., 2005]. The reasons for these features of California

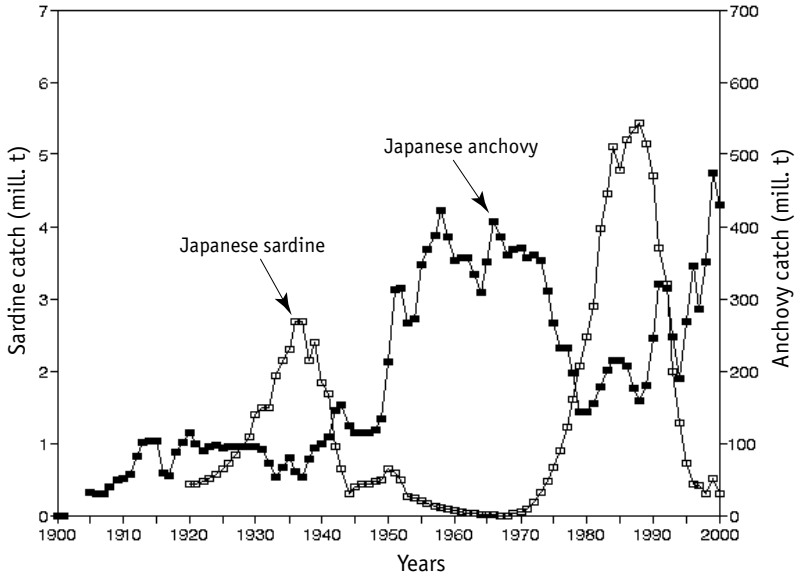

Fig. 6.7. Japanese anchovy *Engraulis japonicus* catch by Japanese fleet (dark squares) compared to the Japanese sardine *Sardinops melanosticus* catch (white squares) in the period of 1905–2000

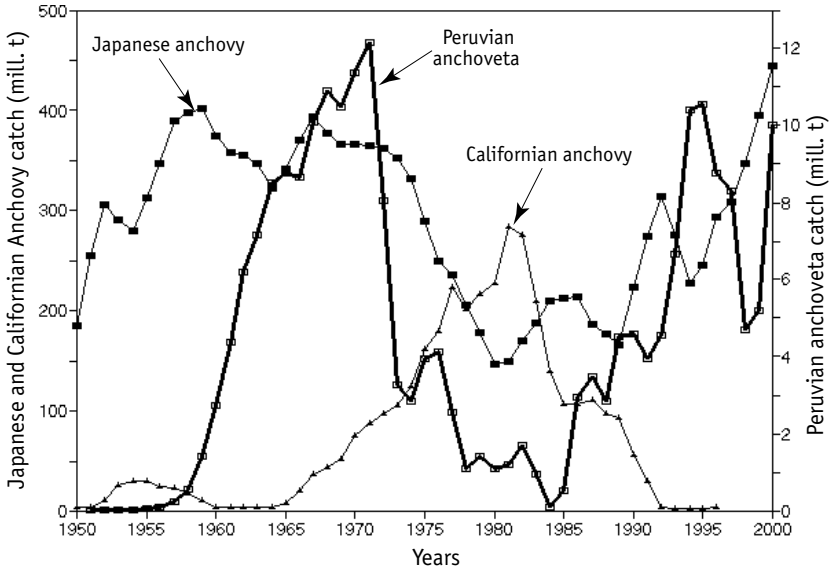

Fig. 6.8. Catch dynamics of Peruvian anchoveta *Engraulis ringens* (bold line), Japanese anchovy *E. japonicus* (dark squares) and California anchovy *E. mordax* (triangles) in the period of 1950–2000 (3-year smoothing)

anchovy and sardine population dynamics have not been entirely explained yet, but are well discussed in the literature [Schwartzlose et al., 1999].

Dynamics of Japanese anchovy catches closely correlate with the changes of Pacific squid (*Todarodes pacificus*) catches (see Chapter 5, Fig. 5.21). Pacific squid is the most productive species in the region (maximal catch is about 0.7 million tons), with a similar lifetime to anchovy (about 2 years). Fluctuations of anchovy and squid catches are virtually identical ($r = 0.82$). As is suggested [Kang et al., 2002], the increase of squid population is the consequence of biomass increase of the principle forage species of anchovy and squid, which are euphauziids and amphipods.

It should be noted that dynamics of total Japanese anchovy and Pacific squid catches are in opposite phase with the index of Pacific Decadal Oscillation (PDO), which characterizes changes in the average temperature of the ocean surface (Fig. 6.9). This confirms that the periods of synchronous increase of Peruvian anchoveta and Pacific squid correspond to cool climatic phases, whereas decrease of the populations of these species

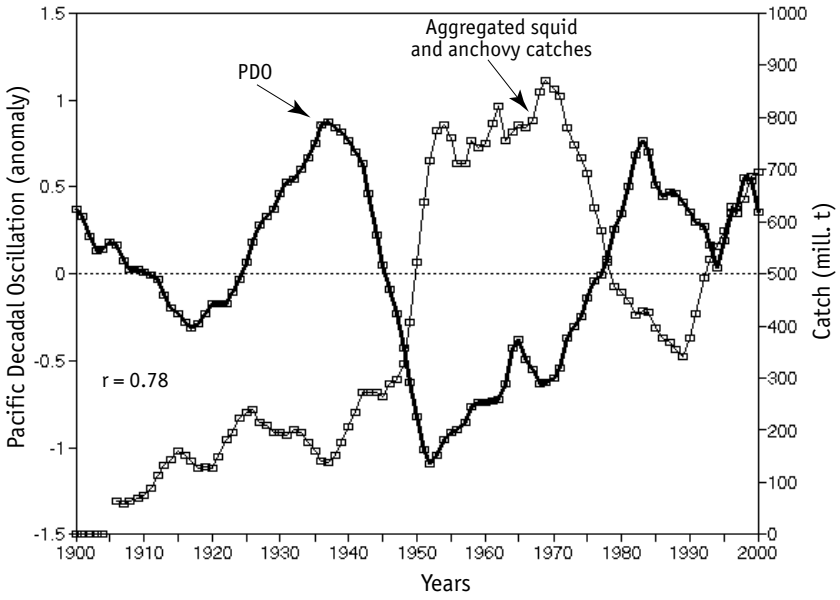

Fig. 6.9. Opposite phase dynamics of Pacific Decadal Oscillation (PDO, 13-year smoothing), (bold line) and aggregated commercial catches of Pacific squid *Todarodes pacificus* and Japanese anchovy *Engraulis japonicus* (white squares, 5-year smoothing)

proceeds as the periods of warming begin, and await the next cooling period to recover.

Contrary to the North Pacific, in the Benguela upwelling region, population outbursts of the South-African anchovy (*Engraulis capensis*) are observed in the warm periods, whereas the population of South-African sardine (*Sardinops ocellata*) is observed in the cool periods. Fig. 6.10 shows that changes in Japanese anchovy, Pacific squid, and the South-African sardine are antiphase to climatic index PDO, which characterizes the long-term fluctuations of the average temperature of the North Pacific surface.

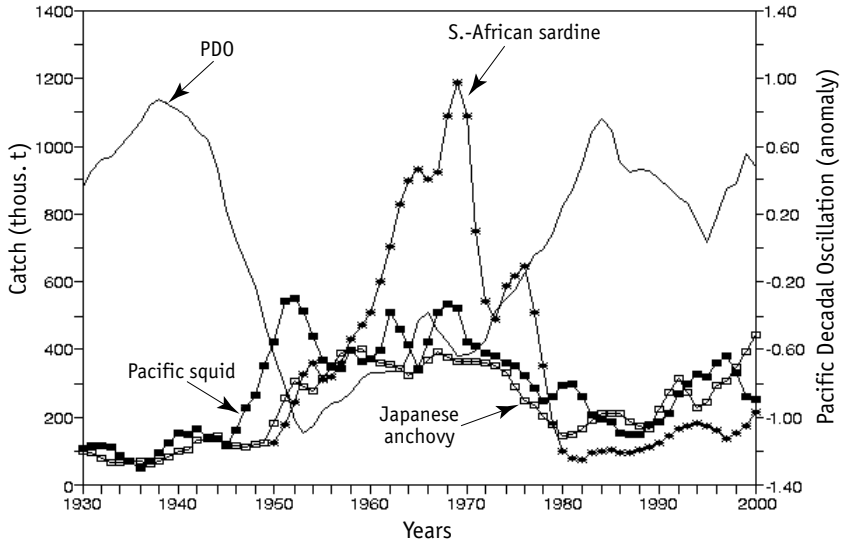

Fig. 6.10. Dynamics of Pacific Decadal Oscillation (PDO, thin line, 13-year smoothing), Japanese anchovy *Engraulis japonicus* (white squares), Pacific squid *Todarodes pacificus* (dark squares) and South African sardine *Sardinops ocellata* (asterisks) commercial catches in the period of 1930–2000

Fig. 6.11 shows dynamics of global and regional Pacific climate indices and catch fluctuations of Peruvian and Japanese anchovies and Pacific squid. Catches of these species are in opposite phase with changes in Global dT, PDO and ALPI indices; the increase of catch volume is observed in the cool periods, whereas warming periods demonstrate their decrease. Nevertheless, there are deviations from this routine. In Fig 6.11 we show that populations of all three species under consideration decreased in the period of temperature increase in 1980s, and increased in the period of 1990s, when Global dT

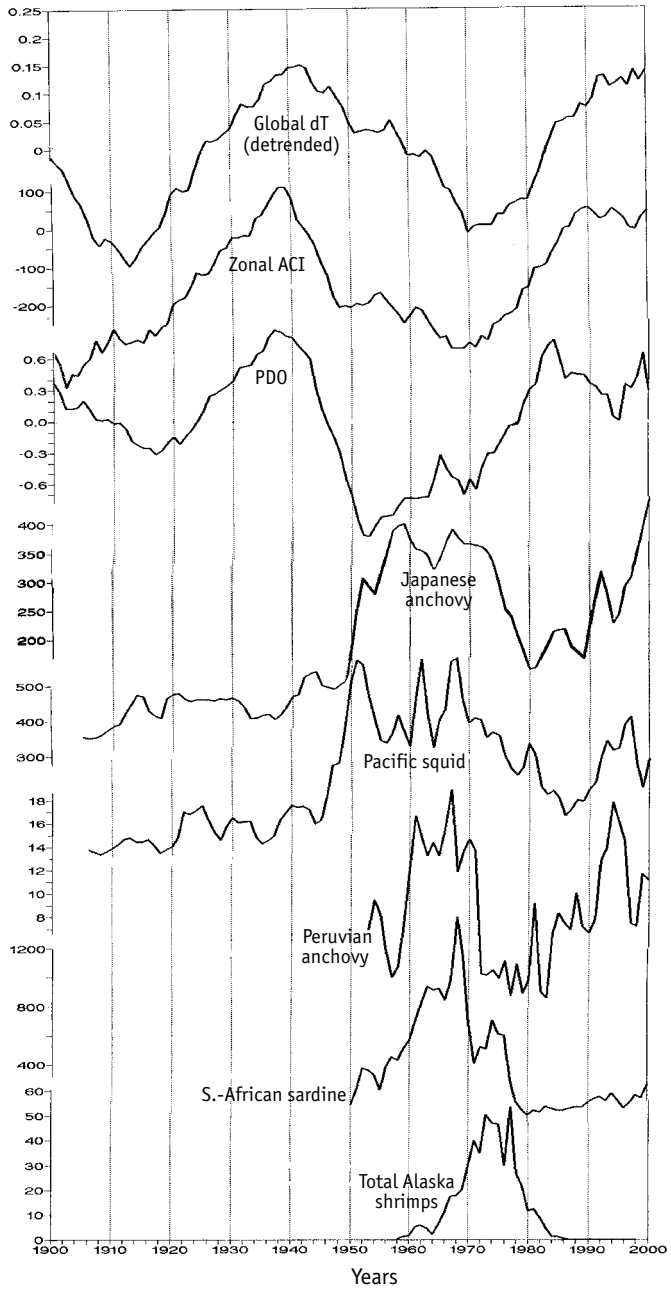

Fig. 6.11. Dynamics of climatic indices and commercial catches of Pacific squid, Peruvian anchovy, Japanese anchovy, South-African sardine and Total Alaska Shrimps in the Pacific region. Symbols: PDO — Pacific Decadal Oscillation; ACI — Atmospheric Circulation Index

increase rate decelerated, but had not yet begun decreasing. Apparently, this fact is in contrast with specific reactions of these species to only temperature changes. However, the dynamics of specific Pacific climatic indices, PDO first of all, and ALPI, show typical deviations from Global dT dynamics. Whereas the Global dT gradually increased during the period 1970s–2000s, by the mid 1980s the growth of PDO had already begun to change — with a 10-year decrease. Pacific climatic indices reflect regional climatic changes more directly than does Global dT, and relatively early increases of both anchovy and squid catches since the mid 1980s may be related to response of the populations on temperature decreases during the cooling period of North Pacific region during the late 1980s, early 1990s.

CHAPTER 7

MODELING

JUSTIFICATION OF THE STOCHASTIC MODEL OF CLIMATE FLUCTUATIONS

Analyses of climatic time series shown in the previous Chapter has provided the following:

- In the recent one and half thousand years, climate fluctuations demonstrate well expressed 50–70-year cycles.
- The intensity of recurrence of this cyclic behavior has increased over the recent 1000 years, and is now fixed at the maximum level, which will be preserved for at least the next 100 years.
- Instrumental measurement series of Global dT, Arctic dT and the Atmospheric Circulation Index (ACI) also demonstrate approximately 60-year periodicity.

Based on these current concepts about periodicity of climate and biota fluctuations, a stochastic model of cyclic climatic fluctuations is developed below. It allows forecasting of the climate changes for the next several decades.

It is known that the problem of forecasting future values of a time series according to its behavior in the past is one of the most complicated in applied statistics. The classical approach invokes the use of correlations (linear statistical dependence) of neighboring signal values and forecasts for one or more steps ahead formed as a sum of a defined number of the previous values, taken with the weighting coefficients, all this generates a linear autoregression model. The values of weight coefficients (autoregression coefficients) are determined by minimization of the sum of these past forecast error squares. A methodological basis for forecasting is a hypothesis that the

stationary mode of the signal, i.e. that the correlation values between neighbor values in the series, determined for the past, will remain at that level in future. If this hypothesis is true, statistical forecasting for each time-step forward which is based on correlation with the previous values, significantly decreases standard deviation compared with any other forecasting alternatives and, in fact, is the optimal choice.

However, as forecasting not for only one but for several steps ahead, as in classical linear models, the forecast variances begin growing rapidly and several steps later yields an asymptotic limit, which is the value of general variance of the forecasted process. The latter means that the autoregression prediction is reduced to a trivial level, when a simple mean value of the signal calculated from the previous values is taken as a predictor.

Also, the factor confounding the application of such classical forecast results is often a predominance of low frequency signal variations, which is equivalent to disruption of the stationary mode hypothesis. One of the standard methods increasing stationarity is the transition from the initial time series to a series of sub-increments. However, this approach replaces the task of forecasting values of the initial series with the task of forecasting its sub-increments and the increased signal noise.

A more effective solution, which increases both stationarity and the «long-range ability» of the predictor, is achieved by applying the parametric trend of the time series. If we succeed in this, forecasting of several steps ahead is reduced to a simple extrapolation of the trend function values to future time intervals of a given length. In this case, the role of classical linear forecasting is reduced to a slight adjustment of the trend forecasts for several steps ahead from the current time using sequential correlations of the signal deviations from the trend.

Unfortunately, efficient constructions of trends dependent upon only a few parameters is not possible in most common situations. However, due to the existence of strong harmonic components for climatic time series this is possible and, consequently, «long-range» forecasting is also possible by invoking the cyclic trend with a given period. For this style of forecasts, the key factor determining its efficiency is the correct determination of the period of the dominant cyclic trend (after which, determination of amplitudes and phases of harmonics is the exclusive technical problem). It should be emphasized that after analyzing real data we have rejected the model containing several harmonics (although it is recognized as a general case resulting from the existence of several harmonics), and retained just one, which represents the do-

minant oscillation. This decision was made after consideration of the need for the enhanced statistical significance of our forecasts, for which it is necessary to introduce the minimum necessary number of parameters to the model.

As discussed above, the determination of the period of the cyclic trend is the fundamental problem of forecast construction. In the following, this problem is solved via two methods, the selection of which depends on the length of the analyzed series. If a series is «tentatively long», the period is determined from the maximum (the peak value) of its power spectrum estimate. However, if the series is «short», estimation from the power spectrum is insignificant. Thus, the predominant period is sought directly, looking for that which is similar to or has the same period of the cyclic trend by identifying that with the best fit to the series analyzed, that which generates the minimum residual variance. In general, both approaches are equivalent, but the use of the power spectrum plot, if possible, is preferable, because it gives a possibility of visual comparison of the competing alternatives of the predominant period. Two alternatives are discussed below.

After the period of cyclic trend has been determined (see Chapter 1), the remaining parameters of the model should be identified. This can be accomplished by the least-square method, however, a robust alternative has been used, providing stablility, despite large deviations from the cyclic trend in the data The approach is discussed in detail below.

A model of climate fluctuations was developed using «long-term reconstructed» time series and short «instrumentally measured» series (for details of the time series see Chapter 1):

- The series of mean annual winter temperatures, reconstructed from Greenland ice core samples representing 1420 years (552–1975);
- The series of summer temperatures, reconstructed from the growth rings of the Arctic pine tree for the recent 1400 years (500–1990);
- The series of mean annual winter temperatures, reconstructed from the growth rings of California pine tree for 1480 years (500–1980), and overall time series for 7979 years (6000 A.C.–1979 A.D.);
- The series of reconstructed fluctuations of sardine and anchovy populations in the California Current zone for 1450 years (500–1950; the series comprises a total of 145 counts aggregated by decade increments, and;
- The series of experimental observations, mean annual temperature over 140 years (1861–2000);
- The series of measurements from which the Atmospheric Circulation Index (ACI) is produced for 110 years (1891–2000).

Spectral analysis of all these time series yielded a predominant oscillation period within 50–70 years over the recent 1000 years of climate evolution. It should be noted that the winter temperature series reconstructed from Greenland's ice core samples seems to be the most reliable source of information.

Following is a formal description of all details of numerical procedure of a prognostic model based on application of the cyclic trend and the approximation via autoregression of the signal deviation from the trend.

DESCRIPTION OF A FORMAL MODEL OF CLIMATIC FLUCTUATION PERIODICITY

A fundamental property of time series under consideration is their strong periodicity. Let us present the time series $x(t)$, $t = t_0, \ldots, t_0 + N - 1$ as the following sum:

$$x(t) = \xi(t) + F(t), \tag{1}$$

where t_0 is the initial year of the time series,

$x(t)$ is the catch volume in the year t,

$F(t)$ is the trend to be identified,

$\xi(t)$ is a stochastic component.

Let us present the identified component of the variations $F(t)$ as a cyclic trend having m number of given periods T_i, $i = 1, \ldots, m$ [Anderson, 1976; Kashyap, Rao, 1983):

$$F(t) = \sum_{i-1}^{m} \left(B_i \sin\left(\Theta_i(t)\right) + D_i \cos\left(\Theta_i(t)\right) + G, \right. \tag{2}$$

where $\Theta_i(t) = 2\pi_i(t - t_0)/T_i$,

B_i, D_i are the unknown amplitudes,

G is the unknown constant of static shift.

Formula (2) may be presented as follows:

$$F(t) = \sum_{i-1}^{m} \left(A_i \cos\left(\Theta_i(t) - \varphi_i\right) + G, \right. \tag{3}$$

where $A_i^2 = B_i^2 + D_i^2$;

$tg(j_i) = B_i/D_i$.

The stochastic component $\xi(t)$ can be presented by an autoregression model [Box, Jenkins, 1974] of the given order p (or AR(p)-model):

$$\xi(t) = -\sum_{k=1}^{p} a_k x(t-k) + \varepsilon(t), \tag{4}$$

where p is the autoregression order,

a_k are unknown parameters of autoregression,

$\varepsilon(t)$ is the residual signal, which is assumed to be Gaussian white noise with a mean equal to zero and unknown variance s^2.

A combination of formulae (1) and (4) gives the following general expression of the model:

$$x(t) = -\sum_{k=1}^{p} a_k x(t-k) + \sum_{i=1}^{m} B_i \sin(\theta_i(t)) + D_i \cos(\theta_i(t)) + G + \varepsilon(t). \tag{5}$$

Therefore, the unknown parameters of the model (5), which values should be determined from the available data, are the following: p of autoregression parameters a_k, $2m$ of harmonics B_i and D_i amplitudes, static shift constant G and variance s^2 of the residual signal $\varepsilon(t)$. Let us determine values of these parameters from the maximum likelihood method [Kashyap, Rao, 1983], for the case where Gaussian noise $\varepsilon(t)$ coincides with the least square method. Let us denote the $(p + 2m + 1)$-dimensional column-vector as $Y(t)$:

$$Y(t) = (-x(t-1), \ldots, -x(t-p), \sin(\Theta_1(t)), \cos(\Theta_1(t)), \ldots, \sin(\Theta_m(t)), \cos(\Theta_m(t)), 1)^T, \tag{6}$$

where the upper index T denotes vector transposition, and c is the vector-column of parameters of the same dimensionality:

$$c = (a_1, \ldots, a_p, B_1, D_1, \ldots, B_m, D_m, G)^T \tag{7}$$

Then the model (5) may be presented in the following compact form:

$$x(t) = c^T Y(t) + \varepsilon(t) \tag{8}$$

The vector of parameters c may be determined from minimization of the square sum:

$$\sum_{t=t_0+p}^{t_0+N-1} \varepsilon^2(t) = \sum_{t=t_0+p}^{t_0+N-1} \left(x(t) - c^T \cdot Y(t)\right)^2 \to \min_c. \tag{9}$$

Solution for the task (9) is readily described by:

$$c = A_i^{-1} \cdot R_0, \tag{10}$$

where the matrix is $A_0 = \sum_{t=t_0+p}^{t_0+N-1} Y(t) \cdot Y^T(t)$;

the vector is $R_0 = \sum_{t=t_0+p}^{t_0+N-1} x(t) \cdot Y(t)$;

and the signal variance estimation $\varepsilon(t)$ is:

$$s^2 = \frac{\sum_{t=t_0+p}^{t_0+N-1} \varepsilon^2(t)}{(N-p)}. \qquad (11)$$

Estimations by formulae (10) and (11) are made usingthe least square method. It is known that least square method estimations are rather sensitive to the presence of data outliers. A very low percentage of such outliers (often even one percent) leads to a strong shift of estimates away from their «real» values. This is the well known «robustness» problem of the estimation methods [Huber, 1984]. One of the ways to increase the robustness of estimations is the use of the maximum likelihood method assuming that the residual signal $\varepsilon(t)$ is distributed according to combined distribution density rather than the pure Gaussian law. For small values of ε, this combined distribution density coincides with the normal distribution law, whereas at high values it coincides with the Laplace distribution. This distribution is of the following density [Huber, 1984]:

$$p(\varepsilon) = \frac{\beta}{s} \cdot \exp\left(-\frac{\varepsilon^2}{2s^2}\right) \text{ at } |\varepsilon| \le s \cdot a; \qquad (12a)$$

$$p(\varepsilon) = \frac{\beta}{s} \cdot \exp\left(-\frac{a}{s} \cdot \left(|\varepsilon| - \frac{as}{2}\right)\right) \text{ at } |\varepsilon| > s \cdot a. \qquad (12b)$$

where a is the so-called robustness parameter, usually equal 1–3 (here $a = 2$ is used);

s is the scale parameter (analogous to standard deviation in the Gaussian law);

β is the normalization constant:

$$\beta = \beta(a) = 1 / \left(2\left(\exp(-a^2/2)/a + \int_0^a \exp(z^2/2)dz\right)\right). \qquad (12c)$$

For the case (12 a, b, c), the maximum likelihood method leads to the following maximizing task (with the accuracy up to an additive constant depending exclusively on the parameter a):

$$J(c,s)=\sum_{t=t_0+p}^{t_0+N-1}\ln\left(p(\varepsilon(t))=-(N-p)\cdot(s)-\frac{1}{2s^2}\sum_{|\varepsilon(t)|\le sa}\varepsilon^2(t)-\right.$$

$$-\frac{a}{s}\sum_{|\varepsilon(t)|>sa}|\varepsilon(t)|\to\max_{c,\,s}. \qquad (13)$$

The equation (13) can be solved numerically, by combining the generalized Newton method for searching for a vector c and the method of simple iteration in searching for parameter s:

$$c^{(j+1)}=c^{(j)}+A^{-1}\left(c^{(j)},s^{(j)}\right)\cdot R\left(c^{(j)},s^{(j)}\right),s^{(j+1)}=\chi^{-1}\left(c^{(j)},s^{(j)}\right), \qquad (14)$$

where $j = 0, 1, \ldots$ is the iteration index. The matrix $A(c, s)$ and the vector $R(c, s)$ are calculated according to the following formulae:

$$A(c,s)=\sum_{t=t_0+p}^{t_0+N-1}F''(\varepsilon(t),s)\cdot Y(t)\cdot Y^T(t),\ R(c,s)=\sum_{t=t_0+p}^{t_0+N-1}F'(\varepsilon(t),s)\cdot Y(t), \qquad (15)$$

$$\text{where } F'(\varepsilon,\,s)=\begin{cases}\varepsilon,\ \text{under}\,|\varepsilon|\le a\\ sa\cdot\text{sign}(\varepsilon),\text{under}\,|\varepsilon|>as\end{cases}-F''(\varepsilon,\,s)=\begin{cases}1,\ \text{under}\,|\varepsilon|\le a\\ 0,\text{under}\,|\varepsilon|>as\end{cases}. \qquad (16)$$

The function $\chi(c, s)$ is determined by the following formula:

$$\chi(c,s)=\frac{\sqrt{\gamma^2+4a}-\gamma}{2a}, \qquad (17)$$

$$\text{where}\qquad a=\frac{\sum_{|\varepsilon|\le as}\varepsilon^2(t)}{(N-p)},\quad \gamma=\frac{a\cdot\sum_{|\varepsilon|>as}|\varepsilon(t)|}{(N-p)},\quad \varepsilon=x(t)-c^T\cdot Y(t). \qquad (18)$$

Deduction of the formula (17) is based on the following. If we consider the dependence of the value (13) on the parameter s, it can be noted that the main component of this dependence is determined by the presence of multiplier $1/(2s^2)$ and a/s. If δs is a small variation of s, then the corresponding variations of sums:

$$\sum_{|\varepsilon(t)|\le as} \varepsilon^2(t) \text{ and } \sum_{|\varepsilon(t)|>as} |\varepsilon(t)|, \tag{19}$$

multiplied by $1/(2s^2)$ and a/s, are much lower (which for small δs values can be equal even zero) than variations of the values $1/(2s^2)$ and a/s themselves, multiplied by corresponding sums from (19). Therefore, if we estimate the variation of $J(c, s)$, caused by δs, the values (19) can be assumed to be almost constant and, therefore, the following formula can be obtained:

$$\delta J(c,s) \approx -\frac{(N-p)}{s} \cdot \left(1 - \frac{a}{s^2} - \frac{\gamma}{s}\right) \cdot \delta s. \tag{20}$$

Assuming the condition $\delta I(c, s) = 0$ follows the quadratic equation relative to the unknown value $r = 1/s$: $\alpha r^2 + \gamma r - 1 = 0$, which has the unique positive root $r = \chi = \left(\sqrt{\gamma^2 + 4a} - \gamma\right) / (2a) = 1/s$. Let us now remember that, in fact, the values of α and γ depend on s and consider the latter equation as an iteration procedure for refinement of the s parameter value (the second of equations (14)). Also, if the robustness parameter a is found to be high enough, $\gamma = 0$ and according to the formula (20) $s = \sqrt{\alpha}$ that coincides with formula (11).

The iteration procedure begins with the initial approximation using the least square method (10), (11) and converges very rapidly, over 5–10 iterations.

The autoregression values of order p, the number of harmonics m and their periods T_i must be decided before identification of the model (5) parameters. The autoregression order p below is always set with a value of 2 as a minimum, which promotes reflection of the full variety of arbitrary oscillations [Box, Jenkins, 1974]. As concerns selection of m and T_i period values, two approaches were used (see below).

Here it should be noted that the forecasting technique under discussion may be used for any climatic time series that demonstrates clearly expressed monochromatic components, and particularly for time series of the catch of the major oceanic commercial fishes,. The periods of predominant harmonics may be taken from either the series forecasted (the first approach, 1) or spectral and spectral-time analysis of other long-term climatic time series (the second approach, 2).

1. Applying the first approach, the number of harmonics and their periods are determined directly from the time series. Let us nominally subdivide the time series into «long-term» and «short-term» ones. If the series contains not less than 64 counts, it is accepted to be long-term, otherwise it is short-term. On the basis of these criteria practically all series of fish catch statistics fall within the short-term category. The long-term time series, from which basis a model can be devised, are the climatic data series, shown in Chapter 2.

For the long-term time series, the number of harmonics m and the values of their periods T_i were determined from estimations of the power spectra of the corresponding series. The value m varied from 1 to 6, usually ranging from 3 to 4. The values of periods T_i were selected related to peak values of the power spectra estimates. Despite our conditional classification of the long-term time series, they are aqctually rather short-term for application of common spectral procedures, based on the use of the Fourier transform. For such series, regarding the frequency resolution, the more appropriate method is autoregression approximation [Marple, 1990]. This method consists of the estimation of the model parameters:

$$x(t) + \sum_{j=1}^{q} a_j x(t-j) = \eta(t), \qquad (21)$$

where α_j, $j = 1, \ldots, q$ are autoregression parameters,

$\eta(t)$ is the residual signal assumed to be the Gaussian white noise with mean of zero and σ^2 variance.

In the formula (21) we use different notations for parameters of AR(q)-model compared to the same parameters of the AR(p)-model in formulas (4) and (5) in order to emphasize that these models are designed for different purposes. The autoregression members in formulas (4) and (5) were introduced to describe the basic properties of the signals' stochastic fluctuations around the determined cyclical trend. Therefore, for these formulae a low order $p = 2$ has been used. The model (21) is designed for description of the spectral structure of the signal. For this purpose, a higher order of autoregression q is required. The higher the order q value, the more sensitive the power spectrum estimation is. At the same time, an increase of the q value order leads to increasing of statistical fluctuations of the estimation. Hence, selection of the q value requires a compromise between sensitivity and stability of the estimation. Usually, is it assumed that $q = N/5 - N/3$, where N is the number of increments in the time sequence. We have used $q = 20$. When

parameters of the model (21) have been determined, the spectral estimation is calculated using the following formula:

$$S_{xx}(w) = \frac{\sigma^2}{2\pi\left|1 + \sum_{j=1}^{q} a_j \exp(-iwj)\right|^2}, \qquad (22)$$

where ω is the cyclical frequency: $\omega = 2\pi/T$;

T is the measurment period of the sampling interval (currently, 1 year);

i is the imaginary unit.

These AR-methods of the power spectrum estimation differ from each other due to the model (22) parameter calculation technique. We have used Burg's maximum entropy method due to its higher reliability and provision of the best frequency resolution for short time series [Marple, 1990].

For short series (which are more exactly «very short») model (5) was used, in which $p = 2$ and a single harmonic in the cyclical trend ($m = 1$). Due to a small number of samples the value of the single period T_i cannot be reliably estimated from the power spectrum. That is why the period value was determined by solving the problem of determining s^2 minima after estimation of the autoregression parameters a_1 and a_2, amplitudes B1 and D_1, and static shift G for some sample period value: $s^2(T_1) \to \min$. The latter minimization problem was solved using the golden section method.

After specification of the models, they were used to forecasts of time series for 60 years beyond the available time series. The forecasting method is described below. For some time series, which implicitly should be non-negative (for example, the volume of fish catches), the prognosis curve does become negative. Such values were reinterpreted to equal zero equal, i.e. the low value threshold of zero has been applied.

2. When using the second approach, a model with the cyclic trend having a single period is used. The value of this periodicity is estimated from analyses of climatic time series. Previously, we have used the values of cyclic trend periods which have been obtained directly from the analysis of the available time series, which are estimations of their power spectra or trend periods that provide minimal residual variances. However, such values may be «too adaptive» to the data. Adaptation of the model parameters to features of the data behavior is not always positive.

If dynamics of major commercial fish catches are used as climatic process indicators, we meet several ambiguities. First, as mentioned above,

the series of catch statistics are too short. Second, the catch volume may depend on both natural reasons and economical behavior of the subject fisheries, that include market situations, overexploitation, availability presence of energy resources for processing, military conflicts in different parts of the World Ocean, etc. The long-term forecasting (even for 10–20 years ahead) of these factors is impossible. Thus, the great share of anthropogenic reasons which affect the catch volume relate to the stochastic noise «constant» of the data, and is then best modeled by autoregressive terms within the model.

Taking into account the above basic concepts, a conclusion is possible that the values of period lengths applied in the model (5), estimated from the initial data sets, include extreme effects of arbitrary factors. At the same time, the values of period lengths taken from the global climatic processes, which are remain negligibly affected by human activity. These processes affect productivity of the major commercial fishes in a complex fashion. Thus, the concept appears to support the use of model (5) for the prediction, but values of the periodicities used should be those derived from the period icities of climatic processes rather than the catch volume time series. Thus, cyclic trends used in model (5), which provides the principal fishery forecasting function, will be more reliable.

To estimate the periodicity of the processes, both long-term climatic time series of about 1500 years and the shorter series based on instrumental measurements, none of which exceed 150 years in length, were used. As shown in Chapter 1, spectral analysis of all the long time series yield results where the period of predominant oscillations are within the range of 50–70 years over the recent 1000 years of climate evolution.

Periods of long climatic time series may be taken from Table 1 (Chapter 1).

For the shorter instrumental time series, the following periods were obtained:

- For Global dT, it is 55 years (estimated from the power spectrum) and 64 years (period estimated from the conditions at the minimum residue variance);
- For ACI, it is 50 years (estimated from the power spectrum) and 58.5 years (period estimated from the conditions at the minimum residue variance).

MODELING PROCEDURE FOR PREDICTIVE CURVES

For the predictions, the so-called «bootstrap»-techniques [Efron, Tibshirani, 1986] have been used. This model allows calculation of a predictive curve, together with its standard deviations. Actually, the procedure requires the generation of a large number M of independent random realizations of artificial trajectories (M was taken equal to 1000) in model (5), that cover the future time interval of the specified length. These trajectories differ from one another due to the different independent realizations of the white noise (t) component. All other parameters (including variance s^2) are the same. Each trajectory represents a scenario of possible process behavior in the specified future time interval, according to model (5). Thus, for each projection we obtain a batch (an ensemble) of M samples of artificial trajectories, which fill the «band» in the (t, x) plane. For each t value, in the future the average value can be calculated from the Sum of the M values, which correspond to different realizations, and their standard deviations (the «band width»). These average values form a predictive curve with its standard deviations.

CHAPTER 8

FORECASTING OF FLUCTUATIONS IN THE MAIN COMMERCIAL SPECIES POPULATION

THE APPROACH TO FORECASTING COMMERCIAL FISH POPULATION DYNAMICS

The possibility of forecasting fluctuations in populations of some commercial fish for 30–40 years is based on the concept of direct relationships between the dynamics of fish population abundances and periodic climate changes. In brief, these concepts are the following:

As shown in Chapter 1, for the recent 1500 years the predominant periodicity of climatic fluctuations was ~60 years, varying from 55 to 76 years. The second periodicity of these climate changes, by intensity, is about 30 years, but it is practically unobserved in the available multiyear series of commercial catches.

The intensity of the ~60-year predominant periodicity increases continuously within the recent 500–1000 years, reaching its maximum at the end of the 20th century. We therefore hypothesize that, it will remain the predominant period for at least the next 100 years.

Analyses of the time series of instrumentally measured Global dT for the last 140 years and Atmospheric Circulation Index (ACI) for the last 110 years revealed oscillations of these indices with approximately 50–70-year periodicity. This confirms the continuation of approximately 50–70-year periodicity of climate fluctuations at present. It should also be noted that there is a practically complete coincidence of the temperature fluctuations reconstructed from Greenland ice core samples and the Global dT from the instrumental measurements during the last 140 years (see Chapter 1 for examples).

Also, relating the long-term changes in the California sardine and anchovy populations, using paleontological data, a 55–57-year predominant periodicity has been observed in the alternating fluctuations of their populations during the recent 1700 years (see Chapter 1). According to historical chronicles from Japan [Kawasaki, 1994], the periodicity of Japanese sardine population outbursts that occurred over the last 400 years, is also about 50–60 years and, generally, correspond with with climate cycle patterns (Fig. 8.1). The outbursts of the Japanese sardine population occur within the rapid temperature ascent phase and, then rapidly begin to fall on attaining the regional temperature maxima.

For the majority of large fish commercial populations, catch statistics time series are relatively short. For Pacific salmon, Japanese sardine and California sardine, the data time series are about 80 years long; for the Atlantic spring-spawning herring it is 93 years; for North-East Arctic cod — about 100 years; for Peruvian sardine and Pollock — about 50 years; for European sardine, South-African sardine and South-African anchovy — about 40 years;

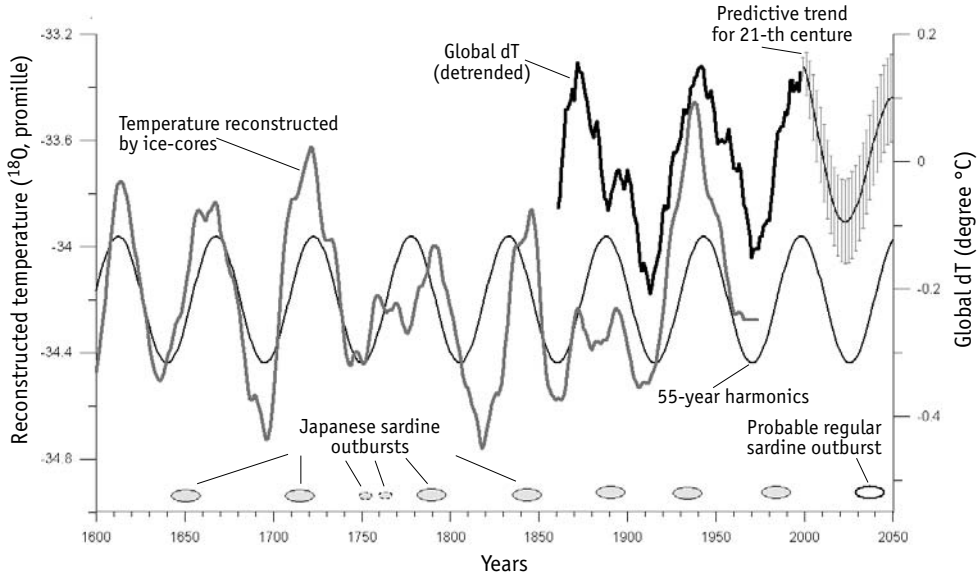

Fig. 8.1. Cyclic temperature fluctuations and Japanese sardine outbursts (ellipses) for the last 400 years based on historical Japanese chronicles for the periods of 1640–1880, and based on fishery catch statistics from 1920–2000. The empty ellipse represents the probable period of the next sardine outburst. Symbols: thin line shows 55-year harmonics; bold grey line shows temperature reconstructed from Greenland ice core samples; bold black line shows detrended Global dT; thin black line presents predicted trend for the 21th century, denoted by model standard deviations, shown using vertical hatches (13-year smoothing)

and for Chilean jack mackerel — only about 30 years. This limitation does not allow tracking the correspondence between catch fluctuations and climatic indices for all these species. However, for the species with the longest time series of statistical data (exceeding 80 years), the coherences between catches and climatic fluctuations are rather clearly observed.

Generally, dynamics of the largest commercial populations in the Atlantic correlate with approximately 60-year fluctuations of climatic indices. In particular, as shown in Chapter 2, the long-term changes in the spawning and commercial biomass of Atlantic spring-spawning herring correlates with dynamics of climatic indices with maxima in 1940s and 1990s and a minimum in 1960s–1970s. The dynamics of North-East Arctic cod population is close to that of Atlantic spring-spawning herring population, delayed by about 10 years. The catch curve of the cod commercial resource biomass, shifted backward by 10 years, correlates quite well with both the dynamics of the herring population and climatic index trends in the region. The reasons for the delay in cod commercial resource biomass changes relative to the climatic index trend are not yet known. However, the relationship to dynamics of Arctic dT Global dT, the ice free area of the Barents Sea, and water inflow of Atlantic water into the Arctic region is obvious.

Fluctuations in catches of European sardine and South-African anchovy are virtually identical, and likely due to the development of warm climatic epoch from 1980–2000.

Concerning those species with relatively short time series, such as Alaska pollock and Chilean jack mackerel, we have observed only a single cycle of fluctuations in their populations from the period of 1960–2000. However, this cycle also correlates well with the dynamics of global and regional climatic indices having approximately 60-year periodicity.

The fluctuation coherency of climate and dynamics of the populations of several major pelagic fish species allows the development of a scheme for projecting possible changes in their populations for the coming decades using a predictive model based on the analysis of long time series with a predominant climatic periodicity of about 50–70 years.

The approximately 60-year periodicity applied represents a mean value that is statistically correspondent with the most probable climate periodicity. Under more realistic local conditions, generated within each productive region, the dynamics of the individual major commercial populations have definite deviations from the general climatic «model-mean» periodicity, which must be taken into account.

SYNTHESIS OF PREDICTIVE TRENDS

Direct application of our «climatic» model for the projections with respect to real-world statistical catch time series evolved as follows. The specific cyclical period used for each of the analyzed catch time series were either selected from previously identified predominant periods of climatic time series or were determined by analysis of each series by searching for a period with the minimal residual values. A trend detected using one method or the other was used to extend the observed data series into the future by 55 years, i.e using the average period of the dominant cycle for the local climatic time series (see Chapter 1).

The commercial species under consideration are subdivided into 2 groups. The first group unites species, for wich the increase of population abundance is observed during the warming periods, i.e. in the phase with fluctuations of Global dT, zonal ACI, PDO, and ALPI. These species are Pacific salmon, Japanese, Peruvian, California and European sardines, Chilean jack mackerel, Atlantic spring-spawning herring, North-East Arctic cod, Alaska pollock, and South-African anchovy. The second group comprises species whose populations increase during the «cooling» periods. They are Peruvian and Japanese anchovies, South-African sardine, and Pacific squid.

Shown below are the «model» projection curves for the perspective of 50 years for 14 major commercial species under the condition that the intensity of their commercial exploitation will evolve and remain at historically reasonable levels.

Predictive trends for the first group of species

Pacific salmon (Fig. 8.2). The period of cyclic trend obtained from analysis of the time series of total Pacific salmon commercial catches is 59 years, i.e. practically equal to the mean 60-year periodicity. According to our predictive trend model, the total population of Pacific salmon catches will decrease until the 2020s, and after that will start increasing. The amplitude of the long-term oscillations of Pacific salmon population is 2.5–3.0X.

Japanese sardine (Fig. 8.3). The cyclical trend period obtained from analysis of the time series of Japanese sardine catches is 55 years, i.e. is close to the mean 60-year climatic periodicity but coincides with the 55-year periodicity obtained from the analysis of the most reliable series of recon-

structed temperature values from the 1500-year Greenland ice core time series. According to the projection trend, total population of Japanese sardine will decrease until the end of the 2010s, after which it will begin increasing. The amplitude of the long-term fluctuations of the Japanese sardine population abundance is extremely high, reaching 2–3 orders of magnitude.

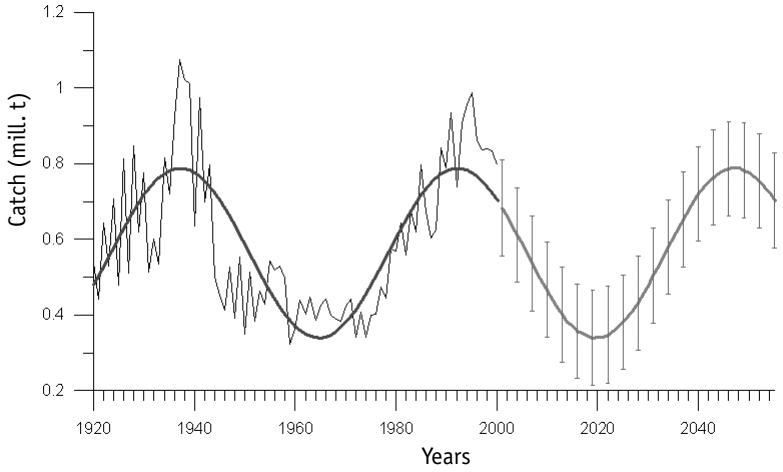

Fig. 8.2. The projected trend of total commercial catches (bold line) of Pacific salmon *Oncorhynhus* spp. with a 50 year future perspective. Thin line shows commercial catch; bold line shows predicted trend marked with standard deviation vertical bars

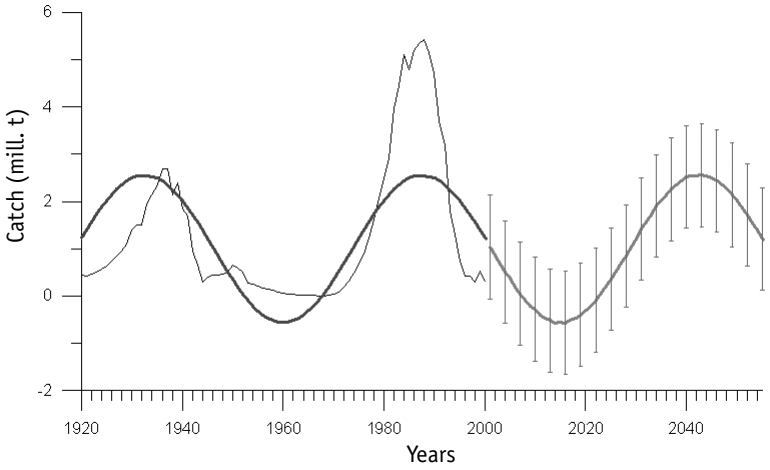

Fig. 8.3. The projected trend of total commercial catches (bold line) of Japanese sardine *Sardinops melanosticus* for the next 50 years. (The symbols are similar to those in Fig. 8.2 ?)

California sardine (Fig. 8.4). The cyclic period trend obtained from analysis of the time series for total catches of California sardine equal 55 years, i.e. is close to the mean 60-year climatic periodicity and also coincides with the 55-year periodicity obtained from the most reliable series of reconstructed temperature values of the 1500-year Greenland time series. According to our trend projection, the total population of California sardine will de-crease until the end of 2010s, after that will begin increa-sing. The amplitude of the long-term fluctuations of this population is extremely high, reaching 2–3 orders of magnitude. Dynamics of total California sardine catches has a specific feature. Contrary to the population outburst happened in 1920s–1930s, the outburst that occurred during the 1970s–1990s was mainly provided by sardine populations from the Gulf of California, and Baja California bays.

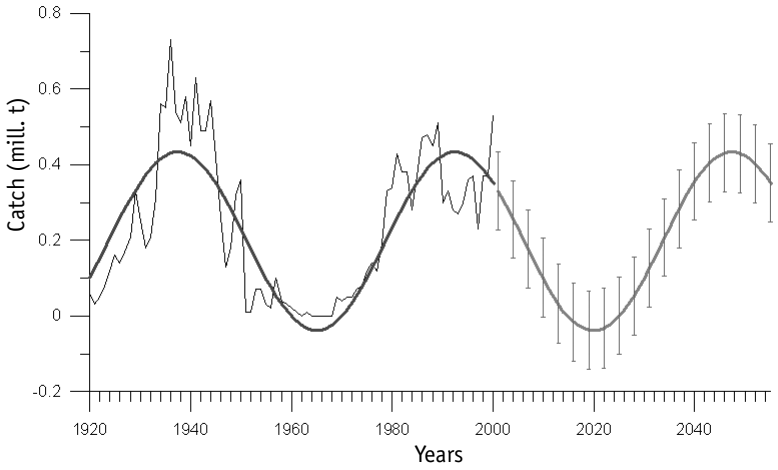

Fig. 8.4. The projected trend of total commercial catches (bold line) of California sardine *Sardinops caerulae* for the perspective of 50 years. (The symbols are similar to those in Fig. 8.2)

Peruvian sardine (Fig. 8.5). The cyclic period trend obtained from analysis of the time series for total catches of Peruvian sardine equals 55 years, i.e. is close to the mean 60-year climatic periodicity and again coincides with the 55-year periodicity, obtained from the most reliable series of reconstructed temperature values of the 1500-year Greenland ice core time series. According to our projected trend, the total population of Peruvian sardine will decrease until the mid-late 2010s, and afterward will begin increasing. The amplitude of the long-term fluctuations of this population is extremely high, reaching 2–3 orders of magnitude.

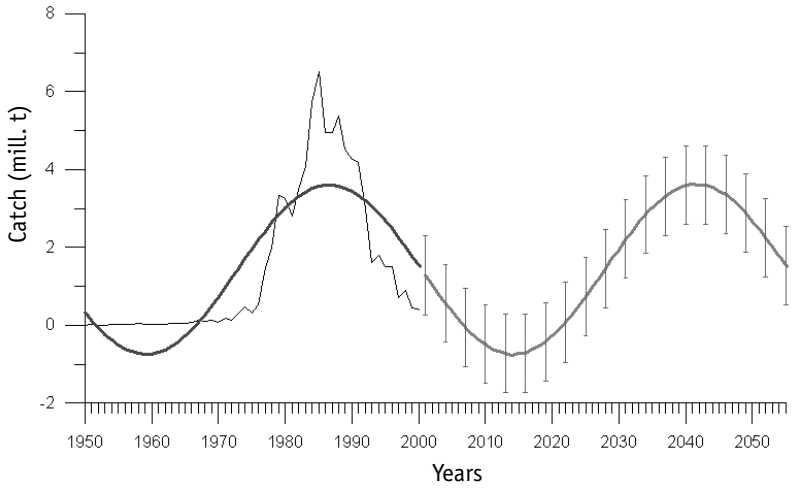

Fig. 8.5. The projected trend of total commercial catches (bold line) of Peruvian sardine *Sardinops sagax* for the perspective of 50 years. (The symbols are similar to those in Fig. 8.2)

European sardine (Fig. 8.6). The cyclic period trend obtained from analysis of the time series for total catches of European sardine equals 55 years, i.e. is close to the mean 60-year climatic periodicity and coincides with the 55-year periodicity, obtained from the most reliable series of reconstructed

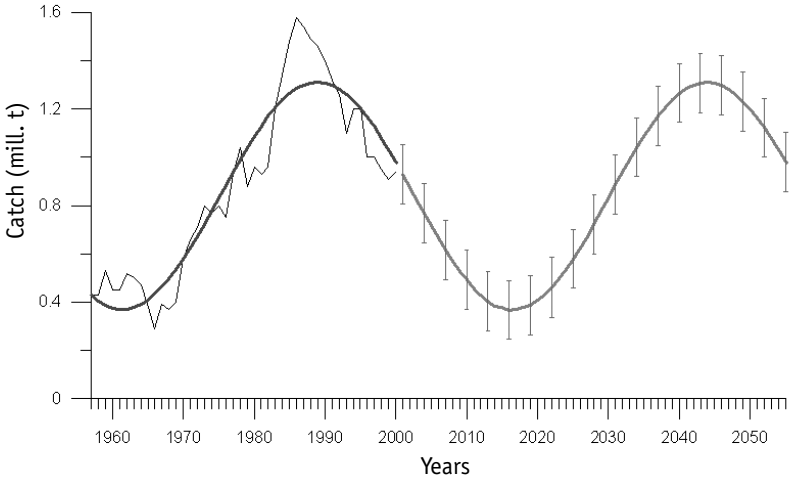

Fig. 8.6. The projected trend of total commercial catches (bold line) of European sardine *Sardina pilchardus* for the perspective of 50 years. (The symbols are similar to those in Fig. 8.2)

temperature values of the 1500-year Greenland ice core time series. According to our projected trend, the total population of European sardine will decrease until the mid-late 2010s, and afterward will begin increasing. The amplitude of the long-term fluctuations of this population is 3–4X.

Chilean jack mackerel (Fig. 8.7). The statistics series of Chilean jack mackerel catches is only 35 years. The cyclic trend period obtained from analysis of the total catch time series is approximated by the period of 55 years. According to the projected trend, the total population of Chilean jack mackerel will decrease until the early 2020s and then will begin increasing. The amplitude of the long-term fluctuations may be estimated to be approximately as 2–3X.

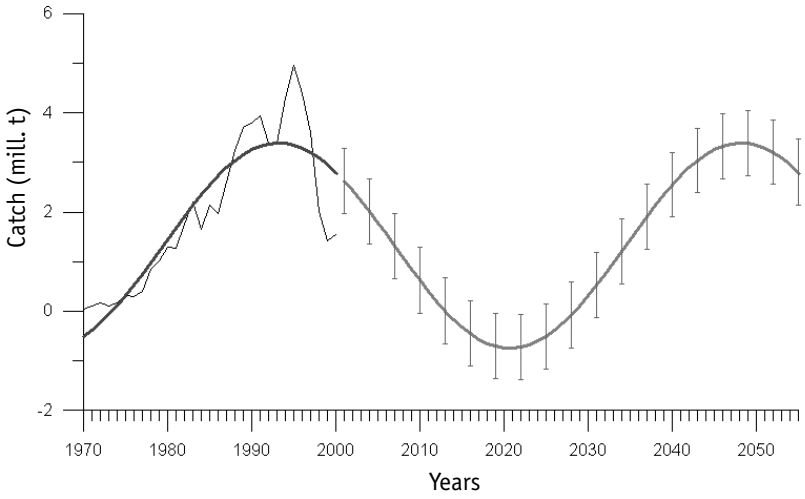

Fig. 8.7. The projected trend of total commercial catches (bold line) of Chilean jack mackerel *Trachurus murphyi* for the future 50 years. (The symbols are similar to those in Fig. 8.2)

Atlantic spring-spawning herring (Fig. 8.8). The analyzed series for Atlantic spring-spawning herring represents dynamics of the spawning stock biomass. This index is tightly related to general biomass of its commercial stock (r = 0.95, see Chapter 3). The cyclic period trend obtained for the 87-year time series is approximately 65 years. This exceeds the mean 55–60-year periodicity, but falls within the range of the general 50–70-year periodicity of climatic fluctuations. According to our projected trend, the total biomass of the Atlantic spring-spawning herring commercial stock will increase

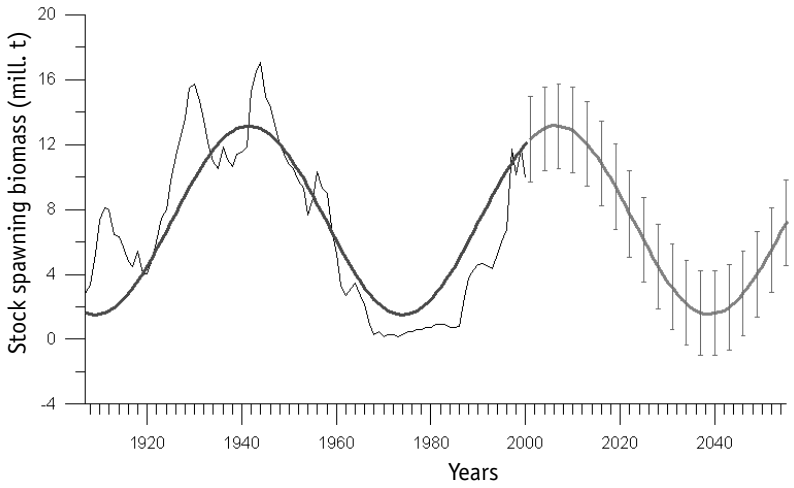

Fig. 8.8. The projected trend of total stock spawning biomass (bold line) of Atlantic spring-spawning herring for the next 50 years. (The symbols are similar to those in Fig. 8.2)

until the early 2010s, and then will begin decreasing. The amplitude of the long-term fluctuations of this population is 3–4X.

North-East Arctic cod (Fig. 8.9). The reconstructed time series of commercial North-East Arctic cod biomass is almost 100 years [Hylen, 2002].

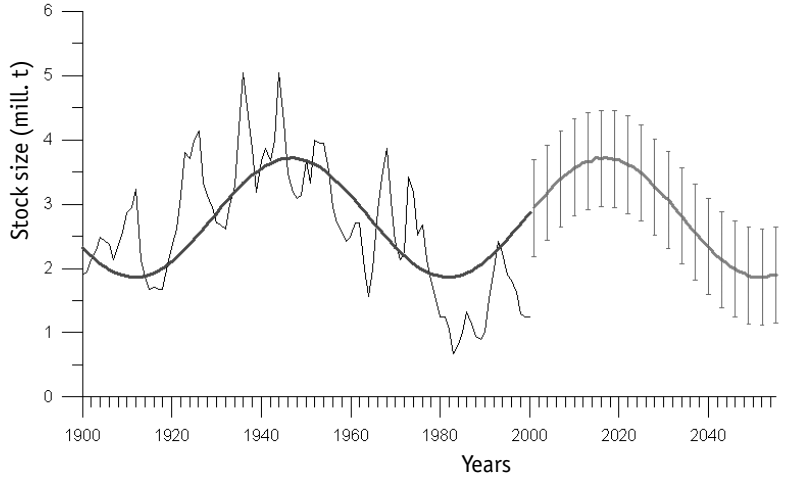

Fig. 8.9. The projected trend of total commercial stock size (bold line) of North-East Arctic cod *Gadus morhua* for the next 50 years. (The symbols are similar to those in Fig. 8.2)

As shown in Chapter 3, the dynamics of commercial North-East Arctic cod biomass is delayed by 8–10 years compared with the curve of commercial herring biomass. For North-East Arctic cod, the cyclic period trend is approximately 70 years, and within the background of this trend the cod commercial resource biomass shows approximately 10-year oscillations. This exceeds the mean 55–60-year periodicity, but falls within the general range of 50–70-year periodicity of climatic fluctuations. According to our projected trend, the total biomass of the North-East Arctic cod commercial resource will increase until the late 2010s–early 2020s; and afterward it will begin decreasing until 2040s. The amplitude of the long-term fluctuations of this population is 3–4X.

Alaska pollock (Fig. 8.10). The time series of Alaska pollock total catches is a bit longer than 50 years. The cyclic trend period is approximated by 55 years. According to our projected trend, the total commercial biomass of Alaska pollock will decrease until the early 2020s; after that it will begin increasing (see Chapter 3). Amplitude of the long-term fluctuations of total biomass may be estimated by 2–3X values — in the first approximation only.

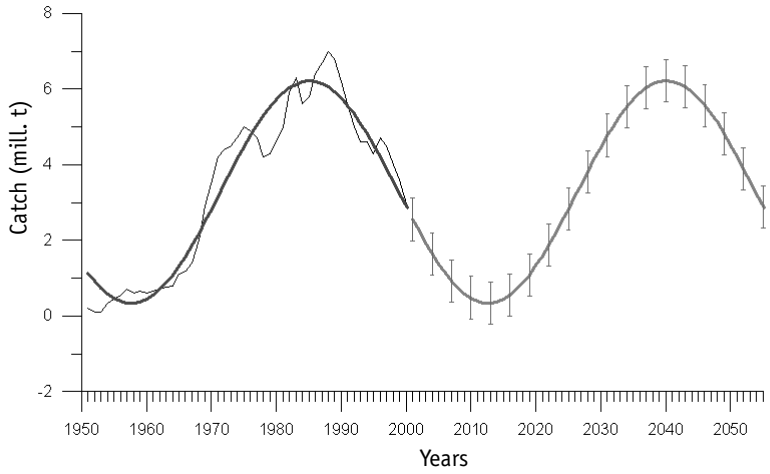

Fig. 8.10. The projected trend of total commercial catches (bold line) of Alaska pollock *Theragra chalcogramma* for the next 50 years. (The symbols are similar to those in Fig. 8.2)

South-African anchovy (8.11). For South-African anchovy catches, the cyclic trend period of the time series is 55 years. According to our projected trend, the total commercial biomass of this species will decrease until the

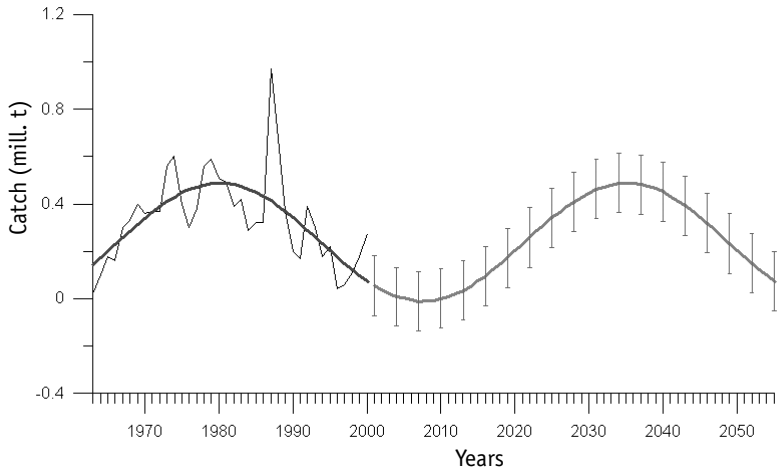

Fig. 8.11. The projected trend of total commercial catches (bold line) of South-African anchovy *Engraulis capensis* for the next 50 years. (The symbols are similar to those in Fig. 8.2)

early 2010s; after in which it will begin increasing (see Chapter 3). Amplitude of the long-term fluctuations may be estimated to be within 5–10X — in the first approximation only.

Predictive trends for the second group of species

Japanese anchovy (Fig. 8.12). The cyclic period of time series trend for Japanese anchovy catches is only about 50 years (see Chapter 6). According to our projected trend, the total commercial biomass of Japanese anchovy will increase until the early 2010s, and then will begin decreasing. The amplitude of the long-term fluctuations may be estimated to be within 5–10X — in the first approximation only.

Pacific squid. Dynamics of squid catches virtually coincide with the long-term changes in Japanese anchovy catches (see Chapter 6). Therefore, the cyclic trend of statistical series of catches and predictive trend of Pacific squid coincide with these of Japanese anchovy. In this relation, Pacific squid population will increase until the early 2010s; after that in will begin decreasing. The amplitude of the long-term fluctuations may be estimated to be within 5–10X — in the first approximation.

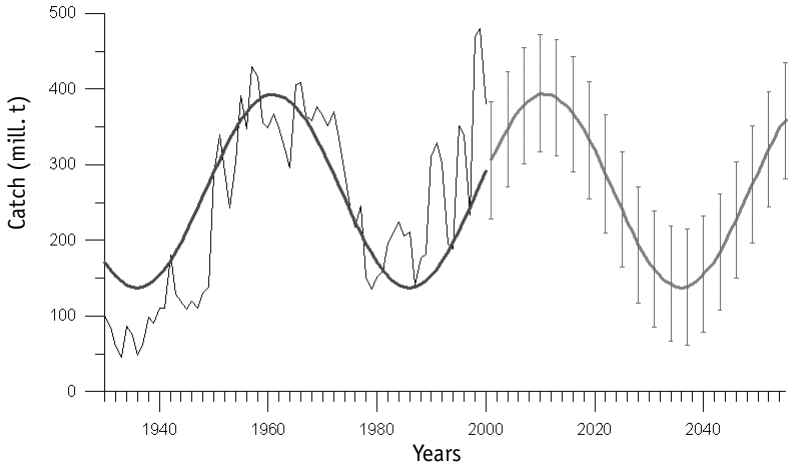

Fig. 8.12. The projected trend of total commercial catches (bold line) of Japanese anchovy *Engraulis japonicus* for the bext 50 years. (The symbols are similar to those in Fig. 8.2)

South-African sardine (Fig. 8.13). The cyclic period trend of the time series for South-African sardine catches is approximately 50 years. According to our projected trend, total commercial biomass of its population will increase until the early 2010s; afterward it will begin decreasing. The amplitude of the long-term fluctuations may be estimated by 5–10X — in the first approximation.

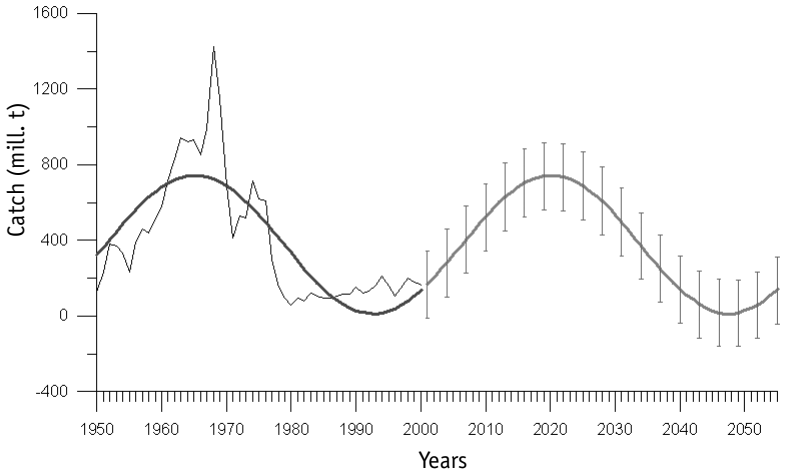

Fig. 8.13. The projected trend of total commercial catches (bold line) of South-African sardine *Sardinops ocellatus* for the next 50 years. (The symbols are similar to those in Fig. 8.2)

Peruvian anchoveta. Predictive trend of catches of this, the most productive fish species, is of great practical interest. However, the features of Peruvian anchoveta population dynamics related to sharp oscillations of its population due to the effects of strong El Niños do not allow strict application of the above-discussed approach. An approximate predictive trend of this species, presented in Chapter 6 (see Fig. 6.6), shows that the population biomass will increase until the early 2020s; after that its long-term decrease will begin always within the continuous background of sharp oscillations, caused by strong El Niño events.

Comments in brief

Predictive trends for some major commercial species characterize probable directions of the population changes for future perspectives of 10, 20 or 30 years. However, it does not allow the use of this approach for shorter-term forecasts. The concepts relating fluctuations of the fish productivity to cyclic climate changes allow better management of the commercial resource exploitation by providing broader temporal perspectives and thus more realistic estimation of the large-scale fishery effects on likely changes in population abundance.

CONCLUSION

The long-term climate periodicity and fish productivity were determined by applying several analytical methods to various time series. For the recent 1500 years, the results of spectral analysis of the climate reconstruction series from Greenland ice core samples and tree rings of long-lived trees indicate the predominance of 50–70-year cyclical climate fluctuations. Application of the Time-Frequency spectral Analysis (TFA) allowed detection of not only average characteristics of climatic cycle periodicity during this period, but also trace their distribution changes with time. From our TFA analysis, the intensity of the 50–70-year climate periodicity increased continuously during the recent thousand years including the 20th century and will likely be preserved at this level for, at least, more 100 years.

According to reconstructed data, California sardine and anchovy population outbursts during the recent 1700 years and Japanese sardine during the recent 400 years have also shown this 60–70-year periodicity.

According to instrumental measurements, analyses of the dynamics of various climatic indices for the recent 140 years show that the 60–70-year cyclical climate periodicity is predominant for Global dT, Arctic dT, Atmospheric Circulation Index (ACI), Atmospheric transfer anomalies (AT anomalies), Pacific Decadal Oscillation (PDO), Aleutian Low Pressure Index (ALPI), and sea ice coverage of Barents Sea and Sea of Okhotsk. Analogous periodicity was determined for fluctuations of Balkhash basin lake volume, rainfall along the west coast of the USA, and Neva River level rise.

According to the fishery statistics data for 50–100 years, fluctuations of the many large commercial fish populations of Pacific and Atlantic Oceans:

anchovies, sardines, herrings, cod, salmons, etc. correlate with the dynamics of global and regional climatic indices.

What are the probable mechanisms of climate effects on dynamics of the population abundance is the basic question, for which no well defined answer is available, to date. Among the major commercial species, two basic groups are identified, for which population maxima correlate with the warming or cooling climate periods e.g. Global dT increase or decrease. This does not mean that temperature alone causes long-term fluctuations of the fish population. For example, Japanese sardine population outbursts occur during periods of increasing Global dT. However, ocean temperatures within the zone of the Oyashio and Kuroshio Currents' mixing, which is the main sardine reproduction site in the region, decreased during this period due to cold Oyashio Current intensification as a result of an overall increase of atmospheric and oceanic circulations in the North Pacific.

The maximum of zooplankton biomass in the North Pacific region occurs during the cooling down period, whereas maxima of the major commercial fish populations are observed during the warming periods in this region.

Correspondence of the long-term trends of the indices that characterize dynamics of atmospheric pressure (ALPI and ACI) and temperature (Global dT, Arctic dT, and PDO) fields, prompts the hypothesis that the interchange of climate warming and cooling periods results from significant changes in atmospheric and oceanic circulation, i.e. force and direction of winds and currents. Subsequently, such changes should be well observed in the vast upwelling zones, along California or Peru, for example. Unfortunately, even in these regions the observation series are not long enough for reliable detection of long-term changes in hydrological indices. The alteration of anchovy and sardine population blooms in these large upwelling zones indicates the existence of unknown yet specific oceanographic conditions, which cause the selective increases in single species populations, while the others decline.

The concept of a «cascade» mechanism of climate fluctuation influences on fish productivity via changes in the primary production and zooplankton production is not confirmed by observational data. In the oceanic ecosystem with a multistage complex of foodweb relations, the major part of plankton production is consumed within the planktonic species network itself. The role of fish as the main consumer in the ecosystem does not seem predominant: the nekton consumes less than 10% of the planktonic coenosis production [Shuntov, 2001].

Irrespective of that fact, if real mechanisms of the climatic influence on the populations are known, we may use global and regional climatic indices to plan for the future dynamics of commercial stocks.

Dynamics of large populations of important pelagic fish with high fecundity is reliant upon the strategy of «risky breeding», given the high individual fish breeding potential. Each female sardine or anchovy can produce up to and over a hundred thousand eggs, each of which is a potential descendant, the majority of which will die within the very early stages of their life. The biological purpose for producing such great numbers of eggs is the ultimate realization of a «happy occurrence» (encountering a set of preferable oceanographic and biological circumstances), which ultimately leads to the high survivability of as many as possible of the abundant spawn. Bakun and Broad [2003] labeled this mechanism using the term «loophole», which means an «ecological window» of environmental conditions, that support the occurrence of an abundant generation. Thus, it is the low or high probability of the successful breeding rather than trophic indices of individual ecosystems that is the main factor in the consequent dynamics of abundant pelagic fish populations with their high breeding potentials.

Occurrences of abundant generations result from the influence of many natural factors, the concurrences of which promote more favorable conditions that provide for higher survivability of larvae, and thus increases the probability of an overall growth of the resource population. Following on, to increase this latter probability, favorable conditions for both larval survival and juvenile growth are required, which in turn promote higher population recruitment. In the «favorable» climatic periods, the frequency of concurrent conditions providing for larval survival and growth of juveniles increases. This leads to the more frequent occurrence of high recruitment to populations of the major pelagic fishes, which form the basis of commercial fisheries in the more productive regions of the World Ocean.

Thus, fluctuations of the fish productivity are determined by the fact that each multiannual climatic period is characterized by the favorable or unfavorable frequency of occurrence of various types of weather, hydrological, and hydrobiological conditions necessary for juveniles survival.

Climate and dynamics of local Pacific salmon populations. The dynamics of large commercial populations correlate with climate changes, which include long-term processes developing over decades in aquatic areas concurrences millions of square kilometers. At the same time, the population dynamics of some individual salmon stocks are not at all well correlated with

the trends of global climatic indices. Total catches within the various regions comprise local and subregional commercial stock landings. As the catch data are combined within a region, the relationship tightens between climate changes and long-term dynamics of the overall salmon population. As this regional integration expands the relationship significantly increases and reaches higher levels of statistical confidence for large regions in the North Pacific. Thus, the long-term changes in the overall salmon population of larger, more integrated regions are in better correlation with dynamics of global (Global dT or ACI) compared with more localized (PDO or ALPI) climatic indices of the North Pacific.

The possibility of forecasting of climate and fish productivity fluctuations is provided by the similarity of the patterns of long-term dynamics of the populations of some abundant pelagic fish species and those of climate changes. Correspondence of the fluctuations in fish productivity and cyclic climate changes are found with the largest commercial populations. These exhibit 60–70-year population cycle fluctuations, within which two approximately 30-year phases of rise and fall of fish productivity are outlined. The long-term dynamics of the main commercial stocks is simply never observed in any so-called «equilibrium» state.

The cyclic character of the climate changes and populations of abundant fish species provides the possibility to estimate the probable trend of long-term changes in some commercial species populations over the perspective of several future decades. The model developed from the long-term (up to 1500 years) climatic time series allowed us to project likely abundance changes in these major regional commercial populations for the perspective of 30–50 years beyond the most recently available time series.

The question about large-scale fisheries as the main reason for the commercial population fluctuations has been examined for a long time and remains ambiguous today. One of the reasons for that ambiguity is the prevailing conventional opinion about assuming constancy of commercial fish stock reproduction conditions. In direct contrast with this opinion, the results we have obtained show that the long-term changes in the fish productivity are related to cyclic climate fluctuations, habitat and related reproduction conditions.

The concepts about relationships between long-term fluctuations in fish productivity with more or less regular patterns of climate change provide an opportunity to forecast alterations within long epochs of increasing or decreasing stock populations of major commercial fish population. One of the best known examples is the dramatic declines of the Atlantic spring-spaw-

ning herring population and catches in the 1960s. Apparently, applying the concepts linking the relationships between population fluctuations with climate changes would help avoid the sudden collapses of the herring fishery at the peak of fishing effort. The second example is the rise and fall of the Japanese sardine catch in 1970s–1990s. It has been reliably determined that direct natural and climatic causes rather than excessive catch resulted in the abrupt decrease of the Japanese sardine population. In the history of blooms and decline of the California sardine in the period of 1920s–1940s and Peruvian sardine in 1970s–1990s the lead role is also attributable to climatic-oceanographic factors. Extremely high amplitudes of Peruvian anchovy population dynamics also illustrate the dominant effects of climate and oceanographic- changes on catch oscillations for this most productive species.

The results obtained from our work show that the trends within multiyear commercial fish resource dynamics are generally determined by the large-scale changes in climate-related oceanographic conditions. However to date, the conventional opinion that these variations are due to «commercial population exploitation» is generally proposed from the unsubstantiated assumption that commercial resource abundance changes depend exclusively on the interaction within the «resource-fishery» system. «Although the concept of the precautionary approach is presented as the recent cardinal revision of the methodology in the field of commercial resource management and regulation, it retains some arbitrary assumptions about the stablility of the resource (and catch), underlying system and equilibrium resource states, commercial resource management — controlled via fishery intensity changes, etc.» [Shuntov, 2003, p. 67–68].

Forecasting of climate-related dynamics of the populations allows prediction of exchanges amongst the main commercial species in the major fishery regions. This provides the opportunity to hitherto predict the control measures for the fishery, which would prevent excessive commercial stock exploitation within the long-term decline phase or, on the other hand, intensify the commercial focus during the growth and colonization phase of commercial stock populations [Csirke, 1984]. This approach would also increase reliability of investments in multiyear projects involving fishery fleets and processing enterprise construction, which are typically oriented toward a definite species composition and the level of the resource base. Application of our understanding of the relationships between fish productivity fluctuations with climate changes will promote more rational use of the ocean resources, but will require more accurate monitoring and esti-

mation of the climatic change dynamics compared with available historical data [Chavez et al., 2003].

These concepts about cyclical climate and biota changes provide an opportunity to predict the direction of the long-term changes ongoing in the various regional natural communities due to natural forces. This also allows for more real estimation of anthropogenic influences on resource population dynamics and for planning and enforcement of environmental protection measures with the forward looking perspective of several decades.

Acknowledgements
We would like to express our deepest appreciation to VNIRO authorities and our colleagues who helped us in preparation and publication of this book. We are also particularly grateful to Dr. Gary D. Sharp from the Center for Climate / Ocean Resources Study, Salinas, California, USA for his deep interest to the problem of fish stock fluctuations in relation to climate changes, priceless comments and amendments to the text, and great contribution to scientific editing of the manuscript.

LIST OF ABBREVATIONS

ACI — Atmospheric Circulation Index

ALPI — Aleutan Low Pressure Index

Anomaly AT — Anomaly of air mass transfer direction

Arctic dT — Mean surface air temperature of circumpolar zone from 60 to 85° N

CSB — Commercial Stock Biomass

Global dT — Mean surface air temperature for all the Earth

NAO — North Atlantic Oscillation

PDO — Pacific Decadal Oscillation

SSB — Spawning Stock Biomass

SST — Sea Surface Temperature

REFERENCES

Abrosov V.N. 1973. Balkhash Lake. L.: Nauka.— 179 p. (Rus).

Aebisher N.J., Coulson J., Colebrook J. 1990. Parallel long-term trends across four marine trophic levels // Nature.— V. 347.— P. 753–755.

Aksnes D.L., Blindheim J. 1996. Circulation patterns in the North Atlantic and possible impact of population dynamics of Calanus finmarchicus // Ophelia.— V. 44.— P. 7–28.

Aleksandrov E.I., Bryazgin N.N., and Dementiev A.A. 2003. Tendencies in the changes of the surface air temperature and atmospheric fallouts in the North Polar region in the second part of the 20th century // The study of climate changes and ocean and atmosphere interactions in Polar zones: Proc. AARI vol. 446.— P. 31–40. (Rus).

Alekseev G.A. 2003. The studies of Arctic climate changes in the 20th century // The study of climate changes and ocean and atmosphere interactions in Polar zones: Proc.— AARI V. 446.— P.6–21. (Rus).

Alekseev G.A., Aleksandrov E.I., Svyashchennikov P.N., and Kharlanenkova N.E. 2000. On the relationship of climate oscillations in the Arctic and in the middle and low latitudes // Meteorology and hydrology.— No. 6.— P.5–17. (Rus).

Alheit J., Hagen E. 1997. Long-term climate forcing of European herring and sardine populations // Fish. Oceanogr.— V. 6.— P. 130–139.

Alheit J., Niquen M. 2004. Regime shifts in the Humboldt Current ecosystem // Progress in Oceanography.— V. 60. № 2–4.— P. 201–222.

Anderson T. 1976. Statistical analysis of time series. — M.: Mir.— 755 p. (Rus).

Anonymous. 2002. Report of the Arctic Fisheries Working Group.— ICES CM 2002 / ACFM: 19.— 22 p.

Aranchibia H., Cubillos L., Arcos D., Grechina A., Vulugron L. 1995. The fishery of horse mackerel (Trachurus symmetricus) in the South Pacific Ocean with notes of fishery off central-southern Chile // Scientia Marina.— V. 59. № 3–4.— P. 589–596.

Averkiev A.S., Bulaeva V.M., Gustoev D.V., and Karpova I.P. 1997. Methodical recommendations for the use of superlong-term method of hydrometeorological element forecasting and the programmed complex «Prism». Murmansk: PINRO.— 40 p. (Rus)

Ayon P., Purca S., Guevara-Carrasco R. 2004. Zooplankton volume trends off Peru between 1964 and 2001 // ICES J. Mar. Sci.— V. 61.— P. 478–484.

Bakun A. 1996. Patterns in the Ocean. California Sea Grant College System.— NOAA.— 323 p.

Bakun A., Broad K. 2003. Environmental «loopholes» and fish population dynamics: comparative pattern recognition with focus on El Niño effects in the Pacific // Fish. Oceanogr.— V. 12. № 4/5.— P. 458–473.

Bakun A., Mendelsson R. 1989. Alongshore wind stress: reconciliation and update through 1986 // The Peruvian upwelling system: dynamics and interactions / Pauly D., Muck P., Mendo J., Tsukayama I. (eds.).— ICLARM Conf. Proc.— № 18.— P. 77–81.

Barnett T.P., Pierce D.W., Saravanan R., Shneider N., Dommenget D., Latif M. 1999. Origins of the midaltitude Pacific decadal variability // Geophysic. Res. Lett.— V. 26. № 10.— P. 1453–1456.

Baumgartner T. R., Soutar A., Ferreira-Bartrina V. 1992. Reconstruction of the history of Pacific sardine and Northern Pacific anchovy populations over the past two millennia from sediments of the Santa Barbara basin // CalCOFI Rept.— № 33.— P. 24–40.

Beamish R., Bouillon D. 1993. Pacific salmon production trends in relation to climate // Can. J. Fish. and Aquat. Sci.— V. 50.— P. 1002–1016.

Beamish R.J.D., Noakes J., McFarlane G. A., Klyashtorin L.B., Ivanov V.V., Kurashov V. 1999. The regime concept and natural trends in the production of Pacific salmon // Can. J. Fish. and Aquat. Sci.— V. 56.— P. 516–526

Beaugrand G., Brander K.M., Lindley J.A., Sousii S., Reid Ph.C. 2003. Plankton effect on cod recruitmnt in the North Sea // Nature.— V. 426.— P. 661–664.

Bell G., Halpert M., Schnell R., Higgins R., Lavrimor J., Kousky V., Tinker R., Thiaw W., Chelliah M., Artusa A. 2001. Climate assessment for 1999 // Bull. Amer. Meteorol. Soc.— V. 81. № 6.— P.1328–1350.

Bigler B., Welch D., Helle J. 1996. A review of size trends among North Pacific salmon // Can. J. Fish. and Aquat. Sci.— V. 53.— P. 455–465.

Birman I.B. 1985. Marine period of life and problems of Pacific salmon stock dynamics. M.: Agropromizdat.— 208 p. (Rus).

Bochkov Yu.A. 1982. Back observationof water temperature in the 0–200 m layer at the Kola meridian in Barents Sea (1900–1981) // Ecology and fishery of bottom fishes in North European basin: Proc. PINRO.— P.113–122. (Rus).

Boitsov V.V., Lebed' N.I., Ponomarenko V.P., Ponomarenko I.Ya., Tereshchenko V.V., Tretyak V.L., Shevelev M.S., and Yaragina N.A. 1996. Barents Sea cod. Murmansk: PINRO.— 285 p. (Rus).

Bondarenko M.V., Krovnin A.S., and Serebryakov V.P. 2003. Ranking of abundance and survival coefficients of the generations in the early ontogenesis of commercial fishes in Barents Sea. M.: VNIRO.— 187 p. (Rus).

Borisov V.M., Elizarov A.A. 1989. Long term variations and abiotic conditions in the ecosystem of the Barents Sea // J. Fish. Biol.— Suppl. A.— V .35.— P. 139–144.

Borisov V.M., Ponomarenko V.P., and Semenov V.N. 2001. Bioresources of Barents Sea and fishery in the second part of the 20th century // Ecology of commercial species in Barents Sea. Chinarina A.D. (Ed.). Apatity: Izd. KNTs RAS. — P.1 39–195. (Rus).

Box J. and Jenkins G. 1974. Analysis of time periods. Forecast and control. In 2 issues M.: Mir.— 40 p. and 197 p. (Rus).

Brander K.M., Dickson R.R., Shepherd J.G. 2001. Modeling the timing of plankton production and its effect on recruitment of cod (Gadus morhua) // ICES J. Mar. Sci.— V. 58.— P. 962–966.

Brander K.M. 2003. ICES/GLOBEC Cod and Climate Change Programme — results and achievements // GLOBEC Internat. Newsletter.— V. 9. № 2.— P. 20–22.

Briffa K.R., Bartholin T.S., Eckstein D., Jones P.D., Karlen W., Schweingruber F.W., Zetterberg P. 1990. A 1400 year tree-ring record of summer temperatures in Fennoscandia // Nature.— V. 346.— P. 434–439.

Brodeur R. 1988. Zoogeography and trophic ecology of the dominant epipelagic fishes in the northern North Pacific // The Biology of the Subarctic Pacific.— Bull. Ocean Univ. Tokyo.— № 26. Part II.— P. 1–29.

Brodeur R., McKinnell S., Nagasava K., Pearcy W., Radchenko V., Takagi S. 1999. Epipelagic nekton of the North Pacific Sub-Arctic and transition zones // Progr. Oceanogr.— V. 43.— P. 365–398.

Brodeur R., Ware D. 1992. Long-term variability in zooplankton biomass in the subarctic Pacific Ocean // Fish. Oceanogr.— V. 1(1).— P. 32–35.

Brodeur R., Ware D. 1995. Interdecadal variability in distribution and catches rates in epipelagic nekton in the Northeast Pacific Ocean // Can. Spec. Publ. Aquat. Sci.— V. 121.— P. 329–356.

Bulatov O.A. 2003. Pollock fishery and reserves in Bering Sea. Coll. Analit. Ref. Inform. Series «Economics, information and fishery control».— M.: VNIERKh.— Iss. 2.— P. 101–114. (Rus).

Bulatov O.A. 2003. The fishery and condition of the walleye pollock stock in the Bering Sea in 1979–2002 // PICES 12-th annual meeting.— Seoul, Korea. Abstracts.— P. 130.

Bulatov O.A. 2004. Bering Sea pollock: breeding, resources and strategy of the fishery control. Thes. Doct. Biology Diss.— M.: VNIRO.— 48 p. (Rus)

Bulatov O.A. 2005. Estimation of total permissible catch and modern control system of pollock fishery in Bering Sea. Analit. Ref. Inform. Series «Water biological resources, their state and use» — M.: VNIERKh.— Iss. 2.— P.2–40. (Rus).

Carrasco S., Lozano O. 1989. Seasonal and long-term variations of zooplankton volumes in the Peruvian sea, 1964–1987 // The Peruvian upwelling system: dynamics and interactions / Pauly D., Muck P., Mendo J., Tsukayama I. (eds.).— ICLARM Conf. Proc.— № 18.— P. 82–85.

Chavez F., Barber R. 1987. An estimate of new production in the equatorial Pacific // Deep-Sea Res.— V. 34.— P. 1229–1243.

Chavez F., Barber R., Sanderson M. 1989. The potential primary production of the Peruvian upwelling ecosystem 1953–1984 // The Peruvian upwelling system: dynamics and interactions / Pauly D., Muck P., Mendo J., Tsukayama I. (eds.).— ICLARM Conf. Proc.— № 18.— P. 50–63.

Chavez F., Ryan J., Lluch-Cota S.E., Niquen M.C. 2003. From anchovies to sardines and back: Multidecadal change in the Pacific Ocean // Science.— V. 219.— P. 217–219.

Clark A., Frid Ch.L.J., Nicholas K.R. 2003. Long-term predation based control of a central-west North Sea zooplankton community // ICES J. Mar. Sci.— V. 60.— P. 187–197.

Corten A. 1999. A proposed mechanism for the Bohuslan herring periods // ICES J. Mar. Sci.— V. 56.— P. 207–220.
Csirke J. (chairmen). 1984. Report of working group on fisheries management? Implications and interactions // Reports of the expert consultation to examine changes an abundance and species composition of neritic fish resources.— FAO Fisheries Report. № 291.— V. 1.— P. 67–90.
Cury Ph., Bakun A., Crawford R., Jarre A., Quinones R., Shannon L., Verheye H. 2000. Small pelagic in upwelling systems: patterns of interaction and structural changes in «wasp-waist» ecosystems // ICES J. Mar. Sci.— V. 57.— P. 603–618.
Cury Ph., Roy C. 1989. Optimal environmental window and pelagic fish recruitment success in upwelling areas // Can. J. Fish. and Aquat. Sci.— V. 46.— P. 670–680.
Cury Ph., Roy C., Mendelsson R., Bakun A., Husby D., Parrish R. 1995. Moderate is better: exploring nonlinear effects on the California northern anchovy (*Engraulis mordax*) // Climate change and northern fish populations / Beamish R.J. (ed.).— Can. Spec. Publ. Fish. Aquat. Sci.— V. 121.— P. 417–424.
Cushing, D. H. 1969. The regularity of the spawning season of some fishes.//J. Cons. int. Explor. Mer. 33.— P. 81–92.
Cushing D.H. 1971. The dependence of recruitment on parent stock in different groups of fishes // J. Cons. int. explor. mer.— V. 33.— P. 340–362.
Cushing D.H. 1978. Upper trophic levels in upwelling areas // Upwelling ecosystems, Boje R., Tomczak M. (eds.).— N.Y.: Springer.— P. 101–110.
Cushing, D. H. 1980. The decline of the herring stocks and the gadoid outburst // J. Cons. int. Explor. Mer.— V. 39.— P. 70–81.
Cushing D.H. 1982. Climate and fisheries.— U.K., Academ. Press.— 373 p.
Cushing D.H. 1990. Plankton production and year-class strength fish populations: an update of the match/mismatch hypothesis // Adv. Mar. Biol.— V. 26.— P. 249–293.
Cushing D.H. 1995. The long-term relationship between zooplankton and fish // ICES J. Mar. Sci.— V. 52.— P. 611–626.
Dansgaard W., Johnsen S.J., Reeh N., Gundestrup N., Clausen H.B., Hammer C.U. 1975. Climatic changes, Norsemen and modern man // Nature.— V. 255.— P. 24–28.
Datsenko N.M., Monin A.S., Berestov A.A., Ivanenko N.N., and Sonechkin D.M. 2004. On oscillations of global climate for the last 150 years // Dokl. RAN. vol. 399. No. 2.— P. 253–256. (Rus).
Dement'eva A.F. 1976. Biological substantiation of the fishery forecasts.— M.: Pishchevaya Promyshlennost'.— 236 p. (Rus).
Dragesund O. 1971. Comparative analysis of year-class strength among fish stocks in the North Atlantic // Fiskeridir. skr. Ser. havunders.— № 16.— P. 49–64.
Dulepova E.R. 2002. Comparative bioproductivity of macro-ecosystems of Far East seas. Vladivostok: TINRO-centre.— 273 p. (Rus).
Dzerdzeevsky B.L. 1943. On warming-up in Arctic // Izv. AN SSSR. Ser. Geofizika i Geografiya.— V. 5.— P. 60–69. (Rus).
Edwards M., Richardson A.J. 2004. The impact of climate change on phenology of the plankton community and trophic mismatch // Nature.— V. 430.— P. 881–884.
Efron B., Tibshirani R. 1986. Bootstrap methods for standard errors, confidence intervals and other measures of statistical accuracy // Statistic. Sci.— V. 1.— P. 54–77.

Ekaikin A.A., Lipenkov V.Ya., Peti Zh.R., and Masson-Dellmot V. 2002. The fifty-year cycle in changes of ice accumulation and ice isotopic composition at the Vostok station // Proc. Glaciological Symp. The future of glaciosphere under the condition of changing climate. Pushchino, May 2002, Iss. 94.— P. 163–173. (Rus).

Elizarov A.A. 2001. Proceedings of G.K. Izhevsky: their modern sounding // Ryb. Khoz.— No. 2.— P. 28–30. (Rus).

Elizarov A.A., Grechina A.S., Kuznetsov A.N., and Sokolov V.A. 1989. Reconstruction in ecosystems of the World Ocean in relation to changes in conditions of the atmosphere-ocean system // Biological grounds of the population dynamics and fish catch forecasting.— M.: VNIRO.— P. 29–46. (Rus)

Ellertsen B., Fossum P., Solemdal P., Sundby S. 1989. Relation between temperature and survival of eggs and first-feeding larvae of Northeast Arctic cod // Rapp. et proc.-verb. reun. cons. int. explor. mer.— V. 191.— P. 209–219.

Enomoto H. 1991. Fluctuations of snow accumulation in the Antarctic and sea level pressure in the southern hemisphere in the last 100 years // Climatic change.— V. 18.— P. 67–87.

Fair L.F. 2003. Critical elements of Kvichak River sockeye salmon management // Alaska Fish. Res. Bull.— V. 10.— № 2.— P. 95–103.

Fiksen O., Utne A.C.W., Aksnes D.L., Eiane K., Helvikand J.V., Sundby S. 1998. Modeling the influence of light, turbulence and ontogeny on digestion rates in larval cod and herring // Fish. Oceanogr.— V. 7.— № 3–4.— P. 355–363.

Garrod D.J., Jones B. 1974. Stock and recruitment relationship in the Northeast Arctic cod stock and the implications for management of the stock // J. Cons. int. explor. mer.— V. 36.— P. 35–41.

Garrod D.J., Shumacher A. 1994. North Atlantic Cod: The Broad Canvas // ICES Mar. Sci. Symp.— V. 198.— P. 59–76.

Garrod D.J. 1967. Population dynamics of Arcto-Norwegian cod // J. Fish. and Aquat. Sci.— V. 24.— P. 145–190.

Girs A.A. 1971. Multiyear oscillations of atmospheric circulation and long-term meteorological forecasts. L.: Gidrometeroizdat.— 480 p. (Rus)

Godo O.R. 2003. Fluctuation in stock properties of north-east Arctic cod related to long-term environmental changes // Fish and Fisheries.— V. 4.— P. 121–137.

Graybill D. 1980. Time Series Data Library by R. Hyndman and M. Akram.— http://www.personal.buseco.monash.edu.au/-hyndman/TSDL.

Gritsenko O.F. 2002. Migratory fishes of Sakhalin Island (systematization, ecology, fishery).— M.: VNIRO.— 248 p. (Rus).

Gulland J.A. 1982. Fish stock assessment.— John Wiley & Sons, Chichester.— 320 p.

Hare S., Mantua N. 2000. Empirical evidence for North Pacific regime shifts in 1977 and 1989 // Progress in Oceanography.— V. 47.— № 2–4.— P. 103–146.

Helle J., Hoffman M. 1998. Changes in size and age at maturity of two North American stocks of chum salmon before and after a major regime shift in the North Pacific Ocean // N. Pacif. Anadrom. Fish. Comm. Bull.— № 1.— P. 81–89.

Huber P. 1984. Robustness in statistics. M.: Mir. 303 p. (Rus).

Hunt G.L. 2003. Ecosystem studies of subarctic seas // GLOBEC Int. Newsletter.— V. 9.— № 2.— P. 30–32.

Hylen A. 2002. Fluctuations in abundance of Northeast Arctic cod during 20-th century // ICES Mar. Sci. Symp.— V. 215.— P. 543–550.

Hylen A., Dragesund O. 1973. Recruitment of young Arcto-Norwegian cod and haddock in relation to parent stock size // ICES J. Mar. Sci.— V. 64.— P. 57–68.

Ishida Y., Ito S., Kaeriyama M., McKinnell S., Nagasawa K. 1993. Recent changes and size of chum salmon in the North Pacific Ocean and possible causes // Can. J. Fish. and Aquat. Sci.— V. 50.— P. 290–295.

Izhevsky G.K. 1961. Oceanologic grounds for formation of commercial productivity of the seas.M.: Pishchepromizdat.— 216 p. (Rus)

Jacobsen T. 1996. The relationship between spawning stock and recruitment for Atlantic cod stocks // ICES C.M. 1996 / G:15.— 22 p.

James A. 1988. Are clupeoid microphagists herbivorous or omnivorous? A review of the diets of some commercially important clupeids // S. Afr. J. mar. Sci.— V. 7.— P. 161–177.

Johannesson K., Vilchez R. 1980. Note on hydroacoustic observations of changes in distribution and abundance of some common pelagic fish species in the coastal waters of Peru, with special emphasis on anchoveta // Workshop on the Effects of Environmental Variation on the Survival of Larval Pelagic Fishes/ Sharp G.D. (ed.).— IOC Workshop Rept.— Unesco, Paris.— № 28.— P. 287–323.

Jones P.D., Osborn T., Briffa K., Folland C., Norton E., Alexander L., Parker D., Rayner N. 2001. Adjusting for sampling density in grid box land and ocean surface temperature time series // J. Geophysic. Res.— V. 106.— P. 3371–3380.

Jonsson J. 1994. Fisheries of Iceland, 1600–1900 // ICES Mar. Sci. Symp.— V. 198.— P. 3–16.

Kaeriyama M. 1998. Dynamics of chum salmon populations released from Hokkaido // N. Pacif. Anadrom. Fish. Comm. Bull.— № 1.— P. 90–102.

Kaeriyama M. 1999. Hatchery programmes and stock management of Salmonid populations in Japan // Stock enhancement and sea ranching / Howell B., Moksness E., Svasend T. (eds.).— Oxford: Fishing News Books.— P. 153–167.

Kaeriyama M., Urawa S. 1992. Future research by the Hokkaido salmon hatchery for the proper maintenance of Japanese Salmonid stocks // Proc. Int. Workshop on future salmon research in the N. Pacific Ocean.— Nat. Res. Inst. Far Seas Fish.— Shimizu, Japan.— P. 57–62.

Kaeriyama M. 1989. Aspects of salmon ranching in Japan // Physiol. Ecol. Jap. Spec.— V. 1.— P. 625–638.

Kang S., Kim Y., Kim G., Parк H. 2002. Long-term changes in zooplankton and its relationship with squid Todarodes pacificus catch in Japan-East Sea // Fish. Oceanogr.— V. 11(6).— P. 337–346.

Karklin V.P., Yulin A.V., Karelin I.D., and Ivanov V.V. 2001. Climatic oscillations of ice coverage of Arctic seas of the Siberian shelf // Proc. AARI. No. 443.— P. 5–12. (Rus).

Karpenko V.I. 1998. Early marine life span of Pacific salmons.— M.: VNIRO.—165 p. (Rus).

Kash'yap R.L. and Rao A.R. 1983. Composition of dynamic stochastic models on experimental data.— M.: Nauka.— 384 p. (Rus).

Kawasaki T. 1992a. Climate-dependent fluctuations in far eastern sardine population and their impacts on fisheries and society // Climate variability, climate change and fisheries / Glantz M. (ed.).— Cambridge Univ. Press.— P. 325–355.

Kawasaki T. 1992b. Mechanisms governing fluctuations in pelagic fish populations // S. Afr. J. mar. Sci.— V. 12.— P. 873–879.

Kawasaki T. 1994. A decade of the regime shift of small pelagics. FAO expert consultation (1983) to the PICES III (1994) // Bull. Jap. Soc. Fish. Oceanogr.— V. 58.— P. 321–333.

Kawasaki T., Omori M. 1995. Possible mechanisms underlying fluctuations in the Far Eastern sardine population inferred from time series of two biological traits // Fish. Oceanogr.— V. 4(3).— P. 238–242.

Kislov A.V., Krenke A.N., Kitaev L.M., Shuvaev N.L., and Volodin E.M. 2000. Reproduction of temperature, fallouts and ice cover by the IVM model within the AMR II experiment // Physics of atmosphere and ocean. Izv. RAN.— V. 36(4).— P. 446–462. (Rus).

Klige R.K., Danilov I.D., and Konishchev V.N. 1998. The history of hydrosphere.— M.: Nauchnyi mir.— 368 p. (Rus).

Klyashtorin L.B. 1997. Pacific salmon: climate-linked long-term stock fluctuations // PICES Press.— Newsletter N. Pacif. Sci. Org.— V. 5.— P. 2–34.

Klyashtorin L.B. 1998a. Cyclic climate changes and Pacific salmon stock fluctuations. A possibility for long-term forecasting // NPAFC Techn. Rept.— Workshop on climate change and salmon production Vancouver, Canada. March 26–27, 1998.— P. 6–7.

Klyashtorin L.B. 1998b. Long-term climate change and main commercial fish production in the Atlantic and Pacific // Fish. Res.— V. 37.— P. 115–125.

Klyashtorin L.B. 2001. Climate change and long-term fluctuations of commercial catches. The possibility of forecasting // FAO Fish. Techn. Paper.—№ 410.— 86 p.

Klyashtorin L.B. and Lyubushin A.A. 2005. On dependence of global temperature anomaly on the world fuel consumption // Modern global changes of the environment.— V. 1. Nauchnyi mir.— 520 p. (Rus).

Klyashtorin L.B. and Sidorenkov N.S. 1996. Long-term climatic changes and pelagic fish reserve fluctuations in Pacific region // Izv. TINRO.— V. 119.— P. 33–54. (Rus).

Klyashtorin L.B. and Smirnov B.P. 1992. Pacific salmons: the state of reserves and reproduction // Obzor. Inform. Ser. Akvakul'tura. Iss. 2.— M.: VNIIERKh.— P. 1–36. (Rus).

Klyashtorin L.B., Lyubushin A.A. 2003. On the coherence between dynamics of the world fuel consumption and global temperature anomaly // Energy and Environ.— V. 14.— № 6.— P. 773–782.

Klyashtorin L.B., Smirnov B.P. 1995. Climate-dependent salmon and sardine stock fluctuations in the North Pacific // Climate change and northern fish fluctuations / Beamish R. (ed.).— Can. Spec. Publ. Fish. Aquat. Sci.— V. 121.— P. 687–689.

Konchina Yu. 1991. Trophic status of the Peruvian sardine and anchovy // J. Ichtiol.— V. 31.— P. 59–72.

Konchina Yu.V. 1991. On the trophic status of Peruvian anchovy and sardine // J. Ichtiol.— V. 31.— Iss. 2.— P. 240–252. (Rus).

Konchina Yu.V. and Pavlov Yu.P. 1999. On the question of jack mackerel generation abundance // J. Ichtiol.— V. 39.— Iss. 5.— P. 784–791. (Rus).

Korel'sky V.N. (Ed.). 1996. Fishery in Japan.— M.: Izd. Ekspeditor.— 160 p. (Rus).

Kryisov A.I. 2000. Dynamics of Atlantic-spring-spawning herring population in the early ontogenesis. Thes. of Biologics Candidate Dissertation.— M.: VNIRO.— 23 p. (Rus).

Kryizhov V.N. 2002. Regional features of climatic changes in the North Europe and the West Siberia in the 20th century // Proc. All-Rus. Conf. «Scientific aspects of ecological problems in Russia». June 13–16, 2001.— M.: Nauka.— P. 133–139. (Rus).

Ladd C., Hunt G.L., Stabeno Ph. 2002. Climate mixing and phytoplankton on the southeast Bering Sea shelf // PICES 11-th annual meeting. Quindao. October 18–26, 2002. Abstracts.— P. 81.

Laewastu T. 1993. Marine climate, weather and fisheries.— Oxford: Fishing News Books.— 204 p.

Lasker R. 1978. The relation between oceanographic conditions and larval anchovy food in the California Current: identification of the factors leading to recruitment failure // Rapp. et proc.-verb. reun. Cons. int. explor. sci. mer.— V. 1073.— P. 212–230.

Lasker R. 1981a. Factors, contributing to variable recruitment of the northern anchovy (Engraulis mordax) in the California Current: contrasting years 1975 through 1978 // Rapp. et proc.-verb. reun. Cons. int. explor. sci. mer.— V. 178.— P. 375–388.

Lasker R. 1981b. The role of a stable ocean in larval fish survival and subsequent recruitment // Marine fish larvae: morphology, ecology and relation to fisheries / Lasker R. (ed.).— Univ. Wash. Press, Seattle.— V. 131.— P. 80–87.

Lasker R. 1985.What limits clupeoid production? Can. J. Fish. and Aquat. Sci.—V. 42 (Suppl. 1).— P. 31–38.

Ljuingman L. 1880. Contributions towards solving the question of the secular periodicity of great herring fisheries // U. S. Comm. Fish and Fisheries Rept.— № 7.— P. 497–503.

Lluch-Belda D., Crawford R., Kawasaki T., MacCall A., Parrish R., Shwartzlose R., Smith P. 1989. World-wide fluctuations of sardine and anchvy stock. The regime problem // S. Afr. J. Mar. Sci.— V. 8.— P. 195–205.

Lluch-Belda D., Hernandez-Vazquez S., Hernandez-Vazquez S., Salinas-Zavala C., Shwartzlose R. 1992a. The recovery of the California sardine as related to global change // Calif. Coop. Ocean. Fish. Invest. Rept.— V. 33.— P. 50–59.

Lluch-Belda D., Schwartzlose R.A., Serra R., Parrish R., Kawasaki T., Hedgecock D., Crawford R.J.M. 1992b. Sardine and anchovy regime fluctuations of abundance in four regions of the world oceans: a workshop report // Fish. Oceanogr.— V. 1(4).— P. 339–347.

Logerwell E.A., Smith P.E. 2001. Mesoscale eddies and survival of late stage Pacific sardine (Sardinops sagax) larvae // Fish. Oceanogr.— V. 10.— P. 13–25.

Longhurst A. 1971. The clupeoid resources of tropical seas // Oceanography and Marine Biology. An annual review № 9 / Barney H.(ed.).— London: Allen & Unwin.— P. 300–304.

Mackas D.L., Goldblatt R., Lewis A.G. 1998. Interdecadal variation in developmental timing of Neocalanus plumchrus populations at Ocean Station P in the subarctic North Pacific // Can. J. Fish. and Aquat. Sci.— V. 55.— P. 1878–1893.

Mackas D.L., Tsuda A. 1999. Mesozooplankton in the eastern and western subarctic Pacific: community structure, seasonal life histories, and interannual variability // Progress in Oceanography.— V. 43.— P. 335–363.

Makarov A.A. 1998. The world power generation and Eurasian energetic space.— M.: Energoatomizdat.— 280 p. (Rus).
Mann K.H., Lazier J.R.N. 1996. Dynamics of marine ecosystems: biological-physical interactions in the oceans.— U.K. Blackwell Publ. Ltd.— 394 p.
Mantua N., Hare S. 2002. The Pacific decadal oscillation // J. Oceanogr. Soc. Jap.— V. 58.— P. 35–44.
Mantua N., Hare S., Zhang Y., Wallace J., Francis R. 1997. A Pacific interdecadal climate oscillation with impacts on salmon production // Bull. Amer. Meteorol. Soc.— V. 78.— № 6.— P. 1069–1079.
Marple S.L.-jr. 1990. Digital spectral analysis and its applications.— M.: Mir.— 584 p. (Rus).
Marshall C., Kjesbu O., Yaragina N., Solemdal P., Ulltang O. 1998. Is spawner biomass a sensitive measure of the reproductive and recruitment potential of Northeast Arctic cod? // Can. J. Fish. and Aquat. Sci.— V. 55.— P. 1766–1783.
Mayama H., Ishida Y. 2003. Japanese studies on the early ocean life of juvenile salmon // N. Pacif. Anadrom. Fish Comm. Bull.— № 3.— P. 41–67.
McGowan J.A. 1995. Temporal change in marine ecosystems // Natural climate variability on decade to century time scales.— Wash. D.C.: Nat. Res. Council. Nat. Acad. Press.— P. 555–571.
Megrey B.A., Hinckley S. 2001. Effect of turbulence on feeding of larval fishes: a sensitivity analysis using an individual-based model // ICES J. Mar. Sci.— V. 58.— P. 1015–1029.
Mendelsson R., Mendo J. 1987. Exploratory analysis of anchoveta recruitment off Peru and related environmental series // The Peruvian anchoveta and its upwelling ecosystem: three decades of change / Pauly D., Tsukayama I. (eds.).— ICLARM Studies and reviews.— IMARPE. Peru, Phillipines.— V. 15.— P. 294–306.
Minobe S. 2000. Spatio-temporal structure of the pentadecadal climate oscillations over the North Pacific // Progress in Oceanography.— V. 47.— P. 381–408.
Minobe S. 1997. A 50–70 year climatic oscillation over the North Pacific and North America // Geophysic. Res. Lett.— V. 24.— P. 683–686.
Minobe S. 1999. Resonance in bi-decadal and penta-decadal climate oscillations over the North Pacific: role in climatic regime shifts // Geophysic. Res. Lett.— V. 26.— P. 855–858.
Monin A.S. and Shishkin Yu.A. 2000. Climate as the physical problem // Uspekhi Fizicheskikh Nauk.— V. 170(4).— P. 419–445. (Rus).
Muck P. 1989. Major trends in the pelagic ecosystem off Peru and their implications for management // The Peruvian upwelling system: dynamics and interactions / Pauly D., Muck P., Mendo J., Tsukayama I. (eds.).— ICLARM Conf. Proc.— № 18.— P. 386–403.
Murphy G.I. 1961. Oceanography and variations in the Pacific sardine populations // CALCOFI Rept.— V. 8.— P. 55–64.
Mysak L.A. 1986. El Niño interannual variability and fisheries in the Northeast Pacific Ocean // Can. J. Fish. and Aquat. Sci.— V. 43.— P. 464–497.
Naidenov V.I. and Kozhevnikova I.A. 2003. Why floods are so often? // Priroda.— No. 9.— P. 12–20. (Rus).

Nakata K., Hada A., Matsukawa Y. 1994. Variations in food abundance for Japanese sardine larvae related to Kuroshio meander // Fish. Oceanogr.— V. 3.— P. 39–49.

Nakken O. 1994. Causes of trends and fluctuations in the Arcto-Norwegian cod stock // ICES Mar. Sci. Symp.— V. 198.— P. 212–228.

Niebauer H.J. 1999. The 1997–1998 El Niño in the Bering Sea as compared with previous ENSO events and «Regime Shift» of the late 1970s // PICES Sci. Rept.— № 10.— P. 101–104.

Nikolaev Yu.V. and Alekseev G.V. (Ed.). 1989. Structure and variability of large-scale oceanologic processes and fields in the Norwegian energetically active zone.— L: Gidrometeoizdat.— 128 p. (Rus).

Nordklim data set –1. 2001.— http// www.smhi.se/hfa.coord/nordklim/nkds.htm

Norton J.G., Schwing F.B., Pickett M.H., Husby D., Moore Ch.S. 2001. Monthly mean coastal upwelling indices, west coast of South America 1981 to 2000: trends and relationships // NOAA Techn. Memorandum NOAA-TM-NMFS-SWFSC–316.— 35 p.

Noto M., Yasuda I. 2003. Empirical biomass model for the Japanese sardine, *(Sardinops melanosticus)*, with sea surface temperature in the Kuroshio extention // Fish. Oceanogr.— V. 12(1).— P. 1–9.

Odate K. 1994. Zooplankton biomass and its long-term variations in the western North Pacific Ocean // Bull. Tohoku Region. Fish. Res. Lab.— V. 56.— P. 115–173.

Oozeki Y. 1999. Pelagic fish management // Bull. Tohoku Nat. Fish. Res. Inst.— № 62.— P. 165–169.

Oozeki Y., Nakata H. (eds.). 2002. Report of an APN/GLOBEC-SPACC workshop on the causes and consequences of climate-induced changes in pelagic fish productivity in East Asia // GLOBEC Rept.— № 15.— 12 p.

Ording A. 1941. Studies on annual growth zones in spruce and pine // Rept. Norweg. Inst. Forestry.— V. 25.— № 7(2).— P. 101–354 (in Norwegian, with English summary).

Ottersen G., Loeng H. 2000. Covariability in early growth and year-class strength of Barents Sea cod, haddock and herring: the environmental link // ICES J. Mar. Sci.— V. 57.— P. 339–348.

Ottersen G., Loeng H., Raknes A. 1994. Influence of temperature variability on recruitment of cod in the Barents Sea // ICES Mar. Sci. Symp.— V. 198.— P. 471–481.

Ottestad P. 1942. On periodical variations in yield of the great sea fisheries and possibility establishing yield prognosis // Fiskeridir. skr. Ser. havunders. (Rept. of Norwegian fisheries and marine investigations).— V. 7.— № 5.— P. 3–11.

Owen R.W. 1981. Microscale plankton patchiness in the larval anchovy environment // Rapp. et proc.-verb. reun. Cons. int. explor. sci. mer.— V. 178.— P. 364–368.

Parrish R.H., Nelson C.S., Bakun A. 1981. Transport mechanisms and reproductive success of fishes in the California Current // Biol. Oceanogr.— V. 1.— P. 175–203.

Parrish R.H., Schwing F.B., Mendelsson R. 2000. Mid latitude wind stress: the energy source for climatic shifts in the North Pacific Ocean // Fish. Oceanogr.— V. 9.— P. 224–238.

Pauly D., Jarre A., Luna S., Sambilay V. Jr., De Menndiola B.R., Alamo A. 1989. On the quality and types of food ingested by Peruvian anchoveta // The Peruvian upwelling system: dynamics and interactions / Pauly D., Muck P., Mendo J., Tsukayama I. (eds.).— ICLARM Conf. Proc.— № 18.— P. 109–124.

Pauly D., Muck P., Mendo J., Tsukayama I. (eds.). 1989. The Peruvian upwelling system: dynamics and interactions.— ICLARM Conf. Proc.— № 18.— 438 p.

Pauly D., Palomares M. L., Gayanilo F. C. 1987. VPA estimates of the monthly population, length composition, recruitment, mortality, biomass and related statistics of Peruvian anchoveta 1953–1981 // The Peruvian anchoveta and its upwelling ecosystem: three decades of change / Pauly D., Tsukayama I. (eds.).— ICLARM Studies and Reviews.— Callao, Peru, IMARPE.— № 15.— P. 142–165.

Pauly D., Tsukayama I. (eds.). 1987. The Peruvian anchoveta and its upwelling ecosystem: three decades of change.— ICLARM Studies and Reviews.— Callao, Peru, IMARPE.— № 15.— 351 p.

Pearcy W., Aydin R.K., Brodeur R. 1999. What is carrying capacity of the North Pacific for Salmonids?— PICES Press.— V. 7(2).— P. 17–23.

Pearcy W., Fisher J., Anma G., Meguro T. 1996. Specific associations of epipelagic nekton of the North Pacific Ocean, 1978–1993 // Fish. Oceanogr.— V. 5.— P. 1–20.

Peterman R.M., Bradford M.J. 1987. Wind speed and mortality rate of marine fish, the northern anchovy (Engraulis mordax) // Science.— V. 235.— P. 354–356.

Pomeranets K.S. 1993. Floods in Neva River mouth // Priroda.— No. 10.— P. 9–19.(Rus).

Pomeranets K.S. 1999. On statistics of floods in St.-Petersburg // Meteorology and Hydrology.— No. 8.— P. 105–110. (Rus).

Pomeroy L. 1979. Secondary production mechanisms of continental shelf communities // Ecol. Proc. Coastal and Mar. Syst. Proc. Conf. Ecol., Thalahasse.— P. 103–186.

Ponomarenko I.Ya. 1973. The influence of fodder and temperature conditions on the cod bottom fry survivability in Barents Sea // Proc. PINRO.— Iss. 34.— P. 210–222. (Rus).

Ponomarenko I.Ya. 1996. Formation of generations and the role of environmental conditions. Dynamics of populations // Barents Sea cod (Boitsov V.V., Lebed' N.I., Ponomarenko V.P., Ponomarenko I.Ya., Tereshchenko V.V., Tretyak V.L., Shevelev M.S., and Yaragina N.A.) Murmansk: PINRO.— P. 157–192. (Rus).

Ponomarenko I.Ya., Yaragina N.A. 1980. Relation between mature and immature specimens among cod of different ages and sizes in 1978–1981.— ICES G.M. 1981 / G: 22.— 20 p.

Ponomarev V.I., Trusenkova O., Trousenkov S., Kaplunenko D., Ustinova E., Polyakova A. 1999. The ENSO signal in the Northwest Pacific // PICES Sci. Rept.— № 10.— P. 9–31.

Pravdin I.F. 1940. The review of investigations of Far East salmons // Izv. TINRO.— V. 18.— P. 1–108. (Rus).

Qiu,B. 2002. The Kuroshio extension system: its large-scale variability and role in midaltitude ocean-atmosphere interaction // J. Oceanogr. Soc. Jap.— V. 58.— P. 57–75.

Reid P.C., Battle E., Batten S., Brander K. 2000. Impacts of fisheries on plankton community structure // ICES J. Mar. Sci.— V. 57.— P. 495–502.

Reid P.C., Planque B., Edwards M.E. 1998. Is observed variability in the long-term results on the continious plankton recorder survey a response to climate change? // Fish. Oceanogr.— V. 7.— № 3–4.— P. 282–288.

Richardson A.J., Schoeman D.S. 2004. Climate impact on plankton ecosystems in the Northeast Atlantic // Science.— V. 305.— P. 1609–1612.

Ricker W.E. 1954. Stock and recruitment .J .Fish. Res. Board Can.— V. 11.— P. 559–623.

Ricker W.E. 1972. Hereditary and environmental factors affecting certain salmonid populations // The stock concept in Pacific salmon / Simon R.C. (ed.).— Vancouver: H.R. MacMillan Lectures in Fisheries. UBC.— P. 27–160.

Ricker W.E. 1995. Trends in the average size of Pacific salmon in Canadian catches // Climate change and northern fish populations / Beamish R. (ed.).— Can. Spec. Publ. Fish. Aquat. Sci.— V. 121.— P. 593–602.

Rodionov S.N. 1995. Atmospheric teleconnections and coherent fluctuations in recruitment to North Atlantic cod stocks // Climate change and northern fish populations / Beamish R. (ed.).— Can. Spec. Publ. Fish. Aquat. Sci.— V. 121.— P. 45–55.

Roemnich D., McGowan J. 1995. Climatic warming and decline of zooplankton in the California Current // Science.— V. 267.— P. 1324–1326.

Rogers J.C. 1984. The association between the North Atlantic Oscillation (NAO) and Southern Oscillation in the northern hemisphere // Monit. Weather Rev.— V. 112.— P. 1999–2015.

Rothschild B.J. 1986. Dynamics of marine fish populations.— Harvard Univ. Press. Cambridge, Mass.— 277 p.

Rothschild B.J., Osborn T.R. 1988. The effect of turbulence on planktonic contact rates // J. Plankton Res.— V. 10.— P. 465–474.

Ryther J. 1969. Photosynthesis and fish production in the sea // Science.— V. 166 (3091).— P. 72–76.

Saetersdal G., Loeng H. 1987. Ecological adaptation of reproduction in North-East Arctic cod // Fish. Res.— V. 5.— P. 253–270.

Sakurai Y., Kiyofuji H., Saitoh S., Hiyama Y. 2000. Changes in inferred spawning area of Todarodes pacificus (Cephalopoda: Ommastrephidae) due to changing environmental conditions // ICES J. Mar. Sci.— V. 57.— P. 24–30.

Schlesinger M. E., Ramankutty N. 1994. An oscillation in the global climate system of period 65–70 years // Nature.— V. 367.— P. 723–726.

Schwartzlose R.A., Alheit J., Bakun A., Baumgasrtner T., Cloete R., Crawford R., Fletcher W., Green-Ruiz M.Y., Hagen E., Kawasaki T., Lluch-Belda D., Lluch-Cota S., MacGall A., Matsuura Y., Nevarez-Martinez M., Parrish R., Roy C., Serra R., Shust K., Ward M., Zuzunaga J. 1999. Worldwide large-scale fluctuations of sardine and anchovy populations // S. Afr. J. mar. Sci.— V. 21.— P. 289–347.

Schwing F., O'Farrell M., Steger J., Baltz K. 1996. Coastal upwelling indices west coast of North America.— NOAA Techn. Memorandum NMFS-SWFSC–231.— 208 p.

Schwing F.B. 1998. Patterns and mechanisms for climate change in the North Pacific: the wind did it // Status and trends of the major roundfish, flatfish, and pelagic fish stocks in the North Sea: thirty-year overview. Proc. 'Aha Huliko'a Hawaiian Winter Workshop, 1996 / Serchuk G., Kirkegaard F.M.E., Daan N. (eds.).— ICES J. Mar. Sci.— V. 53.— P. 1130–1145.

Seliverstov A.S. 1974. Some factors affecting abundance of Atlantic spring-spawning herring generations. Thes. Biologics Candidate Diss.— M.: VNIRO.— 24 p. (Rus).

Semko R.S. 1937. Kamchatka red salmon biology // Proc. Kamchatka Div. TINRO.— P. 1–120. (Rus).

Serra J.R. 1983. Changes a in the abundance of pelagic resources along the Chilean cost // FAO Fish. Rept.— V. 2.— № 291.— P. 255–284.

Shabalova M., Weber S.I.H. 1999. Patterns of temperature variability on multidecadal to centennial timescales // J. Geophys. Res.— V.105. № 24.— P. 31.023–31.041.
Shaporenko S.I. 1993. Balkhash Lake: yesterday, today, tomorrow // Priroda.— No. 9.— P. 47–50. (Rus).
Sharp G.D. 2003. Future climate change and regional fisheries: a collaborative analysis // FAO Fish. Techn. Pap.— № 452.— 75 p.
Sherman K., Solow A., Jossi J., Kane J. 1998. Biodiversity and abundance of the zooplankton of Northern shelf ecosystem // ICES. J. Mar. Sci.— V. 55.— P. 730–738.
Shugimoto T. 2001. Interannual-interdecadal variations in plankton biomass and the physical environment in the North-West Pacific // PICES Sci. Rept.— № 18.— P. 132–136.
Shugimoto T. 2002. Interannual-interdecadal variations in plankton biomass and the physical environment in the North West Pacific // Report of APN/GLOBEC-SPACC workshop on the causes and consequences of climate-induced changes in pelagic fish productivity in East Asia / Oozeki Y., Nakata (eds).— GLOBEC Rept.— № 15.— P. 12.
Shugimoto T., Tadokoro K. 1997. Interannual-interdecadal variations in zooplankton biomass, chlorophyll concentration and physical environment in the subarctic Pacific and Bering Sea // Fish. Oceanogr.— V. 6(2).— P. 74–93.
Shugimoto T., Tadokoro K. 1998. Interdecadal variations of plankton biomass and physical environment in the North Pacific // Fish. Oceanogr.— V. 7.— № 3–4.— P. 289–299.
Shuntov V.P. 1986. The state of knowledge of multiyear cyclic changes in the fish populations of Far East seas // Biol. Moray.— No. 3.— P. 3–14. (Rus).
Shuntov V.P. 1991. Is the global warming deleterious for biological resources of Bering Sea? // Ryb. Khoz.— No. 9.— P. 27–30. (Rus).
Shuntov V.P. 2001 Biology of Far Eastern seas of Russia. vol. 1. Vladivostok: TINRO-centre.— 580 p. (Rus).
Shuntov V.P. 2003. Control of marine biological resources: illusions and reality // Thes. rep. intern. conf. «Rational environmental management and control for marine bioresources: ecosystemic approach. September 23–26, 2003.— Vladivostok.— P. 67–73. (Rus).
Shuntov V.P. and Temnykh O.S. 2004. If the ecological capacity of North Pacific is exceeded in relation with high population of salmons: myths and reality // Izv. TINRO.— V. 138.— P. 19–36. (Rus).
Shuntov V.P. and Vasil'kov V.P. 1982. Epochs of atmospheric circulation and dynamics of Far East and California sardine periodicity // J. Ichtiol.— V. 22.— Iss. 1.— P. 187–199. (Rus).
Slobodkin L.R. 1960. Ecological energy relationship at the population // Amer. Naturalist.— V. 93.— P. 213–236.
Smirnov N.P., Vorob'ev V.N., and Kochanov S.Yu. 1998. North-Atlantic oscillation and climate.— St.-Pb.: Izd. RGGMU.— 121 p. (Rus).
Smirnova N.F. and Smirnov N.P. 2000. Atlantic cod and climate.— St.-Pb.: Izd. RGGMU.— 222 p. (Rus).
Smith P. 2000. Chapter 2. Pelagic fish early life history: CalCOPHI overview // Fisheries Oceanography: an integrative approach to fisheries ecology and management / Hurrison P., Parsons T. (eds.).— Blackwell Science.— P. 8–28.

Solow A.R. 2002. Fisheries recruitment and North Atlantic Oscillation // Fish. Res.— V. 54.— P. 295–297.

Sonechkin D.M. 1998. Climate dynamics as a non-linear Brownian motion // Int. J. Bifurcation and Chaos.— V. 8(4).— P. 799–803.

Starovoitov A.N. 2003. Dog salmon in Far East seas — biological characteristics of the species. 1. Seasonal distribution and migrations in Far East seas and open areas of the Northwest Pacific // Izv. TINRO.— V. 132.— P. 43–81. (Rus).

Statgraphics. 1988. Statistic Graphic System by Statistical Graphic Corporation. Users Guide Publ.— 440 p.

Steele J.N. 1998. From carbon flux to regime shift // Fish. Oceanogr.— V. 7.— № 3–4.— P. 176–181.

Steele J.N., Collie J.S. 2005. Functional diversity and stability of coastal ecosystems. Chapter 22 // The SEA: The Global Coastal Ocean / Robinson A.R., Brink K. (eds.).— Harvard Univ. Press. (in press).

Sundby S. 1997. Turbulence and ichtyoplankton: influence on vertical distributions and encounter rates // Scientia Marina.— V. 61.— Suppl. 1.— P. 159–176.

Sundby S., Ellersten B., Fossum P. 1994. Encounter rates between first feeding cod larvae and their prey during moderate to strong turbulent mixing // ICES Mar. Sci. Symp.— V. 198.— P. 393–405.

Tadokoro K. 2001. Long-term variations of plankton biomass in the North Pacific // PICES Sci. Rept.— № 18.— P. 132–136.

Taylor G., Southards Ch. 2002. Long-term climate trends and salmon population // Climate & Salmon.— http://www.ocs.orst.edu/reports/climate_fish.html.

Temnykh O.S., Starovoitov A.N., Glebov I.I., and Sviridov V.V. 2003. Pacific salmons in pelagic communities of Far East seas // Izv. TINRO.— V. 132.— P. 112–153. (Rus).

Toresen R., Ostvedt O.J. 2000. Variation in abundance of Norwegian spring-spawning herring throughout of 20-th century and the influence of climatic fluctuations // Fish and Fisheries.— V. 1.— P. 231–256.

Trenberth K.E., Hurrell J.W. 1995. Decadal coupled atmosphere-ocean variation in the North Pacific Ocean. Climate change and northern fish population // Climate change and northern fish fluctuations / Beamish R. (ed.).— Can. Spec. Publ. Fish. Aquat. Sci.— V. 121.— P. 14–24.

Ueda H., Kaeriyama M., Urawa S. 2001. Recent progress in salmon migration research in Japan // PICES Sci. Rept.— № 18.— P. 199–201.

Ulltang O. 1996. Stock assessment and biological knowledge: can prediction uncertainty be reduced? // ICES J. Mar. Sci.— V. 53.— P. 659–675.

Ustinova E.I., Sorokin Yu.D., and Khen G.V. 2002. Interannual variability of thermal conditions of the Sea of Okhotsk // Izv. TINRO.— V. 130.— P. 44–51. (Rus).

van Der Lingen C. 2002. Diet of sardine Sardinops sagax in the Southern Benguela upwelling ecosystem // S. Afr. J. mar. Sci.— V. 24.— P. 301–316.

Vangengeim G.Ya. 1940. The long-term temperature and ice break-up forecasting // Proc. State Hydrological Institute.— Iss. 10.— P. 207–236. (Rus).

Verheye H., Richardson A. 1998. Long-term increase in crustacean zooplankton abundance in the southern Benguela upwelling region (1951–1996): bottom-up or top-down control? // ICES J. mar. Sci.— V. 55 (4).— P. 803–807.

Verheye H., Richardson A., Hutchings L., Marska G., Gianacouras D. 1998. Long-term trends in the abundance and community structure of coastal zooplankton in the Southern Benguela system, 1951–1996 // S. Afr. J. mar. Sci.— V. 19.— P. 317–332.

Vinnikov K.Ya. 1986. Climate sensitivity. M.: Gidrometizdat.— 225 p. (Rus).

Vittel's L.A. 1946. Cyclones of the Northern seas and Arctic warming-up // Meteorologia i Gidrologiya.— No. 5.— P. 32–40. (Rus).

Vize V.Yu. 1937. The reasons for Arctic warming-up // Sov. Arktika.— No. 1.— P. 2–18. (Rus).

Vladimirov V.A. 1997. The problems of resources use and perspective forecasting of marine mammals dynamics of Far East seas of Russia // Ryb. Khoz.— No. 3.— P. 20–25. (Rus).

Vladimirov V.A. 2002. On the problem of climatic determinacy of the long-term dynamics of North-Pacific pinnipeds populations // Marine mammals (investigation results in the period of 1995–1998). Council on marine mammals.— M.: Izd. Katran.— P. 143–176. (Rus).

Wada T., Jacobson L. 1998. Regimes and stock-recruitment relationship in Japanese sardine 1951–1995 // Can. J. Fish. and Aquat. Sci.— V. 55.— P. 2455–2463.

Wada T., Oozeki Y. 1999. A population dynamics model for the Japanese sardine—why the sardine shows such large population fluctuations? // Bull. Tohoku Nat. Fish. Res. Inst.— № 62.— P. 171–180.

Walsh J. 1981. A carbon budget for overfishing off Peru // Nature.— V. 290.— P. 300–304.

Watanabe Y., Zenitani H., Kimura R. 1995. Population decline of Japanese *s*ardine Sardinops melanosticus owing to recruitment failures.// Can. J. Fish. and Aquat. Sci.— V. 52.— P. 1609–1616.

Willie-Echeverria T., Wooster W. 1998. Year to year variations in Bering Sea ice cover and some consequences for fish distributions // Fish. Oceanogr.— V. 7.— P. 159–170.

Yanez E., Barbieri M., Silva C., Nieto K., Espinola F. 2001. Climate variability and pelagic fisheries in Northern Chile // Progress in Oceanography.— V. 49.— P. 581–596.

Yasuda I., Sugasaki H., Watanabe Y., Minobe S., Oozeki Y. 1999. Interdecadal variations in Japanese sardine and ocean climate // Fish. Oceanogr.— V. 8.— P. 18–24.

Yndestad H. 2002. The code of long term fluctuations of Norwegian spring spawning herring.— ICES Annual Sci. Conf., Copenhagen.— CM 2002 / Q:02.— 2 p.

Yudanov I.G. 1964. Abundance of Atlantic spring-spawning herring with respect to secular climatic changes. In book: Materials of fishery investigations of the North basin. Murmansk.— Iss. 4.— P. 9–13. (Rus).

CONTENTS

ABOUT THE AUTHORS

LEONID B. KLYASHTORIN (Doctor of Sciences in Marine biology & Fisheries) was born 1934. Since 1958–1965 worked in the Institute Oceanology Ac. Sci. Russia on the primary production in the oceans. Since 1968 until today he works in the Federal Institute for Fisheries and Oceanography (VNIRO). Since 1968–1980 research on the Marine and Freshwater Fish Respiration (the book: L. Klyashtorin «Water Respiration and oxygen requirements of fishes». Pishevaya industry Publishing, Moscow, 1982, 168 p., in Russian), 1980–1990 research on Salmon Ranching and Nature Salmon Stock dynamics. From 1990 until now: Research on the relations between Climate and Long-Term Fish Stock dynamics. Published 131 papers in Scientific journals. Main recent publication — the book: L. Klyashtorin, A. Lyubushin «Cyclic climate changes and fish productivity». VNIRO Publishing, Moscow, 2005. 234 p. (in Russian).

ALEXEY A. LYUBUSHIN (Doctor of Science in Geophysics) was born 1954. He graduated from Moscow Physical Technical Institute. Since 1984 until now he works in the Institute of Physics of the Earth Ac. Sci. Russia and since 1994 also in International Institute of Earthquake Prediction Theory and Mathematical Geophysics Ac. Sci. Russia). He is a professor of Moscow State Geological Prospecting Academy, Department of High Mathematical Modeling. Research interests: multidimensional signal processing, wavelet analysis, point process statistics, artificial networks, geophysical monitoring, earthquake prediction, seismic hazard assessment. Published 108 papers in Scientific journals. Main recent publication: (books), L. Klyashtorin, A. Lyubushin «Cyclic climate changes and fish productivity» VNIRO Publishing, Moscow, 2005. 234 p. (in Russian) and A. Lyubushin «Geophysical and ecological monitoring system date analysis». NAUKA Publishing, Moscow, 2007, 228 p. (in Russian).

Klyashtorin Leonid B., Lyubushin Alexey A.

CYCLIC CLIMATE CHANGES AND FISH PRODUCTIVITY

Chief Publisher *G.P. Korotkova*
Design *V.V. Veselova*
Proof reading *L.I. Filatova*

Signed for printing 23.11.2007. Format $70 \times 100^{1}/_{16}$.
Content 14,0 sheets. Run 200 copies. Order №

VNIRO Publishing
17, V. Krasnoselskaya Street,
Moscow, 107140, Russian Federation

Tel.: (499) 264–65–33
Fax: (499) 264–91–87

This book considers relationships between climate changes and fish productivity of ocean ecosystems.

Analyses of climate index fluctuations and populations of major commercial fish species for the last 1500 years allowed us to characterize the 50-70 year climate fluctuations and fish production dynamics.

Our simple stochastic model suggests that it is possible to predict the likely trends of basic climatic indices and thus some commercial fish populations for several decades ahead.

The results we obtained allowed us to revisit and illuminate the old question: which factor is more influential for the long-term fluctuations of major commercial stocks, climate or commercial fisheries?

VNIRO Publishing